



# State of Wildfires 2024-25

- 1
- 2
- 3 Douglas I. Kelley<sup>1,\*</sup>, Chantelle Burton<sup>2,\*</sup>, Francesca Di Giuseppe<sup>3,\*</sup>, Matthew W. Jones<sup>4,\*</sup>, Maria L. F.
- 4 Barbosa<sup>1,5</sup>, Esther Brambleby<sup>4</sup>, Joe R. McNorton<sup>3</sup>, Zhongwei Liu<sup>6</sup>, Anna S. I. Bradley<sup>2</sup>, Katie
- 5 Blackford<sup>7</sup>, Eleanor Burke<sup>2</sup>, Andrew Ciavarella<sup>2</sup>, Enza Di Tomaso<sup>8</sup>, Jonathan Eden<sup>9</sup>, Igor José M.
- 6 Ferreira<sup>10</sup>, Lukas Fiedler<sup>11,12</sup>, Andrew J Hartley<sup>2</sup>, Theodore R. Keeping<sup>13</sup>, Seppe Lampe<sup>14</sup>, Anna
- 7 Lombardi<sup>8</sup>, Guilherme Mataveli<sup>4,10</sup>, Yuquan Qu<sup>15</sup>, Patrícia S. Silva<sup>16</sup>, Fiona R. Spuler<sup>17,18</sup>, Carmen B.
- 8 Steinmann<sup>19,20</sup>, Miguel Ángel Torres-Vázquez<sup>21</sup>, Renata Veiga<sup>22</sup>, Dave van Wees<sup>23</sup>, Jakob B. Wessel<sup>24</sup>,
- 9 Emily Wright<sup>2</sup>, Bibiana Bilbao<sup>25,26</sup>, Mathieu Bourbonnais<sup>27</sup>, Gao Cong<sup>28</sup>, Carlos M. Di Bella<sup>29,30</sup>,
- 10 Kebonye Dintwe<sup>31</sup>, Victoria M. Donovan<sup>32</sup>, Sarah Harris<sup>33</sup>, Elena A. Kukvaskaya<sup>34</sup>, Brigitte N'Dri<sup>35</sup>,
- 11 Cristina Santín<sup>36,37</sup>, Galia Selaya<sup>38,39</sup>, Johan Sjöström<sup>40</sup>, John Abatzoglou<sup>41</sup>, Niels Andela<sup>23</sup>, Rachel
- 12 Carmenta<sup>42</sup>, Emilio Chuvieco<sup>43</sup>, Louis Giglio<sup>44</sup>, Douglas S. Hamilton<sup>45</sup>, Stijn Hantson<sup>46</sup>, Sarah Meier<sup>47</sup>,
- 13 Mark Parrington<sup>8</sup>, Mojtaba Sadegh<sup>48</sup>, Jesus San-Miguel-Ayanz<sup>49</sup>, Fernando Sedano<sup>49</sup>, Marco Turco<sup>50</sup>,
- 14 Guido R. van der Werf<sup>51</sup>, Sander Veraverbeke<sup>4,15</sup>, Liana O. Anderson<sup>52</sup>, Hamish Clarke<sup>53</sup>, Paulo M.
- 15 Fernandes<sup>54</sup>, Crystal A. Kolden<sup>55</sup>
- 16
- 17 **Affiliations:**
- 18 <sup>1</sup> Water and Climate Science, UK Centre for Ecology & Hydrology, Wallingford OX10 8BB, U.K.
- 19 <sup>2</sup> Hadley Centre, Met Office, Fitzroy Road, Exeter, UK, EX1 3PB
- 20 <sup>3</sup> European Centre for Medium-range Weather Forecast, Shinfield Park, Reading RG29AX, United Kingdom
- 21 <sup>4</sup> Tyndall Centre for Climate Change Research, School of Environmental Sciences, University of East Anglia,
- 22 Norwich Research Park, Norwich, UK, NR4 7TJ
- 23 <sup>5</sup> Federal University of São Carlos, Rodovia Lauri Simões de Barros, km 12 - SP-189 - Aracaju, Buri - São Paulo,
- 24 18290-000, Brazil
- 25 <sup>6</sup> National Centre for Earth Observation, University of Leicester, Space Park Leicester, 92 Corporation Road,
- 26 Space City, Leicester, LE4 5SP, UK
- 27 <sup>7</sup> Department of Life Sciences, Imperial College London, Chemistry Building CHEM062, South Kensington,
- 28 London, SW7 2AZ, UK
- 29 <sup>8</sup> European Centre for Medium-Range Weather Forecasts, Robert-Schuman-Platz 3, 53175 Bonn, Germany
- 30 <sup>9</sup> Centre for Agroecology, Water and Resilience, Coventry University, Wolston Ln, Ryton-on-Dunsmore, Coventry
- 31 CV8 3LG, UK
- 32 <sup>10</sup> Earth Observation and Geoinformatics, National Institute for Space Research (INPE), Astronautas Avenue
- 33 1758, São José dos Campos, Brazil, 12227-010
- 34 <sup>11</sup> Institute of Oceanography, Center for Earth System Research and Sustainability, University of Hamburg,
- 35 Bundesstraße 53, 20146 Hamburg, Germany
- 36 <sup>12</sup> International Max Planck Research School on Earth System Modelling, Max Planck Institute for Meteorology,
- 37 Bundesstraße 53, 20146 Hamburg, Germany
- 38 <sup>13</sup> World Weather Attribution, Centre for Environmental Policy, Imperial College London, Weeks Building, 16-18
- 39 Prince's Gardens, London SW7 1NE
- 40 <sup>14</sup> Water & Climate, Vrije Universiteit Brussel, Pleinlaan 2, 1050 Brussel, Belgium
- 41 <sup>15</sup> Faculty of Science, Vrije Universiteit Amsterdam, De Boelelaan 1100, Amsterdam, Netherlands, 1081 HV
- 42 <sup>16</sup> School of the Environment, Yale University, 195 Prospect St, New Haven, CT 06511, USA
- 43 <sup>17</sup> Department of Meteorology, University of Reading, Brian Hoskins Building, Whiteknights Road, Earley Gate,
- 44 Reading, RG6 6ET, UK
- 45 <sup>18</sup> The Alan Turing Institute, British Library, 96 Euston Rd., London NW1 2DB
- 46 <sup>19</sup> Institute for Environmental Decisions, Department of Environmental Systems Science, ETH Zurich
- 47 <sup>20</sup> Federal Office of Meteorology and Climatology MeteoSwiss, Operation Center 1, P.O. Box 257, 8058
- 48 Zurich-Airport, Switzerland
- 49 <sup>21</sup> Environmental Remote Sensing Research Group, Department of Geology, Geography and Environment,
- 50 Universidad de Alcalá, Calle Colegios 2, Alcalá de Henares 28801, Spain
- 51 <sup>22</sup> Laboratory for Environmental Satellite Applications (LASA), Department of Meteorology, Federal University of
- 52 Rio de Janeiro
- 53 <sup>23</sup> BeZero Carbon Ltd, 25 Christopher Street, London, EC2A 2BS, UK
- 54 <sup>24</sup> Department of Mathematics and Statistics, University of Exeter, Harrison Building, University of Exeter, North
- 55 Park Road, EX4 4QF Exeter, United Kingdom
- 56 <sup>25</sup> Biology, Departamento de Estudios Ambientales, Universidad Simón Bolívar, Valle de Sartenejas, Aartado
- 57 89000, Caracas, Venezuela
- 58 <sup>26</sup> UMR Art-Dev 5281, Université Paul Valéry Montpellier, Site Saint-Charles, France , UMR 5281, Site
- 59 Saint-Charles 1, Rue du Professeur Henri Serre, F-34090 Montpellier, France



- 60 <sup>27</sup> Earth, Environmental and Geographic Sciences, University of British Columbia - Okanagan, 1177 University  
 61 Way, Kelowna, BC, Canada V1V 1V7  
 62 <sup>28</sup> Department of Geography, University of Hong Kong, 10F, The Jockey Club Tower, Centennial Campus,  
 63 Pokfulam Road, Hong Kong  
 64 <sup>29</sup> Departamento de Métodos Cuantitativos y Sistemas de Información, University of Buenos Aires, Av. San  
 65 Martín 4453 (1417), CABA, Argentina  
 66 <sup>30</sup> IFEVA (Agricultural Physiology and Ecology Research Institute), Av. San Martín 4453 (1417), CABA, Argentina  
 67 <sup>31</sup> Department of Environmental Science, University of Botswana, Plot 4775 Notwane Rd, Gaborone Botswana  
 68 <sup>32</sup> West Florida Research and Education Center, School of Forest, Fisheries, and Geomatics Sciences, University  
 69 of Florida, 5988 Highway 90, Milton, FL 32583  
 70 <sup>33</sup> Fire Risk, Research and Community Preparedness, Country Fire Authority, Burwood East, Victoria, Australia  
 71 <sup>34</sup> Laboratory of Experimental and Applied Ecology, V.N. Sukachev Institute of Forest Siberian Branch of the  
 72 Russian Academy of Sciences - separate subdivision of the FRC KSC SB RAS, 50/28 Akademgorodok,  
 73 Krasnoyarsk, Russian Federation, 660036  
 74 <sup>35</sup> Natural Sciences, Nangui Abrogoua University, 02 BP 801 Abidjan 02  
 75 <sup>36</sup> Research Institute of Biodiversity (IMIB), CSIC-University of Oviedo-Principality of Asturias, IMIB, Research  
 76 Building, Mieres Campus, Mieres, Spain, 33600  
 77 <sup>37</sup> Biosciences, Swansea University, Wallace Building, Singleton Campus, Swansea, UK, SA2 8PP  
 78 <sup>38</sup> Research and action, ECOSCONSULT, Calle Tte. H. Balcazar No. 24, Santa Cruz de la Sierra  
 79 <sup>39</sup> Research, Fundacion Innova, Calle Tte. H. Balcazar No. 24, Santa Cruz de la Sierra  
 80 <sup>40</sup> Fire and Safety, RISE Research institutes of Sweden, Box 857, 51515 Borås, Sweden  
 81 <sup>41</sup> School of Engineering, University of California, Merced, 5200 N Lake Rd, Merced, CA, 95343, USA  
 82 <sup>42</sup> Tyndall Centre for Climate Change Research, School of Global Development, University of East Anglia,  
 83 Norwich Research Park, Norwich, UK, NR4 7TJ  
 84 <sup>43</sup> Environmental Remote Sensing Research Group, Department of Geology, Geography and Environment,  
 85 Universidad de Alcalá, Calle Colegios 2, Alcalá de Henares 28801, Spain  
 86 <sup>44</sup> Department of Geographical Sciences, University of Maryland, College Park, MD 20742  
 87 <sup>45</sup> Marine, Earth, and Atmospheric Science, North Carolina State University, 2800 Faucette Drive, Raleigh, North  
 88 Carolina, USA, 27603  
 89 <sup>46</sup> Program in Earth System Sciences, Faculty of Natural Sciences, Universidad del Rosario, Bogotá, Colombia.  
 90 <sup>47</sup> Land, Environment, Economics and Policy Institute (LEEP), Department of Economics, University of Exeter,  
 91 Rennes Drive EX4 4ST Exeter, United Kingdom  
 92 <sup>48</sup> Department of Civil Engineering, Boise State University, Boise, ID, USA  
 93 <sup>49</sup> Disaster Risk Management Unit (E.1), Directorate E (Space, Security, and Migration), European Commission  
 94 Joint Research Centre, European Commission, Rue du Champ de Mars 21, 1050 Brussels, Belgium  
 95 <sup>50</sup> Regional Atmospheric Modelling (MAR) Group, Regional Campus of International Excellence Campus Mare  
 96 Nostrum (CEIR), Department of Geography, University of Hong Kong  
 97 <sup>51</sup> Meteorology and Air Quality, Wageningen University and Research, Droevendaalsesteeg 3-3 A, 6708 PB,  
 98 Wageningen, the Netherlands  
 99 <sup>52</sup> Cemaden/MCTI, 500 – Distrito de Eugênio de Melo, São José dos Campos – São Paulo, Brazil  
 100 <sup>53</sup> FLARE Wildfire Research, School of Agriculture, Food and Ecosystem Sciences, University of Melbourne,  
 101 Grattan St, Parkville, 3010, Australia  
 102 <sup>54</sup> ForestWISE—Collaborative Laboratory for Integrated Forest & Fire Management, Centre for the Research and  
 103 Technology of Agro-Environmental and Biological Sciences, Universidade de Trás-os-Montes e Alto Douro,  
 104 Quinta de Prados, Vila Real, Portugal, 5000-801  
 105 <sup>55</sup> Wildfire Resilience Center, School of Engineering, University of California, Merced, 5200 N Lake Rd, Merced,  
 106 CA 95343, USA

107

108 \*These authors contributed equally to this work.

109

110 Correspondence to:

111 [doukel@ceh.ac.uk](mailto:doukel@ceh.ac.uk)

112 [chantelle.burton@metoffice.gov.uk](mailto:chantelle.burton@metoffice.gov.uk)

113 [Francesca.DiGiuseppe@ecmwf.int](mailto:Francesca.DiGiuseppe@ecmwf.int)

114 [matthew.w.jones@uea.ac.uk](mailto:matthew.w.jones@uea.ac.uk)

115

116 **Key words:** Wildfire, Extreme Fire, Attribution, Climate Change



## 117 Abstract

118 Climate change is increasing the frequency and intensity of extreme wildfires globally, yet  
 119 our understanding of these high-impact events remains uneven and shaped by media  
 120 attention and regional research biases. The State of Wildfire Project systematically tracks  
 121 and analyses global fire activity and this, its second annual report, covers the March 2024 to  
 122 February 2025 fire season. During the 2024-25 fire season, fire-related carbon (C) emissions  
 123 were totalled 2.2 Pg C, 9% above average and the 6th highest on record since 2003, despite  
 124 below-average global burned area (BA; 3.7 million km<sup>2</sup>). Extreme fire seasons in South  
 125 America's rainforests, dry forests and wetlands, and in Canada's boreal forests pushed up  
 126 the global C emissions total. Fire C emissions were over four times above average in Bolivia,  
 127 three times above average in Canada, and ~50% above average in Brazil and Venezuela.  
 128 Wildfires in 2024-25 caused 100 fatalities in Nepal, 34 in South Africa, and 30 in Los  
 129 Angeles, with additional fatalities reported in Canada, Côte d'Ivoire, Portugal, and Turkey.  
 130 The Eaton and Palisades fires in Southern California caused 150,000 evacuations and  
 131 US\$140 billion in damages. Communities in Brazil, Bolivia, Southern California, and  
 132 Northern India were exposed to fine particulate matter at concentrations 13-60 times WHO's  
 133 daily air quality standards. We evaluated the causes and predictability of four extreme  
 134 wildfire episodes from the 2024-25 fire season, including in Northeast Amazonia  
 135 (January-March 2024), the Pantanal-Chiquitano border regions of Brazil and Bolivia  
 136 (August-September 2024), Southern California (January 2025), and the Congo Basin  
 137 (July-August 2024). Anomalous weather created conditions for these regional extremes,  
 138 while fuel availability and human ignitions shaped spatial patterns and temporal fire  
 139 dynamics. In the three tropical regions, prolonged drought was the dominant fire enabler,  
 140 whereas in California, extreme heat, wind, and antecedent fuel build-up were the dominant  
 141 enablers. Our attribution analyses show that climate change made extreme fire weather in  
 142 Northeast Amazonia 30–70 times more likely, increasing burned area roughly fourfold  
 143 compared to a scenario without climate change. In the Pantanal–Chiquitano, fire weather  
 144 was 4–5 times more likely, with up to 35-fold increases in burned area. In Southern  
 145 California, climate change made larger burned area 89% more likely, with burned area up to  
 146 25 times higher. The Congo Basin's fire weather was 3–8 times more likely with climate  
 147 change, with a 2.7-fold increase in burned area. Socioeconomic changes since the  
 148 pre-industrial period, including land-use change, also likely increased burned area in  
 149 Northeast Amazonia. Our models project that events on the scale of 2024-25 will become up  
 150 to 57%, 34%, and 50% more frequent than in the modern era in Northeast Amazonia, the  
 151 Pantanal-Chiquitano, and the Congo Basin, respectively, under a middle-of-the-road  
 152 scenario (SSP370). Climate action can limit the added risk, with frequency increases kept  
 153 below 15% in all three regions under a strong mitigation scenario (SSP126). In Southern  
 154 California, the future trajectory of extreme fire likelihood remains highly uncertain due to  
 155 poorly constrained climate-vegetation-fire interactions influencing fuel moisture, though our  
 156 models suggest that risk may decline in future. This annual report from the State of Wildfires  
 157 Project integrates and advances cutting-edge fire observations and modelling with regional  
 158 expertise to track changing global wildfire hazard, guiding policy and practice towards  
 159 improved preparedness, mitigation, adaptation, and societal benefit. Thirteen new datasets  
 160 and model codebase's presented in this work are available from the State of Wildfires  
 161 Project's Zenodo community (<https://zenodo.org/communities/stateofwildfiresproject>, last  
 162 access: 11 August 2025).

## 163 Short Summary

164 The second State of Wildfires report examines extreme wildfire events from 2024 to early  
 165 2025. It analyses key regional events in Southern California, Northeast Amazonia,  
 166 Pantanal-Chiquitano, and the Congo Basin, assessing their drivers, predictability, and  
 167 attributing them to climate change and land use. Seasonal outlooks and decadal projections



are provided. Climate change greatly increased the likelihood of these fires, and without strong mitigation, such events will become more frequent.

## 1. Introduction

### 1.1. Background

The potential for wildfires is growing under climate change, with increases in the frequency and intensity of drought and periods of fire-favourable weather driving reductions in vegetation (fuel) moisture and priming landscapes to burn more regularly, intensely, and severely (Seneviratne et al., 2022; UNEP, 2022a; Jones et al., 2022; Abatzoglou et al., 2019; Cunningham et al., 2024a). Additionally, human activities and land use change can contribute to or exacerbate the risk of extremely large, fast-moving or intense fires, especially in tropical forests where people are the primary cause of ignition and forest degradation (Lapola et al., 2023). Recent years have been marked by a series of extreme wildfire events spanning the globe (Abatzoglou et al., 2025), with record levels of burned area (BA) occurring in the 2019-2020 Australian “Black Summer” bushfires (Abram et al., 2021; Canadell et al., 2021) and a series of high-ranking wildfire seasons occurring in quick succession in the western US (2020 and 2021; Higuera & Abatzoglou, 2020), Siberia (2020 and 2021; Zheng et al., 2023), varying parts of Europe (e.g. 2017, 2022, 2023; European Commission Joint Research Centre, 2023, 2024, 2025), South America (2019, 2020, 2023, 2024; Kelley et al., 2021; Barbosa et al., 2022; Silveira et al., 2020; Mataveli et al., 2024, 2025), and Canada (2023, 2024; Jones et al., 2024b; Jain et al., 2024; Byrne et al., 2024; Kolden et al., 2024). The 2024-25 fire season was marked by extreme fire extent and emissions in Amazonia and the Pantanal-Chiquitano (Mataveli et al., 2025; Kolden et al., 2025) and a second consecutive year of extreme fire extent and emissions in Canada (Kolden et al., 2025; Parrington and Di Tomaso, 2025). The 2024-25 fire season also saw extreme fire activity in equatorial Africa, which went broadly under-reported despite fires triggering record rates of forest loss (stand-replacing fire extent) in the region (World Resources Institute, 2025). Meanwhile, extremely destructive and costly individual fires affected Southern California (Barnes et al., 2025; Woolcott, 2025) and Jasper National Park in Alberta (Parks Canada, 2024; Insurance Bureau of Canada, 2025). Widespread regional anomalies in high fire activity were also seen in northern India leading to severe haze events (CAMS, 2024).

The prominence of recent extreme wildfires and wildfire seasons notably contrasts with overall trends in the area burned by fires globally. A distinctive trend has emerged towards enhanced fire activity and severity in forests and other fuel-rich environments, which is occurring amidst increasingly frequent and intense droughts and heatwaves, particularly in the extratropics (Jones et al., 2024a, Cunningham et al., 2024a). Due mostly to a reduction in the global savannahs tied to landscape fragmentation and changing rainfall patterns, global BA has fallen since the beginning of this century by around one-quarter (Andela et al., 2017; Jones et al., 2022; Chen et al., 2024). Critically, this decline in fire extent masks major shifts in the distribution of fires globally, with regions such as eastern Siberia and the western US and Canada experiencing a more than 40% increase in BA since 2000 (Jones et al., 2022; Zheng et al., 2021) and regions such as southeast Australia also showing significant increases over longer periods despite high interannual variability (Canadell et al., 2021). Likewise, there have been shifts in the global distribution of BA from non-forests to forests globally and from the tropics to the extratropics, with the increased prevalence and severity of forest fires emitting increasing quantities of forest carbon stocks each year and driving increasing fire carbon (C) emissions globally (Kelley et al., 2019; Jones et al., 2024a). Hence, focussing exclusively on global aggregated BA extent underplays the scale and magnitude of the significant shifts in wildfire activity and impacts that are underway across many world regions. An increase in forest and peatland burning is particularly concerning





221 due to the rich ecosystem services that these regions provide, including C storage and  
 222 biological and cultural diversity (UNEP, 2022b). The intensification of fire regimes in  
 223 environments that are less fire-adapted is of high importance because these ecosystems are  
 224 expected to be least resilient to such changes (Grau-Andrés et al., 2024) and because they  
 225 are often home to communities relying directly on the forest (Newton et al., 2022; Shepherd  
 226 et al., 2020; Schleicher et al., 2018).

227  
 228 The extreme wildfire events of recent years have significantly impacted societies and  
 229 ecosystems across the globe (Cunningham et al., 2024a, 2024b; 2025). Since 1990, wildfire  
 230 disasters have directly killed or injured at least ~18,000 people, a conservative measure  
 231 based on incomplete records and reporting biased to the global Northern countries (updated  
 232 from Jones et al., 2022; Centre for Research on the Epidemiology of Disasters, 2024). In  
 233 2023, 232,000 people were evacuated due to wildfires in Canada alone (Jain et al., 2024;  
 234 Kolden et al., 2024). Also since 1990, fires are estimated to have caused on the order of 1.5  
 235 million premature deaths globally per year through degraded air quality related to fine  
 236 particulate matter (PM<sub>2.5</sub>; Johnston et al., 2021; Xu et al., 2024; Chen et al., 2021). Degraded  
 237 air quality related to fires is experienced most strongly in the tropics (Pai et al., 2022) and  
 238 often disproportionately affects the elderly, the young, the infirm, and traditional communities  
 239 with poor public services or means of protection (Carmenta et al., 2021; Johnston et al.,  
 240 2021).

241  
 242 As anthropogenic emissions of CO<sub>2</sub> remain persistently high, the world's natural C sinks in  
 243 forests, peatlands, and other ecosystems are increasingly pivotal to moderating increases in  
 244 atmospheric CO<sub>2</sub> concentration (Friedlingstein et al., 2025). Intact forests are often relied  
 245 upon for delivering national plans for reaching Net Zero (Smith et al., 2023) and offering sites  
 246 for nature based solutions (NBS). Yet, massive wildfire emissions from boreal forests and  
 247 soils in Siberia and Canada across the years 2020, 2021, and 2023 amount to over 1 billion  
 248 tonnes of C, a gross flux comparable in magnitude to annual CO<sub>2</sub> emissions from fossil fuel  
 249 combustion in India, the EU27 or the USA (Friedlingstein et al., 2025; Zheng et al., 2023). In  
 250 a natural fire regime, these gross emissions would likely be recuperated through post-fire  
 251 recovery. However, the greater vegetation mortality and loss of ecosystem function  
 252 associated with more widespread and severe fires contribute to shifts in local to regional  
 253 terrestrial carbon budgets from sinks to sources (Zheng et al., 2021; Gatti et al., 2021; Nolan  
 254 et al., 2021a; Phillips et al., 2022; Harrison et al., 2018; Jones et al., 2024a). Loss of  
 255 vegetation during extreme fire seasons can also have wider lasting effects on ecosystems,  
 256 for instance by reducing the habitat area available to endemic species (Ward et al., 2020;  
 257 Carmenta et al., 2025).

258  
 259 Extreme fires can moreover impact the livelihoods of various communities and landowners  
 260 who depend on intact natural landscapes. For example, the lands, territories and cultural  
 261 heritage of traditional communities and Indigenous Peoples can be degraded and  
 262 transformed by wildfires, raising climate justice issues that compound a legacy of  
 263 colonisation, dispossession and forced cessation of cultural practices (Garnett et al., 2018;  
 264 Barlow et al., 2018; Lapola et al., 2023; Pascoe et al., 2024). Further, conflating the  
 265 detrimental impacts of wildfire types has also stigmatised small-scale intergenerational fire  
 266 use and led to prohibitive fire governance that affects local communities (Carmenta et al.,  
 267 2021; Barlow et al., 2020; Pascoe et al., 2024).

268  
 269 Mitigating and adapting to increases in wildfire potential are growing priorities of  
 270 policymakers and require coordination with many other stakeholders. National and  
 271 international disaster management centres are seeking to enhance predictive capacity, while  
 272 fire management agencies are expanding or re-allocating their resources to rapidly suppress  
 273 fires to avoid them becoming too large, fast, or intense (e.g. Bowman et al., 2020). A number  
 274 of international organisations such as the UN Environment Programme (UNEP, 2022a), the  
 275 World Bank (2020, 2024a), the Organisation for Economic Co-operation and Development



(OECD, 2023), and a range of other inter- or non- governmental organisations are producing reports that consolidate evidence on the changing risk of extreme fires and identify best practices for mitigating their impacts, including through land management and urban/rural planning. Many land managers are developing and implementing approaches such as fuel reduction (Fernandes and Botelho, 2003; Stephens et al., 2012; Moreira et al., 2020; Chuvieco et al., 2023; Hsu et al., 2025). Wildfire response agencies are exploring innovative approaches to detecting and responding to fires, and there is rising interest in the prospect of integrated fire management around the world (Food and Agriculture Organization of the United Nations, 2024). Operators of C market projects and forest carbon-conservation initiatives, such as REDD+ are particularly wary of the risks that wildfires present to the permanence of C offsets, which often feature as a key tool in national policies and international initiatives for achieving Net Zero emissions (Barlow et al., 2012; Smith et al., 2023).

Amidst extreme wildfires and wildfire seasons, stakeholders increasingly turn to scientists for answers. How extreme was this fire event in a historical context? Is climate change amplifying fire occurrence? Can we disentangle the factors responsible in order to target those in policy and management? Will we see more wildfires like this in the future? Did land use or management factors exacerbate or ameliorate the problem? Could we have predicted these events and how can we improve early warning systems and preparedness in the future? What is the role of climate and socioeconomic factors, such as land use, in reducing risk of extreme wildfires in future?

While observational, statistical, and modelling tools for assessing extreme wildfire drivers and predicting wildfire occurrence are advancing rapidly, their application to studying extreme wildfire seasons or events on timescales relevant to public and political interest remains limited. The State of Wildfires report represents a new initiative to systematically catalogue extreme wildfire events at annual frequency and explain their occurrence, predictability and attribution to climate and land use changes. The report incorporates recent methodological advances in disentangling the drivers of four selected extreme wildfire events to fuel dryness, fuel load, and weather, and ignition and suppression factors. By applying these methodological advances in conjunction with models of global change, we quantify the change in likelihood of the past year's events under climate and land use changes. Observable fire metrics (e.g. BA) are the target variable of our causal inference and attribution work, which thereby advances on more common climate attribution studies that attribute change in fire-favourable meteorological conditions to climate change. Overall, this report capitalises on recent advances in the study of extreme fire events and seasons to provide timely information about shifting fire regimes and their causes. The findings of the report are relevant to organisations involved in prevention and combat efforts, policymakers, the media, and the wider public.

## 1.2. Objectives of this Report

The State of Wildfires report aims to deliver actionable information to policy and practice stakeholders and wider society. In rising to this challenge, we aim to spur scientific and technological innovation including stimulating development of better tools for understanding and predicting extreme fires. In this edition we:

1. Regionally identify extreme individual wildfires or extreme wildfire seasons of the period March 2004-February 2025, and place them in context of recent trends.
2. Quantify the impacts of extreme events in terms of the exposure of population, physical assets (built environment), and carbon projects to fire as well as degraded air quality.



- 329 3. Shortlist a selection of four extremes (extreme individual wildfires or extreme wildfire  
 330 seasons) with notable impacts on society or the environment, which we term the  
 331 'focal events'.
- 332 4. Diagnose the contributions of both fuel dryness and load, ignitions, and suppression  
 333 to the occurrence of each focal event.
- 334 5. Assess the capacity of operational predictive systems to predict each focal event.
- 335 6. Attribute each focal event to anthropogenic influences by testing the role of climate  
 336 change and socioeconomic factors such as land use, land use change, and human  
 337 ignitions.
- 338 7. Provide an outlook on the probability of extreme events in the coming fire season  
 339 (commencing March 2025).
- 340 8. Project future changes in the probability of each focal event under future climate  
 341 scenarios.

342  
 343 Key methodologies used to achieve the above objectives are summarised as follows. To  
 344 address objectives 1 and 2, we build a comprehensive dataset of fire metrics including BA,  
 345 fire counts, fire C emissions, and individual fire properties (size and rate of growth) for  
 346 consistent world regions and quantitatively identify anomalies in these metrics during the  
 347 past fire season (Giglio et al., 2018; van der Werf et al., 2017; Andela et al., 2019). To  
 348 address objectives 3 and 4, we leverage weather forecasts from the European Centre for  
 349 Medium-Range Weather Forecasts (ECMWF) at different time horizon from medium (1-15  
 350 days) to long range (up to 4 months ahead) and additionally employ two state-of-the-art fire  
 351 models, *Controlar Fogo Local Analise pela Máxima Entropia* - English "Local Fire Control  
 352 Analysis by Maximum Entropy" (ConFLAME; Kelley et al., 2019; Barbosa et al., 2025b) and  
 353 *Probability of Fire* (PoF; McNorton et al., 2024) to pinpoint the causes of the extreme fire  
 354 events of 2024-25. To address objective 5, we employ projections of fire weather from the  
 355 Hadley Centre Large Ensemble (HadGEM3-A, Ciavarella et al., 2018) to attribute change in  
 356 the Fire Weather Index (FWI) to climate change, and we drive ConFLAME (Kelley et al.,  
 357 2019; Barbosa et al., 2025b) with outputs from both HadGEM3-A and separately with the  
 358 Intersectoral Impacts Model Intercomparison Project 3a (ISIMIP3a) and Joint UK Land  
 359 Environment Simulator Earth System model (JULES-ES; Mathison et al., 2023) to attribute  
 360 extreme BA to climate and land use changes (Burton, Lampe et al., 2024). To address  
 361 objective 6, we use seasonal outlook of FWI from the Copernicus Emergency Management  
 362 Service (Di Giuseppe et al., 2024). To address objective 7, we again pair ConFLAME with  
 363 JULES-ES (Mathison et al., 2023) to project future changes in BA under several future  
 364 climate and land use scenarios and provide a comprehensive assessment of past and future  
 365 extreme wildfire events.

366  
 367 The State of Wildfires report was launched in 2024 and is an annual report that can harness  
 368 and adopt new methodologies brought forward by the scientific community in the interim  
 369 between its yearly publication. Over the coming years and decades, we aim to enhance the  
 370 tools presented in this report to predict extremes with increasing lead times, monitor  
 371 emerging situations in near-real time, and explain their causes rapidly, thus enhancing our  
 372 ability to deliver timely insights to decision-makers when they are most needed.

## 373 2. Extreme Wildfire Events of 2024-25

### 374 375 2.1. Methods

376  
 377 We catalogued the extreme regional wildfire events or annual fire seasons in the period  
 378 March 2024-February 2025 based on a combination of anomalies in the distribution of  
 379 several observable fire metrics from Earth observations (**Section 2.1.1** and **Section 2.1.2**).  
 380 In this work, the global fire season is defined as occurring in March-February windows  
 381 oriented around the annual minima of global fire activity in boreal spring (see further details



382 in **Section 2.1.1.2**). As a new development for this edition of the report, we added statistics  
 383 describing anomalies in fire intensity during the 2024-25 fire season, complementing  
 384 anomaly statistics provided in the prior edition related to BA, fire emissions, fire size, and  
 385 rate of growth.

386  
 387 Due to the diversity of environmental settings in which fires occur and the range of  
 388 ecological, economic, or societal impacts caused, defining an extreme fire or an extreme fire  
 389 season remains inherently challenging. To date, extreme fires have commonly been defined  
 390 by their BA extent, by their feedback on the global climate, and by their socio-economic and  
 391 ecological impacts (Linley et al., 2022, 2025; Driscoll et al., 2024). We reviewed the range of  
 392 approaches that can be taken to identify extreme wildfire events in our inaugural report (see  
 393 **Appendix A** of Jones et al., 2024b) and so do not revisit this in the current article.

394  
 395 While an extreme fire event or extreme fire season may be visible as a significant anomaly  
 396 against historical Earth observations, the scientific community seeks to apply a more  
 397 comprehensive definition of extreme fire, including its impacts on society and the  
 398 environment. To catalogue extreme events that were not necessarily visible in Earth  
 399 observations, regional expert panels were constructed and given responsibility for identifying  
 400 extreme events of the past fire season (**Section 2.1.3**). The expert panels were given  
 401 flexibility to identify and catalogue wildfire characteristics or impacts that are considered  
 402 regionally extreme but are not necessarily captured by Earth observations. Examples of  
 403 extremes that can be captured by expert assessment (but not by Earth observations)  
 404 include: suppression difficulty; fatalities and structure loss; impacts on human health and  
 405 wellbeing; impacts on agricultural and other economic sectors; impacts on biodiversity, and;  
 406 impacts on diverse ecosystem services such as recreation, tourism, or other cultural values.  
 407 Hence, **Section 2.2** identifies a variety of impactful events displaying a broad range of  
 408 characteristics and impacts that can occur across diverse fire regimes (e.g. Archibald et al.,  
 409 2009; Cunningham et al., 2024a, 2024b; Keeley, 2009).

410  
 411 As a new development for this report, we added several new analyses providing context to  
 412 the observed extremes in fire during the past fire season (**Section 2.1.4**). Specifically, we  
 413 added an analysis of extreme fire weather days for the 2024-2025 fire season allowing the  
 414 spatial and temporal context of extreme fires with extreme fire weather to be described.

## 415 416 **2.1.1. Earth Observations of Fire**

### 417 418 **2.1.1.1. Input Datasets**

419  
 420 We assembled observations of burned area (BA), synonymous with fire extent, for the period  
 421 March 2002-February 2025 from the National Aeronautics and Space Administration (NASA)  
 422 product MCD64A1 (collection 6.1). MCD64A1 provides daily BA observations at 500 m  
 423 spatial resolution with global coverage and is based on retrievals from the Moderate  
 424 Resolution Imaging Spectroradiometer (MODIS) sensors mounted to the Terra and Aqua  
 425 satellites (Giglio et al., 2018, 2021).

426  
 427 We also produced a global record of individual fires for the period March 2002-February  
 428 2025 by updating the Global Fire Atlas (Andela et al., 2019) through February 2025, driven  
 429 by the 500m MODIS BA data. The Global Fire Atlas algorithm clusters burned cells into  
 430 individual fires, tracks their daily progression, and logs attributes such as fire size and mean  
 431 daily rate of growth. Our updates are provided at Andela and Jones (2025). The Global Fire  
 432 Atlas is one of several products tracking daily fire progression and identifying individual fires  
 433 at global scale based on moderate resolution satellite data (Andela et al., 2019; Laurent et  
 434 al., 2018; Artés et al., 2019). The product uses the MODIS BA product. The smallest unit of  
 435 disaggregation is 500m and the shortest timestep on which the expansion of a fire can be



observed is daily. Given its resolution, the Global Fire Atlas is expected to represent the dynamics of large fires better than smaller fast-moving fires.

In addition, we gathered estimates of fire carbon (C) emissions for the period March 2024–February 2025 from two models driven by Earth observations of active fires or BA: firstly, the Global Fire Assimilation System (GFAS) product, provided operationally by the Copernicus Atmospheric Services (CAMS) at 0.1 degree spatial resolution and daily temporal resolution (Kaiser et al., 2012; European Centre for Medium-Range Weather Forecasts, 2024), and; secondly, the Global Fire Emissions Database (GFED; version 4.1s) product at 0.25 degree spatial resolution and daily temporal resolution (van der Werf et al., 2017). GFAS is driven by the fire radiative power (FRP) retrievals in the MODIS active fire product MCD14A1 and biome-level relationships between FRP and biomass consumed based on GFED3 (Kaiser et al., 2012). For the 1997–2016 period, GFED4s is driven by MODIS BA data (MCD64A1 collection 5) supplemented with small fire BA based on MODIS active fire data, and a model for biomass productivity and fuel consumption (van der Werf et al., 2017). For the post-2016 period, emissions are based on active fire detections scaled to emissions using pixel-based scaling factors derived from the 2003–2016 overlapping period.

As a new analysis developed for the 2024–25 report, we added summaries of the peak (95th percentile) intensity of the fires detected in the Global Fire Atlas. The underlying data for this analysis were daily observations of fire radiative power (FRP) from the NASA active fire products MOD14A1 and MYD14A1 (Giglio et al., 2016). FRP measures the rate of radiant energy emitted by a fire, which is directly related to the fire's intensity and fuel consumption. MOD14A1 and MYD14A1 each provide FRP observations at two different times of the day, with the MOD14A1 dataset produced based on retrievals from the MODIS sensor aboard NASA's Terra satellite, which overpasses at around 10:30 AM and 10:30 PM local time, and the MYD14A1 dataset produced based on retrievals from the MODIS sensor aboard NASA's Aqua satellite, which overpasses at around 1:30 PM and 1:30 AM local time. In our case, daytime and nighttime observations of FRP were combined into a single dataset of active fire detections obtained from any satellite overpass and either MODIS sensor. To minimize potential uncertainties, we excluded FRP measurements associated with large MODIS scan angles ( $>50^\circ$ ), and normalized the FRP measurements by pixel size (Li et al., 2024).

The upcoming decommissioning of the Terra and Aqua satellites on which the MODIS instruments are mounted pose potential challenges for evaluating long-term data records of BA and estimated emissions from wildfires. The wider community requires continued development of BA and active fire products from sensors such as VIIRS (e.g., Parrington et al., 2025).

#### 2.1.1.2. *Input Data Uncertainties*

We note that the MODIS BA product data used in our analyses of anomalies in BA and individual fire properties (via the Global Fire Atlas) are known to be conservative due to the limitations to detecting small fires (e.g. agricultural fires) based on surface spectral changes at 500m resolution. Recent work has shown that including detections of small active fires increases global BA estimates by 93% (Chen et al., 2023). However, variability and trends in regional BA totals using datasets that include small fires do not differ significantly from the variability and trends present in the MODIS BA product (Chen et al., 2023). Hence, inclusion or exclusion of small fires tends to generate biases in central estimates of BA in one direction or the other, in line with the sensitivity of different sensors to different fire types. Uncertainty in the detection of small fires is larger than in the case of fires detected in the MODIS BA product, due to limited validation (van der Werf et al., 2017). The MODIS BA product with resolution of 500 m is deemed highly suitable for addressing the research questions of this report, which focus on more impactful fires that tend to burn larger areas.





Uncertainties in the BA estimation can be approached by comparing different existing global BA products. For instance the estimations of BA from the NASA MCD64A1 product, which is the basis for the calculations of this paper are 40% lower than ESA FireCCIS311, based on Sentinel-3 reflectance and VIIRS active fires, and 20% lower than the estimations provided by the Copernicus Land service (March 2024-Feb 2025 period). Comparing these estimates with the BA derived from higher resolution sensors, such as Sentinel-2 MSI would probably double the estimations of MCD64A1, as it was observed in Africa (Chuvieco et al., 2022) and the GFED5 BA product (Chen et al., 2024).

Uncertainties in fire carbon emissions estimates from GFED4.1s are on the order of  $\pm 20\text{-}25\%$  at 1 standard deviation for global totals (van der Werf et al., 2017; van der Werf et al., 2010). Uncertainties in GFED4.1s stem from uncertainties in BA, the amount of biomass consumed per unit BA, and the carbon emitted per unit biomass burned. Revisions to BA input data, discussed above, have tended to influence GFED central estimates of fire C emissions to a greater degree than the uncertainties around central estimates (van der Werf et al., 2017; Chen et al., 2023). Uncertainties in fire carbon emissions estimates from GFAS are on the order of approximately  $\pm 25\%$  at 1 standard deviation for global totals. Uncertainties are introduced by missed active fire detections, either below the detection threshold of the MODIS instruments, or not observed during the limited diurnal coverage of Low Earth Orbiting satellites, assumptions made for biome classifications, coefficients used to convert observed thermal anomalies to consumed dry matter, and emission factors used to estimate emitted quantities of carbon and pyrogenic pollutants. Variation in C emissions estimates on the order of approximately 20-60% has been observed in studies comparing multiple emissions products (Wiedinmyer et al., 2023).

The fire radiative power (FRP) data provided by the MOD14A1 and MYD14A1 products are subject to several well-documented uncertainties that affect both the detection of active fires and the precision of retrieved energy estimates (Giglio et al., 2016; Wooster et al., 2021). Omission errors typically arise when fires are obscured by clouds or, in some cases, dense smoke incorrectly flagged as clouds during masking procedures (Atwood et al., 2016). Additional omissions occur when the mid-infrared (MIR) radiance levels of small, low-intensity fires fall below detection thresholds, which is most common in the case of sub-canopy or peatland combustion (Schroeder et al., 2008; Roberts et al., 2018). Temporal gaps in satellite coverage also contribute, as MODIS instruments observe any given location only up to four times per day, often missing short-lived events or peak fire activity in the late afternoon (Roberts and Wooster, 2014). Commission errors, by contrast, typically occur when non-fire thermal anomalies are misclassified as active fires. False positives can be caused by sunglint on water or clouds or by thermally anomalous surfaces such as bare soils, urban infrastructure, gas flares, and volcanic eruptions, which produce elevated MIR radiance that mimics fire signatures (Wooster et al., 2021). Contextual detection algorithms help mitigate these errors by comparing candidate pixels to local background conditions. These approaches have been particularly successful in reducing commission errors, which are often below 10% (Giglio et al., 2016; Wooster et al., 2021). In contrast, uncertainties in omission errors and FRP observations remain less well characterised (Wooster et al., 2021; Li et al., 2024).

### 2.1.1.3. Regional Burned Area, Carbon Emissions and Fire Count Totals

We calculated regional totals of BA and C emissions based on a variety of regional layers defined in Table 1. The regional layers represent a range of biogeographical boundaries (e.g. biomes), geopolitical boundaries (e.g. countries), and values used in scientific reports (e.g. by the Intergovernmental Panel on Climate Change; IPCC). We calculated monthly totals of BA and fire C emissions for each region by aggregating monthly BA and daily C emissions data, summing the data from the input datasets both spatially and temporally as



544 required. In the case of fire C emissions, we also calculated the mean estimate of fire C  
545 emissions from GFED4.1s and GFAS, regionally.

546

547 We adopt a March-February definition of the global fire season (e.g. the latest global fire  
548 season spans March 2024-February 2025). Due to an annual lull in the global fire calendar  
549 in the boreal spring months, fire season BA totals are least sensitive to the shifts in fire  
550 season cutoffs of 1-2 months if the fire season centres on spring (Boschetti and Roy, 2008).  
551 This makes the global fire season centred on spring a pragmatic option for the study of  
552 interannual variability or trends in fire extent (Boschetti and Roy, 2008). The period  
553 March-February is specifically oriented at the end of the austral fire season and before  
554 widespread fires have begun in the boreal extratropics. The regions where this global  
555 definition of the fire season is most problematic are: northern hemisphere South America,  
556 Southeast Asia, and Central America (Giglio et al., 2013).

557

558 In addition, we calculated totals of regional fire counts for each global fire season based on  
559 the number of individual fire ignition points present within each region, using ignition point  
560 vectors from the Global Fire Atlas. The resolution of the MODIS data supplied to the Global  
561 Fire Atlas algorithm is 500 m and hence fires that are smaller in scale are omitted. Regional  
562 or national systems may record greater fire counts due to the inclusion of smaller fires.

563



**Table 1:** Regional layers to which global Earth observations were disaggregated and used to define regions with extreme wildfire seasons or extreme individual wildfire attributes. Regional layers are available from Jones et al. (2025).

Layer	Short Form	Source	Notes
Biomes	NA	Olson et al. (2001)	
Continents	NA	ArcGIS Hub (2024)	
Continental Biomes	NA	Olson et al. (2001), ArcGIS Hub (2024)	Spatial intersect of biomes and continents.
Ecoregions	NA	Olson et al. (2001)	Ecoregions are geographically inset within biomes.
Countries	NA	EU Eurostat (2020)	
UC Davis Global Administrative Areas (GADM) Level 1	GADM-L1	UC Davis (2022)	First sub-national administrative level, such as states of the US or provinces of China. Version 4.1.
Intergovernmental Panel on Climate Change <i>Sixth Assessment Report (AR6) Working Group I (WGI) Reference Regions</i>	IPCC AR6 WGI Regions	Iturbide et al. (2020)	
Global C Project <i>Regional C Cycle Assessment and Processes (RECCAP2) Reference Regions</i>	RECCAP2 Regions	Ciais et al. (2022)	
Global Fire Emissions Database (GFED) Basis Regions	GFED4.1s Regions	van der Werf et al. (2006)	

#### 2.1.1.4. Cross-Product Intercomparison of Regional Burned Area Totals

In this report, to characterise the dependence of our findings on BA product choices, we add a supplementary comparison between the regional BA totals detected by the MCD64A1 BA product and two other BA products. The first product was the ESA Climate Change Initiative FireCCIS311 product, derived from Sentinel-3 SYN reflectance and Visible Infrared Imaging Radiometer Suite (VIIRS) active fires (Lizundia-Loiola et al., 2022; see **Figure S1**). FireCCIS311 is provided at a spatial resolution of 300 m and is based on a contextual algorithm based on Sentinel-3 SYN surface reflectance (SYN combines OLCI and SLSTR reflectance), guided by active fire detections from VIIRS. The second product is NASA's VIIRS BA product (VNP64A1 v002; Zubkova et al., 2024; Giglio et al., 2024; see **Figure S1**), generated using an adaptation of the MODIS MCD64A1 Collection 6.1 algorithm, applied to 750 m VIIRS imagery and active fire detections. The hybrid algorithm uses dynamic thresholds on composite imagery derived from a burn-sensitive vegetation index and temporal texture measures, enabling it to distinguish fire-induced changes from other land surface changes. It identifies the burn date at 500 m resolution for each grid cell, with prior probabilities of burned/unburned areas informed by cumulative VIIRS active fire observations.



The FireCCIS311 product has been computed since 2019, and hence our cross-product comparisons focus on the fire seasons March 2019–February 2025. We followed identical approaches as described in prior sections to calculate regional BA totals and to quantify anomalies of the past fire season. With very few exceptions, we find a high level of consistency between the MCD64A1, FireCCIS311, and VIIRS VNP64A1 BA products with regards to both the regional BA totals and the geographical distribution of anomalies and rankings of BA in the 2024–25 fire season versus previous fire seasons since 2019 (**Figure S1**; Jones et al., 2025). This analysis adds confidence that regional anomalies identified in the MCD64A1 BA product are generally replicated across products from different space agencies using different algorithms applied to different combinations of Earth-observing sensors. The MCD64A1 BA product will soon discontinue due to the decommissioning of MODIS sensors aboard NASA's Terra and Aqua satellites. Consistency across products is an encouraging finding for the continuity of our annual reporting.

## 2.1.2. Identifying Extreme Fire Seasons and Events from Earth Observations

### 2.1.2.1. Regions with Extreme Wildfire Seasons

Anomalies in BA, fire C emissions, and fire counts in the latest global fire season (March 2024–February 2025) were calculated in several ways:

- (i) as relative anomalies (expressed in %) from the annual mean during all previous March–February periods since 2002 (2003 for fire C emissions);
- (ii) as standardised anomalies (standard deviations) from the annual mean during all previous March–February periods since 2002 (2003 for C emissions);
- (iii) as a rank amongst all March–February periods since 2002 (2003 for fire C emissions), March 2024–February 2025 inclusive.

In this report, anomalies in fire C emissions are reported based on the two-model mean estimate from GFED4.1s and GFAS, however anomalies based on the GFED4.1s or GFAS estimates individually are also available via Jones et al. (2025).

We identified regions in which the latest fire season was potentially classifiable as ‘extreme’ based on the rank of BA, C emissions, and fire count amongst all fire seasons. For visualisation purposes, we identified regions in which the latest fire season ranked in the top 5 of all annual fire seasons on record (see **Section 2.2.1**). The BA data for the period March 2002–February 2025 includes 23 fire seasons, while the C emissions data for the period March 2003–February 2025 includes 21 fire seasons. Hence, a top-5 ranking translates approximately to a fire season in the upper quartile of those on record.

We further characterised the onset, peak, and cessation of anomalous monthly BA in March 2024–February 2025. First, we identified the month of the event's peak as the maximum difference between monthly BA values in March 2024–February 2025 and the climatological mean monthly values from the prior March–February periods. Thereafter, the event's onset and cessation were defined as the bounds of consecutive months with above-average BA prior to and following the peak but limited to the March 2024–February 2025 period.

The annual data and anomalies produced using these methods are available from Jones et al. (2025).



### 638 **2.1.2.2. Regions with Extreme Individual Wildfire Attributes**

639 We identified regions in which large or fast-moving fires occurred in the latest fire season  
 640 based on records of individual fires from the Global Fire Atlas (Andela et al., 2019). For each  
 641 region (**Table 1**) and year, we estimated the size of the largest fire, the daily rate of growth of  
 642 the fire that spread most rapidly, the size of the 95th percentile fire, and the daily rate of  
 643 growth of the 95th percentile fire. In the Global Fire Atlas, the daily rate of growth for any  
 644 given fire is determined by calculating the average daily rate of growth at which the fire  
 645 advanced across all its constituent cells. This method includes cells burned by the head,  
 646 flank, and backfire and produces lower spread rates than if the calculation were based solely  
 647 on the cells burned by the head fire.

649 As a new analysis developed for the 2024-25 report, we also identified regions in which  
 650 intense fires occurred in the latest fire season based on the Global Fire Atlas and FRP  
 651 observations from the MODIS active fire datasets (MOD14A1 and MYD14A1). Regional  
 652 values were calculated per fire season across two steps as follows. First, each fire present in  
 653 the Global Fire Atlas was assigned a peak intensity value equivalent to the 95th percentile of  
 654 all FRP measurements (daytime and nighttime) occurring within the perimeter and date  
 655 range of the fire. Second, the regional summary values were taken to be the mean of all  
 656 peak (95th percentile) intensity values from the cohort of fires occurring in a region and fire  
 657 season. This approach effectively masks FRP measurements to fires that occur in the Global  
 658 Fire Atlas prior to averaging, meaning that the fire intensity anomalies presented here relate  
 659 to the same set of fires as the fire size and fire rate of growth statistics.

661 Anomalies in each fire attribute were calculated relative to other fire seasons since 2003  
 662 using the same metrics as for BA (see *i-iii* above), and we identified regions in which the  
 663 latest fire season featured fires with potentially extreme attributes based on the ranking of  
 664 the individual fire metrics amongst all fire seasons.

666 The annual data and anomalies produced using these methods are available from Jones et  
 667 al. (2025).

### 670 **2.1.3. Identifying Extreme Fire Seasons and Events from Expert Consultation**

#### 673 **2.1.3.1. Role of Expert Consultation**

674 We assembled a panel of regional experts from each continent (**Table A1**) to contribute to  
 675 the identification, description, and characterisation of extreme wildfire seasons or impactful  
 676 events in the latest fire season. A key role of the expert panel was to catalogue regional  
 677 events that significantly impacted society or the environment but which may not have been  
 678 detected by Earth-observing satellites due to issues such as scale, short duration, timing of  
 679 overpass, and cloud or canopy cover. This includes (but is not limited to) wildfires that  
 680 impacted society by causing fatalities, evacuations, displacement (e.g. homelessness),  
 681 direct structure or infrastructure loss or damage, degradation of air or water quality, loss of  
 682 livelihood, cultural practice or other ways of life, and loss of economic productivity. This  
 683 definition also includes (but is not limited to) wildfires that impact the environment via  
 684 disturbance to vulnerable ecosystems, biodiverse areas, or ecosystem services such as C  
 685 storage. This approach recognises that Earth observations do not provide a complete record  
 686 of all impactful fires. We do not define ubiquitous quantitative thresholds of impact by any of  
 687 the measures outlined above, but rather invite in-region experts to identify events that  
 688 triggered impacts that were sufficient in magnitude to infiltrate public and political discourse.  
 689 The sources of information available for cataloguing regional events include national/regional  
 690 fire records, land and fire management agencies reports, disaster management reports,





news reports, and social media. A second key role of our expert panel was to describe and contextualise the impacts of the fire seasons highlighted as extreme by Earth observations or regional assessment (see **Section 2.2.3**).

The year in review by continent, produced by the expert panel, is presented in **Appendix A**.

#### 2.1.3.2. *Shortlisting of Focal Events*

In later sections of this report, we conducted various analyses to understand the causes and predictability of a selection of extreme wildfire seasons or events during March 2024-February 2025 (see **Sections 4-6**). We limited the number of analyses to three globally prominent focal events of the 2024-25 global fire season because the approaches used are not operational and time is required to train and optimise our models regionally.

In discussion with our expert panel, we prioritised the three events studied in this report by weighing up the anomalies in Earth observations during the latest fire season as well as a suite of impacts that these extremes had on people and the environment. The focal events are notable for their international significance even where they have not attracted international media attention and where they have been highly relevant and recognized within and beyond their region.

#### 2.1.4. *Contextualising Analyses*

##### 2.1.4.1. *Contemporaneous Extremes in Fire Weather*

In the supplementary material edition of this report, we introduce routine summaries of the extreme (95<sup>th</sup> percentile) fire weather days during the March 2024-February 2025 global fire season based on the Fire Weather Index (FWI), a common metric of fire danger developed by the Canadian Forest Service as part of the Canadian Forest Fire Danger Rating System (CFFDRS; van Wagner, 1987). The FWI comprises various components that consider the influence of weather on fire danger, with 2m temperature, 10m wind speed, precipitation, and 2m relative humidity as prerequisite variables. Higher FWI values are generally seen during droughts, heatwaves and strong winds as these conditions are conducive to wildfires in environments with sufficient fuel load (Jolly et al., 2015; Di Giuseppe, 2016; Jones et al., 2022). We base our analysis of extreme (95<sup>th</sup> percentile) fire weather on the FWI dataset derived from the Copernicus Climate Change Service ERA5 reanalysis (Hersbach et al., 2020; Vitolo et al., 2020) and maintained by the Copernicus Emergency Management Service (CEMS, version 4.1, 2019). The same statistics are reported for the 2024-25 fire season as in the case of fire observational datasets, including (i) ranks, (ii) proportional anomalies, and (iii) standardised anomalies amongst all fire seasons since 2002 (**Figure S2**). Full discussion of the methodology and results are provided in **Supplementary Text S2**. The data produced using these methods are available from Turco et al. (2025).

##### 2.1.4.2. *21<sup>st</sup> Century Trends in Burned Area*

To place recent extremes in the context of fire trends of the past two decades, we update our regional analyses of trends in annual BA from Jones et al. (2022). In addition to reporting trends in *total* BA, we also present trends in *forest* BA as these regularly diverge from total BA trends (**Figure S3**), following Jones et al. (2024a). Full discussion of the methodology and results are provided in **Supplementary Material S2**.



## 743 2.2. Results

744

### 745 2.2.1. Extreme Fire Seasons and Events of 2024-25 from Global Earth 746 Observations

747

#### 748 2.2.1.1. Global Summary

749

750 According to the MODIS BA product, 3.7 million km<sup>2</sup> burned globally during the 2024-25  
 751 global fire season (March 2024-February 2025), 9% below the average of previous fire  
 752 seasons (4.0 million km<sup>2</sup>) since 2002 and overall ranking 16th (i.e., 8th lowest) of all fire  
 753 seasons since 2002 (Jones et al., 2025). Despite this, fire C emissions were 9% above  
 754 average at 2.2 Pg C during the 2024-25 global fire season, which ranks 6th amongst all fire  
 755 seasons since 2003 (based on annual averages of GFED4.1s and GFAS estimates; see  
 756 **Section 2.1.2**; Jones et al., 2025). The 2024-25 fire season therefore followed a similar  
 757 pattern as in the 2023-24 fire season, with above-average emissions occurring despite  
 758 below-average BA at the global level. These anomalies, signifying lesser fire extent but more  
 759 severe fires than average, are emblematic of a reported trend towards increased fire extent  
 760 and intensity in carbon-rich environments such as forests (Jones et al., 2024a). It is  
 761 important to note that the MODIS BA product is uncorrected for missed small fire detections  
 762 as in the case other estimates (e.g. Chen et al., 2023; Lizundia-Loiola et al., 2022), meaning  
 763 that the estimated BA extents from MODIS are conservative (i.e., *at least* 3.7 million km<sup>2</sup>  
 764 burned globally during 2024-25).

765

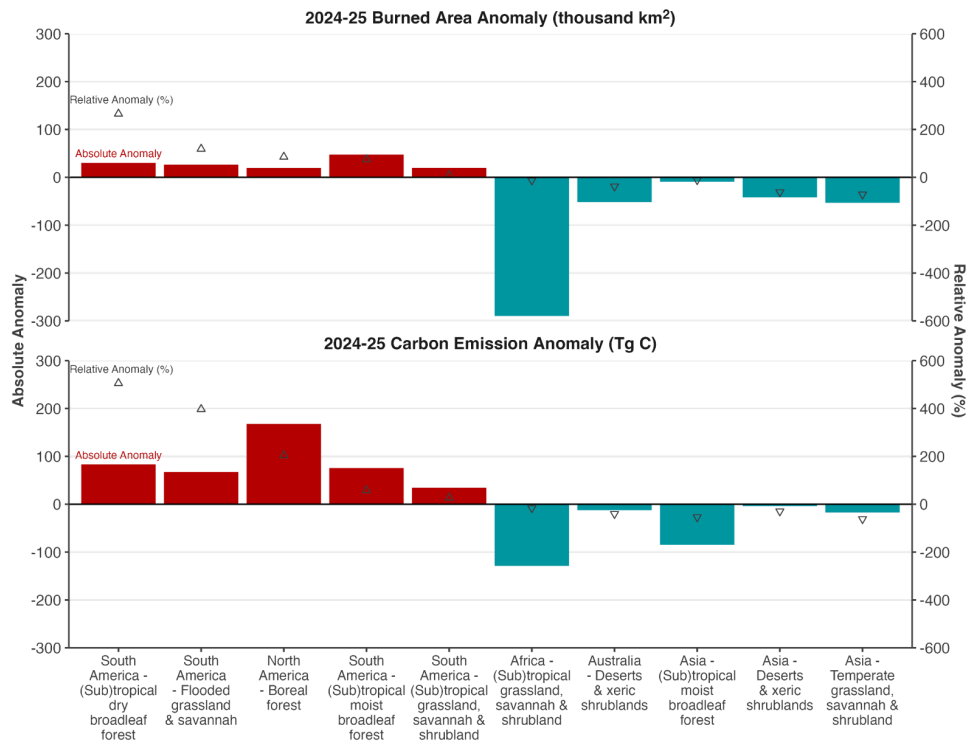
766 Stark regional contrasts in the anomalies in BA, fire C emissions and individual fire  
 767 properties are visible in the Earth observations at various regional scales (**Figure 1, Figure**  
 768 **2, Figure 3**). The three countries with greatest positive anomalies in BA and C emissions  
 769 during 2024-25 were Bolivia, Brazil, and Canada (**Table 2, Table 3**), marking a second  
 770 consecutive year in which the Americas experienced an anomalous fire season.

771

772 On the scale of continental biomes (**Figure 1, Figure 2, Figure 3**), the greatest BA and fire  
 773 C emissions anomalies of 2024-25 were seen in the North American boreal forests (mostly  
 774 in Canada), the South American moist tropical forests (mostly in Amazonia), the South  
 775 American dry tropical forests (mostly in the Chiquitano dry forests of Bolivia), and the South  
 776 American grassland and savannah biome (mostly in the Cerrado region). On the other hand,  
 777 it was a second consecutive year the African savannahs experienced a low fire season. In  
 778 the world's tropical savannah regions, which contribute around 70% towards global BA, the  
 779 total BA in the 2024-25 fire season was 290 thousand km<sup>2</sup> (12%) below average in Africa,  
 780 slightly above average in South America, and slightly above average in Australia (**Figure 2**).  
 781 Total BA across the global (sub)tropical grassland, savannah, and shrubland biome was 290  
 782 thousand km<sup>2</sup> (10%) below average, and the 6th lowest on record, but still contributed 70%  
 783 towards total global BA during 2024-25. Correspondingly, the C emitted by fires in global  
 784 savannahs was 102 Tg C (10%) below average in 2024-25.

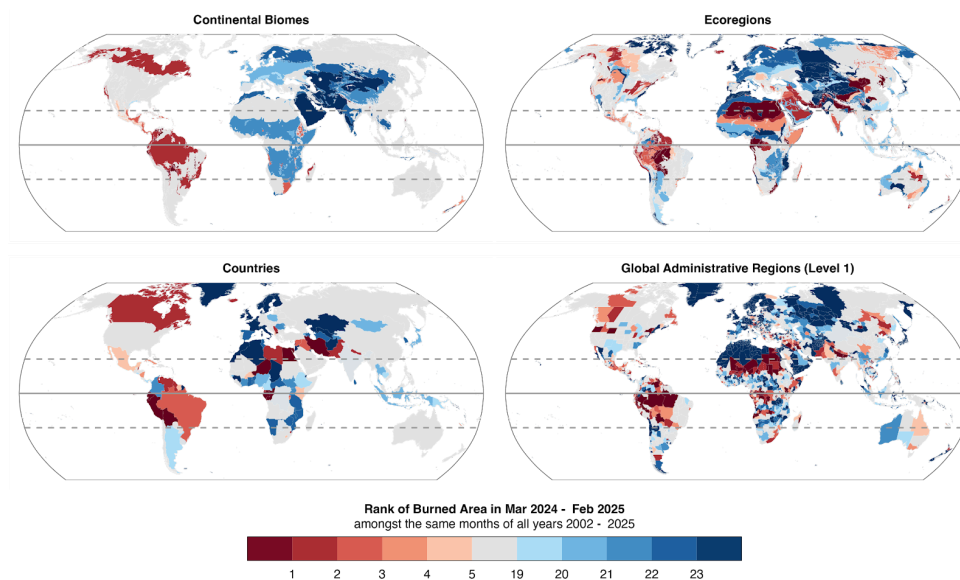
785

786

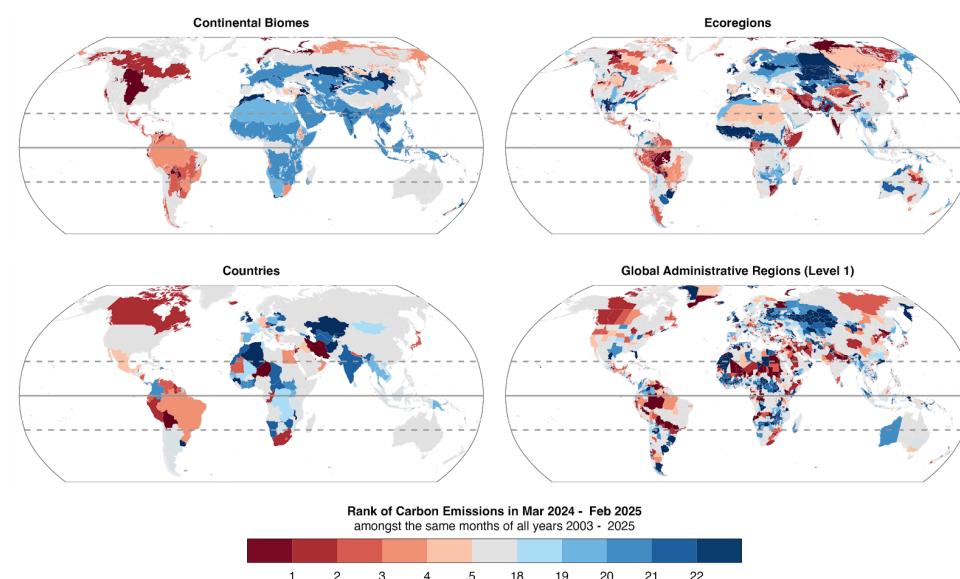


787

788 **Figure 1:** Anomalies in burned area (BA) and carbon (C) emissions for selected continental  
789 biomes in the 2024-25 global fire season (March 2024-February 2025), versus the average  
790 of prior fire seasons since 2002. The selected regions all experienced BA anomalies of over  
791  $\pm 20$  thousand km<sup>2</sup> or C emissions anomalies over  $\pm 30$  Tg C during the 2024-25 global fire  
792 season. Relative changes (%) are also marked by triangular symbols and can be read on the  
793 secondary axis.



794  
795 **Figure 2:** Ranks of BA during March 2024–February 2025 versus previous March–February  
796 periods ( $n = 23$  global fire seasons), at the scales of **(top left)** continental biomes, **(top**  
797 **right)** ecoregions, **(bottom left)** countries and **(bottom right)** level 1 administrative regions.  
798 Results for regions with high-ranking (top 5 years) or low-ranking (bottom 5 years) events  
799 are highlighted. The timing of BA anomalies is shown in **Figure S4**.  
800



801  
802 **Figure 3:** Rank of fire C emissions during March 2024–February 2025 versus all  
803 March–January periods since 2003 ( $n = 22$  global fire seasons), at the scales of **(top left)**  
804 continental biomes, **(top right)** ecoregions, **(bottom left)** countries and **(bottom right)** level  
805 1 administrative regions. We consider C emissions estimates from two products (GFAS and



806 GFED), first calculating the mean emissions value from the two products, then ranking the  
 807 values.

808

809 **Table 2:** Summary of the largest positive anomalies in burned area (BA) during the 2024-25  
 810 fire season on national and sub-national scales. Anomalies are expressed relative to all  
 811 previous fire seasons 2002-2024 ( $n = 23$ ). The table includes the top ten countries ranked by  
 812 the magnitude of their absolute BA anomalies and the top 30 level 1 administrative regions  
 813 (e.g. states or provinces) grouped into countries where applicable. Extended data for all  
 814 countries and region layers are available from Jones et al. (2025).

Region Name	BA during the 2024-25 fire season (thousand km <sup>2</sup> )	Absolute BA anomaly (thousand km <sup>2</sup> )	Relative BA Anomaly (%)	Ranking of the 2024-25 fire season
<b>Bolivia</b>	<b>107</b>	<b>+67</b>	<b>+169</b>	<b>1</b>
Santa Cruz (Department of Bolivia)	65	+49	+311	1
Beni (Department of Bolivia)	36	+15	+74	4
<b>Brazil</b>	<b>243</b>	<b>+59</b>	<b>+32</b>	<b>3</b>
Mato Grosso (State of Brazil)	68	+22	+49	4
Pará (State of Brazil)	36	+20	+119	1
Mato Grosso do Sul (State of Brazil)	23	+11	+90	2
Amazonas (State of Brazil)	9	+6	+254	1
São Paulo (State of Brazil)	10	+4	+67	4
<b>Canada</b>	<b>46</b>	<b>+21</b>	<b>+86</b>	<b>2</b>
Northwest Territories (Territory of Canada)	16	+12	+281	3
British Columbia (Province of Canada)	8	+5	+154	4
Alberta (Province of Canada)	7	+4	+123	2
<b>Venezuela</b>	<b>43</b>	<b>+15</b>	<b>+52</b>	<b>2</b>
Apure (State of Venezuela)	16	+5	+41	2
Bolívar (State of Venezuela)	6	+3	+133	1
<b>Niger</b>	<b>13</b>	<b>+10</b>	<b>+257</b>	<b>1</b>
Tahoua (Department of Niger)	5	+4	+967	1
<b>Burkina Faso</b>	<b>33</b>	<b>+9</b>	<b>+39</b>	<b>5</b>
Sahel (Region of Burkina Faso)	6	+6	+1226	1
<b>Angola</b>	<b>374</b>	<b>+9</b>	<b>+2</b>	<b>8</b>
Moxico (Province of Angola)	61	+8	+15	3
Huíla (Province of Angola)	20	+6	+49	1
Cunene (Province of Angola)	18	+5	+35	5
Bié (Province of Angola)	20	+4	+25	1
<b>Congo (Republic of the)</b>	<b>41</b>	<b>+8</b>	<b>+25</b>	<b>1</b>
<b>Sudan</b>	<b>82</b>	<b>+8</b>	<b>+11</b>	<b>8</b>
North Darfur (State of Sudan)	15	+9	+168	1
<b>Mali</b>	<b>77</b>	<b>+7</b>	<b>+10</b>	<b>6</b>
Gao (Region of Mali)	13	+12	+1383	1
<b>Other</b>				
Queensland (State of Australia)	100	+19	+24	5
Heilongjiang (Province of China)	23	+14	+164	2
Zabaykal'ye (Territory of Russia)	23	+11	+88	3
North-Western (Province of Zambia)	45	+10	+29	1
Sakha (Republic of Russia)	27	+9	+55	6
Amur (Region of Russia)	20	+8	+70	4
Zamfara (State of Nigeria)	9	+5	+95	4
Oregon (State of United States)	7	+5	+285	1
Jilin (Province of China)	7	+4	+186	4
Sankuru (Province of Dem. Rep. Congo)	11	+4	+58	1

815





**Table 3:** Summary of the largest positive anomalies in carbon (C) emissions during the 2024-25 fire season on national and sub-national scales. Anomalies are expressed relative to all previous fire seasons 2003-2024 (n = 22). The table includes the top ten countries ranked by the magnitude of their absolute C emissions anomalies and the top 30 level 1 administrative regions (e.g. states or provinces) grouped into countries where applicable. Extended data for all countries and region layers are available from Jones et al. (2025).

Region Name	C emitted during the 2024-25 fire season (Tg C)	Absolute C emissions anomaly (Tg C)	Relative C emissions Anomaly (%)	Ranking of the 2024-25 fire season
<b>Canada</b>	<b>282</b>	<b>+189</b>	<b>+204</b>	<b>2</b>
Northwest Territories (Territory of Canada)	104	+85	+441	2
Alberta (Province of Canada)	56	+42	+297	2
British Columbia (Province of Canada)	55	+36	+196	2
Saskatchewan (Province of Canada)	43	+28	+184	3
Manitoba (Province of Canada)	11	+5	+74	4
<b>Bolivia</b>	<b>187</b>	<b>+148</b>	<b>+383</b>	<b>1</b>
Santa Cruz (Department of Bolivia)	157	+136	+637	1
Beni (Department of Bolivia)	23	+11	+86	3
La Paz (Department of Bolivia)	4	+2	+79	4
<b>Brazil</b>	<b>314</b>	<b>+111</b>	<b>+55</b>	<b>4</b>
Mato Grosso (State of Brazil)	86	+29	+50	6
Amazonas (State of Brazil)	35	+25	+237	1
Mato Grosso do Sul (State of Brazil)	30	+23	+323	1
Pará (State of Brazil)	59	+22	+61	4
Tocantins (State of Brazil)	22	+5	+33	5
São Paulo (State of Brazil)	8	+5	+190	1
Rondônia (State of Brazil)	22	+3	+16	7
Roraima (State of Brazil)	5	+2	+81	5
<b>Venezuela</b>	<b>26</b>	<b>+8</b>	<b>+47</b>	<b>3</b>
Bolívar (State of Venezuela)	5	+2	+97	1
<b>Mexico</b>	<b>29</b>	<b>+6</b>	<b>+26</b>	<b>5</b>
<b>South Africa</b>	<b>18</b>	<b>+3</b>	<b>+24</b>	<b>2</b>
<b>Angola</b>	<b>146</b>	<b>+3</b>	<b>+2</b>	<b>9</b>
Moxico (Province of Angola)	28	+5	+21	3
Bié (Province of Angola)	9	+2	+35	1
Huíla (Province of Angola)	7	+2	+37	1
<b>Peru</b>	<b>7</b>	<b>+2</b>	<b>+51</b>	<b>2</b>
<b>Russian Federation</b>	<b>179</b>	<b>+2</b>	<b>+1</b>	<b>9</b>
Sakha (Republic of Russia)	75	+32	+74	3
Zabaykal'ye (Territory of Russia)	31	+14	+78	4
Amur (Region of Russia)	25	+8	+46	5
Arkhangel'sk (Region of Russia)	2	+2	+1776	1
<b>Congo (Republic of the)</b>	<b>10</b>	<b>+2</b>	<b>+24</b>	<b>2</b>
<b>Other</b>				
Queensland (State of Australia)	31	+4	+14	7
Oregon (State of United States)	7	+4	+130	3
Idaho (State of United States)	5	+3	+139	3
North-Western (Province of Zambia)	22	+2	+12	1
Alto Paraguay (Department of Paraguay)	6	+2	+55	2
Mai-Ndombe (Province of Dem. Rep. Congo)	7	+2	+36	1



### 823 2.2.1.2. *An Unprecedented Fire Season in South America*

824

825 There were pronounced and widespread positive anomalies in BA in 2024-25 across South  
 826 America during 2024-25 (**Figure 1, Figure 2**). Several South American biomes experienced  
 827 extremely high or even record-setting BA in the 2024-25 fire season (**Figure 1**). The South  
 828 American (sub)tropical dry broadleaf forests, principally comprising the Chiquitano and  
 829 Chaco dry forests, experienced a record-breaking fire season, with the 42 thousand km<sup>2</sup>  
 830 burned exceeding the average since 2002 by a factor of 3.6 and the 100 Tg C emitted  
 831 exceeding the average since 2003 by a factor of 6. In the South American (sub)tropical moist  
 832 broadleaf forests, principally comprising the Amazon rainforest, BA was 47 thousand km<sup>2</sup>  
 833 (75%) above the average since 2002, which is the second-highest year on record, and C  
 834 emissions were correspondingly 76 Tg C (58%) above average. Finally, in the South  
 835 American Flooded grassland and savannah biome, which principally includes the seasonally  
 836 inundated Pantanal region, BA was 26 thousand km<sup>2</sup> (119%) above the average since 2002,  
 837 which is also the second-highest year on record, and C emissions were correspondingly 67  
 838 Tg C (397%) above average. Across South America as a whole, BA was 120 thousand km<sup>2</sup>  
 839 (35%) above average and C emissions were 263 Tg C (84%) above average, producing the  
 840 highest C emissions total on record for the continent.

841

842 The spatial breadth of the record-setting or high-ranking anomalies in fire extent, emissions,  
 843 size, rate or spread and intensity (**Figure 2, Figure 3, Figure 4**), as well as their impact on  
 844 society and the environment, made the last fire season unprecedented on the continent.  
 845 **Appendix A (Section A6)** discusses the unprecedented South American fire season of  
 846 2024-25 in greater detail, including its impacts and regional context, relying also on  
 847 information from regional fire monitoring systems and reporting.

848

849 Fifteen of South America's 115 ecoregions experienced new record levels of BA or C  
 850 emissions during 2024-25 (**Figure 2, Figure 3**) and 72 of South America's ecoregions  
 851 experienced BA or C emissions in the top three years on record (**Figure 2, Figure 3**).  
 852 Regions with record levels of BA or C emissions included the Chiquitano dry forests and the  
 853 Pantanal wetlands of Bolivia and central-west Brazil. In nearby southern and southwestern  
 854 parts of Amazonia, five moist forest and seasonally flooded (várzea) ecoregions also  
 855 showed record-breaking BA or C emissions. The widespread positive BA anomalies in  
 856 southern and southwest Amazonia, the Chiquitano and the Pantanal were visible in the  
 857 MODIS BA dataset from March and April 2024, peaking in August-November 2024 before  
 858 subsiding around November (**Figure S4**). In the Guianan shield region, encompassing much  
 859 of Northeast Amazonia (north of the Amazon river and the Rio Negro tributary) and the  
 860 Guianan forests of Venezuela, Guyana, and Suriname, four moist forest and swamp forest  
 861 ecoregions also experienced record-breaking levels of BA or C emissions (**Figure 2, Figure**  
 862 **3**). Here, BA anomalies peaked around March-April before subsiding in May in northern  
 863 parts but persisted through to December in areas closer to the equator (**Figure S4**).

864

865 At the national level within South America, the most significant anomalies in BA during the  
 866 2024-25 fire season occurred in Bolivia, where BA was 67 thousand km<sup>2</sup> (169%) above  
 867 average and fire C emissions were 148 Tg C (383%) above average, the greatest values on  
 868 record in the country (**Figure 2, Figure 3; Table 2, Table 3**). In Brazil, BA was 59 thousand  
 869 km<sup>2</sup> (32%) above average and emissions were 111 Tg C (55%) above average during  
 870 2024-25, making it the country's third highest fire season on record for BA after 2007-08 and  
 871 2010-11. Additionally, Venezuela recorded an anomaly of +15 thousand km<sup>2</sup> (+52%), its  
 872 second-highest BA total after 2023-24. Anomalies in these three countries are highlighted  
 873 due to global totals of BA and C emissions (**Table 2, Table 3**). On sub-national scales, the  
 874 2024-25 fire season saw record-breaking BA or C emissions in four states of Brazil (Pará,  
 875 Amazonas, Mato Grosso do Sul, and São Paulo), one department of Bolivia (Santa Cruz), 3  
 876 States of Venezuela (Bolívar, Delta Amacuro, Monagas). Other record-breaking anomalies  
 877 were seen at sub-national levels across South America (**Figure 2, Figure 3**), including in 6



regions of Guyana, 7 regions of Peru, 2 districts of Suriname, 8 provinces of Ecuador, as well as some parts of Chile and Colombia (**Figure 2**, **Figure 3**), clearly signalling the large geographical breadth of the extremes on the continent during the 2024-25 fire season.

For most regions of South America, the anomalies in BA and C emissions were explained by particularly large, fast moving and intense fires, rather than above-average fire counts (**Figure 4**). In Brazil, data on individual fire characteristics from the Global Fire Atlas showed new record fire sizes at the 95th percentile threshold for 6 states (Amapá, Mato Grosso, Mato Grosso do Sul, Paraná, Rondônia, and São Paulo). In Mato Grosso, Mato Grosso do Sul, and São Paulo, 95th percentile fire sizes were 105-266% above average, driving record breaking BA despite fire counts being 18-54% below average. Meanwhile, three states (Mato Grosso, Mato Grosso do Sul, and São Paulo) all saw the fastest rates of growth at the 95th percentile threshold, and 5 states (Mato Grosso do Sul, Paraná, Rio de Janeiro, Roraima, and São Paulo) experienced the most intense fires on record (measured per the average fire's 95th percentile intensity value; **Figure 4**). Unlike in other parts of Brazil, the fire count anomaly (+154%) was record-breaking in Amazonas during 2024-25, combining with the 95th percentile fire size anomaly (+60%) to produce the record-breaking BA. Similar patterns were observed across South America, with anomalies in fire size, rates of growth, and intensities generally being more widespread than anomalies in fire count (**Figure 4**). Some notable exceptions were 5 regions of Peru, 5 regions of Ecuador, 3 regions of Colombia, and 3 regions of Guyana, where record-setting fire counts were observed, as well as in parts of Venezuela where high-ranking fire counts occurred (**Figure 4**).

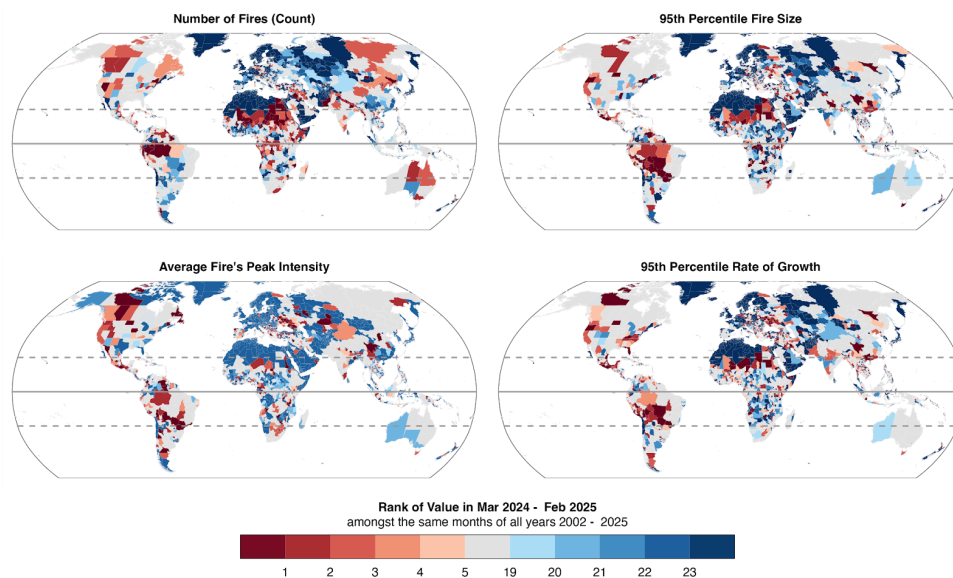


**Figure 4:** Ranks of selected individual fire properties during the March 2024-February 2025 fire season versus previous March-February periods ( $n = 23$  global fire seasons), including (top left) fire count, (top right) 95th percentile fire size, (bottom left) the average value of a the peak intensity (95th percentile FRP within fire perimeters) considering all regional fires, and (bottom right) 95th percentile daily rate of growth. Results are shown at the scale of states or provinces (GADM administrative level 1 regions).



### 909 2.2.1.3. *A Second Consecutive Extreme Fire Year in North America*

910 The 2024-25 fire season was the second-highest fire year on record for BA and C emissions  
 912 in the North American boreal forests, with BA 86% above the average since 2002 (+20  
 913 thousand km<sup>2</sup>) and C emissions 3 times the average since 2003 (+168 Tg C). These large  
 914 anomalies follow the record-breaking 2023-24 fire season when BA was five times above  
 915 average and C emissions were seven times above average, marking two consecutive years  
 916 of extreme fire activity in the North American boreal forests. Elsewhere, BA extent was in the  
 917 top three years on record in the North American (sub)tropical moist broadleaf forest  
 918 (concentrated in Latin America), and in the North American mediterranean forests,  
 919 woodlands and scrub (concentrated in Southern California). Across North America as a  
 920 whole, BA was 31 thousand km<sup>2</sup> (35%) above average and C emissions were 194 Tg C  
 921 (112%) above average, the second highest totals on record for both metrics.

922  
 923 Eleven of North America's 189 ecoregions experienced new record levels of BA or C  
 924 emissions during 2024-25 (**Figure 2, Figure 3**), with these regions principally concentrated  
 925 in northwest Canadian taiga and tundra, mountain forests of the northwest US and  
 926 southwest Canada (principally in Oregon and Alberta), and moist tropical forest ecoregions  
 927 of mesoamerica (principally in Mexico), but also including the Central Valley grasslands of  
 928 California and the northeast coastal forests of the US. More broadly, but with a similar  
 929 geographical distribution, 44 North American ecoregions experienced BA or C emissions in  
 930 the top three years on record (**Figure 2, Figure 3**). The positive BA anomalies in  
 931 extratropical North America were visible in the MODIS BA dataset from April 2024 in western  
 932 regions (e.g. mountain forests of the northwest US and southwest Canada), July-August  
 933 2024 in the central regions (e.g. Canadian tundra and taiga), and late into the 2024 summer  
 934 in eastern regions (e.g. northeast coastal forests; **Figure S4**). Thereafter, BA anomalies  
 935 were consistently observed through summer (July-September 2024) and in some cases  
 936 persisted through October 2024.

937  
 938 In Canada, BA was 21,000 km<sup>2</sup> (86%) above average and C emissions were 189 Tg C  
 939 (204%) above average during 2024-25, marking the country's second highest fire season on  
 940 record immediately following the record-breaking fire season of 2023-24 (**Figure 2, Figure**  
 941 **3; Table 2, Table 3**). Notably, the anomalies of 2024-25 were concentrated in the western  
 942 Canadian states of British Columbia, Alberta and northwest Territories which all saw the  
 943 second-highest BA or C emissions on record, with large anomalies in the range of  
 944 120-440%, second only to the 2023-24 fire season. More generally, record levels of BA or C  
 945 emissions were less spatially extensive in North America than in South America, though the  
 946 US states of Oregon, Wyoming, and New York saw record BA, as did several mesoamerican  
 947 states of Mexico, Guatemala, and Costa Rica (**Figure 2, Figure 3**).

948  
 949 For western Canada, individual fire metrics from the Global Fire Atlas were also anomalous  
 950 and highly-ranked amongst previous years, but generally fell short of the records set in the  
 951 2023-24 fire season (**Figure 4**). For example, fire counts were 170-190% above average in  
 952 Alberta and British Columbia, ranked second (behind 2023-24), whereas anomalies in 95th  
 953 percentile fire size and rate of growth were not particularly large. Meanwhile, the explanation  
 954 for the anomalous BA in some states of the northwest US was not consistent, with some  
 955 states experiencing above-average fire counts, some experiencing above-average fire sizes,  
 956 but few experiencing both.

957  
 958 **Appendix A (Section A4)** provides a more complete summary of the fire season in North  
 959 America based on the regional panel assessment.

960



#### 961 **2.2.1.4. A Mixed Picture in Africa**

962  
 963 For the second consecutive year, BA was around 290 thousand km<sup>2</sup> (12%) below the  
 964 average of previous fire seasons in the African (sub)tropical grassland, savannah and  
 965 shrubland biome, and the 3rd lowest on record (**Figure 2**), but still contributed 56% towards  
 966 the global BA total and 86% towards total BA in Africa. BA anomalies in the African  
 967 savannahs have a significant influence on the continental BA anomalies, and indeed BA  
 968 across Africa as a whole was 313 thousand km<sup>2</sup> (12%) below average.

969  
 970 Despite the low fire activity in Africa during 2023, several exceptions emerged in both central  
 971 and northern Africa. Record levels of BA were observed in several parts of the Congo Basin  
 972 (**Figure 2, Figure 3**) due to an unusually high number of fires (**Figure 4**). BA in the Republic  
 973 of Congo was 25% above average, the highest on record, and similarly fire C emissions  
 974 were 25% above average (**Table 2, Table 3**). In the Democratic Republic of the Congo, the  
 975 Mai-Ndombe and Sankuru provinces each experienced record levels of BA or fire C  
 976 emissions with anomalies in the range of 36-58% (**Table 2, Table 3**). These anomalies were  
 977 centred on several western ecoregions of the Congo Basin, including the Atlantic Equatorial  
 978 coastal forests where BA was more than triple the annual mean, Western Congolian swamp  
 979 forests where BA was twice the annual average and the Central Congolian lowland forests  
 980 where BA was 77% above average, and the Northwestern Congolian lowland forests where  
 981 BA was 55% above average.

982  
 983 Likewise, several northern regions of Angola experienced record BA (**Figure 2, Figure 3**,  
 984 **Table 2, Table 3**). In northern Africa, Mali, Niger, Chad and Sudan all saw high BA in various  
 985 states or regions that encompass the semi-arid Sahel region, though these anomalies  
 986 notably occur against a low baseline in most cases due to the typically sparse vegetation  
 987 fuel loadings in such regions. **Appendix A (Section A1)** provides a more complete summary  
 988 of the fire season in Africa based on the regional panel assessment.

#### 989 990 **2.2.1.5. A Low Fire Year in Eurasia**

991  
 992 Asian and European biomes generally experienced a low fire year that contributed towards  
 993 the below-average global BA total in 2024-25 (**Figure 1, Figure 2**). BA was around 50  
 994 thousand km<sup>2</sup> (71%) below average in the Asian temperate grassland, savannah and  
 995 shrubland biome, 42 thousands km<sup>2</sup> (62%) below average in the Asian xeric shrublands, and  
 996 9 thousand km<sup>2</sup> (11%) below average in the Asian (sub)tropical broadleaf forests. The  
 997 below-average fire extent in all of these regions translated into below-average C emissions,  
 998 though not in direct proportion because the combustion of vegetation per unit BA also varied  
 999 compared with previous years (**Figure 1**). For example, while BA was 11% below average in  
 1000 the Asian (sub)tropical broadleaf forests, C emissions were 54% (85 Tg C) below average  
 1001 signifying that areas that did burn tended to do so with anomalously low severity. Across  
 1002 Asia as a whole, the total BA was 99 thousand km<sup>2</sup> (26%) below average during 2024-25,  
 1003 the 4th lowest annual total on record, and C emissions were 119 Tg C (28%) below average,  
 1004 the 5th lowest on record.

1005  
 1006 While most regions of Asia experienced a low fire year in general, there were some notable  
 1007 exceptions. Many states of northeast India and Nepal experienced high-ranking or  
 1008 record-breaking levels of BA or C emissions (**Figure 2, Figure 3**), highlighting a coherent  
 1009 regional-scale anomaly during 2024-25. Similarly, in northeast Asia where 2 provinces of  
 1010 China (Heilongjiang and Jilin; **Table 2**), 2 provinces of South Korea, and 7 prefectures of  
 1011 Japan experienced record-breaking BA or C emissions and many neighbouring regions  
 1012 likewise experienced high-ranking fire years (**Figure 2, Figure 3**). **Appendix A (Section A2)**  
 1013 provides a more complete assessment of the fire season in Asia.

1014





1015 Though less impactful on the global BA and C emissions totals than in the vast Asian  
1016 biomes, the 2024-25 fire season was notably another low fire year in Europe. For example,  
1017 BA was 13 thousand km<sup>2</sup> (59%) below average in the European temperate broadleaf and  
1018 mixed forests, 12 thousand km<sup>2</sup> (40%) below average in the European temperate grassland,  
1019 savannah and shrubland biome. Across Europe as a whole, the total BA was 30 thousand  
1020 km<sup>2</sup> (49%) below average during 2024-25, the 4th lowest annual total on record, and C  
1021 emissions were 5 Tg C (22%) below average, the 7th lowest on record.

1022

1023 Despite the low fire activity in Europe, there were several exceptions in southeast Europe. In  
1024 regions of Serbia, North Macedonia, and western Turkey experienced record high BA or C  
1025 emissions in 2024-25. Further north, several eastern regions of Ukraine experienced  
1026 record-breaking fire C emissions, with some suggesting a link between elevated ignitions  
1027 and the ongoing conflict in the country (European Commission Joint Research Centre,  
1028 2025). **Appendix A (Section A3)** provides a more complete assessment of the fire season  
1029 in Europe based on regional panel assessment.

1030

#### 1031 2.2.2. Focal Events of this Report

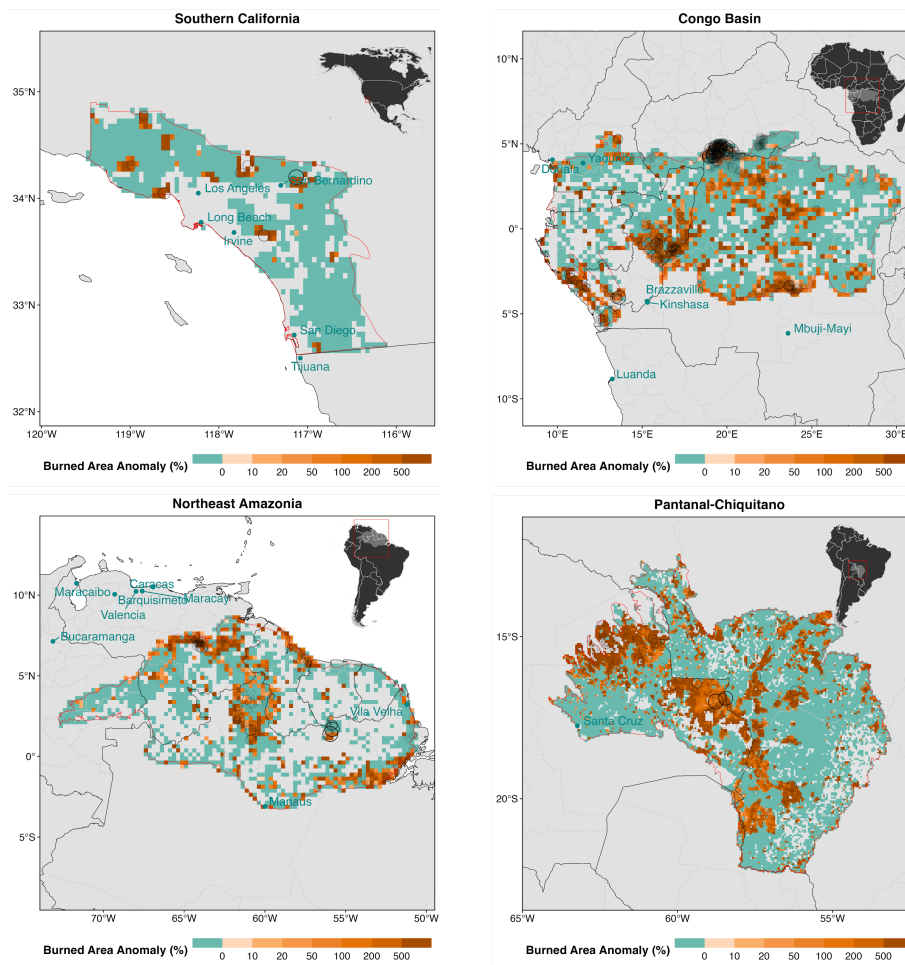
1032

1033 In this year's report, we identify four focal events with global relevance for further study  
1034 across **Sections 4-6**. The four events are Northeast Amazonia, the Pantanal-Chiquitano,  
1035 Southern California, and the Congo Basin (**Figure 5**), and our reasons for selecting these  
1036 particular events are detailed below. In **Sections 4-6**, our analyses explain the causes of  
1037 each of the events (**Section 4**), evaluate the predictability of the events (**Section 4**), attribute  
1038 the events to climate change and land use factors (**Section 5**), and predict the likelihood of  
1039 similar events under future climate change scenarios (**Section 6**).

1040



1041



1042

1043

1044 **Figure 5:** Spatial distribution of burned area (BA) anomalies during 2024-25 relative to the  
1045 mean annual BA (%). BA is shown at 0.25° resolution (Northeast Amazonia and Congo  
1046 Basin) or 0.05° resolution (Pantanal and southern California). Fire ignition points (open  
1047 circles) from the Global Fire Atlas are also shown for the fires with sizes in the upper quartile  
1048 regionally during 2002-2025, with the largest fires for each region displaying as the largest  
1049 and most visible circles.

1050

#### 1051 2.2.2.1. Northeast Amazonia (January-March 2024)

1052

1053 The Northeast Amazonia region here refers to the moist tropical forest ecoregions northeast  
1054 of the Amazon river and the Rio Negro tributary, mostly including Amazonia but also  
1055 including the Guianan Shield forests that extend into Venezuela, Guyana, Suriname, and  
1056 French Guiana (**Figure 5**). We specifically target the period January-March 2024. In this  
1057 region, as in other parts of the northern hemisphere tropics, our global March-February fire  
1058 season definition can be misaligned with local fire seasonality, specifically where fire  
1059 seasons span two calendar years. Although this event straddles the boundary between the  
1060 2023-24 and 2024-25 fire seasons, we include it here to ensure that significant fire activity is  
1061 not excluded solely due to the constraints of our reporting framework. **Section 2.2.1**



discusses the regional anomalies that led this region to be identified (e.g. **Figure 2, Figure 3**), with further review of the fire season provided by our expert panel in **Appendix A (Section A6)**. It emerges as a major event of global relevance for the following reasons:

- **Record-breaking burned area in forests:** The area of forest burned was more than four times (+332%) the average, and the highest on record, while total BA (including non-forests) was also 67% above average. In forests, 8 continuous months of the fire season (March-September 2024) had BA above the climatological mean, peaking in March 2024. The most pronounced anomalies occurred in the Northern Amazonian savannas around Roraima, the forest-savanna transition zones of northern Venezuela and southern Guyana, and the coastal ecosystems near the Guyana-Suriname border (**Figure S5**).
- **Carryover from the previous fire season:** A new record for total BA had been set in the previous fire season (2023-24) mostly due to an anomalously high count of large fires in non-forests. The transition of anomalously high fire activity into forest environments during the 2024-25 fire season was a distinguishing factor.
- **Anomalous fire counts:** The large BA anomalies were explained by an anomalously high number of fires, with 1,500 (52%) more fires than the average fire season.
- **Widespread forest loss:** Highest rates of forest loss (stand-replacing fire extent) since 2016 recorded in Amazonia with 60% attributed to wildfires.
- **Disproportionate impact on rural, traditional populations and Indigenous territories:** Fires degraded air quality and destroyed crops, homes, and native vegetation, intensifying food and water insecurity for those living in the region, including Indigenous peoples. The compounded effects of fire and drought deepened the humanitarian crisis in the Yanomami Territory and local organizations estimate at least 70,000 people across urban and rural areas without access to clean water.

#### 2.2.2.2. *Pantanal and Chiquitano (August-September 2024)*

The Pantanal-Chiquitano region here refers to the areas draining into the Pantanal (IBGE, 2021), the world's largest tropical wetland area, and the Chiquitano dry forest ecoregion in Bolivia (**Figure 5**). We specifically target the period January-March 2024, when the most substantial anomalies in BA were observed (**Figure S6**). **Section 2.2.1** discusses the regional anomalies in Brazil and Bolivia that led this region to be identified (e.g. **Figure 2, Figure 3**), with further review of the fire season provided by our expert panel in **Appendix A (Section A6)**. It emerges as a major event of global relevance for the following reasons:

- **Record-Breaking burned area:** BA in the Pantanal-Chiquitano region was almost triple (+196%) the annual average, and the highest on record. This anomaly included a +466% BA anomaly in forests. There were 8 continuous months (March-October) with BA above the climatological mean, oriented around a peak in August 2024.
- **Record-Breaking carbon emissions:** Fire C emissions were 6 times (+502%) the annual mean, driven up by the large anomaly in forest fire C emissions in the period.
- **Record fire size and spread:** The 95th percentile fire size for the region was over three times (+226%) the average and the 95th percentile rate of growth was 88% above average, signifying that large, fast-spreading fires drove up the anomalous BA total in the region.
- **Severe air quality degradation:** Over 900  $\mu\text{g}/\text{m}^3$  of fine particulate matter ( $\text{PM}_{2.5}$ ) was recorded in September 2024, which is 60 times above WHO standard.
- **Economic losses:** Agribusiness losses due to wildfires reached R\$ 1.2 billion (~US\$222 million) in the Pantanal, the biome's main economic sector.
- **Challenges in response:** 78 days of firefighting effort which involved multiple actors was marked by significant access and logistical challenges in remote regions, making it difficult to reach and support isolated communities.



### 1115 2.2.2.3. *Southern California (January 2025)*

1116  
 1117 Southern California here refers to the Mediterranean portions of seven counties in California  
 1118 (Los Angeles, Orange, Riverside, San Bernardino, San Diego, Santa Barbara, and Ventura;  
 1119 **Figure 5**). The Mediterranean portions are defined based on the ecoregional definition of the  
 1120 US Environmental Protection Agency (EPA, 2024). Although California as a whole did not  
 1121 experience a particularly strong fire season in 2024-25 from the vantage of BA or fire C  
 1122 emissions (e.g. **Figure 2**, **Figure 3**), the regional expert panel identified the numerous  
 1123 wildfires affecting LA and surrounding counties in January 2025 as a major event of the  
 1124 2024-25 fire season (see **Appendix A Section A4**), with the Palisades and Eaton fires in  
 1125 particular leading to loss and damage in the suburbs of LA. We specifically target the period  
 1126 January 2025 when the most substantial anomalies were observed (**Figure S7**). Southern  
 1127 California emerges as a major event of global relevance for the following reasons:

- 1128 • **High fatalities and structure loss.** Over 11,500 homes were destroyed across Los  
 1129 Angeles County, and at least 30 lives were lost (Los Angeles County Coroner, 2025;  
 1130 Wikipedia, 2025). The Palisades Fire damaged or destroyed nearly 8,000 structures,  
 1131 while the Eaton Fire impacted over 10,000 structures (CALFIRE, 2025; Wikipedia,  
 1132 2025).
- 1133 • **Mass evacuations.** At least 153,000 people evacuated, with up to 200,000 under  
 1134 evacuation warnings or orders during the peak of the crisis (USGS, 2025b; NPR,  
 1135 2025; Wikipedia, 2025).
- 1136 • **Air quality impacts.** Air and municipal water quality were heavily impacted by the  
 1137 fires, contributing to negative health outcomes for thousands. During the fires, peak  
 1138  $PM_{2.5}$  levels were recorded at  $483\mu g/m^3$  (an order of magnitude greater than the  $35$   
 1139  $\mu g/m^3$  daily standard set by the US Environmental Protection Association), part of a  
 1140 prolonged period of Hazardous air quality (California Air Resources Board, 2025).
- 1141 • **Water quality impacts.** Municipal water supplies were considered unsafe for several  
 1142 weeks following the fires for tens of thousands of residents in the affected areas (City  
 1143 of Pasadena, 2025). In response to the fires outside Los Angeles, over 8.3 million  
 1144 cubic meters of water from federal reservoirs in central California, a move which has  
 1145 been criticised because this water did not supply southern California, happened well  
 1146 after the fires were controlled, and because it would otherwise have been used for  
 1147 irrigation in the Central Valley (Levin et al., 2025).
- 1148 • **Exceptional economic loss.** Total economic losses were estimated at US\$140B  
 1149 including property destruction, health costs, business disruption, and infrastructure  
 1150 impacts, making this one of the most costly wildfire events in US history (LAEDC,  
 1151 2025; UCLA Anderson School of Management, 2025).
- 1152 • **Wider economic disruption.** The fires are projected to cause US\$4.6-8.9 billion in  
 1153 lost economic output over five years, 25,000-50,000 job-years lost, and labour  
 1154 income reductions of US\$1.9-3.7 billion (LAEDC, 2025). The Palisades and Eaton  
 1155 fires affected almost 2,000 businesses (LAEDC, 2025). As LA is also the largest port  
 1156 on the US Pacific coast, the fires impacted broader supply chains that run through  
 1157 the port of LA (Terrill, 2025).
- 1158 • **High insured losses.** Industry estimates have placed insured losses in the range of  
 1159 to US\$20-75 billion (Li and Yu, 2025; Morningstar DBRS, 2025; Insurance Insider,  
 1160 2025), placing substantial additional stress on the already volatile home insurance  
 1161 market in California and on most global reinsurers.
- 1162 • **Housing and affordability crisis.** Thousands of affordable housing units were  
 1163 destroyed, worsening Southern California's housing shortage, displacing large  
 1164 numbers of lower-income residents, and exacerbating the problem of homelessness  
 1165 in the region (Mattson-Teig, 2025; Li and Yu, 2025; Booth, 2025). This triggered a  
 1166 ripple mass displacement into both surrounding communities and beyond in the  
 1167 months following the fires (NYT, 2025).



- **Debris flows.** The geology of southern California is highly conducive to erosion and debris flows after wildfires. Several debris flows following high-intensity rainfall events in the weeks after the fire produced further damage and required hundreds of additional evacuations in and near the affected areas (USGS, 2025a).

The fires in Southern California have already been subject to several detailed investigations, which found that the fires were driven by exceptionally late onset of winter rains that extended the fire season into January, unseasonably warm winter temperatures, fuel buildup from very wet conditions in the prior year to two, and powerful Santa Ana winds exceeding 130 km/h, creating extreme fire weather conditions that propelled fires to progress downhill from wildlands into the built environment and become an urban conflagration (Barnes et al., 2025; Garrett, 2025). The potential for extreme wildfires to develop under dry downslope winds was predicted several days in advance, including by the National Interagency Fire Center (NIFC), the National Weather Service (NWS), and the Storm Prediction Center (SPC; see summary by Wikipedia, 2025) as well as by specialist commentators (e.g. Swain, 2025).

#### 2.2.2.4. *Congo Basin (July-August 2024)*

The Congo Basin region here refers to the moist tropical forest ecoregions of equatorial Africa (**Figure 5**). **Section 2.2.1** discusses the regional anomalies that led this region to be identified (e.g. **Figure 2**, **Figure 3**), with further review of the fire season provided by our expert panel in **Appendix A (Section A6)**. It emerges as a major event of global relevance for the following reasons:

- **Record-breaking burned area:** Highest-ranked BA on record at 28% above the annual mean due to there being 4,000 (20%) more fires than in the average year. There were 7 continuous months with BA above the climatological mean. The largest fire anomalies were observed during July and August (**Figure S8**), especially in southern Democratic Republic of the Congo, northern Angola, and parts of the Republic of the Congo.
- **Unprecedented role of fire in primary forest loss:** Forest loss statistics from the recent Global Forest Watch report (Goldman et al., 2025) showed that wildfires were the dominant driver of a more than doubling (+150%) of rates of forest loss in the Republic of the Congo and the Democratic Republic of the Congo during 2024 versus 2023, representing the highest rates of primary forest loss since 2015.
- **Sparse reporting and poor media coverage:** Reporting on the occurrence, drivers, and consequences of fire is extremely sparse in this region, including by government agencies and the international and national news media. This demonstrates that extreme fire events in this region are often overlooked, making it an intriguing case study to investigate in this report.

### 3. **Impact Assessments**

In this edition of the report, we introduce new routine regional assessments of fire impacts on society in terms of population exposure to fire, physical asset exposure to fire, the exposure of carbon projects to fire, and the degradation of air quality through emissions of fine particulate matter (PM<sub>2.5</sub>). For our air quality analysis, estimates are generated for the focal events only (**Section 2.2.2**). In all other cases, estimates are provided for each of the regional layers detailed in **Table 1**, mirroring our approach to providing regional summaries of BA, C emissions, and individual fire properties (**Section 2.1.2**).



### 1217 **3.1. Methods**

1218

#### 1219 **3.1.1. Population Exposure Assessment**

1220

1221 Population exposure estimates are produced using the global risk assessment platform  
 1222 CLIMADA (Aznar-Siguan and Bresch 2019). CLIMADA has previously been validated and  
 1223 applied to systematically quantify exposed population to a variety of natural hazards globally,  
 1224 such as river floods (Kam et al. 2021) and tropical cyclones (Stalhandske et al., 2024; Kam  
 1225 et al. 2024). The BA hazard set is set up using the MCD64A1 MODIS BA product (Giglio et  
 1226 al. 2018). The original BA data are aggregated monthly on a regular grid with a resolution of  
 1227 150 arcsec and expressed as the fraction of total cell area burned. For the spatial distribution  
 1228 of exposed population, we use Gridded Population of the World (Doxsey-Whitfield et al.,  
 1229 2015), which is spatially reaggregated on the same grid as the hazard using the LitPop  
 1230 exposure layer (Eberenz et al. 2020). The population exposed to wildfires is estimated by  
 1231 multiplying the BA fraction (BA expressed as a fraction of burnable area) of each cell by the  
 1232 population present in each grid cell. As a complementary approximation to the main  
 1233 analysis, a single displacement share is derived by comparing population exposure  
 1234 estimates with reported displacement figures from the Internal Displacement Monitoring  
 1235 Center (IDMC, 2025), acknowledging that exposure only partially translates into impact.  
 1236 Event records are matched to BA observations following the methodology described in  
 1237 Riedel et al. (2025). We compute the ratio between recorded impacts and exposed values  
 1238 for each event and provide the median of these damage ratios across events.

1239

1240 The data produced using these methods are available from Steinmann et al. (2025).

1241

#### 1242 **3.1.2. Physical Asset Exposure Assessment**

1243

1244 Physical asset exposure estimates are produced using the global risk assessment platform  
 1245 CLIMADA (Aznar-Siguan and Bresch 2019). CLIMADA has previously been validated and  
 1246 applied to systematically quantify economic impacts resulting from exposure of physical  
 1247 assets to a variety of natural hazards globally (Stalhandske et al. 2024), including fires (Lüthi  
 1248 et al. 2021). The exposure layer LitPop (Eberenz et al. 2020) was used to spatially distribute  
 1249 national-scale macroeconomic indicators as a function of night light intensity (Román et al.  
 1250 2018) and population density (Doxsey-Whitfield et al., 2015) within national geographical  
 1251 domains. We disaggregate country-based produced capital estimates (World Bank, 2024c)  
 1252 for the year 2018 to approximate physical asset density in US dollars (US\$). Physical asset  
 1253 exposure to wildfires is estimated by multiplying the BA fraction of each cell by the physical  
 1254 asset totals present in each grid cell (analogous to our analysis of population exposure,  
 1255 **Section 3.1.1**). In addition to this analysis, a single overall loss fraction is provided  
 1256 recognising that exposure tends to overstate actual asset damage. This fraction is derived  
 1257 by comparing modelled exposure estimates with asset damages from wildfire events, as  
 1258 reported in the Emergency Events Database (EM-DAT; Delforge et al. 2025) maintained by  
 1259 the Centre for Research on the Epidemiology of Disasters (CRED). Event records are  
 1260 matched to BA observations following the methodology described in Riedel et al. (2025). We  
 1261 compute the ratio between recorded impacts and exposed values for each event and provide  
 1262 the median of these damage ratios across events.

1263

1264 The data produced using these methods are available from Steinmann et al. (2025).

1265

#### 1266 **3.1.3. Carbon Projects Exposure**

1267

1268 We estimated the exposure of carbon offset projects to fire by combining a large set (n=927)  
 1269 of project boundaries for forestry projects in Latin America (n=394), northern America  
 1270 (n=316), Eurasia (n=150), Africa (n=60), and Australasia (7) with information on fire and





climate. Project boundaries were sourced from BeZero Carbon Ltd., who have collated and digitised boundaries for all nature-based projects in the Voluntary Carbon Market (VCM). Information on annual BA was derived from the MCD64A1 collection 6.1 data (Giglio et al., 2018) and this was combined with information on land cover from MCD12Q1 collection 6.1 (Sulla-Menashe et al., 2019) to separate forest from non-forest fires. To evaluate drought conditions, we calculated the 12-month Standardized Precipitation Evapotranspiration Index (SPEI) using data from ERA5-Land (Muñoz-Sabater et al., 2021) calibrated over the 1980-2014 period.

We evaluated fire activity during the 2024 calendar year in the context of long-term trends in drought and fire risk. First, to assess how 2024 compared to previous years since 2001, we calculated the number of carbon projects affected by fire in each year and the average percentage of project area burned per year (%). Second, to place this in the context of climate change, we calculated the 2024 drought anomaly as the 2024 SPEI minus the long-term average SPEI (1980-2023).

#### 3.1.4. Air Quality Impact Assessment

The human health risks associated with fire smoke pollution are well established. Smoke contains a toxic mix of gases, including ozone and carbon monoxide, as well as fine particulate matter ( $PM_{2.5}$ ) that can carry heavy metals and environmentally persistent free radicals (Hamilton et al., 2021; Andreae, 2019; Fang et al., 2023). Even short-term exposure to these pollutants has been associated with increased risk of cardiovascular and respiratory illnesses, including asthma exacerbation, reduced lung function, and acute infections (Johnston et al., 2021; Xu et al., 2024; Chen et al., 2021; Xu et al., 2023; Aguilera et al., 2021; Zhang et al., 2025). Furthermore, wildfire smoke contributes to increased mortality, particularly among vulnerable populations. In addition to these physiological effects, heavy smoke can significantly reduce visibility, compounding health risks by increasing the likelihood of injuries during regular driving, evacuation, or emergency response (Gill and Britz-McKibbin, 2020), and generates lasting mental health effects amongst exposed or displaced communities (Humphreys et al., 2022).

To quantify the contribution of fires to degraded air quality we used the global model framework utilised by the Copernicus Atmosphere Monitoring Service (CAMS) to simulate concentrations of fine ( $<2.5 \mu m$  diameter) particulate matter ( $PM_{2.5}$ ; Peuch et al., 2022). One of the key objectives of CAMS is to monitor and forecast global atmospheric composition including smoke from vegetation fires. Fires in CAMS are prescribed by the Global Fire Assimilation System (GFAS; Kaiser et al., 2012), which calculates hourly estimates of biomass burning emissions by assimilating fire radiative power (FRP) observations from satellite-based sensors and by means of land cover-dependent conversion (FRP to dry matter) and emission factors (dry matter to emitted gas or aerosol species per biome) describing the rate at which about 40 smoke constituents are released into the atmosphere. This study uses GFAS version 1.4, which is the version used currently for the NRT production input of CAMS global and regional forecast services, plus some improvements that include the use of VIIRS FRP retrievals. Spurious FRP observations of no vegetation fire origin are filtered out in GFAS with a static map. GFAS ingests active fire information together with a characterization of its uncertainty, including an uncertainty component related to the satellite sensor detection limit and a solution for partial observational cloud coverage.

Simulations are run with the Integrated Forecasting System extended with modules of atmospheric composition (IFS-COMPO), which describe source, sink, and transport processes of the main reactive trace gases (Flemming et al., 2015; Huijnen et al., 2016) and aerosol species (Morcrette et al., 2009; Remy et al., 2022, 2024) and which, together with satellite observations, is at the core of the CAMS system for the global domain. Mass fluxes of atmospheric constituents from the surface into the atmosphere are either prescribed from



CAMS pre-compiled emissions inventories, with some aspects of on-line simulated temporal variability, as in the case of pollutants from the burning of fossil fuels for transportation and electricity, or estimated online at every time step in the IFS when strongly dependent on meteorological conditions as in the case of desert dust and sea salt aerosol and of biogenic fluxes of CO<sub>2</sub>. The resolution used is the current operational resolution of 40 km, with 137 vertical levels. GFAS biomass burning emissions are estimated at 0.1° resolution based on FRP observations from the MODIS sensor on both the Terra and Aqua satellites (Giglio et al., 2016) and from the VIIRS sensor on the Suomi NPP satellite (Csiszar et al., 2014). The vertical distribution of fire emissions within the simulation follows the GFAS IS4FIRES injection height estimation (Sofiev et al., 2012; Remy et al., 2017).

To isolate the contribution of extreme fire events to atmospheric PM<sub>2.5</sub> concentrations, two sets of forecast experiments are run for specific focal events using a similar assessment framework. In the first (“with local fires”), all emission sources of PM<sub>2.5</sub> were considered including those of anthropogenic, dust, biogenic and other natural origin. In the second (“no local fires”), biomass burning emissions from within the focal event are excluded. The difference in simulated PM<sub>2.5</sub> concentrations between the two runs then represents the fire contribution to PM<sub>2.5</sub> within the region.

After PM<sub>2.5</sub> concentrations had been simulated at a 3-hourly temporal, and 40 km spatial, resolution, we summarised the influence of fires in the region to a daily population-weighted mean PM<sub>2.5</sub> concentration at ground-level (in units of µg/m<sup>3</sup>) for each focal region. Population data for the year 2020 from the Gridded Population of the World (GPW) dataset version 4 (Doxsey-Whitfield et al., 2015) were used to weight the values of PM<sub>2.5</sub> concentration in each grid cell of the focal regions, producing a weighted mean value for PM<sub>2.5</sub> concentration for each simulated date. This process was repeated for each simulation (“with local fires” and “no local fires”), and daily differences between the simulations were used to assess the additional number of days with poor air quality caused by fires in the focal regions.

To illustrate the scale and intensity of wildfire smoke health-relevant exposure within the 2024-2025 fire season, total population-weighted PM<sub>2.5</sub> and the isolated contribution of fires to population-weighted PM<sub>2.5</sub> in a focal region are compared against the World Health Organisation 24-hour mean (15 µg/m<sup>3</sup>) standard for daily PM<sub>2.5</sub> exposure (WHO, 2021).

1359

## 1360 3.2. Results

1361

### 1362 3.2.1. Population Exposure

1363

During the 2024-25 fire season, we estimate approximately 100 million people to have been exposed to wildfires worldwide. Exposure was most pronounced across South and Southeast Asia, as well as Central and East Africa. At the country level, India and the Democratic Republic of the Congo show the highest numbers, with around 15 million people affected in each (Figure 6; Figure S9). Nigeria, China, Mozambique, and South Sudan also were also exposed substantially, each with more than 5 million people affected. At the subnational level, we estimate the highest population exposures in Uttar Pradesh State (India) with over 4.6 million people, Heilongjiang Province (China) with 3.7 million, and Punjab State (India) with 3.6 million exposed (Figure 6; Figure S9). Several provinces in the Democratic Republic of the Congo also exceed 2 million, illustrating how national-level exposure is often driven by a few highly affected administrative regions.

1375

Some of the countries with the most extreme anomalies in fire BA and C emissions, most notably Bolivia, Brazil, and Canada, accounted for only a small share of absolute global population exposure, and showed negative (Canada) to modest positive (e.g. Bolivia and Brazil) anomalies (Figure 6; Figure S9). This decoupling highlights the relevance of the



spatial distributions of both BA and population to population exposure, which might be low when extensive fires occur in remote places.

Several of the countries with the highest absolute exposures, such as in India and the Democratic Republic of the Congo, showed negative anomalies on a national level, related to the fact that fire-related population exposure in these regions is more recurrent. Nonetheless, on a subnational level, some regions of these countries show considerable positive anomalies, such as in India's Uttar Pradesh State where 4.6 million people were exposed (146% above average) and about half a million being exposed in the provinces Kasai-Central (+33%) and Kongo-Central (+27%) in the DRC.

Population exposure anomalies were also high in relative terms across parts of the Middle East and the Balkans (e.g. Jordan, Iran, Iraq, North Macedonia, Albania), the Andes region (e.g., Peru, Ecuador), the Northern coast of South America (Venezuela, Guyana, Suriname; broadly encompassing our focal region of Northeast Amazonia), and Central Sahel (e.g., Niger), as well as isolated cases such as Nepal and Iceland. For example, Jordan shows divergent anomalies in population exposure (+201%) resulting from large subnational regions of Balqa (+322%) and Irbid (+393%). These patterns of exposure mostly align with patterns in BA and carbon emissions (**Section 2**), in the Middle East and the the Balkans, Andes, Northern coast of South America and Central Sahel. Although the absolute number of people affected in some of these countries remains low, the relative anomaly marks a sharp departure from historical patterns.

It is important to distinguish between the exposed and affected population. Based on 521 events in the years 2008-2025 recorded by IDMC (2025), we estimate the damage ratio of exposed to displaced population to amount to 3.0%. While nearly 100 million people were exposed to wildfire activity in the 2024-25 season, only a small fraction - 20,046 people (IDMC, 2025) - were formally displaced (0.02%). Note, however, that this figure likely understates the true scale of disruption, as displacement records are incomplete. Many affected individuals may not be forced to leave their homes but still experience substantial short- and long-term consequences, including health burdens (Gould et al., 2024) and financial distress such as short-term earning disruptions (Borgschulte et al., 2024), increased missed mortgage payments (Ho et al., 2023), declines in property values (Huang and Skidmore, 2024), and lasting reductions in income later in life (Meier et al., 2025). Moreover, recent cases have emphasised that the number of people impacted by wildfire smoke can be many times higher than the number of people directly exposed to fire (Jones et al., 2024b; Kolden et al., 2024, 2025; Johnston et al., 2021). As such, these records should be viewed as a conservative lower bound on the broader human impacts of wildfire exposure.

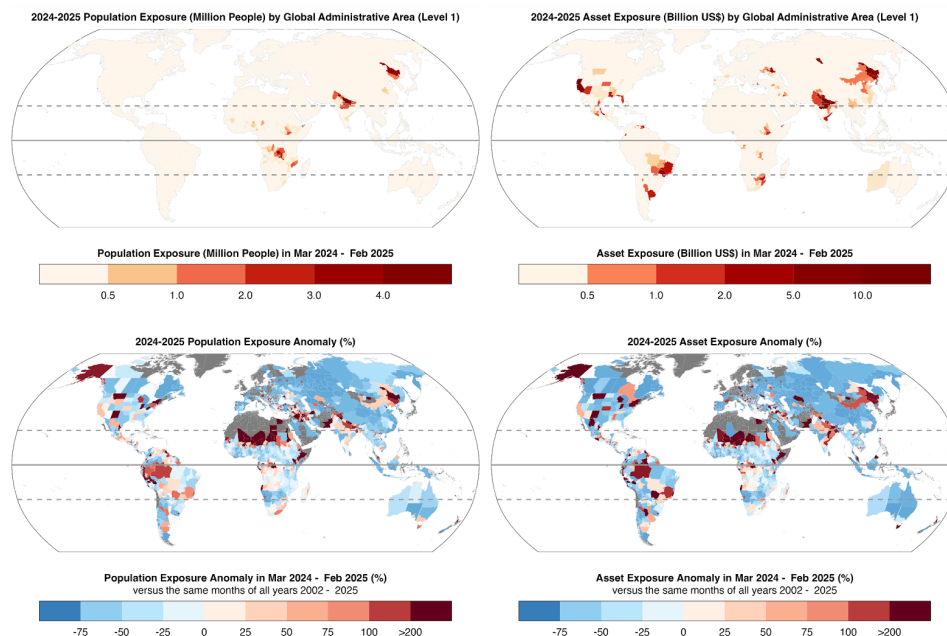


**Figure 6:** (left panels) Population and (right panels) physical assets exposed to burned area (BA) during the 2024-25 global fire season. The figure shows (top panels) the number of people or the asset value (billion US\$) exposed to fire and (bottom panels) the relative anomaly versus all years since 2002. Results are shown at the national scale in Figure S9.

### 3.2.2. Physical Asset Exposure

We estimate that physical assets exposed to wildfires during the 2024-25 season amounted to US\$215 billion worldwide. The highest asset exposures were concentrated in a mix of middle- and high-income countries, led by India (US\$44 billion), the United States (US\$26 billion) and China (US\$17 billion), followed by Venezuela, South Africa, and Brazil (Figure 6; Figure S9). While India, and to a lesser extent Brazil and China, ranked highly in both population and asset exposure, the asset exposure landscape broadens to include developed countries such as the United States and South Africa (US\$14 billion). This divergence not only reveals different spatial patterns of wealth and infrastructure but also the concentration of high-value assets in certain subnation regions (Figure 6; Figure S9). For instance, South Africa's Gauteng province, its economic hub, ranked among the most exposed globally at US\$8 billion, despite the country's moderate population exposure. Similarly, in the United States, California alone accounted for over US\$17 billion in exposed assets, driven largely by the severe January 2025 wildfires (US\$14 billion) discussed in Section 2.2.3. These estimates are still low in comparison to damage records provided by EM-DAT for the LA fires (US\$52.5 billion). This difference is likely caused by an underestimation of the affected exposure, which consisted of exceptionally high-value structures not represented by LitPop. This also explains the underestimation of the asset exposure anomaly in California, which is less pronounced (+60%) than in other states and regions of the world (Figure 6).

In contrast, Central African countries such as the Democratic Republic of the Congo, Nigeria, and Mozambique, which featured prominently in population exposure, did not rank highly in terms of exposed assets (Figure 6; Figure S9). The exception is South Sudan



(US\$4 billion), where asset exposure remains substantial. The data also highlights high absolute asset exposure in Mexico, Turkey, and the Russian Federation, each with national totals around US\$8 billion. At the subnational level, exposure was concentrated in economically important regions, including Izmir in Turkey (US\$3 billion), Mexico City (Distrito Federal; US\$3 billion), and Russia's Kemerovo and Rostov regions (approximately US\$3 billion each). These patterns underscore how wildfire-related asset exposure is shaped by the intersection of fire occurrence with concentrated infrastructure and economic activity.

Asset exposure anomalies for the 2024-25 fire season, expressed relative to the same months of all previous fire seasons from 2002-2024 ( $n = 23$ ), reveal several hotspots with unusually high physical asset exposure. Notable positive national-level anomalies were concentrated across the Middle East (e.g., Iraq, Syria), Southeast Europe and the Balkans (e.g., Albania, Bosnia and Herzegovina, Greece), parts of the Sahel and Horn of Africa (e.g., Niger, Eritrea), and the northern tropical of South America (e.g., Ecuador, Colombia, Guyana) (**Figure 6; Figure S9**). At the subnational level (**Figure 6; Figure S9**), pronounced relative anomalies were observed in regions not necessarily among the highest in absolute asset exposure. For example, many of the strongest asset exposure anomalies were highly localised, including regions of Chad, Sudan, Brazil, and Pakistan, where this season's values sharply deviate from past levels (**Figure 6; Figure S9**). In contrast, while California recorded the highest total asset exposure, its relative anomaly was modest, reflecting its regular exposure to fire. These spatial contrasts underscore that extreme fire seasons can affect both high-value regions and those with historically lower risk.

A comparison between asset exposure anomalies and BA anomalies (**Figure 6**) shows areas of both alignment and divergence. Overlaps are evident in Venezuela, western Brazil, Niger, and parts of India and Bolivia, where elevated fire activity coincided with high asset exposure. In contrast, strong BA anomalies in parts of equatorial Africa and Russia were not matched by anomalous asset exposure. This disconnect underscores that fire activity alone is not a sufficient proxy for physical asset impact. Rather, extensive burns in remote or forested areas may have limited consequences for built infrastructure, whereas smaller fires near wildland-urban interfaces can generate disproportionately high asset exposure (Calkin et al., 2023).

As with population exposure, asset exposure does not equate to realised impact. Comparing modelled exposed assets with reported EM-DAT figures, economic losses from 105 historic wildfire events in the time period 2002-2025 show a damage ratio of around 29% of exposed asset value. While a modelled US\$215 billion in physical assets were exposed to wildfires in 2024-25, a smaller sum of US\$57 billion in realised damages was recorded by EM-DAT, or around one-quarter of our exposure estimate. Note, that these figures reflect differences in scope and data quality. EM-DAT's total economic damage records may include indirect losses, such as business interruption and sectoral impacts. Its definition is broad, source-dependent, and rarely disaggregated. Thus, reporting is uneven and regionally biased due to variation in local capacity and data availability (Mazhin et al., 2021, Jones et al., 2023). In contrast, our modelled asset exposure offers a consistent estimate of physical assets at risk, representing the maximum potential asset loss. Yet, it does not represent realised or total economic damage. While both measures have limitations, together they help to characterise the scale of global wildfire-related economic impacts.

### 3.2.3. Carbon Projects Exposure

Forestry projects can provide cost effective climate mitigation and co-benefits to society and biodiversity, though their outcomes depend on complex interactions between project activities and their local ecological and social context (Holl and Brancalion, 2020). Wildfires present a growing threat to forest carbon offset projects, posing risks to the permanence of stored carbon (Anderegg et al., 2020) and thus credit integrity (Badgley et al., 2022) and the





financial viability of project activities (Conte and Kotchen 2010, Michaelowa et al., 2021). Forestry projects can focus on emissions avoidance (e.g. REDD+), emissions removal (e.g. afforestation or forest restoration), or a combination (e.g. improved forest management). Here we evaluate fire activity during the 2024 calendar year across an unprecedented number of forestry projects in the Voluntary Carbon Market (VCM), and place results in the context of long term trends in fire risk.

The 2024 fire season was characterized by anomalously high fire activity across the 927 projects evaluated. In total 169, or 18% of projects recorded BA in 2024, a record over the observational period (2001-2024) (Figure S10 (a)). This coincided with record annual BA with 1.6% of project areas affected on average (Figure S10 (b)). Regional drought extremes were likely responsible for the observed uptick in fire activity during 2024, with drought conditions in 72% of projects exceeding the long-term (1980-2023) average and, in 13% of projects, exceeding extreme (SPEI < -2) drought conditions (Figure S10 (c)).

Interestingly, observed anomalies vary regionally and further depend on project activities. Exceptional drought conditions in Latin America resulted in a record number of projects being affected by fire but total BA was just short of previous peak years. In this region, many projects focus on the avoidance of deforestation (38%), and in addition to climate, fire risk is driven by changing land cover and land use over time (Alencar et al., 2015). In comparison, in northern America a smaller number of projects are prone to fire annually and the majority (93%) of projects focus on improved forest management. Here, a record average burned area was observed, but the total number of projects affected was modest and aligned with average drought conditions. Africa had the highest average BA but 2024 was a low fire year, aligned with long term BA trends in African savannas and woodlands (Andela et al., 2014), and a relatively large number of projects focused on afforestation or forest restoration (52%), which may result in decreasing fire activity over time.

Notably, despite increasing fire risk, about 46% of projects did not experience any BA over the observational period, and 67% of projects were at moderately low risk from fire (with less than 0.5% burned annually in the forests within a 50-km buffer zone around the project).

Aligned with long-term changes in fire weather (Jolly et al., 2015, Abatzoglou et al., 2019), we found that the majority of forest carbon projects faced anomalous drought conditions in 2024. The 2024 fire season affected a record number of forest carbon projects globally, resulting in an unprecedented annual percentage of BA within project boundaries. High-integrity forest carbon projects can help to mitigate global climate change, and we find some evidence that these interventions are also reducing fire risk locally. Nonetheless, the quality of carbon credits issued by nature-based projects depends on the permanence of the carbon emissions avoided or removed, which we show to be increasingly at risk.

#### 3.2.4. Air Quality Impact

Here, we present estimates of the concentration of fine particulate matter ( $PM_{2.5}$ ) that the average person in the Pantanal-Chiquitano region experienced due to wildfire smoke emissions (the population-weighted  $PM_{2.5}$  concentration; **Figure 7**). In the Pantanal-Chiquitano, the population-weighted  $PM_{2.5}$  concentration exceeded the WHO daily  $PM_{2.5}$  daily standard of  $15 \mu g/m^3$  on most days from August to November (**Figure 7**), with only 30 days between July and October falling below the threshold, most of which were in early July. Considering fire emissions alone, the average person experienced  $PM_{2.5}$  above  $15 \mu g/m^3$  on 16 additional days between July to October due to local fire emissions, which is slightly lower (20%) than previous 30% estimate of the contribution of Brazilian deforestation fires to  $PM_{2.5}$  (Reddington et al. 2015). September marked the peak pollution month where the average person experienced  $PM_{2.5}$  concentrations of  $61 \mu g/m^3$  and fires accounted for approximately 59% of the pollution mass ( $\sim 36 \mu g/m^3$ ). In comparison to **Figure 7**,

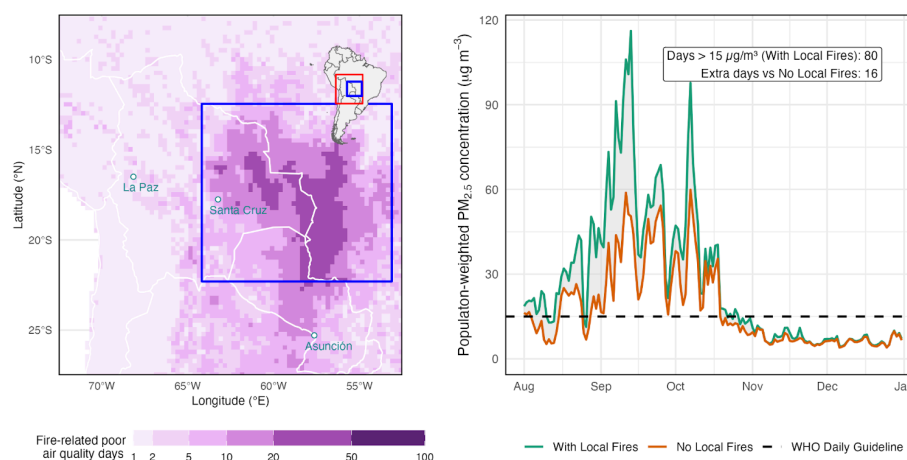




non-population weighted daily concentrations met or exceeded the US Environmental Protection Agency's 24-hour maximum standard of  $150 \mu\text{g}/\text{m}^3$  on five days. Though no comparable single-day maxima standard exists under WHO or Brazilian air quality regulations, this highlights the potential of extreme pollution exposure in low population regions closer downwind of South American fire occurrence. Furthermore, even in the absence of fires, background pollution levels are already severely degraded; the presence of fire emissions, however, significantly worsens air quality conditions. Furthermore, this analysis has focused only on the impact of local fires, yet the overall seasonality of PM matches the fire season in South America. This suggests that while local fires are enhancing exposure to pollution there is likely to be a significant contribution from longer-range fire smoke transport to the region.

1570

To help contextualize model findings, we also examined model results for the January 2025 Los Angeles (LA) wildfire (not shown). The modelled  $\text{PM}_{2.5}$  results for the LA region were muted, with a maximum population-weighted daily concentration of  $29 \mu\text{g}/\text{m}^3$  on January 17. However, observational reports of the LA fire document much more extreme pollution, including a  $480 \mu\text{g}/\text{m}^3$  one hour peak and a  $93 \mu\text{g}/\text{m}^3$  daily mean peak on January 8th (US EPA, 2025; Briscoe and Rainey, 2025). This discrepancy likely stems from insufficient spatial and temporal resolution in both the model and the analysis region, which cannot capture the rapid and highly localized plume behaviour typical of urban or wildland-urban interface fires. It illustrates why high-resolution modelling that captures community scale air quality analysis of short-lived extreme events are needed for comprehensive impact assessments of fires as they encroach into populated regions. Benchmarking model performance against documented local maxima could guide improvements and enhance reliability for future health risk evaluations in all burning environments.



1584

**Figure 7:** Poor air quality days caused by anomalous fire activity in the Pantanal-Chiquitano region during the 2024-25 fire season. **(Left panel)** shows the additional number of days exceeding the World Health Organisation (WHO) daily standard of  $15 \mu\text{g}/\text{m}^3$  as a result of fire emissions occurring within the defined regions (red outlines), over and above the number of poor air quality days caused by all other sources of  $\text{PM}_{2.5}$  (e.g. industrial, transport, and residential) and from fires occurring outside of the defined regions. **(Right panel)** shows a daily time series of population-weighted  $\text{PM}_{2.5}$  concentrations ( $\mu\text{g}/\text{m}^3$ ) under scenarios that include or exclude local fires. The WHO daily standard of  $15 \mu\text{g}/\text{m}^3$  is shown and days exceeding that threshold are counted as poor air quality days.



## 1594 4. Diagnosing Causes and Assessing Predictability

1595

### 1596 4.1. Methods

1597

#### 1598 4.1.1. Predictability of Focal Events of the 2024-25 Fire Season

1599

##### 1600 4.1.1.1. *Short to Medium Range Forecasts*

1601 We evaluated the capacity of two distinct methods to predict fire occurrence over short to  
 1602 medium -range time periods (1 to 15 days): the Fire Weather Index (FWI; van Wagner, 1987;  
 1603 Vitolo et al., 2020) and the Probability of Fire (PoF; McNorton et al., 2024).

1604 FWI is a well-established empirical indicator of fire danger mostly reflecting the influence of  
 1605 meteorological conditions on landscape flammability. It is based on 4 prerequisite weather  
 1606 variables and it describes the impact that atmospheric conditions have on fuel dryness (see  
 1607 **Section 2.1.4.1**). It was originally calibrated for the boreal forests of Canada and assumes  
 1608 constant fuel characteristics. Due to its ease of implementation it is now widely used around  
 1609 the world (Bedia et al., 2015; Di Giuseppe et al., 2016; Abatzoglou et al., 2018; Vitolo et al.,  
 1610 2020; Jones et al., 2022). Here, we used weather inputs from the ECMWF Integrated  
 1611 Forecasting system in its operational configurations at 9 km resolutions.

1612 PoF is one of the outputs of the ECMWF Sparky fire model and aims to improve upon the  
 1613 fire forecasting skill of the FWI (McNorton et al., 2024; Di Giuseppe et al., 2025). The  
 1614 Sparky-PoF is a data-driven fire prediction system that advances on fire danger metrics by  
 1615 modelling not only the effect of meteorological variables on fire likelihood but also (i) the  
 1616 temporal evolution of fuel load and fuel moisture content and (ii) ignition events informed by  
 1617 lightning forecasts, human population density, and road networks. PoF is an example of a  
 1618 new generation of indicators based on machine learning methods that have recently been  
 1619 created to produce more informative operational predictions of wildfire (Shmuel et al., 2025;  
 1620 Di Giuseppe, 2023). One of the practical advantages of PoF is that it can directly output a  
 1621 prediction of the number of fire hotspots when averaged over vast areas which is directly  
 1622 comparable to active fire observations. While these approaches are relatively new, they hold  
 1623 great promise for improving fire forecasting, particularly in fuel-limited biomes where FWI is a  
 1624 weaker predictor of fire activity (Bedia et al., 2015; Jones et al. 2022). PoF leverages  
 1625 medium-range (up to 15 days horizon) weather forecasts and fuel variables that are  
 1626 available from an experimental configuration where IFS is coupled with the Sparky fire model  
 1627 to drive a data-driven classifier, trained on observed hotspots using a XGBoost methodology  
 1628 (Shmuel and Heifetz, 2025; Jain et al., 2020). Predictions of PoF from Sparky showed better  
 1629 skills than FWI in recent events and are available operationally with forecasts up to 10 days  
 1630 in advance (Di Giuseppe et al., 2025).

1631 In general, FWI is effective at capturing the immediate emergence of fire-conductive weather  
 1632 conditions across much of the globe. However, it does not consider the fuel build-up and the  
 1633 state of vegetation in specific biomes other than boreal forests, which is often a critical factor  
 1634 in fire occurrence. As a result, FWI-based systems may predict fire-prone conditions too far in  
 1635 advance of actual fire emergence, particularly in ecosystems where vegetation availability  
 1636 (i.e., fuel) governs ignition potential. In contrast, data-driven models like PoF, which  
 1637 incorporate information on both dead and live fuel moisture content are better able to reflect  
 1638 the delayed response of ecosystems to dry conditions. These models provide a more  
 1639 realistic representation of fire potential in fuel-limited landscapes or in regions where the  
 1640 hydroclimatic cascade delays fire onset. This is especially relevant for wetland biomes,  
 1641 which have been a key focus of analysis this year.



#### 1642 **4.1.1.2. Subseasonal to Seasonal Forecast**

1643

##### 1644 **4.1.1.2.1. Fire weather**

1645 The prediction of fire weather over sub-seasonal to seasonal (up to 6 months ahead) is a  
 1646 relatively unexplored field of research (Roads et al., 2005). Until recently, only a few studies  
 1647 had specifically examined the prediction and predictability of fire weather-related quantities  
 1648 and their connection to actual fire activity globally (Di Giuseppe et al., 2024). Here, we  
 1649 evaluate the ability of cutting-edge seasonal prediction systems to predict anomalies in the  
 1650 FWI, using data available through the Copernicus Emergency Management Service which  
 1651 uses ECMWF's SEAS5 seasonal forecasts as forcing (Di Giuseppe et al., 2024). We  
 1652 probabilistically quantify the likelihood of FWI values exceeding the seasonal mean  
 1653 prediction time steps ranging from 1 to 3 months considering a climate that spans the period  
 1654 1991-2016. These predictions are not designed to inform on the exact location of fire  
 1655 outbreaks, but rather to serve as an indicator of landscape preconditioning to burn. The  
 1656 predictions highlight regions where anomalous fire weather may emerge and thus merit  
 1657 closer monitoring, offering an early signal of where fires could become a concern.

1658 On seasonal timescales, patterns of fire weather are significantly influenced by large-scale  
 1659 climate modes such as the El Niño-Southern Oscillation (ENSO) through variation in  
 1660 temperature and rainfall patterns across the tropics (Latif et al., 1998; Chen et al., 2017;  
 1661 Bedia et al., 2018). In some tropical countries, forecasts of ENSO have been used directly to  
 1662 predict risk of fire and to implement preemptive fire management actions including bans on  
 1663 fire (Pan et al., 2018). For example, major fire anomalies and regional haze events in  
 1664 southeast Asia are thought to have been avoided during the 2023-2024 El Niño, following  
 1665 the implementation of new predictive systems and policy interventions since earlier El Niño  
 1666 years (e.g. 2015) (World Resources Institute, 2016). The effect of other large-scale climate  
 1667 modes is also present in other world regions, such as in the case of the Indian Ocean Dipole  
 1668 (IOD) in the case of Australia (Harris and Lucas, 2019) and several Atlantic and Pacific  
 1669 oscillations in the case of Amazonia (Aragão et al., 2018). The ECMWF's SEAS5 forecasts  
 1670 have been shown to accurately predict the meteorological variability associated with ENSO  
 1671 and their effects on fire activity over timescales of 1 to 2 months ahead (Johnson et al.,  
 1672 2019; Di Giuseppe et al., 2024).

##### 1673 **4.1.1.2.2. Burned Area**

1674 While FWI forecasts can successfully identify regions with elevated fire danger aligning with  
 1675 observed BA anomalies, they tend to indicate broad areas at risk and lack the specificity  
 1676 needed to pinpoint where fires are most likely to occur. This reflects a key limitation:  
 1677 translating fire weather anomalies into accurate predictions of seasonal fire activity is not  
 1678 straightforward, as it requires incorporating additional drivers, namely fuel availability, ignition  
 1679 sources, and suppression capacity. Modeling the complex dynamics among fire and its  
 1680 bioclimatic and human drivers remains a challenge and is the focus of extensive research  
 1681 (e.g. Jones et al., 2022). Nevertheless, when considering forecasting ability in the long range  
 1682 and accuracy, climate remains the most reliable parameter among the drivers of fire activity.  
 1683 Accordingly, we examine the potential of machine learning techniques to forecast BA  
 1684 anomalies, which are being developed to provide targeted forecasts that guide the  
 1685 deployment and coordination of limited firefighting resources amidst increasingly  
 1686 synchronous wildfires (Torres-Vázquez et al., 2025a; Abatzoglou et al. 2021). We employ the  
 1687 model developed by Torres-Vázquez et al. (2025b), which is a hybrid approach combining  
 1688 dynamical seasonal drought forecasts with a statistical climate-fire model based on the  
 1689 Random Forest (RF) algorithm. This model leverages the Standardised Precipitation Index  
 1690 (SPI), aggregated over periods of 3, 6, or 12 months, to capture both antecedent and  
 1691 concurrent climatic conditions that influence fire activity. Calibrated with historical BA and  
 1692 SPI data, the RF model forecasts BA anomalies one month ahead of the fire season. The



system has shown promising predictive skill, successfully capturing BA anomalies across the globe (Torres-Vázquez et al., 2025b).

#### 4.1.1.3. *Uncertainties and forecast skills*

Uncertainty is a key factor in prediction and is likely to increase with forecast horizon. The forecast uncertainty is provided as the spread across a set of ensemble simulations from possible scenarios or by expressing the forecast as probability. Variability across the ensemble of forecast realizations was previously estimated to be in the range of 10%-15% for FWI (Vitolo et al., 2020), and in this study is reported as variance in the forecast values. PoF is a measure that is probabilistic in nature and is reported as probability of occurrence. For long-range predictions, uncertainty is also explicitly incorporated by expressing forecasts in probabilistic terms, specifically as the probability of exceeding (or falling below) certain thresholds, such as the upper and lower tercile.

The quality of fire forecasts is assessed by visually examining how well the forecasts capture the likelihood of key focal fire events. This approach mirrors the way fire management agencies typically interpret and use these indicators during the fire season. It is designed to partially reflect the operational context in which such indices are applied. Similarly, the seasonal predictions of FWI and the probability of above-median BA aim to demonstrate the type of information currently available to support informed decision-making for resource planning at extended lead times.

#### 4.1.2. *Identifying Causes of Focal Events*

We assess the main or concurrent causes of the 2024-25 focal fire events using two complementary modelling frameworks: the Probability of Fire as part of the Sparky modelling complex (McNorton et al., 2024) and the ConFLAME attribution framework (Kelley et al., 2021; Barbosa et al. 2025b). PoF is applied to satellite observations of active fires (Giglio et al., 2018; regridded to 0.1°) and targets a prediction of absolute fire counts on daily timescales. Meanwhile, ConFLAME is applied to satellite observations of BA from MODIS (Giglio et al., 2018; regridded to 0.5°), enabling causality analysis of fire events to key environmental and human-related causes. The ConFLAME analysis is performed on absolute BA fraction and anomalies from the 2002-2025 climatological mean and includes full regional summaries to provide broader context and to better support interpretation of region-wide drivers and trends. Used together, as in this report, the two systems provide complementary analyses of the causes of both active fire hotspots and BA anomalies.

Each model groups predictors into broader categories of causation: weather, fuel and ignitions (**Table S1 in Supplementary Material S4**). Some predictors are shared or overlap between categories due to their interconnected nature (e.g., fuel moisture and weather), but the models are designed to avoid double-counting. To identify the main causes of the fire event, PoF uses an ensemble-based gradient-boosted decision tree classifier (XGBoost), with attribution provided through SHapley Additive exPlanations (SHAP) method taken from the SHAP library (Lundberg and Lee, 2017) values to quantify the influence of each driver group on predicted fire hotspots.

ConFLAME, in contrast, uses a probabilistic Bayesian approach to assess the contribution of each driver group to observed BA, accounting for model uncertainty and fire stochasticity. While PoF is trained globally, ConFLAME is trained separately for each region to capture regional variation in the relationship between fire drivers and BA. Regional influence is particularly relevant for explaining the final BA as it depends on the local variations of fuel and ignition. Local ecology shapes how vegetation and biomass affect burning (Lehmann et al. 2014) and human control can result in promoting fire (e.g. through deforestation or water extraction) or suppressing it (Andela et al. 2017). In ConFLAME causes are combined



through logistic functions, with results expressed in terms of likelihoods for a detectable BA to be associated to a specific cause.

Both systems include uncertainty estimates. PoF reflects uncertainty via probabilistic ensemble outputs and a measure is provided by the error in the predicted number of hotspots. ConFLAME directly quantifies uncertainty from both drivers and model structure, providing confidence intervals for predictions. While neither system is free of limitations, this dual-model setup allows for a more robust assessment of fire causes across different spatial and temporal scales, with prediction of hotspots providing a fine-scale measure of fire activity and BA an integrated assessment of landscape impacts.

The PoF model does not assume that each factor always pushes fire activity in the same direction. For example, while increased fuel moisture generally reduces fire activity by dampening ignition and spread, in some regions, higher antecedent rainfall can lead to greater vegetation growth, increasing available fuel and potentially resulting in more intense fires later. In fuel-limited regions, where grasses and herbaceous plants dominate, high rainfall can boost fuel growth and lead to more burning. But in fuel-rich areas with lots of trees, that same rainfall mostly increases fuel moisture, potentially decreasing fire activity. In contrast, ConFLAME allows you to specify the expected direction of influence. When a factor can both increase or decrease fire activity depending on context, those effects are represented separately in the model. See **Supplementary Material for Section 4** for a detailed description.

## 4.2. Results

### 4.2.1. Predictability of Focal Events

#### 4.2.1.1. Short to Medium Range Forecasts

##### 4.2.1.1.1. Northeast Amazonia

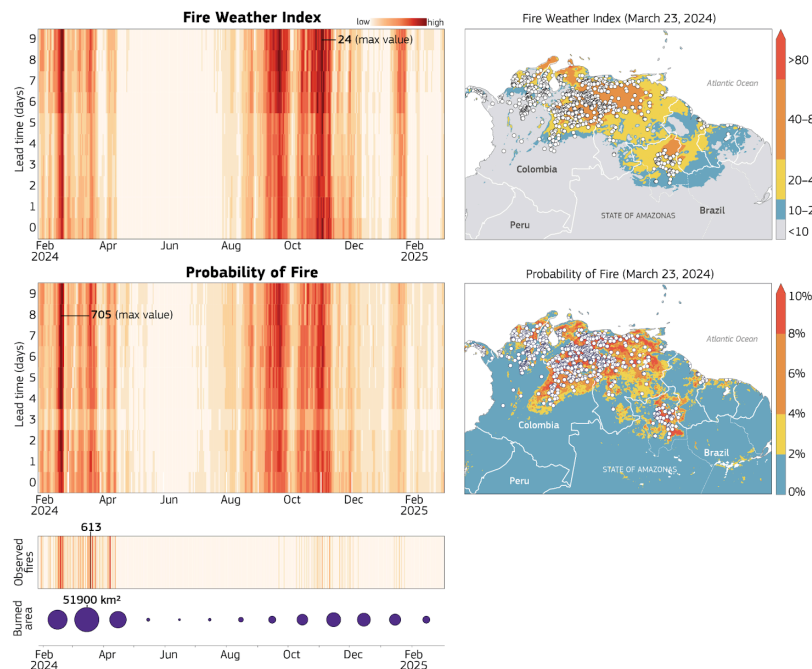
Between January and March, satellites detected over 30,200 fire hotspots, marking the highest number recorded for that period since monitoring began in 1999 (Eschenbacher, 2024). These fires were intensified by persistent extreme drought conditions associated with the El Niño phenomenon, which led to higher temperatures and reduced rainfall (NASA Earth Observatory, 2024c; **Figure 8**). This part of the region lies in the Northern Hemisphere tropics, where the peak of the fire season aligns with boreal winter months. The region is lesser-studied than parts of southern hemisphere Amazonia (Brando et al., 2020; Alencar et al., 2015).

Both FWI and PoF systems identified two main fire seasons in 2024: February-April and August-November. However, around 80% of the total BA concentrated in the early months of the year and only 20% during the second dry season. The total probabilities of PoF values over the focal region translates into a number of predicted hotspots and this is directly comparable to the detections from MODIS. In March, when approximately 60% of the annual BA was recorded, the PoF reached its peak predicting nearly 700 fire hotspots in a single day, closely matching the ~600 observed hotspots. While the FWI also indicated anomalously high fire risk, its peak occurred later in September. The onset of the first fire wave aligned closely with the emergence of fire-prone weather conditions (**Figure 8**), highlighting the role of weather in enabling fire activity. In this region, where over 90% of ignitions are human-driven and fuel availability remains high, atmospheric conditions primarily act as the trigger for widespread burning.



1788 Interestingly, both the PoF and FWI systems failed to capture a lull in fire activity during the  
 1789 second emergence in August–November of fire-conductive conditions showing the limitations  
 1790 of forecasting fire activity rather than fire danger. One possible explanation is that these  
 1791 conditions fell outside typical burning cycles, for example, in agricultural areas where fires  
 1792 are often timed around harvest. This raises an important possibility that the models failed to  
 1793 represent the quiet September period because they have only limited information on human  
 1794 ignition patterns, land ownership and use types, and lesser-studied factors such as fire  
 1795 suppression, policy interventions, and managed or cultural burning practices, underscoring  
 1796 the need for improved human activity data that could significantly improve fire prediction  
 1797 (Jones et al., 2022).

1798



1799

1800 **Figure 8:** Northeast Amazonia forecasts of the FWI and PoF with lead times up to 10 days  
 1801 prior for the period February 2024–February 2025 as an average value over the focal area.  
 1802 The total percentage of PoF values over the focal region translates into a number of  
 1803 predicted hotspots and this is directly comparable to the detections observed by MODIS.  
 1804 The x-axis corresponds to specific dates throughout the year, while the y-axis denotes either  
 1805 observations or the time leading up to the date when a forecast was generated. The vertical  
 1806 colour coherence allows for quick identification of the time windows of predictability  
 1807 associated with the observed fire activity both provided in terms of number of detected active  
 1808 fires per day and total monthly BA (circles). The maps represent a snapshot in time at day 0  
 1809 to allow the comparison of the spatial distribution of the forecasts and the recorded fire  
 1810 activity by MODIS.





#### 1811 **4.2.1.1.2. Pantanal and Chiquitano**

1812

1813 The Pantanal and Chiquitano have been enduring a prolonged dry period since 2019 leading  
 1814 to the 2024 worst water crisis ever recorded in the biome (World Wildlife Fund, 2024).  
 1815 Notably, the Pantanal did not experience its typical flood season in early 2024 and the  
 1816 average area covered by water during the first four months was smaller than that of the  
 1817 previous year's dry periods (Van Dijk et al., 2025). By the end of May 2024, almost the entire  
 1818 Pantanal and Chiquitano region was classified as experiencing extreme drought, the  
 1819 second-highest classification of drought intensity on the Integrated Drought Index (NASA  
 1820 Earth Observatory, 2025a, 2024c). As the Pantanal is a wetland ecosystem, the  
 1821 establishment of dry conditions is a prerequisite for the onset of fire activity. A full  
 1822 hydrological cascade must occur before widespread burning can take place: prolonged  
 1823 precipitation deficits must lead to the reduction of flooded areas, their replacement by  
 1824 grasslands, and the progressive desiccation of both live and dead vegetation. This sequence  
 1825 introduces a natural delay, which explains why fire activity in the region peaked in August  
 1826 and September, well after the onset of dry weather in June (**Figure S11 in Supplementary**  
 1827 **Material S4**).

1828 The total percentage of PoF values over the focal region translates into a number of  
 1829 predicted hotspots and this is directly comparable to the detections from MODIS. The most  
 1830 severe PoF forecast, predicting 971 hotspots, closely matches the 885 observed in late  
 1831 August. At large scales, the FWI offers a useful overview of fire-conducive weather  
 1832 conditions. However, it is the inclusion of fuel characteristics in the PoF that provides the  
 1833 finer spatial granularity (maps in **Figure S11 in Supplementary Material S4**) needed for  
 1834 more accurate and actionable fire risk assessments.

#### 1835 **4.2.1.1.3. Southern California**

1836 California is arguably one of the most extensively studied regions in terms of shifts in fire  
 1837 regimes (see, e.g., Billmire et al., 2014; Littell et al., 2016; Williams et al., 2019; Swain et al.,  
 1838 2025). In 2024, Southern California experienced severe burning in September, with a total of  
 1839 1,200 km<sup>2</sup> burned. Although these fires fell within the typical fire season, the total BA was  
 1840 unremarkable for the region compared to previous years. However, the most significant fire  
 1841 event took place much later, in January 2025, well outside the typical fire period, when the  
 1842 Palisades and Eaton fires broke out in Los Angeles county. The events sparked widespread  
 1843 public debate about how prepared we are to anticipate off-season fires (Woolcott, 2025).

1844 As shown in **Figure S12 (Supplementary Material S4)**, fire-prone weather conditions  
 1845 persist across much of the year, extending well into autumn, a reflection of the expanding fire  
 1846 season driven by climate warming. Yet, in regions like Southern California, fire prediction  
 1847 based solely on weather indicators is often inadequate. The primary causes of the severity of  
 1848 these events was an intensification of the hydrological cycle that exacerbated both wet and  
 1849 dry extremes. Southern California experienced an unusually wet antecedent period prior to  
 1850 intense drying in an unusually dry winter, which created an accumulation of dry fuel setting  
 1851 the ideal conditions for intense fire activity (Swain et al., 2025). Fuel accumulation is a  
 1852 persistent feature throughout the fire season, and therefore does not result in a large  
 1853 difference between the PoF and FWI forecasts when averaged over the Mediterranean  
 1854 areas of California. However, its inclusion in the prediction system allows for the  
 1855 identification of zones with higher susceptibility, which are clearly visible in the  
 1856 accompanying map. Neither the FWI nor PoF metrics could provide adequate warning  
 1857 regarding the magnitude of the winter fire event affecting the wildland-urban interface. These  
 1858 events were driven by atmospheric phenomena influenced by steep orography, which are  
 1859 not resolved by current weather forecasting models. The lack of the required resolution  
 1860 impacts equally on empirical and machine learning methods. This highlights the need for  
 1861 improved high resolution forecasting for fire danger in the wildland-urban interface



#### 1862 **4.2.1.1.4. Congo Basin**

1863 The 2024 dry anomaly in Central Africa has been partly attributed to the co-occurrence of a  
 1864 positive El Niño phase and a warm Indian Ocean Dipole (McPhaden et al., 2024). These  
 1865 conditions tend to shift the West African monsoon northward, leading to suppressed  
 1866 precipitation over the Congo Basin during the core of the rainy season, a pattern observed  
 1867 globally in recent years (Toreti et al., 2024). This event also aligns with a broader trend of a  
 1868 lengthening and intensifying dry season in the Congo rainforest. Satellite analyses over the  
 1869 past few decades show that the dry season is starting earlier and ending later, increasing the  
 1870 region's vulnerability (Jiang, 2019). There are typically two main fire seasons in the Congo  
 1871 Basin: from December to March north of the equator, and from June to September south of  
 1872 the equator. In the equatorial zone, however, fires are not naturally occurring, as precipitation  
 1873 is distributed throughout the year. The expansion of dry seasons both north and south of the  
 1874 equator has led to a situation where fire seasons in the Congo Basin now span almost the  
 1875 entire year with peak activities between July and August and December and March.  
 1876 Compounding this, a decline in lightning activity over the region (Chakraborty and Menghal,  
 1877 2025) suggests that fires are increasingly of human rather than natural origin. This  
 1878 combination of persistent drier-than-average conditions and human-driven ignition means  
 1879 that fire activity is now widespread and weakly correlated with weather patterns. As a result,  
 1880 predictions have a very short predictability window of only a few days (horizon at correlation  
 1881 of lines in **Figure S13**). The detachment of fire activity from natural conditions in the Congo  
 1882 Basin presents a significant challenge for forecasting (**Figure S13**). In these regions, the  
 1883 discriminatory power between fire-prone and non-prone conditions is greatly reduced, and  
 1884 both FWI and PoF tend to overpredict fire occurrence. In particular, FWI fails to capture the  
 1885 complex interactions among fuel availability, ignition sources, and human activity. This  
 1886 limitation is especially pronounced in areas where natural ignitions are infrequent, and fuel  
 1887 dynamics, rather than weather alone, drive fire occurrence and behaviour (**Figure S13**).

#### 1888 **4.2.1.2. Seasonal Predictability from Fire Weather Forecasts**

1889 The year 2024 has been officially declared the warmest year on record, surpassing previous  
 1890 temperature benchmarks (WMO, 2025; NOAA, 2025a). This exceptional warmth has been  
 1891 driven not only by long-term global warming (IPCC, 2023), but also by a combination of  
 1892 short-term ocean-atmosphere anomalies. In particular, extensive and persistent oceanic heat  
 1893 waves have been observed across multiple ocean basins, contributing to elevated sea  
 1894 surface temperatures (Holbrook et al., 2019). These marine heatwaves have been further  
 1895 reinforced by an unusual reduction in low-level cloud cover over parts of the Atlantic Ocean,  
 1896 allowing for increased solar radiation absorption at the ocean surface and amplifying the  
 1897 warming (Ceppi and Nowack, 2021).

1898 Given this overall picture, seasonal forecasts of FWI anomalies successfully captured the  
 1899 broad regional patterns of elevated fire danger, particularly in Northeast Amazonia and parts  
 1900 of Bolivia and Venezuela (**Figure 9**). These forecasts aligned with the widespread drought  
 1901 and above-average temperatures linked to the strongest El Niño since 2015, a concurrent  
 1902 positive Indian Ocean Dipole, and record-breaking ocean heatwaves. Together, these factors  
 1903 intensified drying across equatorial South America, expanding fire-prone conditions well  
 1904 beyond the regions that ultimately experienced the most extreme burning.

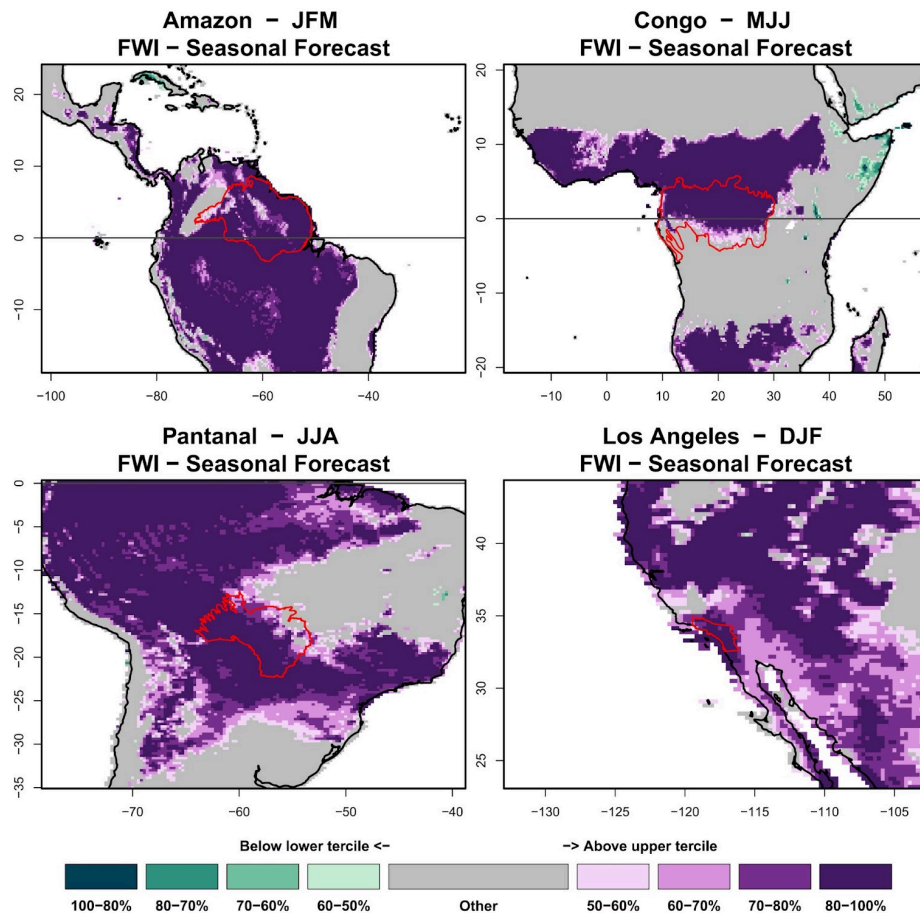
1905 All forecasts issued one month before the fire season showed high confidence (between 60  
 1906 and 90%) in the development of above-normal conditions in our focal regions, all exceeding  
 1907 the 66th percentile of climatological values.

1908 **Figure 9** demonstrates both the strengths and limitations of FWI-based seasonal forecasts.  
 1909 While they provide valuable early warnings by detecting fire weather anomalies, their  
 1910 broad-scale nature can lead to overestimations of fire impact if not combined with



information on fire susceptibility. These findings reinforce the value of FWI in anticipating periods of increased landscape flammability, but also highlight the need to more appropriately model anomalies in fuel load and moisture and to integrate non-climatic factors, such as ignition sources, land use practices, suppression capacity, and landscape accessibility, into fire impact forecasting models to improve precision and operational relevance. Future seasonal-scale forecasts may seek to implement PoF as a predictive tool, which improves upon FWI by tracking fuel loads and moisture and thus the legacy effects of antecedent conditions on landscape flammability.

**Figure S14** presents an example of the burned-area anomaly forecasting system using our hybrid dynamical and Random Forest (RF) approach (**Section 4.1.1.2.2** and Torres-Vázquez et al., 2025b). The maps illustrate the predicted probability of a BA anomaly and whether these predictions could trigger alerts for BA anomalous seasons within a potential early-warning system. Following Torres-Vázquez et al. (2025b), alerts are issued when predicted probabilities exceed thresholds optimized to balance correct detections and false alarms. For the 2024 season, anomalies in South America, notably in drought-affected regions influenced by El Niño conditions, were reasonably well anticipated. However, in other regions, particularly parts of Africa including the Congo basin, there were numerous false alarms, reflecting current limitations in fully capturing regional complexities and non-climatic fire drivers. This first implementation demonstrates operational potential, and future refinements (such as incorporating extended fire records and adjusting region-specific thresholds) could enhance skills by reducing false positives.



1932

1933 **Figure 9:** Seasonal prediction of Fire Weather Index (FWI) during the periods relevant to our  
1934 focal events, presented in probabilistic terms that indicate the likelihood of an increased or  
1935 decreased anomalous fire season.

1936

#### 1937 4.2.2. Identifying Causes of Focal Events

1938 Weather, fuel, and ignitions are the three primary controls influencing the occurrence and  
1939 intensity of fire events (Di Giuseppe et al., 2025). These broad categories can be further  
1940 examined to pinpoint individual factors, for example, precipitation and temperature within the  
1941 weather category or fuel moisture from dead and live vegetation in the fuel category.  
1942 Analysing the single factors can give an idea not only of the probability of the fire to occur  
1943 but also on their intensity and behaviour. For example anomalies above the expected climate  
1944 (here 2003-2023) in the moisture of dead fuel, due to its lower moisture content and higher  
1945 combustibility, often plays a significant role in determining ignition potential. Low live fuel  
1946 moisture increases vegetation flammability, thereby contributing significantly to greater fire  
1947 severity and intensity.

1948 Beyond this descriptive approach, the PoF and ConFLAME causality models enable a  
1949 probabilistic attribution of fire occurrence to the three primary controls. These models



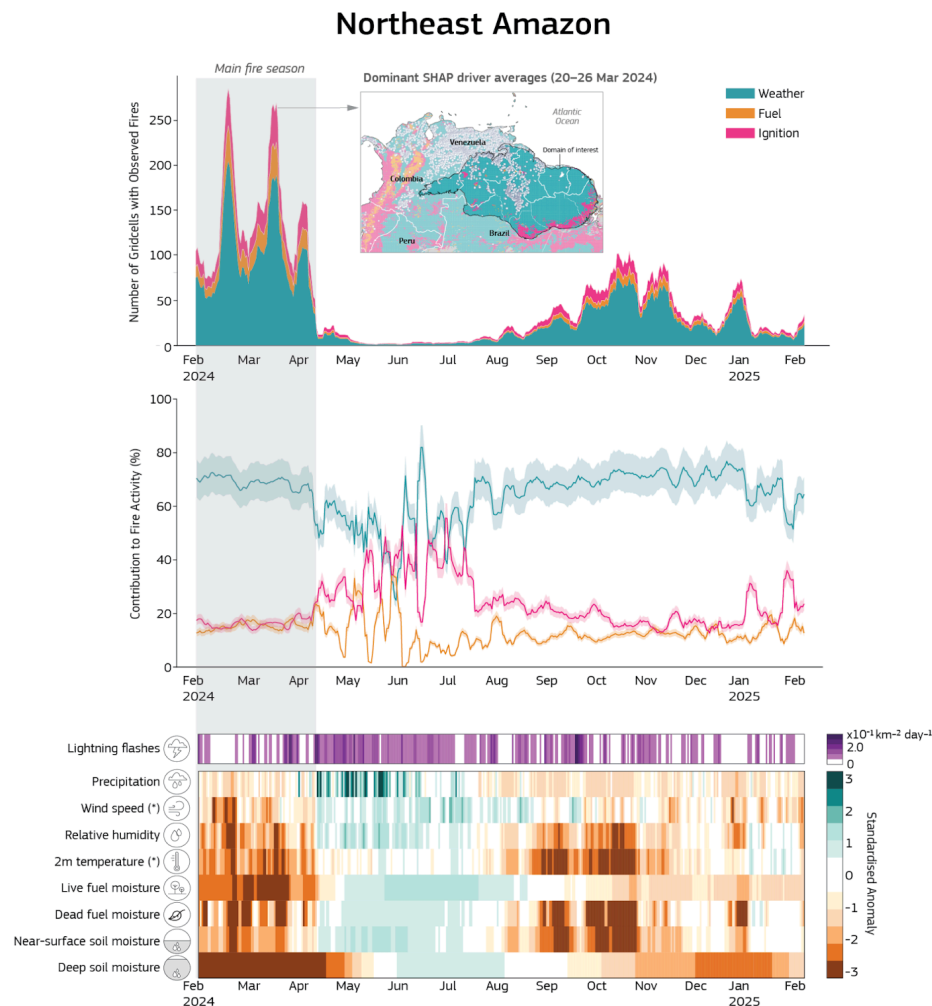
provide attribution even when no fire is recorded: a low probability across all controls reflects an accurate forecast of no fire, while a high probability without observed fire activity could point to successful suppression efforts, fire-prevention policies, or other unaccounted human factors not included in the model forecasts. The discrepancies between the model prediction and the observed fire activity (fire hotspots or BA anomalies) are included to provide a measure of the model uncertainties.

#### 4.2.2.1. Causes of Fire Hotspots during Focal Events

1957

##### 4.2.2.1.1. Northeast Amazonia

According to our Sparky-PoF analysis, the extreme fire activity during the 2024-25 fire season in Northeast Amazonia (described in **Section 2.2.2.1**), was predominantly driven by anomalous dry weather. Northeast Amazonia experienced an exceptionally severe fire season between January and April (**Figure 10**), driven by extreme drought which started in 2023, intensified by the combined effects of El Niño and the Atlantic Meridional Mode, which brought unusually high temperatures and suppressed rainfall. At the peak of the season, during the week of 20-26 March, nearly 2,000 fire hotspots were observed. Fires were fueled by prolonged and intense drying across the entire landscape, which made vegetation highly flammable and enabled rapid fire spread across large areas. On the most severe week of burns our causation analysis shows that weather conditions were the dominant factor, accounting for about 60% of fire activity, while fuel availability and ignition sources each contributed around 20%. During the first part of the year the exceptional dryness meant that soil humidity levels and moisture in both dead and live vegetation fell to among the driest 2% of historical conditions, while deep soil moisture dropped below 1%. The time series of lightning activity (**Figure 10**, bottom panel) further illustrates that ignitions in the region are predominantly human-driven. During the May-August period, lightning activity is high and is linked to storms and rainfall, which tend to suppress fire ignition and spread. As a result, even though lightning increases the relative contribution of ignition to predicted fire activity, doubling its weight to around 40%, this is not reflected in actual fire occurrence or BA. A second, less intense onset of fires occurred between September and January. This was driven by a more superficial drying of the landscape that did not extend into deeper soil layers. Unlike the earlier season, which was associated with hydrological drought, this later period was more reflective of meteorological drought (precipitation deficit).



1982

1983 **Figure 10:** Drivers explaining fire hotspots prediction in Northeast Amazonia. Daily fire  
1984 activity and contributing drivers from February 2024 to February 2025. (**Top panel**) Daily  
1985 count of grid cells with detected fire hotspots, stacked by dominant driver category, fuel,  
1986 weather, or ignition/suppression. A dominant driver is assigned only if its contribution  
1987 exceeds 50% of the total attribution; otherwise, the grid cell is left unclassified (gray). An  
1988 inset map shows the spatial distribution of dominant drivers during the peak fire week,  
1989 highlighting regional heterogeneity in fire causation. (**Middle panel**) Relative contributions  
1990 (%) of each driver category to predicted fire occurrence, with shaded bands indicating  
1991 model-observation uncertainty. (**Bottom panel**) Standardized anomalies (in units of standard  
1992 deviation) for each input driver variable, including lightning flash density. Asterisks (\*)  
1993 indicate reversed anomalies.

1994





#### 1995 **4.2.2.1.2. Pantanal and Chiquitano**

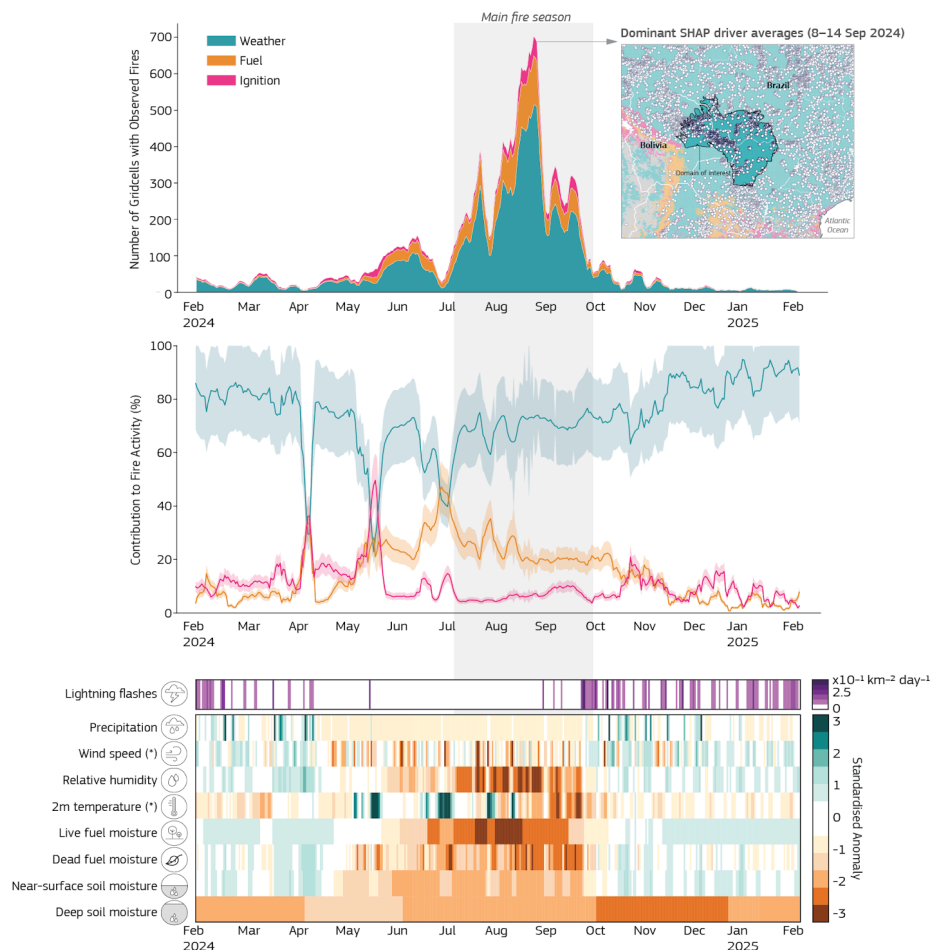
1996 According to our Sparky-PoF analysis, the extreme fire activity during the 2024-25 fire  
1997 season in the Pantanal-Chiquitano (described in **Section 2.2.2.2**), was mainly the result of  
1998 extremely dry weather which had started since 2023. Drought conditions affecting the  
1999 Pantanal and Chiquitano continued into the early months of the 2024-25 fire season  
2000 following multiple years of below-average rainfall (**Figure 11**). Although the year began with  
2001 relatively moist surface conditions, deep soil moisture remained in the driest 15% of  
2002 observed records or 1-2 standard deviations below the mean (**Figure 11**). A wet phase in  
2003 February-April allowed moisture transfer from the atmosphere to surface fuels, but it did not  
2004 infiltrate deeply into the soil. As a result, when surface conditions dried out again at the  
2005 beginning of June, vegetation quickly became highly flammable and primed to ignite.

2006 While fire activity in this region was predominantly controlled by weather (71% mean  
2007 contribution throughout the year), the role of fuel became increasingly important during the  
2008 most intense burning phases (up to 40% during the most intense week between 5 and 14  
2009 August 2024). In fact, the contribution of fuel conditions doubles during these peak events,  
2010 indicating that the persistence of fire-conducive weather over time, rather than the specific  
2011 daily weather, plays a dominant role in driving the most severe fires.

2012 In the Pantanal and Chiquitano, the lack of correlation between fire occurrence and natural  
2013 ignition sources, such as lightning density (**Figure 11**, bottom panel), is even more evident  
2014 than in other regions. When lightning does occur, it is typically accompanied by rainfall due  
2015 to the convective nature of tropical storm systems, further reducing the likelihood of fire  
2016 ignition. The only notable 'dry lightning' event, observed in mid-May, caused a spike in the  
2017 modelled PoF which translated into a spike of fire activity that was observable though small  
2018 in magnitude. Humans are the main source of ignitions in the region (Menezes et al., 2022)  
2019 and, while weather remains the main driver of fire activity overall, fuel conditions are playing  
2020 an increasingly important role in determining the severity and extent of extreme fire events  
2021 (**Figure 11**).



## Pantanal and Chiquitano



2022

2023 **Figure 11:** Drivers explaining fire hotspots in the Pantanal-Chiquitano (as for **Figure 10**).

### 2024 4.2.2.1.3. Southern California

2025 According to our Sparky PoF analysis of the extreme fire activity during the 2024-25 fire  
 2026 season in Southern California (described in Section 2.2.2.3), the results point to a  
 2027 combination of drivers, weather, fuel, and ignitions, each playing an almost equal role in  
 2028 creating the fire prone conditions observed during the two major events in January 2025  
 2029 (Palisades and Eton fires).

2030 Early in the 2024-25 fire season, Southern California was emerging from a two-year period  
 2031 of very wet conditions, with deep soil moisture levels at 2 to 3 standard deviations wetter  
 2032 than the climatological average (**Figure S15**). During the summer of 2024, lightning may  
 2033 have contributed to ignitions, although in these areas most fires are typically human-induced.  
 2034 Overall, fire activity remained relatively low and below the climatological average.



However, the Palisades and Eaton fires in January 2025 were well outside the typical fire season. These fires were clear outliers in terms of their seasonality, triggered by a rare alignment of short-lived but intense fire-prone conditions while fuel moistures remained low (Figure S15). Between 5 and 25 January, favourable weather, fuel availability, and ignition sources aligned leading to create ideal conditions for ignition and rapid fire spread.

In the week preceding the fires, fire weather conditions contributed around 40% to the predicted fire probability, fuel availability 30%, and ignition sources the remaining 20%. Despite the generally moist deep soil conditions, a brief but extreme episode of surface drying (reaching 3 standard deviations below normal) combined with unusually strong winds (also 3 standard deviations above average), was sufficient to create highly flammable conditions at the wildland-urban interface, enabling the fires to ignite and spread rapidly.

#### 4.2.2.1.4. Congo Basin

According to our Sparky-PoF analysis, the extreme fire activity during the 2024-25 fire season in the Congo basin (described in Section 2.2.2.4), was the result of the extreme drought that has affected the regions in recent years.

In 2024-2025, fire activity in the Congo occurred year-round in a region marked by abundant and widespread vegetation cover. The spring wet season (March-May) did not materialise due to extreme and persistent drought conditions. As a result, the second wet season later in the year also brought limited relief, leaving deep soil layers significantly dry (up to 2 standard deviations below climatological norms). The region remains in a prolonged state of water deficit until now (Figure S16).

Throughout the year, weather conditions were the dominant and most stable factor influencing both the number, intensity and duration of fire events. A combination of low rainfall (67% below the climatological average) and elevated temperatures (90% above the climatological average) led to sustained drying of both vegetation and soil, placing them among the driest 2% and 1% of the climatological record, respectively. These conditions maintained highly flammable landscapes across the region (Figure S16).

Most fire ignitions in the Congo basin can be attributed to human activity. Although lightning occurs year-round (Figure S16), it is more frequent during the wet season due to the convective nature of tropical precipitation. However, during these wetter periods, high moisture levels typically prevent fire ignition and spread. In contrast, during prolonged dry spells, even a small number of human-caused ignitions can trigger widespread and persistent fire outbreaks, owing to the highly combustible state of the vegetation.

#### 4.2.2.2. Causes of Burned Area Anomalies during Focal Events

##### 4.2.2.2.1. Northeast Amazonia

According to our ConFLAME analysis of the extreme BA during the 2024-25 fire season in Northeast Amazonia (described in Section 2.2.2.1), weather conditions explained about 40-60% of the BA anomalies, though with fuel conditions acting as an important determinant cause during the periods with greatest fire extent (Figure 12). In the peak month of March 2024, BA exceeded the long-term average (2002-2024) by over 12,000 km<sup>2</sup>. Nearly half of the March 2024 anomaly could be attributed to fuel conditions, while weather anomalies potentially accounted for between 50% and 150% of the BA anomaly (a high-end value of 150% would suggest that weather alone would have caused anomalies exceeding the observed values, but below-average ignitions moderated the BA response; Figure 12). During the secondary peak in BA anomalies during October-November, fuel and weather contributed similarly with fuel rising in importance due to the insufficient water recharge from



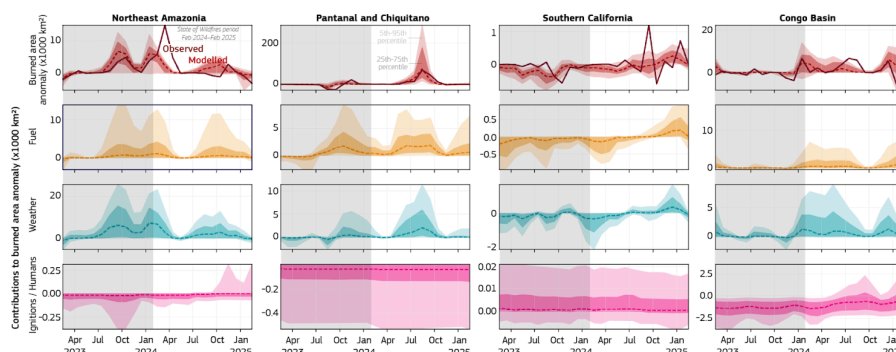
the wet season. Weather and fuel together accounted for between 1,000 km<sup>2</sup> and over 10,000 km<sup>2</sup> of BA anomalies.

Consistent with active fire analysis (**Section 4.2.1.1**), fuel played a key role in determining the geographical distribution of BA during the 2024-25 fire season (**Figure S19**). This is visible in northern regions such as the Forest-Savanna Transition Zone in northern Venezuela and southern Guyana, and the Northern Amazonia Savannas of Roraima and northern Pará, where savanna outcrops are surrounded by rainforest (see maps in **Figure S19**). In the forest landscapes, fuel anomalies and fire weather anomalies drove the predicted anomalies in BA. Interestingly, predicted BA anomalies were large in some parts of the region (e.g. Suriname) but went undetected by the MODIS BA product. The causality framework is very confident in its prediction, raising the question of whether detections were missed, possibly due to dense canopy and persistent cloud cover (Giglio et al., 2006).

Despite widespread BA in early 2024, many parts of the region remained largely unburned. Understanding why is as important as knowing what drove the fires. Our analysis shows that in areas with very low BA fraction (less than 0.5% of burnable area), no single factor (fuel, weather, or human activity) clearly limited fire spread (refer to **Figure S18**). Instead, a combination of factors, such as low ignition rates, patchy fuels, or short dry spells, likely prevented fires from taking hold. On the other hand, in the most severely burned areas (top 5% of BA), the relative importance of fuel and weather was reversed compared to broader patterns. Here, fuel moisture emerged as the primary driver of BA. Drier conditions could have increased BA by 30-40%. Weather still played a role contributing an additional 20% increase, but its influence was secondary to that of fuel.



2104



2105

**Figure 12:** Anomalies in burned area (BA) and driver contributions for each focus region during 2024, relative to the 2002-2024 average. Columns represent regions; rows show different variables. **(Top row)** Modelled and observed BA anomalies, expressed thousand km<sup>2</sup>. Model output shows median, interquartile range (shaded), and 5th-95th percentile range (lighter shading). **(Other rows)** Modelled contributions to BA anomalies from fuel conditions, fire weather, and human/ignition-related factors, also shown in thousand km<sup>2</sup>. These panels highlight which drivers contributed most to regional fire deviations from the historical average in 2024.

2114

#### 2115 4.2.2.2.2. *Pantanal and Chiquitano*

2116 According to our ConFLAME analysis of the extreme BA during the 2024-25 fire season in  
 2117 the Pantanal-Chiquitano (described in **Section 2.2.2.2**), weather conditions explained half of  
 2118 the BA anomalies and fuel conditions explained almost 30% (**Figure 12**). June, July, and  
 2119 August accounted for the most extensive burning in the Pantanal, with 25-75% of the  
 2120 landscape experiencing some fire activity, even if large parts featured only small anomalies.  
 2121 The peak occurred in June, when the BA exceeded climatological values by more than 5,000  
 2122 km<sup>2</sup> (almost triple than the annual mean). This anomaly was primarily driven by weather  
 2123 conditions (50-60%) with fuel (10-20%) and ignition (10-20%) contributing equally. Although  
 2124 fire weather remained favourable in September and October due to persistently high  
 2125 temperatures, overall fire activity was lower than during the earlier peak (**Figure 12 and**  
 2126 **S20**).

2127 We found that ignition sources contributed only 10-20% to the anomalously high fire activity  
 2128 in 2024. However, we caution that our modelling framework only partially captures ignition  
 2129 dynamics, particularly those related to human activities such as farming. This limited  
 2130 representation is reflected in the wide uncertainty range assigned to ignition within the  
 2131 causality framework. Key factors like land clearing, water extraction, and the proximity of  
 2132 ignitions to protected areas are known contributors to extreme fires in the Pantanal (Barbosa  
 2133 et al., 2022) and they are not fully accounted for in our analysis.

2134 Regional differences in fire drivers were evident (**Figure S20**). Fuel conditions played a key  
 2135 role in the fine-scale geographical distribution of BA anomalies. Exceptionally dry fuels  
 2136 affected the Chiquitano dry forests in the east, while weather was the dominant driver in  
 2137 upland regions along the edge of the Pantanal wetlands, such as the Serra do Amolar hills in  
 2138 western Brazil. The most extreme fires were observed where these two influences  
 2139 overlapped, where vegetation was both unusually flammable and atmospheric conditions  
 2140 were conducive to burning.



2141 As for what prevented the fires from becoming even more severe (**Figure S18**), no single  
2142 factor alone limited fire spread, even in the areas that burned most intensely. However, small  
2143 shifts in conditions, such as drier weather, drier fuels, or fewer land-use barriers, could have  
2144 led to 2-12% more BA in the model cells experiencing the greatest fire anomalies regions  
2145 (top 5% of anomalies).

#### 2146 4.2.2.2.3. *Southern California*

2147 According to our ConFLAME analysis of the extreme BA during the 2024-25 fire season in  
2148 Southern California (described in **Section 2.2.2.3**), the most important cause of the extent of  
2149 burned areas was fuel (30% to 60%) closely followed by weather (20-40%), while ignitions  
2150 (20%) was less pronounced than in previous years and acted as reducing factor (**Figure 12**).  
2151 During January 2025, unusually dry fuel conditions played a key role in promoting BA  
2152 anomalies, explaining up to 500 km<sup>2</sup> of the 800 km<sup>2</sup> of the anomalous BA in that month. Fire  
2153 weather conditions, starting as early as October 2024, were also anomalous versus previous  
2154 years. Focusing on the areas with the most extensive burning (top 5% of BA), we found that  
2155 anomalies could have been 30-60% larger under drier fuel conditions and more extreme fire  
2156 weather, with an additional 5% increase if fuel availability anomalies had also been higher  
2157 (**Figure S17 and Figure 4.11**). The substantial suppression efforts deployed is unaccounted  
2158 for in our modelling framework and could be one of the possible reasons the fires did not  
2159 escalate even further.

#### 2160 4.2.2.2.4. *Congo Basin*

2161 According to our ConFLAME analysis of the extreme BA during the 2024-25 fire season in  
2162 the Congo basin (described in **Section 2.2.2.4**), weather conditions explained about 30-60%  
2163 of the BA anomalies, with fuel conditions acting as an important secondary control during the  
2164 periods with greatest fire extent (**Figure 12**). Fuel conditions in the Congo Basin remained  
2165 relatively stable throughout 2024, contributing between 10-35% to fire activity year-round. In  
2166 contrast, the influence of weather conditions varied more substantially, with virtually no  
2167 fire-conducive weather in October-November, outside the typical fire season, and moderate  
2168 levels (5-15%) during peak fire periods, particularly in January and July (see also **Figure**  
2169 **S17**). July stood out as the month with the largest deviation from typical fire patterns. During  
2170 this time, fuel conditions and fire weather contributed almost equally to the BA (**Figure S22**).

2171 ConFLAME indicates widespread anomalous BA across the southern part of the Congo  
2172 basin. These model estimates of BA are larger than the BA detected by satellites (**Figure**  
2173 **S22**). Dense canopy in these remote regions may have led to missed detections of BA.  
2174 Particularly high fire-conducive conditions were predicted across much of southern  
2175 Democratic Republic of the Congo (DRC), as well as northern Angola and parts of the  
2176 Republic of the Congo. However, two notable pockets, in the far northeast of the basin,  
2177 around the border of northeast DRC and South Sudan, and a smaller zone just east of the  
2178 border between the DRC and Republic of the Congo in the north, did not emerge in our  
2179 analysis.

2180 Despite these broad areas of fire-favourable conditions, fires did not become much larger in  
2181 many places. The key reasons for this were moisture and weather limitations. Looking at  
2182 areas at the top 5% of burning, up to 15% more fire could have occurred if fuel had been  
2183 even drier or if atmospheric conditions had been slightly more favourable.





## 2184 5. Attribution to Global Change Factors

2185

2186 Many of the direct drivers and controls on fire events, outlined in **Section 4** (e.g. weather,  
 2187 fuel, moisture, ignition and suppression), are influenced by global change factors such as  
 2188 climate and land-use change. Since the pre-industrial era, global mean temperature has  
 2189 increased by  $\sim 1.3^{\circ}\text{C}$  (Betts et al., 2023; Forster et al., 2025), with greater rates of warming at  
 2190 higher latitudes, adding potential for fuel drying. Climate change has also resulted in altered  
 2191 precipitation patterns, with total rainfall and dry season length increasing or decreasing  
 2192 variably across regions (Polade et al., 2014; Swain et al., 2018; IPCC, 2023a). Meanwhile,  
 2193 changes to fuel load and ignition rates are driven by emissions, climate change and land-use  
 2194 change, with varying effects regionally (Foley et al., 2005; Finney et al., 2018; Romps, 2019;  
 2195 Wang et al., 2024).

2196

### 2197 5.1. Methods

2198

#### 2199 5.1.1. Overview of Attribution Approaches

2200

2201 Fire is a complex phenomenon that impacts societies and ecosystems in many ways, from  
 2202 the extent of BA to the severity of individual fire events. Different user groups seek  
 2203 information on different aspects of fire risk, whether policymakers, communities, fire  
 2204 managers, litigators, or those working to build a broader scientific evidence base. To provide  
 2205 results relevant for a wide range of stakeholders we apply various modelling approaches to  
 2206 fire attribution, drawing on different metrics and attribution techniques, to build a more  
 2207 comprehensive understanding of human influence on recent extreme fire activity. Our  
 2208 approach includes analyses of fire weather indices and BA, alongside a range of attribution  
 2209 metrics suited to these different contexts. Our BA attribution also provides the evidence, in  
 2210 the form of a calibrated probabilistic model, needed to perform future risk projections in  
 2211 **Section 6**.

2212

2213 While most attribution research has focused on the contribution of anthropogenic climate  
 2214 change, humans influence fire occurrence and risk in multiple other ways: the direct  
 2215 influence of people via activities such as land use change and landscape configuration;  
 2216 changes in ignition probability, fire suppression, among others. Considering human-driven  
 2217 climate change separately to changes in human activity, in addition to their combined effect,  
 2218 allows us to disentangle the contributions of local and global environmental change.

2219

2220 Understanding the influence of people or climate on fire and its drivers is inherently  
 2221 challenging, given the complexity of fire processes and the interactions between natural and  
 2222 human systems. Integrating these range of complementary methods - each with its own  
 2223 strengths and limitations, additionally helps build confidence in attribution results that no  
 2224 single method could provide alone. We can therefore identify where there is broad  
 2225 agreement across methods.

2226

2227 To quantify the different ways people affect fire, we apply four types of attribution in this  
 2228 report (**Table 4**), designed to meet diverse user needs and to align with the modelling  
 2229 frameworks currently available:

2230

- 2231 • i) Firstly, our attribution to *anthropogenic climate forcing* explicitly targets the changes  
 2232 driven by anthropogenic greenhouse gas emissions and land-use change, following  
 2233 the IPCC WGI definition (Hegerl et al., 2009; Mengel et al., 2021). We prescribe  
 2234 these emissions in a model to specifically isolate human forcing from natural  
 2235 variability (**Section 5.1.2 and 5.1.3**).
- 2236 • ii) Our attribution to *total climate forcing* considers changes driven by climate change  
 2237 since the pre-industrial period, including both anthropogenic climate forcing and



2238 natural variability in line with the IPCC WGII and the Intersectoral Impacts Model  
 2239 Intercomparison Project 3a (ISIMIP3a) definition of climate change impact attribution  
 2240 (IPCC, 2023b; IPCC 2023c; Mengel et al., 2021). This involves comparing  
 2241 simulations driven with historical reanalysis, our factual, to a detrended  
 2242 counterfactual simulation, where the trend in each climate variable is removed (with  
 2243 both simulations including historical transient land-use change). Therefore only the  
 2244 impacts of climate change are attributed, not distinguishing between anthropogenic  
 2245 or natural causes (Mengel et al., 2021; Burton, Lampe et al., 2024). We perform this  
 2246 between 2003-2019, the overlap between available counterfactual simulations and  
 2247 satellite data used for training in Burton, Lampe et al., 2024.  
 2248 • iii) Our attribution to *socio-economic factors* is applied via the same set of simulations  
 2249 as our attribution to *total climate forcing*. We isolate the role of socio-economic  
 2250 factors by comparing the early industrial period to the late industrial period  
 2251 (1901-1917 versus 2003-2019) using detrended ISIMIP3a data, in which only  
 2252 land-use and population density are allowed to change (Burton, Lampe et al., 2024).  
 2253 • iv) Our attribution to *all forcings* compares the early industrial period in the  
 2254 counterfactual scenario to the last industrial period in the factual scenario, which  
 2255 gives the net effect of all forcings combined (*anthropogenic climate forcing + total*  
 2256 *climate forcing + socio-economic factors*).

2257 The attribution methods described above enable us to assess the influence of climate and  
 2258 socio-economic forcings on fire in each focal region with respect to three different target  
 2259 variables:

- 2260 • i) **Extremes in fire weather during 2024-25.** The FWI is a weather-based indicator  
 2261 of landscape flammability and can provide insight into how fire-prone conditions are  
 2262 likely to be affected by a changing climate.

2263  
 2264 Using the HadGEM3-A large ensemble, we attribute changes in the probability of  
 2265 extreme fire weather conditions to *anthropogenic climate forcing*. This analysis  
 2266 specifically targets the months identified as extreme for each focal event as outlined  
 2267 in **Section 2.2.2** focusing on sub-regional extremes that occur in the model grid cells  
 2268 with the highest FWI values (top 5% of all regional grid cells). By focusing exclusively  
 2269 on these areas of most severe fire weather, this approach provides a proxy for  
 2270 understanding how each forcing influences the locations and times of highest fire risk  
 2271 within the region. We used this methodology as in last year's report. See **Section**  
 2272 **5.1.2** for details.

- 2273 • ii) **Region-wide extreme BA during 2024-25 focal events.** Event specific BA  
 2274 reflects how climate and human factors jointly influence the actual extent of burning  
 2275 during major fire events, offering a direct measure of fire impact on people and  
 2276 ecosystems.

2277  
 2278 Using the ConFLAME model framework we attribute changes in the likelihood of the  
 2279 2024-25 observed total BA across the entire focal region to *anthropogenic climate*  
 2280 *forcing*, *total climate forcing*, *socio-economic factors*, and *all forcings* combined. Like  
 2281 our FWI analysis focuses on the observed peak burning months and captures the  
 2282 overall influence of each forcing on the extent of fire activity at the regional scale.  
 2283 See **Section 5.1.3** for details.

- 2284 • iii) **Background changes in BA this century** using median monthly over recent  
 2285 decades. Background BA shows how climate change is reshaping regional fire  
 2286 regimes over the long term, revealing gradual shifts in baseline fire activity that may  
 2287 go unnoticed in year-to-year variability.

2290



2291 Using fire-enabled dynamic global vegetation models (DGVMs) participating in the  
 2292 Fire Model Intercomparison Project (FireMIP), we attribute changes in median  
 2293 monthly BA averaged over recent decades (2003-2019) to *total climate forcing*,  
 2294 *socio-economic factors*, and *all forcings* combined. This approach provides context  
 2295 on longer-term background fire activity and applies the same methodology as last  
 2296 year's report, though this year focussing on specific focal regions. See **Section 5.1.4**  
 2297 for details.

2298 In each approach we include an explicit estimate of uncertainty. We use bootstrapping to  
 2299 give uncertainty estimates for the FWI Risk Ratios (RR) defined as the ratio between the  
 2300 probability of seeing the observed FWI with the target forcing vs without anthropogenic  
 2301 climate forcing, reported here at 90% confidence intervals. ConFLAME is designed as an  
 2302 uncertainty quantification model (as per our driver assessment, **Section 4.2.4**), giving the  
 2303 likelihood of all possible BA outcomes for each region based on a probabilistic analysis of past  
 2304 burn patterns and environmental conditions. We combine the information from the FireMIP  
 2305 models in a weighted multi-model ensemble to give uncertainty ranges across the models.  
 2306 Each result therefore presents a 5-95<sup>th</sup> percentile probability estimate.

2307 For consistency with last year's report we also report attribution estimates based on methods  
 2308 used in the State of Wildfires 2023-24 report (Jones et al., 2024b):

- 2309 • iv) **Sub-regional extreme BA during 2024-25.** We attribute changes in the  
 2310 likelihood of extreme BA occurring within the model grid cells with the highest BA (top  
 2311 5% of all regional grid cells), focusing on areas where fire activity was most spatially  
 2312 concentrated during peak burning months. This analysis uses the same ConFLAME  
 2313 simulations and forcing scenarios as the region-wide BA attribution and provides  
 2314 insight into how forcings affect the most severely impacted locations within the  
 2315 region. See **Supplementary Text S5.2.3** for discussion of results.

2316 In the coming years, our project seeks to incorporate attribution results based on a broader  
 2317 set of Earth System Models (ESM) to better sample the structural uncertainty arising from  
 2318 differences in process representation across different models (i.e. beyond HadGEM3-A). In  
 2319 this report, we introduce results based on the one ESM as follows:

- 2320 • v) **Background changes in fire weather this decade.** Using the Canadian Earth  
 2321 System Model (CanESM5; Swart et al., 2019), we attribute changes in the frequency  
 2322 of extreme fire weather to *total climate forcing* with the Canadian Fire Weather Index  
 2323 (FWI), identifying how the likelihood of extreme fire weather has changed by  
 2324 comparing the frequency of high Fire Weather Index (FWI) values in pre-industrial  
 2325 and present-day climates. Our analysis covers the years 2016 to 2025, focusing on  
 2326 the climatological months of peak burning during the 2024-2025 fire season. See  
 2327 **Supplementary Text S5.1.2** for methodology and **Supplementary Text S5.2.2** for  
 2328 discussion of results.

2329



**Table 4:** Summary of the attribution approaches used in this report. See **Table S2** for a breakdown on the what each attribution type includes and what each modelling targets.

Term	Definition	Experiments compared	Framework	Application
Event attribution for fire weather and burned area				
Anthropogenic climate forcing	Change in fire weather driven by anthropogenic emissions from greenhouse gases, land-use change and aerosols. As per (Ciavarella et al., 2018; Li et al., 2021)	<b>Factual:</b> HadGEM3-A_ALL: with natural forcing plus human emissions <b>Counterfactual:</b> HadGEM3-A_NAT with natural-only forcing from solar variability and volcanoes	HadGEM3-A attribution ensemble. 0.83 x 0.56 degree resolution	Fire weather (FWI)
			ConFLAME (Kelley et al. 2021; Barbosa et al. 2025b) with merged ERA5/HadGEM3-A product	Burned Area with ConFLAME
Impacts attribution for fire weather and burned area				
Total climate forcing	Changes in FWI since pre-industrial	<b>Factual (2016-2025):</b> present-day climate from CanESM5 SSP585 <b>Counterfactual 1850-1859):</b> Pre-industrial climate simulation	CanESM5 CMIP6 ensemble	FWI
	Changes in BA due to climate change, irrespective of the cause of warming. As per ISIMIP (Intersectoral Impacts Model Intercomparison Project) (Mengel et al., 2021 and Frieler et al., 2024)	<b>Factual (2003-2019):</b> present-day climate (driven by GSWP3-W5E5 reanalysis), CO <sub>2</sub> , land-use and population <b>Counterfactual (2003-2019):</b> Historical climate detrended using seasonally-varying regression on global mean temperature (ATTRICI method, CO <sub>2</sub> fixed at 1901 value, present-day land-use and population)	ISIMIP3a impact attribution. 0.5 degree resolution	FireMIP ensemble and ConFLAME
Socio-economic factors	Changes in BA due to land-use and population change. As per (Burton, Lampe et al., 2024)	<b>Counterfactual (1901-1917):</b> Warming trend removed using ATTRICI method, fixed 1901 CO <sub>2</sub> , limited land use and population change <b>Counterfactual (2003-2019):</b> Warming trend removed using ATTRICI method, fixed 1901 CO <sub>2</sub> , present-day land use and population		
All forcings	Changes in BA due to climate, land-use and population change. As per (Burton, Lampe et al., 2024)	<b>Counterfactual (1901-1917):</b> Warming trend removed using ATTRICI method, fixed 1901 CO <sub>2</sub> , limited land use and population change <b>Factual (2003-2019):</b> Historical climate driven by reanalysis	ISIMIP3a impact attribution	FireMIP ensemble

#### 5.1.2. Attributing Extremes in Fire Weather during 2024-25

We use two complementary approaches to attribute changes in the probability of high fire weather, measured using the Canadian Fire Weather Index (FWI), to anthropogenic climate change. The first method uses a targeted large-ensemble weather model simulation to assess the influence of climate change on the 2024/25 fire seasons directly. The second



method applies a longer-term, probabilistic framework using simulations from a fully coupled Earth system model.

The first approach follows the same methodology used in the previous State of Wildfires report (Jones et al. 2024b). This is an established approach to attribute changes in the probability of high fire weather, measured using FWI, to anthropogenic climate forcing. This method has been previously used by the World Weather Attribution (Barnes et al., 2023; Barnes et al., 2024; Barnes et al., 2025), using outputs from the HadGEM3-A large ensemble (Ciavarella et al., 2018). Our approach builds on the methodology introduced by Stott et al. (2004) for attributing extreme weather events, and it has been applied in other attribution studies targeting fire weather, such as Li et al. (2021).

As outlined in **Section 4.1.1**, the FWI is used operationally and in research contexts to rate fire danger based on meteorological conditions. Due to the availability of model output variables we use maximum daily temperature at 1.5 m as a proxy for noon values, total daily precipitation, mean daily relative humidity at 1.5 m, and mean daily wind speed at 10 m, following Perry et al. (2022). We calculate the daily FWI for the months of 2024-25 peak BA anomaly for each focus region, using the same month and region for validation over the historical time series (1960-2013). Note that at time of writing, data for HadGEM3-A was only available till the end of 2024, so we do not report on Southern California fires using this method.

We validate and bias-adjust the model estimates of high FWI for the period 1960-2013 by comparing a 15-member HadGEM3-A ensemble with ERA5 reanalysis data (C3S, 2024) representing “observed” FWI. The 0.25 degree resolution observed FWI from ERA5 was coarsened by linear interpolation (calculated by extending the gradient of the closest two points) to match the 0.5 degree model grid. We compare the time series of individual components of the FWI (**Figure S49-S55**), and the distribution of the modelled and observed FWI (**Figure S56-S58**), and apply a simple linear regression to find the bias correction required for the 2023 model output. Before bias-adjustment, the modelled FWI is generally higher than the observed FWI for Amazonia and Congo, which modelled FWI compares more favourably to ERA5 in the Pantanal. The correction adjusts the trend and absolute value while maintaining variability, and the model successfully reproduces the observed distribution after applying the correction in each region (see **Supplementary Text S9**).

For the events occurring in the 2024 fire season, we calculate the FWI from the HadGEM3-A model simulations comprising 2 experiments of 525 members each, one driven by all forcings including historical greenhouse gas emissions, aerosols, zonal-mean ozone concentrations, land-use change and natural forcing (ALL), and a second counterfactual simulation with natural-only forcing from solar variability and volcanic emissions, and 1850 land-use (NAT) (**see Table 4**). By applying the bias-adjustment from the previous step, and comparing the fire weather in the two simulations to the 2024-25 observed FWI from ERA5, we calculate the change in probability of high fire weather due to anthropogenic climate forcing. The standard definition of “high fire weather” that we use is the 95th percentile of daily Fire Weather Index (FWI) values across all grid cells and days during the season. However, as in last year’s report and in Burton et al. (2025), when the region is small or when climate conditions significantly influence the higher FWI in our counterfactual, leading to few ensemble members reaching higher FWI values, we need to adjust our definition of extreme. In this year’s assessment, we apply the 90th percentile threshold for the Northeastern Amazonia and Congo regions, as the differences between the factual and counterfactual ensembles are so large that very few counterfactual members reach the 95th percentile of the factual distribution, making the calculation of risk ratios unreliable.



### 2391 5.1.3. Attributing Region-wide Extreme BA during 2024-25

2392 We use the ConFLAME framework for direct BA attribution. For this report, we apply two  
 2393 configurations of the ConFLAME attribution framework to attribute anomalies in BA fraction  
 2394 during the peak burning months of the 2024-25 fire season:

- 2395 • A **near real-time (NRT) setup** for targeting anthropogenic climate forcing, which  
 2396 largely mirrors the configuration used in the drivers attribution section (see **Section**  
 2397 **4**), assesses how human influences affected the likelihood of BA via meteorological  
 2398 driver of fire conditions observed during the specific 2024 events. This setup targets  
 2399 the actual environmental conditions leading up to and during the events, providing  
 2400 the most up-to-date picture of climate and socioeconomic influences. By focusing on  
 2401 the precise timing and location of the event, the NRT configuration provides an  
 2402 up-to-date and high-resolution picture of how anthropogenic climate forcings have  
 2403 influenced the likelihood of extreme fire activity.
- 2404 • The **Inter-Sectoral Impact Model Intercomparison Project (ISIMIP) 3a setup**,  
 2405 previously used with ConFire in last year's report. This setup enables the analysis of  
 2406 how often fire events such as those in 2024 might occur under environmental  
 2407 conditions from 2002 to 2019. While 2024 itself is excluded, we look for similar  
 2408 events in this earlier period to understand how likely they would be without the recent  
 2409 changes in climate and land use. This broader, long-term setup helps us assess how  
 2410 the background risk is shifting over time and complements the more event-specific  
 2411 analysis shown earlier. This setup also directly links to the future projections  
 2412 presented in **Section 6**, which also use ISIMIP. As an addition to last year's report's  
 2413 set up, our ISIMIP set up also includes changes in land use and cover (measured as  
 2414 the difference between tree cover and agricultural fraction since the previous year) in  
 2415 the direct socioeconomic forcing attribution (see **Table S3**).

2416 As each configuration uses data that is somewhat similar to our Fire Weather (in the case of  
 2417 NRT) or FireMIP (when using ISIMIP) set ups, neither setup is fully independent of our other  
 2418 two modelling approaches. However, the fire modelling in ConFLAME captures different  
 2419 components of fire than FWI or FireMIP by attributing BA during the events themselves. The  
 2420 advantage of ConFLAME is that it bridges the gap between event-focused real-time  
 2421 attribution and global process-based fire models. That said, future iterations would benefit  
 2422 from incorporating more independent, preferably observation-driven input datasets to  
 2423 improve robustness and reduce potential structural alignment across methods.

2424 Each attribution experiment involved training ConFLAME using “observed” or reanalysis  
 2425 driving data against MODIS BA (as described in Section 4). We then ran the framework with  
 2426 factual driving data followed by a separate run counterfactual with the effect we aim to  
 2427 attribute (e.g., all forcings, climate, or socioeconomic drivers) removed. We conducted  
 2428 paired ConFLAME factual and counterfactual predictive model simulations at monthly  
 2429 resolution, using a structure similar to that in **Section 4.1.2**, with specific drivers grouped into  
 2430 controls in **Table S1** and evaluated the model following Barbosa (2025; **Section 4.1.2**). We  
 2431 separately train ConFLAME on 50% of the data between 2003-2011 and perform evaluation  
 2432 on years 2012-2019. Further details of the model fitting and validation can be found in  
 2433 **Supplementary Text S5.1.3** and **Supplementary Text S9.1**, respectively.

2434 To determine the impact of total climate forcing, socioeconomic factors and total forcing on  
 2435 increased BA during our focal events using the ISIMIP configuration, we conducted paired  
 2436 sampling of monthly BA in the target months (see Table 4). Total climate forcing's factual  
 2437 driving data uses the same 2003-2019 GSWP3-W5W5 reanalysis data used for training for  
 2438 factual, while we use detrended data for the counterfactual, whereas socioeconomic used  
 2439 detrended data 2003-2019 for factual and 1901-1917 for counterfactual. Total forcing used  
 2440 2003-2019 from GSWP3-W5W5 for the factual and 1901-1917 from detrended





GWSP3-W5W5 for the counterfactual. We used paired sampling to account for uncertainty in the relationships between drivers and BA, ensuring co-variation between experiments (as in Kelley et al., 2021). In total, we drew 1,000 samples across the 17 years of each simulation, resulting in 17,000 paired samples.

We use two key metrics to assess how our target factors have influenced BA during extreme fire events. We report attribution metrics both for the entire region (reported in the main text, **Section 5.2.2**) and for "sub-regional extremes" - the grid cells with the top 5% of BA, to also assess how anthropogenic factors may have influenced the most severely affected areas (in **Supplementary Material S5.2.2**). The Amplification Factor (AF) tells us how much bigger (or smaller) the BA was because of a specific factor. It works by comparing factual BA for BAs as large or larger than what was observed during the target months versus counterfactual. Observed BA is calculated in a manner consistent with the model outputs, by averaging BA across either the entire region or the top 5% of BA within the target region and month. Observations are derived from monthly MCD64A1 data. In near-real-time (NRT) mode, we do this for the specific year of interest. In the ISIMIP setup, we compare across many years (2003-2019). An AF greater than 1 means climate change increased BA. For example, an AF of 2 means twice as much area burned. We calculate this across our model simulations and report both the central estimate (median) value and the range of uncertainties based on 10th to 90th percentiles. Because the Early Industrial factual simulation in our ISIMIP setup includes no human influence on the climate, we first adjusted the target event's BA to the level expected without climate change. This adjustment involved identifying the percentile of the observed BA in the factual simulation, and then finding the BA at that same percentile in the counterfactual simulation

For the NRT set up, we can also use the Risk Ratio (RR), which shows how much more (or less) likely the target factor made a fire event of this size. Similarly to **Section 5.1.2**, it compares the chance of seeing the observed BA under today's climate to the chance under a climate without human influence. A RR above 1 means climate change made the event more likely; a RR below 1 means it made it less likely.

#### 5.1.4. Attributing Background Changes in Burned Area this Century

We assess how BA has changed over recent decades due to climate and socio-economic drivers using the FireMIP ("Fire Model Intercomparison Project") attribution framework developed by Burton, Lampe et al. (2024). This method uses state-of-the-art global FireMIP models, employing each model's native fire scheme, to estimate the contribution of different drivers to BA by comparing simulated fire activity under different ISMIP3a experiments setup. We quantify the effect of *climate forcings* on BA by comparing the present-day factual burned area to the present-day counterfactual BA. The effect of *socio-economic forcings* is assessed by comparing the present-day of the counterfactual simulations to the early-industrial of the counterfactual simulations since long-term climate is stationary in these simulations. Lastly, we find the effect of *all forcings* by comparing the present-day factual BA to the early-industrial counterfactual BA.

The attribution focuses on changes in median monthly BA during 2003-2019 and uses a weighted multi-model ensemble, where weights reflect each model's ability to reproduce observed regional fire anomalies in GFED5 and FireCCI datasets. All results are reported as relative anomalies, and uncertainty is assessed via a random resampling of the weighted ensemble, including a stochastic parameter which accounts for uncertainty on the performance of the entire ensemble. This approach provides a robust and conservative estimate of trends, particularly suited to assessing regional-scale fire responses.



In contrast to last year's report, where results were reported for IPCC AR6 regions containing the focal fire zones, this year we refined the analysis by tailoring the attribution directly to the specific areas featured in the report. This regional adjustment enhances the relevance and interpretability of the attribution results for each case study.

For full details on the method, model evaluation, and baseline results across all IPCC regions, see Burton, Lampe et al. (2024).

## 5.2. Results

### 5.2.1. Extremes in Fire weather during the 2024-25 Focal Events

#### 5.2.1.1. Northeast Amazonia

We find that the fire weather conditions in Northeast Amazonia during January-March 2024 were significantly more likely due to anthropogenic climate forcing, with the probability of experiencing fire weather at or above the levels observed during the event being 32 to 73 times higher in the factual simulations compared to the counterfactual simulations (Figure 13). A substantially larger proportion of the factual ensemble exceeds the observed 90th percentile of FWI from the ERA5 reanalysis than in the counterfactual ensemble (Figure 13), indicating that high fire weather conditions during early 2024 were much more likely in a climate influenced by anthropogenic emissions.

2515  
 2516

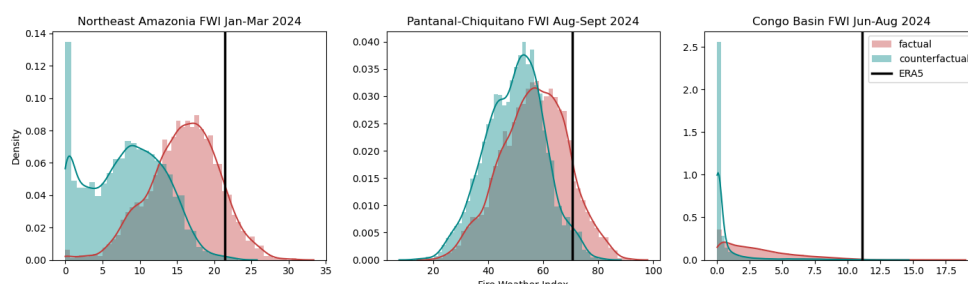


**Figure 13:** High fire weather conditions in 2024/25: Probability distributions of FWI in the HadGEM3 ensemble for the focal fire season in each region, comparing simulations with anthropogenic and natural forcings (red; factual) to natural-only forcings (teal; counterfactual). Black line shows ERA5 reanalysis. The x-axis shows the regional average of high-percentile FWI days: 89th percentile for Jan-Mar in Northeast Amazonia (left), 95th percentile for Aug-Sep in the Pantanal and Chiquitano (middle), and 90th percentile for Jun-Aug in the Congo Basin (right).

2525

#### 5.2.1.2. Pantanal and Chiquitano

The high fire weather conditions experienced during the peak anomaly in fire activity in August-September 2024 were 4.2-5.5 times more likely due to anthropogenic climate forcing (Figure 13). While this increase is smaller than that estimated for Northeast Amazonia, the narrower range suggests we have greater confidence that human influence increased the probability of extreme fire weather conditions in this region.

2533

Our results largely agree with the rapid attribution analysis from the World Weather Attribution (WWA) initiative (Barnes et al., 2024), though with smaller uncertainty ranges, WWA found that the accumulated fire weather conditions, represented by the June Daily



Severity Rating (DSR), were 4.6 (1.1 to 20) times more likely due to human-induced climate change. The DSR, a fire-suppression oriented rescaling of the FWI, is commonly used to assess the cumulative fire weather danger over monthly timescales (Van Wagner, 1987). WWA focused on June conditions because of their role in setting up the severe fire season that followed, and their direct relevance to the large BA that severely impacted wildlife and livelihoods in the Pantanal. Observations also indicated a decrease in annual rainfall of -23.5% (-46% to +5%) in the region, though this trend was not reproduced by climate models (Barnes et al., 2024).

2545

#### 2546 **5.2.1.3. Southern California**

2547

Due to the lack of data availability from HadGEM3-A for 2025, we were unable to perform bespoke FWI attribution analysis for Southern California. However, in previously published analysis, the rapid attribution study by WWA (Barnes et al., 2025) found that the extreme fire weather conditions (peak FWI) in the coastal southern California ecoregion surrounding Los Angeles during January 2025 were 1.37 (0.48 to 3.6) times more likely in comparison to the pre-industrial climate, suggesting that climate change may have lead to a moderate increase in fire weather, though causing a reduction in fire weather is also plausible and within the confidence range. As the impacts of Los Angeles fires related to extreme single days of wildfire spread, the monthly maximum FWI value averaged over the study region was used here. This result is complemented by the increasing likelihood of an extended dry season in the region. Decreased October-December precipitation allowed for protracted fuel drying, resulting in a more likely overlap between dry conditions and the winter Santa Ana winds. Observed trends (ERA5) in the October-December standardised precipitation index found that the dry conditions leading up to the LA fires were 2.4 (0.33 to 20.9) times more likely than in the pre-industrial climate. Using analogue-based attribution (Vautard et al., 2016), the cut-off-low circulation pattern associated with the strong Santa Ana winds around Los Angeles was found to have increased in likelihood by 2.5 (0.4 to 17) times.

2565

#### 2566 **5.2.1.4. Congo Basin**

2567

The high fire weather conditions observed across the Congo Basin during June-August 2024 were unusual in both the factual and counterfactual simulations. Our analysis indicates that these conditions were 3.0-8.0 times more likely due to anthropogenic climate forcing (Figure 13). The entire FWI distribution in the factual ensemble is shifted toward higher values compared to the counterfactual ensemble. This means that across the full range of fire weather conditions, the probability of conditions conducive to burning is substantially greater in a climate influenced by human emissions.

2575

#### 2576 **5.2.2. Region-wide extreme BA during 2024-25**

##### 2577 **5.2.2.1. Northeast Amazonia**

2578

We find strong evidence that anthropogenic climate forcing contributed to increased regional BA during the January-March 2024 fire season in Northeast Amazonia. Our analysis shows a 96% likelihood (very likely under IPCC definitions of confidence) that BA was higher than it would have been without anthropogenic climate forcing (Figure 14). We estimate that regional BA was approximately 4.3 times larger (our *Amplification Factor*) than it would have been in a counterfactual world without anthropogenic climate forcing (Figure 14; Table 5), with a 90% confidence range of 1.02 to 25.32. While the central estimate suggests a quadrupling of BA, the wide uncertainty range reflects the natural variability of fire processes. Nonetheless, even the lower bound supports a small but clear increase.

2588

We assess the risk ratio, the likelihood of an event like January-March 2024 occurring under current climate conditions versus a pre-industrial baseline (Table 5). Based on historical data

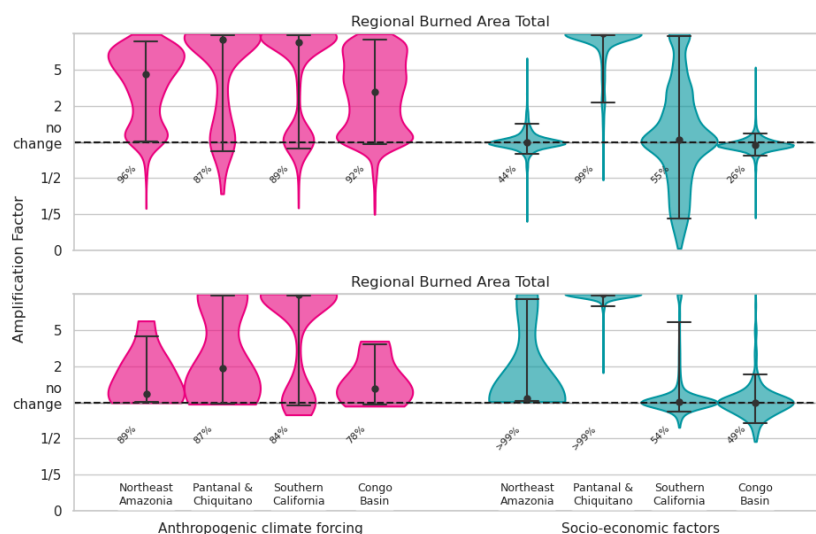


provided as evidence for the model, we estimate that a similar event is now 2.1 times more likely due to anthropogenic climate forcing. This figure captures the longer-term climate signal that would shape the overall frequency of such events. When we control for meteorological variability by comparing simulations with and without anthropogenic forcing but using identical weather patterns from 2024, we see slightly stronger effects (**Table 5**). The risk ratio rises to 2.7, and the upper bound of our Amplification Factor increases dramatically (over 100-fold in some ensemble members). This suggests that climate forcing alone could account for much, or possibly all, of the burning under certain conditions, although the central estimate remains close to our previous assessment.

Climate influence was widespread across Northeast Amazonia, most of the entire region showing a greater likelihood of increased BA due to anthropogenic forcing (**Figure 15**). The strongest attribution signal occurred in the Southern Guiana Shield Fringe Forests, where climate change was very likely ( $\geq 90\%$  confidence) to have increased BA. These forests are particularly important due to their extensive areas of primary rainforest and high ecological sensitivity. In contrast, attribution confidence tapered to around 70-80% in the Guiana Coastal Plain, and only a few localized areas, particularly in savanna mosaics, showed weak or no signal.

The region's ecological heterogeneity, encompassing floodplain forests, natural grasslands, and savanna formations, means fire impacts vary considerably. Some savanna systems are naturally adapted to low-intensity surface fires (Alvarado et al., 2020; Pivello et al., 2021), but increased frequency and intensity of burning can overwhelm their resilience. Fire-sensitive ecosystems, such as humid forests and wetlands, are even more vulnerable, with increased fire pressure posing a long-term threat to ecosystem stability and biodiversity (Alvarado et al., 2020), and it is these ecosystems where anthropogenic climate forcing is most likely causing increase in burning.

For regional BA totals, the likelihood that socioeconomic drivers increased BA was 47% (**Figure 14**), indicating no clear signal that human landscape modification influences the extent of burning in seasons like early 2024. The estimated Amplification Factor was 1.08, but with a wide 90% confidence interval of 0.44 to 7.21 (**Table 5**). The wide confidence range, from potential halving of BA to a seven-fold increase, indicates that our model finds socioeconomic drivers to have a highly uncertain influence on regional fire activity during this period. This uncertainty likely reflects both the limited resolution of the socioeconomic variables used (e.g. population density, broad land cover classes) and the challenge of capturing the complex ways that human activities interact with fire. It is also possible that opposing effects such as suppression in one area versus ignition pressure in another, could be offsetting each other in regional statistics, though the modelling framework does not resolve these interactions explicitly.



2634

**Figure 14:** Probability density of the Amplification Factor (AF) for each region, showing how different factors influenced the extent of burning for each focal region. The top panel displays results for the entire region, while the bottom panel focuses on sub-regional extremes (defined as the grid cells in the top 5% of BA fraction). Anthropogenic climate forcing targets the 2024/25 focal moths using NRT set up with counterfactuals using all HadGEM ensemble members; socioeconomic factors uses the ISIMIP set up, looking at increased likelihood of 2024/255 like events in 2003-2019 with climate trends removed vs 1900-1917. An AF greater than 1 indicates that the factor contributed to an increase in burned area extent; a AF less than 1 indicates a reducing influence; a value near 1 suggests no change. Vases show probability distribution of AF, dots within each vase show central estimate and bars show 90th percentile confidence range. The percentages lower left of each vase shows the likelihood of each factor increasing burned area.

2647

#### 5.2.2.2. *Pantanal and Chiquitano*

The Pantanal and Chiquitano regions showed one of the strongest anthropogenic climate change signals of all focal regions studied here or in previous reports (Jones et al., 2024b). The likelihood that anthropogenic climate forcing increased the observed regional BA is estimated at 88% (**Figure 14**), indicating anthropogenic climate forcing likely drove an increase in BA (**Table 5**). The total BA was 34.5 times higher (our *amplification factor*) in the factual ensemble than in the counterfactual, although the wide uncertainty range of 0.84 to 100 suggests the effect of anthropogenic climate change could range from minimal to extremely large (**Table 5**). When internal meteorological variability is removed (using ensemble-mean), the estimated amplification factor remains largely unchanged. The model-based risk ratio for the event is 3.3, meaning the observed extent was roughly three times more likely due to anthropogenic climate change.

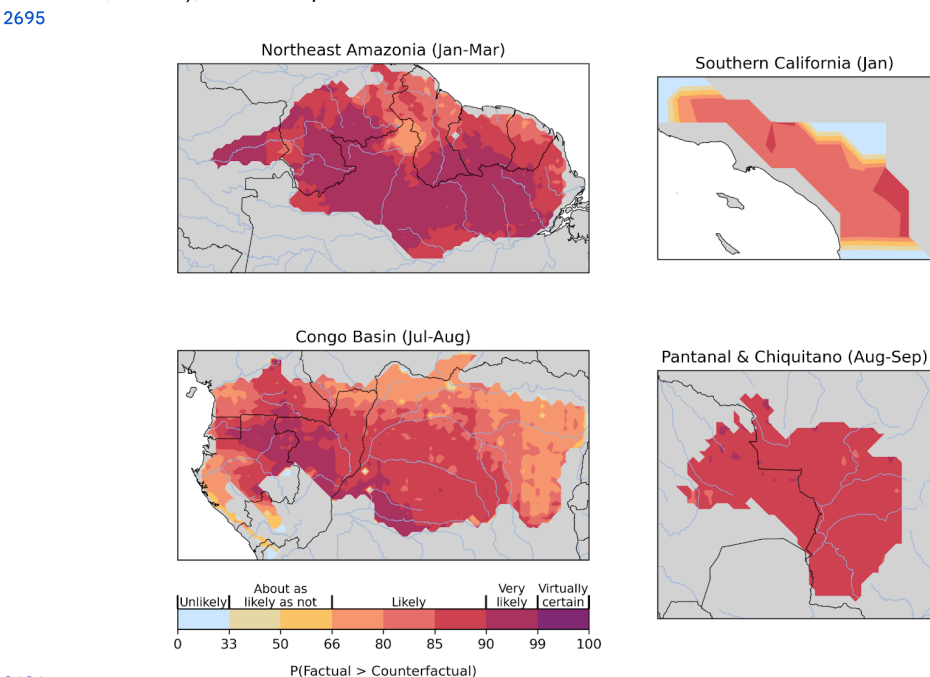
Climate influence was relatively consistent across the region (**Figure 15**). Uniformity in attribution results may reflect the broad scale influence of anthropogenic climate change. It also suggests that climate change is amplifying fire risk even in areas with relatively intact ecosystems or seasonal wetlands, underscoring the vulnerability of these landscapes to the ongoing warming. However, the wide range in uncertainty highlights the need for improved observational data and better representation of fuel-moisture dynamics in fire-prone wetland mosaics such as Pantanal.



Socioeconomic factors show a very strong role for direct human influence in shaping BA anomalies during 2024-like events in the Pantanal and Chiquitano region. At the regional scale, the likelihood that socioeconomic factors increased BA is 99%, with an estimated amplification factor (AF) exceeding 100 (90% confidence interval: 2.12 to 100). This means that even under conservative estimates, human activity at least doubled BA during comparable fire years. In sub-regional extremes, the Amplification Factor range is even more extreme with a central estimate of more than 100 (lower 90% confidence bound of 16.24), with a similarly high likelihood (>99%) that human activity contributed. This implies that the vast majority of burning in these most severely affected areas was directly linked to socioeconomic drivers and would have been extremely unlikely in their absence.

These results confirm that direct human influences, such as land use effects and human ignition sources, can be as significant, or more so, than climate change in raising the likelihood of extreme wildfire events in the Pantanal-Chiquitano region. This is particularly important and promising because these factors can be directly addressed through local policies, incentives and enforcement actions, offering clear and locally isolated pathways for intervention and risk reduction alongside global action on climate change. The consistency between regional and sub-regional attribution indicates that these influences are not just diffuse but are concentrated in areas of greatest impact. Even the lower bounds of the confidence intervals provide compelling evidence that anthropogenic pressure substantially elevated fire outcomes.

These results agree with a growing body of evidence pointing to compounding non-linear effects of human and climatic drivers in the Pantanal (Marques et al., 2021, Barbosa et al., 2022, Santos et al., 2024). While this attribution includes some of the human drivers identified in the region, such as land use change, other key drivers, like wetland degradation and water extraction (which can intensify fire risk by drying out the landscape; Barbosa et al., 2022, 2025b), are not captured here.



2696





**Figure 15:** Regions where anthropogenic climate forcing most likely influenced fire activity during the 2024-25 fire season, based on the ConFLAME Near Real-Time setup. Maps show the probability that burned area (BA) was higher in the factual (climate change-influenced) scenario compared to the counterfactual (no climate change) scenario-based on the proportion of ensemble members where BA was greater in the factual than in the counterfactual scenario. Results are shown for focal fire periods in each region: January-March 2024 for Northeast Amazonia; August-September 2024 for the Pantanal and Chiquitano; June-August 2024 for the Congo Basin; and January 2025 for Southern California. Colourbar descriptive labels are based on IPCC uncertainty definitions (Mastrandrea et al. 2010).

2707

### 2708 5.2.2.3. *Southern California*

2709

Anthropogenic climate forcing likely contributed to the high levels of BA observed in Southern California in January 2025, with a likelihood of increased burning of 89%. The amplification factor (AF) was estimated at 24.8, though with a wide uncertainty range (90% confidence interval 0.89 to 100), indicating that the influence could have ranged from negligible to extremely large. Despite this spread, the ensemble-mean counterfactual results largely agree, reinforcing confidence that anthropogenic climate forcing increased the likelihood of the event. The risk ratio of 2.3 suggests that similar fire conditions are more than twice as likely in the present-day climate compared to a scenario without climate change. This elevated risk was in January, outside the region's typical peak fire season, suggesting that anthropogenic forcing may be expanding the seasonal window during which large fire events can occur.

2721

There is no clear evidence that socioeconomic factors occurring on the landscape increased the likelihood of January 2025-like regional BA in Southern California during 2002-2019. The estimated likelihood of an increase is 55%, with a highly uncertain amplification factor (AF = 1.04 [0.17-85.58]). As with the climate attribution, this likely reflects the small size of the region and limited signal in long-term data.

2727

### 2728 5.2.2.4. *Congo Basin*

2729

Anthropogenic climate forcing likely increased the total area burned across the Congo Basin during June to August 2024. The likelihood of an increase is estimated at 92%, with an amplification factor (AF) of 2.69, meaning the event-scale BA was nearly three times higher than it would have been without forcing. However, there remains some uncertainty: while the best estimate points to a substantial increase, the range spans from a very small influence to a more than 30-fold increase (90% confidence range of 0.96 to 33.96).

2736

When we account for internal climate variability by averaging across all ensemble simulations (rather than using only the observed event conditions), the signal strengthens substantially. In this case, anthropogenic climate change appears to have increased BA by a factor of 15 (90% confidence range: 0.97 to over 100), with a risk ratio of 2.6, which shows a more consistent pattern of increased fire risk due to long-term warming and drying trends. Unlike other regions, where most of the uncertainty stems from how fire responds to environmental conditions, in the Congo Basin uncertainty in the meteorological response to climate change itself plays a larger role.

2745

The influence of climate change also varied significantly within the region. The strongest signal appears in the southern parts of the Congo Basin, particularly the Southern Moist Forests, where our modeling frameworks suggest climate change very likely (90-95% likelihood), using IPCC terms definition **Figure 15** increased BA. Further north, in the DRC's northern moist forests, the likelihood was lower (50-80%), and in the Southern Gabon



2751 transition forests, there was little to no signal. These spatial differences may reflect varying  
2752 sensitivities to rainfall patterns, fuel conditions, or other landscape features, and highlight the  
2753 importance of region-specific analysis.

2754

2755 There is no clear signal that socioeconomic factors increased BA during the June-August  
2756 2024 fires in the Congo. Across the region as a whole, the likelihood of increased burning  
2757 due to population density and land-use change was 26%, with an amplification factor (AF) of  
2758 0.94 (90% confidence interval: 0.70 to 1.17), suggesting a small or even slightly dampening  
2759 influence. At the sub-regional level, attribution remains uncertain. The likelihood of increased  
2760 BA in the most affected grid cells was estimated at 62%, with an AF of 1.00 [0.68-1.69].

2761



**Table 5:** Summary of attribution results for burned area (BA) and fire weather indices during key fire events across Northeast Amazonia (Jan-Mar 2024), Pantanal-Chiquitano (Aug-Sep 2024), Congo Basin (Jul 2024), and Southern California (Jan 2025). Values are reported for both burned area (BA) across the full region and sub-regional extremes -the areas that saw the most burning (see Figure 5). Metrics include the amplification factor (AF; the ratio of BA under the influence of the assessed factor relative to the counterfactual), risk ratio (RR) of fire weather index during the events, and % change in annual mean (background) BA. Results are shown for different configurations: anthropogenic meteorological forcing (using near real-time and ensemble-mean setups), total climate forcing, and socio-economic factors. Values are reported as median [5th-95th percentile] ranges, with likelihoods indicating the confidence that the factor contributed to increased burning or extreme fire weather. Colours indicate IPCC-defined confidence or likelihood categories (Mastrandrea et al., 2010). Where likelihoods are not explicitly provided, colours reflect the lowest plausible category based on the reported confidence range.

Variable	Metrics	Sources	Northeast Amazonia	Pantanal and Chiquitano	Southern California	Congo Basin
Anthropogenic climate forcing						
Fire Weather Index	Risk Ratio (RR)	HadGEM	31.96-72.64	4.16-5.45		3.04-8.00
	RR	CanESM5	1.9 [1.5, 53.3]	12.3 [3.4, 76.9]	1.7 [1.6, 1.8]	1.3 [0.7, 1.7]
	RR	WWA		4.6 [1.1, 20]*	1.37 [0.48, 3.6]+	
	Intensity Delta	WWA		+39% [13%, 71%]*	+5.7% [-10, 27]+	
Burned Area (BA)	Amplification factor (AF)	ConFLAME/ HadGEM ensemble	4.33 [1.02, 25.32]	34.47 [0.84, >100]	24.79 [0.89, >100]	2.69 [0.96, 33.96]
	RR		2.1	3.3	2.3	1.6
	AF	ConFLAME/ HadGEM mean	13.25 [1.02, >100]	>100 [0.82, >100]	>100 [0.82, >100]	14.76 [0.97, >100]
	RR		2.7	3.5	2.9	2.6
Areas of highest BA	AF	ConFLAME/ HadGEM ensemble	1.17 [1.01, 5.13]	1.91 [0.98, >100]	>100 [0.95, >100]	1.29 [0.96, >100]
	R		2.2	2.4	2.9	1.8
	AF	ConFLAME/ HadGEM mean	1.11 [0.95, 1.94]	>100 [0.96, >100]	>100 [0.98, >100]	1.24 [0.84, >100]
	RR		1.6	3.7	3.8	1.3



Variable	Metrics	Sources	Northeast Amazonia	Pantanal and Chiquitano	Southern California	Congo Basin
Total climate change						
BA	AF	ConFLAME/ ISIMIP	1.01 [0.88, 1.15]	>100 [2.73, >100]	1.07 [0.68, 2.83]	1.08 [0.95, 1.43]
Areas of highest BA	AF	ConFLAME/ ISIMIP	1.02 [0.94, 1.13]	>100 [4.92, >100]	1.00[0.91, 1.86]	1.14 [0.87, 3.02]
Background BA		FireMIP	-6% [-11%, - 2%]	10% [6, 15%]	7% [2%, 12%]	54% [45%, 63%]
Socio-economic factors						
Burned Area	AF	ConFLAME/ ISIMIP	0.99 [0.8, 1.41]	>100 [2.12, >100]	1.04 [0.17, 85.59]	0.94 [0.7, 1.17]
Max. Burned Area	AF	ConFLAME/ ISIMIP	1.02 [1.07, 1.13]	>100 [16.24, >100]	1.00 [0.85, 6.65]	1.00[ 0.68, 1.69]
Background Burned Area		FireMIP	10% [3%, 17%]	-7% [-12%, -2%]	-3% [-7%, -1%]	-16% [-21%, -11%]
All forcings						
Burned Area	AF	ConFLAME/ ISIMIP	0.99 [0.81, 1.47]	1.08 [0.44, 7.21]	1.05 [0.26, 64.26]	1.01 [0.86, 1.42]
Max. Burned Area	AF	ConFLAME/ ISIMIP	1.01 [0.96, 1.10]	1.04 [0.98, 8.26]	1.00 [0.86, 12.16]	1.06 [0.73-4.44]
Background BA		FireMIP	1% [-6%, 9%]	3% [-2%, 9%]	2% [-2%, 7%]	25% [18%, 33%]
*WWA results for June DSR and 2774 + January max FWI						
Virtually certain > 99%	Very likely >90%	Likely >66%	About as likely as not 33-66%	Unlikely, <-33%	Very unlikely <10%	Exceptionally unlikely <1%

2772

2773



### 2775 **5.2.3. Background Changes in Burned Area this Century**

2776

2777 We assess how climate and socio-economic drivers have influenced changes in background  
 2778 levels of BA for each focus region using the global fire model attribution framework  
 2779 introduced by Burton, Lampe et al. (2024), adapted this year to match the specific  
 2780 geographic areas analysed in this report (see methods in **Section 5.1.4**). Results represent  
 2781 the change in median monthly BA during 2003-2019 compared to a counterfactual scenario  
 2782 in which anthropogenic climate change or changes in socio-economic factors were removed.  
 2783 This is distinct from our analyses focussing on the attribution of individual focal events in  
 2784 **Sections 5.2.1 and 5.2.2**.

2785

#### 2786 **5.2.3.1. Northeast Amazonia**

2787

2788 Total climate forcing led to a modest but consistent decrease in background BA between  
 2789 2003-2019, with a median change of -6% [-11%, -2%] compared to a counterfactual without  
 2790 climate change. Unlike the earlier attribution method (**Section 5.2.2**), which focused on  
 2791 extreme 2024-like events, this model captures long-term, background fire activity, including  
 2792 broader fuel-climate interactions.

2793

2794 The reduction in BA may reflect increased moisture or changes in vegetation structure that  
 2795 reduce flammability, though the exact mechanism is unclear. Recent observational analyses  
 2796 suggest a rise in wet-season (December to May) rainfall and a reduction in dry days in  
 2797 northern Amazonia over the past two decades (Barichivich et al., 2018; Almeida et al.,  
 2798 2017), which could contribute to these trends if captured in the climate inputs. The  
 2799 underlying models used in this attribution framework used here also features tighter coupling  
 2800 between vegetation, climate, and fire than the event-based approach, which may explain  
 2801 some of the differences, though it remains difficult to determine whether these are due to  
 2802 improved fuel representation or simply reflect a contrast between background and extreme  
 2803 conditions.

2804

2805 Socioeconomic changes are estimated to have increased the background BA in Northeast  
 2806 Amazonia by +10% [3%, 17%] in 2003-2019 compared to 1901-1917. This signal aligns well  
 2807 with the earlier analysis of 2024-like events (**Section 5.2.2.1**) but is more narrowly  
 2808 constrained, reinforcing the role of human-driven changes as a key influence on regional fire  
 2809 activity, as identified in many previous studies. For instance, recent studies on land use and  
 2810 fire dynamics in the Amazonia region points to rising fire activity associated with expanding  
 2811 agricultural areas, secondary vegetation, and newly deforested areas (Silveira et al., 2022).  
 2812 Human activities remain the primary source of ignition, mainly through practices such as  
 2813 deforestation, pasture maintenance, and crop field burning, often intensified under dry  
 2814 conditions (Lapola et al., 2023).

2815

#### 2816 **5.2.3.2. Pantanal and Chiquitano**

2817

2818 We find a modest but robust signal of climate-driven change in background fire activity.  
 2819 Between 2003 and 2019, total climate forcing is estimated to have increased the average BA  
 2820 by 10% [6%, 15%]. The relatively narrow confidence range suggests strong model  
 2821 agreement and indicates that the region's area burned has already been measurably  
 2822 affected by long-term climatic shifts. This aligns with broader lines of evidence that highlight  
 2823 the Pantanal's vulnerability to changes in rainfall patterns and dry season intensity, which  
 2824 influence both fuel availability and flammability (**Section 4.2**). These findings are also  
 2825 consistent with attribution results for extreme events in 2024 (**Section 5.2.2.2**), which also  
 2826 showed a high likelihood of increased burning, albeit with greater uncertainty.

2827



We estimate that socioeconomic drivers contributed a reduction in background BA of 7% [-12%, -2%] compared to pre-industrial conditions. This suggests that long-term changes in land use and management, including shifts in agricultural practices, may have contributed to a modest but consistent suppression of average fire activity over the past two decades. The attribution of socioeconomic influence on BA in the Pantanal presents an interesting contrast with the attribution of focal event BA in the previous section, which suggests that socioeconomic factors very likely increased BA (**Section 5.2.2.2**). This contrast may point to important temporal and functional differences:

- Long-term socioeconomic changes, such as improved fire control in settled areas or changes in land use, could suppress background fire activity.
- Yet, during extreme conditions, these same systems may fail to contain fires, or different areas (e.g. the interface between private properties and protected areas, Barbosa et al., 2022) may dominate the fire signal.

Still, the disagreement raises a cautionary flag. While the two methods target different timescales and use different models, their confidence intervals do not fully overlap, suggesting that at least one framework may be underestimating uncertainty or missing key processes. It also reinforces the importance of using multiple, independent lines of evidence in attribution work and, specifically for the Pantanal, shows that more work is needed to assess the balance between human impact on background vs extreme BA along with the modelling techniques used to assess this.

#### 5.2.3.3. *Southern California*

In Southern California, the models attribute a +7% [2%, 12%] increase in median background BA to total climate forcing. This is consistent with the attribution results for 2025-like events (**Section 5.2.2.3**), though with higher confidence. The agreement across these distinct approaches, despite targeting different fire outcomes (seasonal extremes vs general background activity), provides additional confidence that long-term climate change is influencing baseline fire conditions in the region.

Socio-economic influences contributed a -3% change in background BA, with an uncertainty range of [-7%, 1%]. While not statistically significant, this result is more tightly constrained than those from the earlier analysis of 2025-like events. The modest downward influence may reflect intensifying suppression capacity, declines in human-caused fires due to fire-prevention policies including those targeted to electrical utilities (Jorge et al., 2025; Abatzoglou et al., 2020), or other urban interface factors, though uncertainty remains high.

#### 5.2.3.4. *Congo Basin*

In the Congo Basin, we estimate that total climate change has driven an increase in mean annual BA of 54%, with a tight confidence range of [45%, 63%]. This makes it one of the most robust signals of climate influence across the background fire analyses. These results are consistent with, though slightly stronger and more confident than, the attribution using 2024-like extreme events. The agreement between methods strengthens confidence that climate change is already amplifying baseline fire activity in the region.

This signal likely reflects a clear climate influence on fire-conductive weather, particularly in the southern part of the basin (**Section 4.2.2.4**). While fuel limitations played a role in moderating fire spread (**Figure 12**), the background increase in BA appears strongly tied to meteorological shifts linked to climate change.

Socioeconomic influences appear to have played a moderating role in background fire activity across the Congo Basin. In our process-based model analysis, socioeconomic drivers, including changes in land use, land cover, and population, led to a 16% reduction in





background BA between 2003-2019, with a 90% confidence range of -21% to -11%. This suggests a consistent and substantial dampening effect on fire, possibly reflecting a combination of land fragmentation, land use conversion, or reduced fire use. These results are broadly in line with, though more confidently constrained than, the amplification factor estimated for 2024-like events in the previous attribution method, which indicated limited influence from socioeconomic factors.

## 6. Seasonal and Multi-Decadal Outlook

### 6.1. Methods

#### 6.1.1. Seasonal Forecasts

##### 6.1.1.1. Fire Weather Index

In **Section 4**, we introduced the use of seasonal forecasts of FWI and examined how they performed during the focal events of the 2024-25 fire season. In this section, we present global FWI forecasts from the ECMWF's SEAS5 seasonal prediction system for the months June-August 2025, extending the same approach employed in **Section 4** throughout the boreal summer months of 2025 (see **Section 4.1.1.2.1** for methods).

##### 6.1.1.2. Burned Area

In **Section 4**, we introduced the use of seasonal forecasts of burned areas using a combination of weather driver and ML and examined how they performed during the focal events of the 2024-25 fire season. In this section, we present global BA forecasts from the same system for the months July-September 2025, extending the same approach employed in **Section 4** throughout the boreal summer months of 2025 (see **Section 4.1.1.2.2** for methods).

### 6.1.2. Multi-Decadal Projections

#### 6.1.2.1. Fire Weather Index at Future Global Warming Levels

To calculate how the risk of fire weather extremes might evolve with future warming, we apply the same framework described in **Supplementary Material S5.1.1** but instead of comparing recent climate to the past, we compare it to a set of global warming levels: 1.5 °C, 2.0 °C, 3.0 °C, and 4.0 °C above recent past climate (2016-2025).

For each level of warming, we identify years in the CanESM5 ensemble where the smoothed 11-year running global mean temperature aligns with the target level, and then assess the frequency of extreme 7-day FWI events in those years, as per Liu et al. (2023b) and similar to Otto et al. (2018). Comparing this to the 2016-2025 climate baseline gives us a forward-looking set of Risk Ratios (RR) — RR1.5, RR2.0, etc. These indicate how much more likely such extremes become as the planet warms.

As with the attribution to past climate (**Section S5.1.1**), uncertainties are captured through bootstrapped confidence intervals, enabling meaningful comparison of future risks even when rare extremes are involved.

#### 6.1.2.2. Burned Area in Future Emissions Scenarios

In order to project future changes in BA, we extended the ConFLAME ISIMIP3a modelling approach used in **Section 5.1.3** to future decades under Shared Socioeconomic Pathway (SSP) scenarios SSP126, SSP370, and SSP585, following a similar protocol to UNEP



(2022a). We use the same optimised model as in **Section 5.1.3**, but here we employ bias-corrected global climate model (GCM) outputs from ISIMIP3b (Frieler et al. 2025) for prediction. While ISIMIP3a uses reanalysis data for historical analysis, ISIMIP3b employs GCM data to project future climates and is designed for usage cases requiring a seamless continuation of the historical period into future scenarios.

ISIMIP3b utilizes five bias-corrected GCMs, including historical model output up to 2014 and future scenarios from 2015-2100 under the three SSPs. ISIMIP3b uses surface-based meteorological outputs from ScenarioMIP simulations, which include future forcings from greenhouse gases, aerosols, land-use change, and short-lived climate forcers. The five GCMs used are: GFDL-ESM4 (Held et al., 2019), IPSL-CM6A-LR (Boucher et al., 2020), MPI-ESM1-2-HR (Mauritsen et al., 2019), MRI-ESM2-0 (Yukimoto et al., 2019), and UKESM1-0-LL (Tang et al., 2019; Sellar et al., 2019). As part of ISIMIP3b, each GCM is bias-corrected as described in Lange (2019).

Future ISIMIP3b projections for socioeconomic drivers such as population density or land use change were not available at time of analysis. As such, our simulations exclude future changes in ignition sources or direct land-use modification on both fire and vegetation. To simulate vegetation structure and fuel availability, the JULES-ES dynamic vegetation model was run offline, driven by surface climate variables from each of the five bias-corrected GCMs under each SSP scenario, and scenario-specific CO<sub>2</sub> concentrations to represent CO<sub>2</sub> fertilization, along with prescribed nitrogen deposition but excluding changes in fertiliser application, along with prescribed nitrogen deposition but excluding changes in fertiliser application. The land cover output from JULES-ES was then bias-corrected (using the same mapping procedure as **Section 5.1.3**, based on biases between JULES-ES driven by reanalysis and VCF observations) to maintain consistency with the GCM bias-correction procedures. Our approach provides a probability distribution of future BA representing the uncertainty range from cross-model (GCM) spread in the response of climate and vegetation to emissions for each scenario and year in the period 2010-2100. Years 2010-2014 were adopted from the historical experiment for each GCM, and post-2014 from branched SSP and model specific projections. We describe future changes as significant if the range across GCM projections for a future period does not overlap with the range given by the GCMs for 2010s.

Using this driving data, we generate 1,000-member ensembles for each region and each GCM/SSP combination, using the trained ConFLAME-ISIMIP model described in **Section 5.1.3**. For each 10-year period, we calculate the likelihood of extreme fires by determining the fraction of years within each ensemble member where burned area during the event months exceeds that of the observed focal event. We then average this exceedance fraction across all 1,000 ensemble members to estimate the likelihood for that decade. This process is repeated for each GCM and SSP.

For decades beyond 2010s, we then calculate the increase in the likelihood of 2024/25-like events by taking the ratio of the exceedance frequency in each future decade relative to the 2010s baseline. This is analogous to the risk ratio used in **Section 4**, where the future period acts as the “factual” and 2010s as the “counterfactual” baseline. Following methods outlined in **Section 4**, we perform this analysis for the entire region and for “sub-regional extremes” - the grid cells with the top 5% of BA.

Lastly, we calculated the integrated probability of experiencing a fire event of similar magnitude to our target region within the expected lifespan of a citizen born in 2023 (the year of the latest estimate). According to UN population statistics (United Nations Population Division, 2023), life expectancy at birth is 75.8 years for Brazil, 79.3 years for the USA, and 61.9 years for the Democratic Republic of the Congo (DRC). While the Northeast Amazonia and Congo Basin regions span multiple countries, most fire anomalies in these regions



occurred in Brazil and the DRC, respectively (**Figure 5**). To account for years beyond 2100 in the life expectancy of Brazil and the USA, we extrapolated the annual trend in event probabilities. The integrated probability is calculated as one minus the product of the annual probabilities of not experiencing a fire event like the focal event, across each year from 2025.

## 6.2. Results

### 6.2.1. Seasonal Forecasts of Fire Weather Index and Burned Area Anomalies

As of mid-2025, neither La Niña nor El Niño conditions are present in the tropical Pacific. Instead, the climate system has entered an ENSO-neutral phase, according to the latest report from the National Oceanic and Atmospheric Administration (NOAA, 2025c). This neutral phase is expected to persist through the remainder of summer, and into at least early autumn. While neutral ENSO conditions typically indicate a reduced influence of Pacific sea surface temperature anomalies on global weather patterns, the persistence of anomalously warm ocean conditions and other climate drivers may continue to exert significant influence on regional and global climate variability in the months ahead (Frölicher and Laufkötter, 2018).

May 2025 was the second-warmest May on record globally, with an average temperature of 15.79 °C, 0.53 °C above the 1991-2020 climate and 1.4 °C above pre-industrial levels (Copernicus Climate Changes Service, 2025). While this marked a brief drop below recent consecutive months exceeding 1.5 °C from pre-industrial record, it still reflects the persistent trend of global climate warming (Horton, 2025). Unusually low rainfall and soil moisture across northwestern Europe, including the UK, reached their lowest levels since 1871. This raises serious concerns about crop failures, potential water shortages and wildfire risk (European Commission Joint Research Centre, 2025; UK Environment Agency, 2025). Similar conditions were reported in the US, particularly across Arizona and Texas, where exceptional drought levels led to reservoir depletion, strict water restrictions, and increased wildfire activity (National Centers for Environmental Information, 2025; National Interagency Fire Center, 2025).

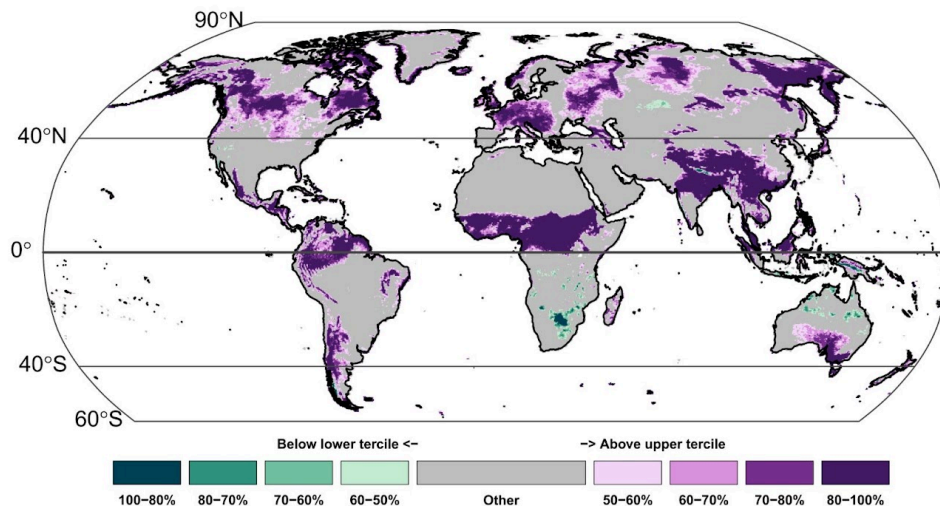
Starting from May, and according to the outlook for the Northern Hemisphere boreal summer of 2025 (June-July-August), anomalous fire weather conditions are anticipated across several key regions with high levels of confidence (in places reaching 80 %). Anomalous fire danger season is expected in Canada, US western states (also see National Interagency Fire Center, 2025), northeast Europe (notably the UK), and parts of Siberia (**Figure 16**). In the equatorial zone, persistent dryness and hydroclimatic anomalies are expected to increase fire danger (confidence level of 60% and higher) in Northeast Amazonia, the Congo Basin, and the Himalayan foothills (affecting areas of India and Nepal). In contrast, a relatively quiet fire season is projected for the Southern Hemisphere, with only Chile and southern Australia showing fire-prone conditions at a moderate level of confidence (>50%).

The BA anomaly forecast (bottom panel of **Figure 16**) displays a distinct pattern from that of FWI, as it models the expected fire response conditioned on both coincident and antecedent climate variables, based on region-specific statistical relationships. For instance, elevated probabilities of above-median BA are projected in the western part of South America, southern California, localized areas of Central America, and central North America. In central Asia, medium-to-high probabilities emerge, particularly in the eastern regions. In Africa, significant signals are observed over the central continent, while in Australia, elevated probabilities are mainly found in the northern regions. Over central Europe, despite a high FWI forecast, limited historical fire activity prevents reliable calibration of the climate-fire model, and therefore no BA forecast is issued for this region.



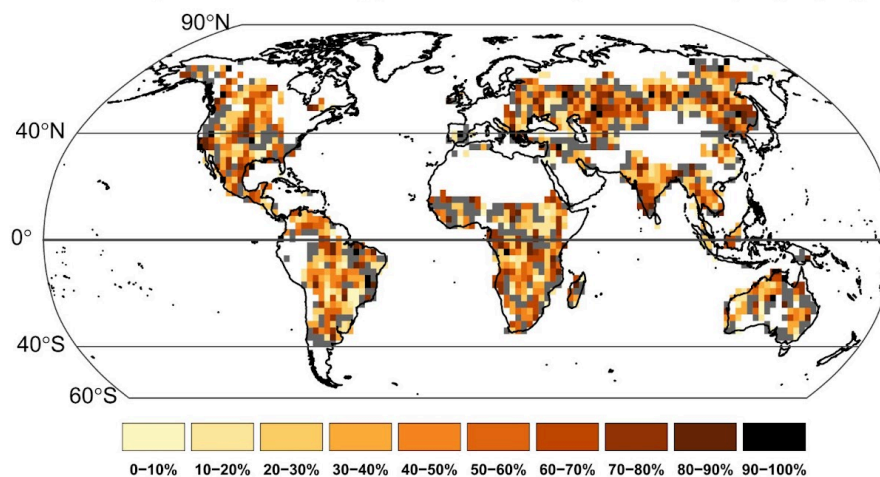
## FWI – Seasonal Forecast

Probabilities Below/Above Normal (Start date: 01/06/2025 | Season June–July–August [JJA])



## Burned area anomaly – Seasonal Forecast

Probability of burned area anomaly (Start date: 01/06/2025 | Season June–July–August [JJA])



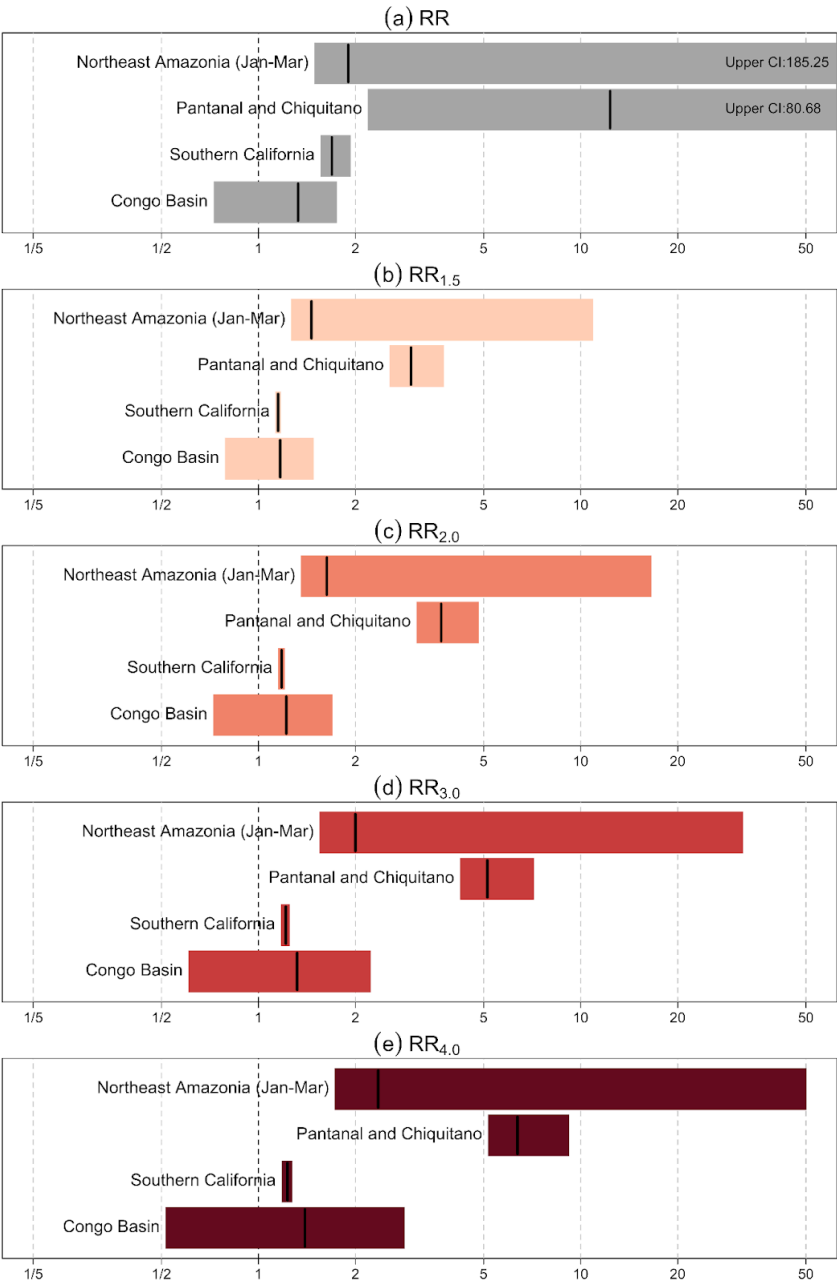
3032

3033 **Figure 16:** Seasonal prediction of Fire Weather Index (FWI) and burned area (BA)  
3034 anomalies for the boreal summer of 2025 (June–July–August). Both forecasts are issued in  
3035 June 2025 and are presented in probabilistic terms: FWI prediction shows the likelihood for  
3036 increased (above the upper tercile) or decreased (below the lower tercile) fire-weather  
3037 conditions; whereas BA prediction shows the probability of BA anomalies being above the  
3038 climatological median. Grey areas are masked where insufficient BA statistics are available  
3039 to perform the predicted mean.  
3040



3041 **6.2.2. Future Changes in Likelihood of Extreme Fire Weather Events**

3042  
3043 In three of the focal regions where climate change significantly increased the likelihood of a  
3044 2024-25-level fire weather event (Section 5.2.1), even greater increases are projected under  
3045 future warming levels of 1.5 °C, 2 °C, 3 °C, and 4 °C (Figure 17).



3046  
3047 **Figure 17:** Risk Ratio (RR) estimates based on the comparison between (a) the past climate  
3048 of 1850-1859 and the recent climate of 2016-2025, (b) the recent climate of 2016-2025 and



the period that global mean surface temperature (GMST) reached **(b)** 1.5 °C, **(c)** 2 °C, **(d)** 3 °C and **(e)** 4 °C for the four extreme wildfire events between 2024 and early 2025 using CanESM5. Bars show 95% confidence intervals (CIs) and central values are shown in bold.

#### 6.2.2.1. *Northeast Amazonia*

In Northeast Amazonia the increased fire weather risk found in **Section 5.2.1.1** during January-March is projected to continue rising under future warming, with increases in probability of 1.5 (95% CI: 1.3-10.8), 1.6 (1.4-16.3), 2.0 (1.6-31.4) and 2.4 (1.7-49.5) at 1.5 °C, 2 °C, 3 °C, and 4 °C of warming, respectively. Compared to southern Amazonia, fires in Northeast Amazonia have gathered less attention from the scientific community and little is known about how future changes in fire weather conditions may impact this region.

Amazonia spans multiple countries, making coordinated fire governance particularly challenging. These countries often have differing political priorities and economic interests, which shape land use policies, enforcement capacity, and investment in fire monitoring and response systems. Such disparities can hinder the implementation of integrated fire management strategies, especially in border regions where transboundary fires may occur but fall under fragmented jurisdictional and institutional frameworks. These institutional and policy asymmetries introduce further uncertainty about how fire risk will evolve in a warming climate. As fire weather intensifies, the region's unique fire season and cross-border governance dynamics should be explicitly considered in fire risk assessments and regional adaptation strategies.

#### 6.2.2.2. *Pantanal and Chiquitano*

The Pantanal and Chiquitano region, which showed the largest historical increase with 4.75 (95% CI: 4.2-5.5, **Section 5.2.1.2**), is set to continue to increase with global warming, with projected increases in probability of 3.0 (95% CI: 2.6-3.6), 3.7 (3.2-4.6), 5.1 (4.4-6.5), and 6.4 (5.4-8.3) at 1.5 °C, 2 °C, 3 °C, and 4 °C of warming, respectively (**Figure 17, b-e**). This is especially concerning for the Pantanal and Chiquitano, where fires are strongly driven by climate, particularly through extreme (Silva et al., 2022; Barbosa et al., 2022) and compound events (Ribeiro et al., 2022; Libonati et al., 2022). The ongoing reduction of wetlands in the Pantanal, often replaced by flammable grasslands (Damasceno-Junior et al., 2021), combined with the projected increase of fire weather conditions (Feron et al., 2024), may indicate a permanent shift in the landscape and its fire regime. This increases the vulnerability of fire-sensitive vegetation and wildlife habitats, while also threatening economic activities that rely on seasonal flooding.

#### 6.2.2.3. *Southern California*

Southern California shows a similar pattern, with the likelihood of 2024-25 extreme fire weather being about 1.7 times higher (95% CI: 1.6-1.8) than in the past, and projected increases in likelihood ranging from 1.1 to 1.3 with rising global temperatures.

#### 6.2.2.4. *Congo Basin*

In contrast, the Congo Basin shows a more modest and statistically non-significant change, with the likelihood of a similar extreme fire weather event to that of the 2024-25 season increasing by a factor of 1.3 from the past to the present. Future projections suggest a wide but uncertain range of change, between 0.5 and 2.7 depending on the warming level.





### 3101 6.2.3. Future Changes in Likelihood of Extreme Fire Events

3102

#### 3103 6.2.3.1. Northeast Amazonia

3104 By the 2040s, under SSP585, the likelihood of an event similar to those of the 2024-25  
 3105 season increases modestly but significantly to 0.12-0.14%, a ~17% increase in frequency  
 3106 compared to the 2010s (**Figure 18; Table 6**). Other scenarios show smaller or even  
 3107 negligible changes over this period. By the end of the century, however, all scenarios project  
 3108 notable increases in event frequency. SSP585 shows the largest rise, with the probability of  
 3109 such an event nearly doubling (up to 1.92 times more frequent). SSP370, reflecting current  
 3110 emissions trajectories, projects a 1.19-1.57 times increase. In contrast, SSP126 illustrates  
 3111 the mitigation potential of low-emission pathways, limiting increases to just 1.09 times (under  
 3112 10% increase) by 2100, significantly lower than under higher-emission scenarios. SSP370  
 3113 only clearly diverges from SSP126 by late century (2090s), though the potential for larger  
 3114 increases appears earlier (**Figure 18**). This divergence between the two scenarios is  
 3115 especially pronounced when focusing on areas with the highest BA (top 5% of grid cells,  
 3116 **Figure S29**). These regions of extreme burning could see a doubling in fire extent by  
 3117 mid-century and at least doubling (potentially tripling) by 2100 under SSP370, with  
 3118 substantial overlap with SSP585 projections (where extreme BA could almost quadruple).

3119 By 2100, SSP126 still shows marginal increases in the likelihood of BA events such as those  
 3120 in 2024 (**Figure 18**), though sub-regional extreme BA see much less significant change  
 3121 (**Table 6; Figure S29**), with frequency ranging from slight decreases (by a factor of 0.91) to  
 3122 modest increases (1.34).

3123 These increases are mainly driven by projected declines in moisture availability (**Figure 18**  
 3124 **Figure S29**). Although fuel availability is expected to decline somewhat, this only marginally  
 3125 offsets the rise in extreme BA likelihood across the region and has virtually no mitigating  
 3126 effect on the highest BA areas. No changes in fuel are statistically significant in our  
 3127 projections.

3128 Most regions of Northeast Amazonia see increases in January-March (JFM) average BA by  
 3129 2100 (**Figure S32**). However, under SSP126, increases in the north, French Guiana,  
 3130 Suriname, and Guyana, are less certain and, if they occur, are smaller. This is reflected in a  
 3131 decreased frequency of extremes across these areas (**Figure S32**). Under SSP370, climate  
 3132 change drives widespread increases in BA, with corresponding rises in extremes nearly  
 3133 everywhere except Roraima (Brazil). Most of Brazil and Venezuela are very likely to see  
 3134 increases in BA even under SSP126, with some moist regions showing rises in extremes  
 3135 under SSP126 and widespread increases under SSP370. Results for SSP585 are similar to  
 3136 those of SSP370, with widespread increases in BA and extremes throughout the region.  
 3137 Importantly, increases in extremes begin in some areas in the near future (**Figures S30-31**).  
 3138 By the 2030-2040s, Amapá (Brazil), northern Pará (Brazil), and southern Suriname are  
 3139 projected to experience more frequent extreme BA events and increased BA under the  
 3140 SSP585 scenario (**Figure S30**). Increases in BA are less certain but still likely under  
 3141 SSP370, with mitigation under SSP126 helping to limit these trends.

3142 Finally, we explored what this means for people's lived experience (**Figure 19**). A person  
 3143 born 75.8 years ago (Brazil's current life expectancy) would have had a 33-36% likelihood of  
 3144 witnessing a fire event like January-March 2024 during their lifetime. This suggests that,  
 3145 although anthropogenic changes have increased the likelihood of such fires (see **Section 5**),  
 3146 these events remain far from certain. Even the modest increases in frequency projected  
 3147 under SSP126 would raise that lifetime likelihood to 41-55% for someone born today (i.e.,  
 3148 2025-2021). Under SSP370 (our current path), the chance rises substantially to 52-69%, and  
 3149 under SSP585, to 55-76%. There is also a substantial rise in the probability of experiencing



multiple such events within a lifetime, for example, under SSP370, there is a 17-32% chance  
 of seeing two such events, compared to just 6-8% for those born in the 1940s.

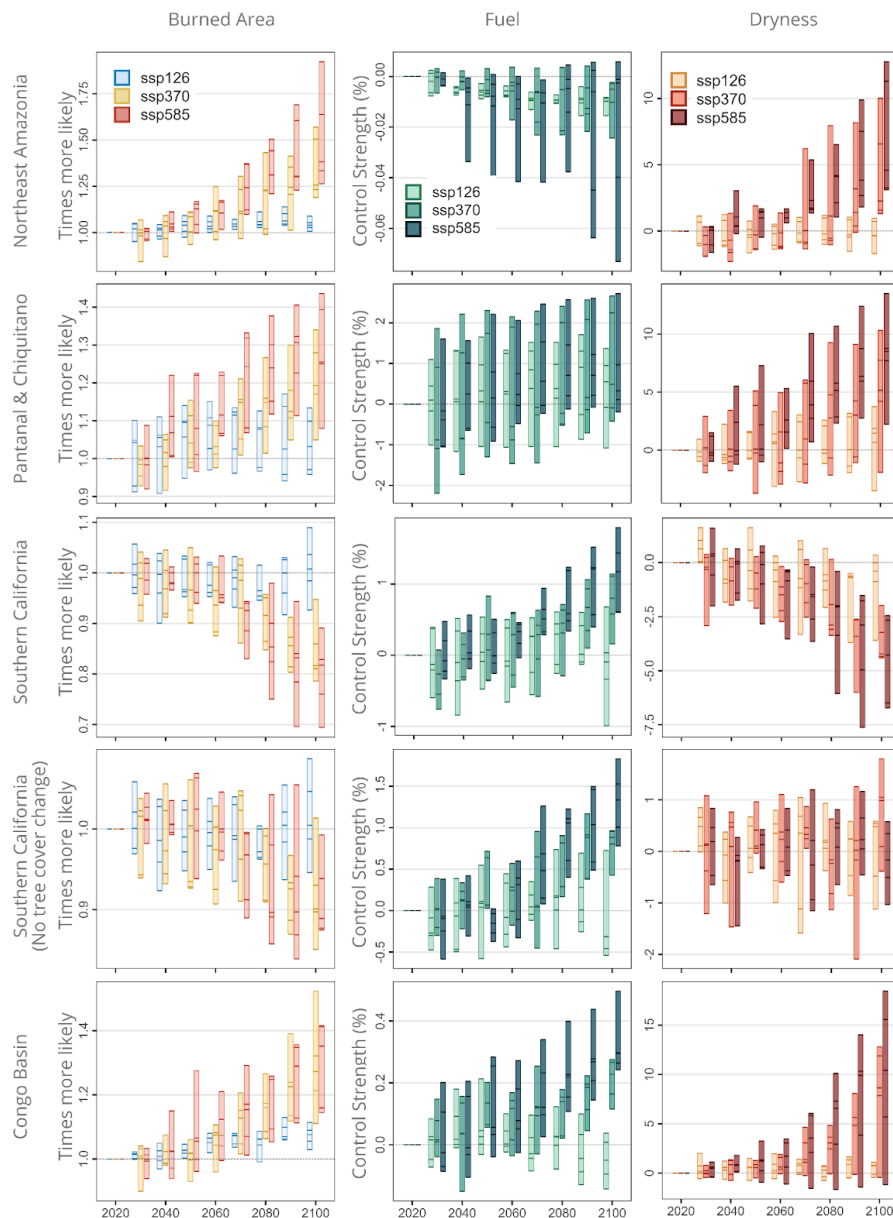


**Figure 18:** Future projections from ConFLAME of the change in likelihood of BA extent of the magnitude seen in the 2024-25 season, along with the contribution of fuel and moisture conditions in years in which BA exceeds the 2024-25 thresholds. Each set of bars shows changes for each decade relative to the 2010-2020 baseline, with each bar representing a different SSP scenario and the spread of bars indicating the variation across GCMs, with individual bars representing different GCMs.

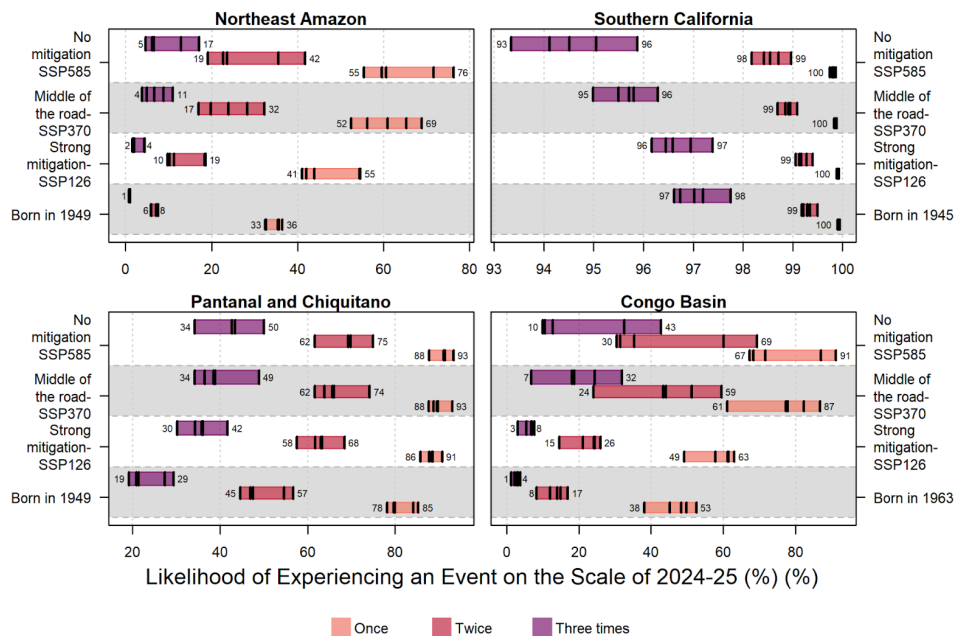


**Table 6:** Summary of the likelihood of extreme events today using reanalysis ‘factual’ and into the future using bias-corrected GCMs for our focal events identified in **Section 4.4.3**. Min and max report range across GCMs. We also determine how much more frequent the events will be at two different time horizons based on each model’s likelihood in the future projections over likelihood during 2010-2020. Asterisks (\*) indicate non-significant changes from 2010-2020 values. Colours show linear increase of likelihood (orange) and frequency (blue) for less frequent, orange for more), where darker shade indicates higher values. The top half of the table displays projections using BA over the entire region, while the bottom shows projections for sub-regional extremes (grid cells with the top 5% BAs).

Region	SSP	Represents	All Region											
			Likelihood(%/year during focal months)						How much more frequent (multiplier)					
			2010-2020		2040-2050		2090-2100		2040-2050		2090-2100			
			min	max	min	max	min	max	min	max	min	max		
Northeast Amazonia	Factual	observed	0.073											
	SSP126	strong mitigation	0.12	0.12	0.12*	0.12*	0.12	0.13	0.97*	1.09*	1.01	1.09		
	SSP370	middle-of-the-road	0.12	0.13	0.12*	0.13*	0.15	0.19	0.93*	1.11*	1.19	1.57		
	SSP585	no mitigation	0.12	0.12	0.12	0.14	0.15	0.23	1	1.17	1.26	1.92		
Pantanal & Chiquitano	Factual	observed	0.19											
	SSP126	strong mitigation	0.09	0.09	0.09*	0.11*	0.09*	0.11*	0.95*	1.14*	0.96*	1.13*		
	SSP370	middle-of-the-road	0.08	0.1	0.09*	0.11*	0.1	0.12	0.98*	1.15*	1.05	1.34		
	SSP585	no mitigation	0.08	0.1	0.09*	0.11*	0.1	0.13	0.97*	1.22*	1.08	1.44		
Southern California	Factual	observed	0.38											
	SSP126	strong mitigation	0.34	0.36	0.33*	0.36*	0.31*	0.38*	0.95*	1.03*	0.93*	1.09*		
	SSP370	middle-of-the-road	0.34	0.37	0.3*	0.37*	0.27	0.33	0.9*	1.05*	0.79	0.95		
	SSP585	no mitigation	0.34	0.35	0.32*	0.36*	0.23	0.31	0.94*	1.03*	0.69	0.89		
Southern California - no tree cover change	Factual	observed	0.42											
	SSP126	strong mitigation	0.38	0.41	0.38*	0.4*	0.37*	0.42*	0.95*	1.04*	0.95*	1.09*		
	SSP370	middle-of-the-road	0.38	0.42	0.36*	0.41*	0.35*	0.39*	0.93*	1.06*	0.85*	1.01*		
	SSP585	no mitigation	0.38	0.41	0.38*	0.41*	0.34*	0.38*	0.94*	1.07*	0.87*	1.00*		
Congo Basin	Factual	observed	0.17											
	SSP126	strong mitigation	0.16	0.18	0.17*	0.18*	0.17	0.19	1*	1.05*	1.03	1.11		
	SSP370	middle-of-the-road	0.17	0.19	0.17*	0.19*	0.21	0.26	0.93*	1.06*	1.11	1.52		
	SSP585	no mitigation	0.17	0.18	0.17*	0.21*	0.2	0.26	0.96*	1.28*	1.15	1.42		



Region	SSP	Represents	Sub-regional extremes												How much more frequent (multiplier)					
			Likelihood(%/year)																	
			2010-2020				2040-2050				2090-2100				2040-2050		2090-2100		2090-2100	
			min	max	min	max	min	max	min	max	min	max	min	max	min	max	min	max	min	max
Northeast Amazonia	Factual	observed	<0.01																	
	SSP126	strong mitigation	0.01	0.02		0.01*	0.02*		0.01*	0.02*		0.01*	0.02*		0.94*	1.38*		0.91*	1.34*	
	SSP370	middle-of-the-road	0.01	0.02		0.01*	0.02*		0.03	0.04		0.03	0.04		0.92*	1.58*		1.98	3.23	
	SSP585	no mitigation	0.01	0.02		0.02	0.02		0.03	0.05		0.03	0.05		1.15	1.64		2	3.6	
Pantanal & Chiquitano	Factual	observed	0.01																	
	SSP126	strong mitigation	0.02	0.03		0.03	0.03		0.03	0.03		0.03	0.03		1.05	1.21		1.03	1.24	
	SSP370	middle-of-the-road	0.02	0.03		0.03*	0.03*		0.03	0.04		0.03	0.04		0.94*	1.23*		1.21	1.45	
	SS585	no mitigation	0.02	0.03		0.03*	0.03*		0.03	0.04		0.03	0.04		0.96*	1.45*		1.26	1.75	
Southern California	Factual	observed	0.27																	
	SSP126	strong mitigation	0.24	0.26		0.24*	0.25*		0.23*	0.27*		0.23*	0.27*		0.96*	1.03*		0.94*	1.12*	
	SSP370	middle-of-the-road	0.24	0.26		0.22*	0.27*		0.2	0.24		0.2	0.24		0.91*	1.08*		0.82	0.97	
	SSP585	no mitigation	0.24	0.26		0.23*	0.25*		0.18	0.23		0.18	0.23		0.9*	1.04*		0.76	0.94	
Congo Basin	Factual	observed	0.01																	
	SSP126	strong mitigation	0.01	0.01		0.01*	0.01*		0.01	0.01		0.01	0.01		0.92*	1.94*		1.02	1.42	
	SSP370	middle-of-the-road	0.01	0.01		0.01*	0.01*		0.02	0.05		0.02	0.05		0.91*	1.37*		1.59	5.07	
	SSP585	no mitigation	0.01	0.01		0.01*	0.04*		0.02	0.05		0.02	0.05		0.69*	3.85*		2.57	3.97	



3167

**Figure 19:** Likelihood of experiencing extreme fire events similar to those of 2024-2025 during the average lifetime of a citizen, based on current life expectancy (2023): Brazil (75.8 years, Northeast Amazonia, the Pantanal-Chiquitano), USA (79.3 years, Southern California), and Democratic Republic of Congo (61.9 years, Congo Basin). Bars show the probability of experiencing at least one, two, or three such events if born today under different scenarios: historical climate (bottom bar in each group), SSP126, SSP370, and SSP585 (subsequent bars, bottom to top). Black vertical lines indicate individual GCM estimates; bar heights show the range across models.

3176

#### 6.2.3.2. Pantanal and Chiquitano

3178

By mid-century (2050), no scenario shows significant increases in the frequency of BA levels such as 2024 at the regional scale (Table 6). All scenarios project modest increases by this point: about 1.14-1.15 times more frequent in SSP126 and SSP370, with slightly higher increases in SSP585 (up to 1.22 times). However, substantial changes emerge later in the century (Figure 18). Under SSP370, the likelihood of these fires becomes significantly higher by the 2070s, with a 1.2-fold (20%) increase relative to historical conditions. By 2100, SSP585 shows the greatest increases, up to 1.44 times more frequent, while SSP370 projects 1.34 times (Table 6). SSP126 demonstrates clear mitigation potential, limiting increases to about 1.13 times, with no significant change throughout the century.

3188

For areas with the highest BA (top 5% grid cells), future changes in the frequency of 2024-like events are significantly different from 2010-2020 for both mid-century (2050) and by 2100 (Table 6). Increases at the sub-regional level are larger than regional averages, though not as dramatic as in Northeast Amazonia: by the end of the century events such as those from the 2024-25 season are expected to increase 1.26 to 1.75 times under SSP585, while SSP126 keeps increases much smaller (1.03-1.24 times). SSP370 projections fall between these (1.21-1.45 times), demonstrating that mitigation could still meaningfully limit the occurrence of extreme fire. Increases in the likelihood of extreme BA in high burning



cells could begin as early as the 2030s under SSP126, driven in part by potential increases in fuel availability, though this effect could level off or reverse by mid-century (**Figure S29**). Under SSP370 and SSP585, increases in frequency of extreme BA start to take hold by the 2040s, though large changes may not emerge until after 2060.

These future extremes will mainly be driven by declining moisture availability over the entire region (**Figure 18**). For the most extreme BA areas, this moisture signal is less certain, and changes in fuel, though uncertain, could be large enough to modulate moisture effects (**Figure S29**).

Increases in BA will likely occur across the region by 2090 under all scenarios except in the wetland core of the Pantanal (**Figure S35**), where responses are much more uncertain. Areas of increased extreme fire behaviour exist even under SSP126, but most of the region is projected to see reductions or little change in extremes. In contrast, SSP370 drives widespread increases in extreme BA across almost the entire region, except the wetlands. However, as **Section 5** and other studies (e.g. Barbosa et al., 2022, 2025b) highlight, recent increases in extreme fire have been driven by the combined effects of climate change and wetland degradation, factor not considered in the future projections. This means increases in wetland fire extremes could arise sooner, even by the 2030s or 2040s under SSP126. Under SSP585, widespread increases in extreme BA may arise as soon as 2030 (**Figure S33**), and by 2040 even SSP126 shows large areas of the Pantanal and Chiquitano with much higher chances of a 1-in-100 event (**Figure S34**). Under the SSP126 scenario, the lower chances of extreme events by 2100 compared to mid-century (2040-2050) reinforce how strong mitigation strategies may alter wildfire trajectory throughout the 21st century in this region.

Finally, in terms of lived experience, someone born in the 1940s would already have had a high chance (78-85%) of witnessing a fire event like 2024 during their lifetime (**Figure 19**), with **Section 5** showing climate and human factors likely contributed substantially. Even under SSP126, this rises to 86-91% for someone born today. The difference is most striking for multiple-event likelihoods. Historically, someone born in the 1940s would have had a 19-29% chance of seeing three such events. Under SSP370, this rises sharply to 34-49%, similar to SSP585 (34-50%). Even under SSP126, the likelihood of seeing two such events exceeds 50% (58-68%), compared to 45-57% historically.

### 6.2.3.3. Southern California

While January 2025 fire activity was likely influenced by anthropogenic climate change (**Section 5.2.2.3**), future projections suggest that similar-scale BA extremes may become less frequent (**Table 6; Figure 18**). However, this depends strongly on how local vegetation responds to rising CO<sub>2</sub> and climate change.

Looking ahead, models do not project a significant increase in the frequency of these regional-scale extremes (**Figure 18**). In fact, under SSP370 - a scenario closely aligned with current emissions trajectories, the likelihood of 2025-like events in terms of January BA slightly declines by a factor of 0.79 to 0.95 by the 2090s versus 2010s. Similar trends are seen under SSP585, though with the potential for stronger decreases. SSP126, however, showed no robust change by the end of the century.

The projected decline in extreme fire activity in Southern California appears to be driven primarily by modelled increases in tree cover, which occurs even with GCMs with declining precipitation, suggesting that it is largely driven by CO<sub>2</sub> fertilisation and enhanced water-use efficiency (**Figure S28**). This effect is more pronounced in drier climates like Southern California, where rising CO<sub>2</sub> concentrations reduce water stress on plants and promote vegetation growth. While this leads to greater fuel loads, our framework also represents tree covers influences on fuel moisture, which can suppress fire risk tipping the balance toward





fewer extreme fire events in many model simulations. CO<sub>2</sub> concentrations are higher in SSP585 and SSP370 compared to SSP126, which explains why this effect is more pronounced in these scenarios. However, when tree cover is held constant at present-day levels, this signal weakens considerably. Under these “fixed tree” simulations, future projections of extreme fire activity become much more uncertain, with wide variation across scenarios all the way to the 2090s (**Figure 18**). Climate projections themselves for the region are mixed. Some models show increases in January precipitation and fewer dry days, while others suggest drier conditions (**Figure S42**). These divergent signals further contribute to uncertainty in fuel moisture and fire behaviour over the coming decade.

Our projections, therefore, rely on modelled tree and shrub cover from a global land surface model, which, while bias-corrected using historical observation (**Figure S28**), is primarily designed to capture broad-scale vegetation patterns. The model includes global plant functional types (PFTs) such as evergreen and deciduous shrubs, which encompass Mediterranean shrublands like those found in Southern California, but also represent structurally similar ecosystems in very different climatic and ecological settings (e.g., tropical savannas, tundra scrub). As a result, while the model tends to perform reasonably well in estimating total woody cover, it may not fully capture the fine-scale ecological gradients or the dominant shrubland dynamics that drive fire activity in this region. In particular, it may miss key features of chaparral systems and their interannual variability. Future work using regionally calibrated vegetation models or integrating remote sensing estimates of fuel structure may help increase confidence in projections for fire-prone shrub-dominated systems like Southern California.

Therefore, while our models suggest a potential future decrease in large-scale fire extremes in Southern California, this outcome depends on how burned area responds to increasing tree cover, and how vegetation itself responds to rising CO<sub>2</sub> and changing climate. Both relationships remain uncertain and will require further investigation. Understanding the evolving links between fuel load, fuel moisture, and ignition risk in the region is essential to refining future fire risk projections in this region.

#### 6.2.3.4. *Congo Basin*

By the 2050s, none of the emission scenarios project a significant increase in the frequency of regional-scale 2024-like fire events (**Table 6**). Both SSP126 and SSP370 project modest changes, ranging from slight decreases to increases of up to 1.28 times more frequent, though wide uncertainty means small decreases remain possible. Substantial increases emerge by 2100, especially under higher-emissions scenarios. Under SSP370, the likelihood of large fire events rises by 1.11-1.52 times, with SSP585 showing similar values. In contrast, SSP126 holds the increase to just 1.03-1.11 times, indicating a meaningful mitigation potential.

For the most extreme fire events (top 5% of grid cells), projected increases in frequency are more substantial (**Table 6**). No scenario shows significant differences by 2050. However, significant and potentially large changes emerge by 2100. Under SSP370, the frequency of these high-BA extremes could rise by up to 5 times relative to historical conditions (range: 1.59-5.07), slightly higher than the 4-fold increase under SSP585 (2.57-3.97). SSP126 limits this increase substantially to just 1.02-1.42 times. These results show that even under a mitigation pathway, some increase in extreme BA is likely, but the scale of that increase is drastically reduced.

The primary driver of increased fire risk in the region is declining moisture availability, with drier conditions projected across much of the basin (**Figure 18**). In the higher-emissions scenarios (SSP370 and SSP585), increased fuel availability may amplify this effect. For the



3306 most extreme fire-prone areas, however, fuel controls show little change, suggesting that  
3307 moisture stress will be the dominant factor shaping future fire behavior (**Figure S29**).

3308

3309 Spatially, increases in BA are relatively uniform across the region, though some local  
3310 differences emerge (**Figures S39-41**). The eastern DRC may experience small decreases in  
3311 July average BA, though increases remain more likely. In contrast, Gabon, Equatorial  
3312 Guinea, and central DRC (particularly south of the Congo River) are projected to see the  
3313 largest increases, with BA doubling or even quadrupling in some areas. Some of these  
3314 increases, particularly along the Gabonese and Equatoguinean coasts, may begin as early  
3315 as the 2030s.

3316

3317 In terms of lived experience, someone born in the DRC in 1963 with a life expectancy of 61.9  
3318 years, would have had a 38-53% chance of experiencing at least one event like that of July  
3319 2024 (**Figure 19**). For those born today, this rises to 49-63% under SSP126, 61-87% under  
3320 SSP370, and as high as 67-91% under SSP585. The likelihood of experiencing multiple  
3321 such events also increases markedly. Under SSP585, someone born today would have a  
3322 30-69% chance of seeing two events, and a 10-43% chance of seeing three. In contrast,  
3323 SSP126 limits this to 15-26% for two events and just 3-8% for three, highlighting the  
3324 powerful influence of mitigation. Indeed, the chance of seeing just one event under SSP126  
3325 is comparable to seeing two under SSP585.



## 3326 7. Conclusions: Summary of the State of Wildfires in 2024-25

3327

### 3328 7.1. Extreme Wildfire Events of 2024-25

3329 • **Global:** A total of 3.7 million km<sup>2</sup> burned globally during the 2024-25 fire season, 9%  
 3330 below the average of previous seasons (4.0 million km<sup>2</sup>), ranking 16th of all fire  
 3331 seasons since 2002. Despite the relatively low area burned, global fire carbon  
 3332 emissions were 2.2 Pg C, 9% above average and the 6th highest on record, driven  
 3333 by intense and high-emission fires in South America and Canada. This pattern  
 3334 reinforces a trend towards growing fire impacts in carbon-rich forest ecosystems,  
 3335 even during years with below-average fire extent globally.

3336 • **South America:** South America experienced an unprecedented fire season setting a  
 3337 new record for carbon emissions. Emissions reached 263 Tg C (84% above  
 3338 average), with BA also 120,000 km<sup>2</sup> (35%) above average. Bolivia, Brazil, and  
 3339 Venezuela each saw high or record-breaking anomalies, with Bolivia setting national  
 3340 records for both BA and C emissions. Record fire activity occurred across multiple  
 3341 biomes including the Chiquitano dry forests, Pantanal wetlands, and southern and  
 3342 Northeast Amazonia. These fires were characterised by extremely large,  
 3343 fast-spreading, and intense events despite fire counts often being average or below  
 3344 average, highlighting a pattern of fewer but larger and more intense fires on the  
 3345 continent. Highlights:

3346 ○ **Northeast Amazonia (Focal Event):** Record-breaking fire activity affected  
 3347 the moist tropical forests north of the Amazon River and Rio Negro, including  
 3348 large portions of Venezuela, Guyana, Suriname, and northern Brazil. Several  
 3349 ecoregions experienced all-time highs in burned area or carbon emissions,  
 3350 with fire activity peaking March-April and again in late 2024. Air quality  
 3351 impacts and environmental degradation were reported across the region.

3352 ○ **Pantanal-Chiquitano (Focal Event):** Extreme fire season across Bolivia and  
 3353 adjacent Brazil, with the Chiquitano dry forest and Pantanal wetlands (the  
 3354 world's largest wetlands) seeing some of the largest fires on record. Bolivia  
 3355 experienced the highest national carbon emissions total ever recorded (187  
 3356 Tg C), with the Santa Cruz department (Bolivia) alone responsible for 157 Tg  
 3357 C. Fires destroyed critical habitat, caused severe air pollution, and threatened  
 3358 biodiversity hotspots. The pantanal recorded PM<sub>2.5</sub> concentrations of  
 3359 903.2 µg/m<sup>3</sup> in September 2024, 60 times the WHO daily standard.

3360 ○ **Amazonas State, Brazil:** A record-breaking year for fire activity in this moist  
 3361 tropical forest region. Fire counts were up +154% versus the long-term  
 3362 average, and BA and fire size reached record levels. The 95th percentile fire  
 3363 size anomaly was +60%. This was one of the few regions in South America  
 3364 where high fire counts *and* severe individual fire behaviour co-occurred.

3365 ○ **Mato Grosso and Mato Grosso do Sul States, Brazil:** Both states saw  
 3366 record-breaking fire intensity and rate of spread. In Mato Grosso, 95th  
 3367 percentile fire size was 266% above average, despite fire counts being 54%  
 3368 below average. Mato Grosso do Sul experienced record emissions (+323%)  
 3369 and fire growth rates, pointing to fast, intense fires likely driven by land-use  
 3370 change and drought.

3371 ○ **Pará State, Brazil:** This state recorded its highest-ever BA (36,000 km<sup>2</sup>) and  
 3372 major emissions anomalies (+61%). Fire activity expanded deep into forested  
 3373 areas, likely linked to land clearing. It was among the most significant  
 3374 subnational contributors to Brazil's fire totals in 2024-25.

3375 ○ **São Paulo State, Brazil:** Unusually high-intensity fires occurred despite a  
 3376 relatively small area burned. 95th percentile fire size and intensity both set  
 3377 new records. Carbon emissions were nearly double the historical average



- (+190%), driven by a combination of unseasonal drought and land-use pressures.
- **Bolívar and Delta Amacuro, Venezuela:** Two states in northeast Venezuela experienced record emissions and BA, with Bolívar seeing a +133% BA anomaly and Delta Amacuro impacted by early-season fire peaks. These fires affected swamp forests and grassland regions.
  - **Coastal and Andean Ecuador, Peru, and Colombia:** Subnational analysis reveals record or high-ranking anomalies in 8 provinces of Ecuador, 7 regions of Peru, and multiple Colombian ecoregions. These include areas in southwestern Amazonia and the eastern Andean slopes, where record fire sizes and intensities occurred despite average fire counts.
  - **Guyana and Suriname:** Six ecoregions in Guyana and two districts in Suriname experienced record fire counts and BA, contributing to the focal Northeast Amazonia event but deserving standalone mention given the extent and duration of the anomalies.
- **North America:** The 2024-25 fire season was the second most severe on record for North America, with total C emissions of 194 Tg C (112% above average) and BA of 31,000 km<sup>2</sup> (35% above average). Canada again saw extreme fire activity for the second year running, with 282 Tg C emitted and over 46,000 km<sup>2</sup> burned, second only to the record-breaking 2023-24 season. In the US, the catastrophic Palisades and Eaton Fires in California in January 2025, which killed at least 30 people, destroyed over 11,500 homes, and caused over \$140 billion in damages. Highlights:
    - **Southern California, USA (Focal Event):** The most disastrous wildfire event in modern US history occurred in Los Angeles County in January 2025 during a severe Santa Ana wind event. The Palisades and Eaton Fires destroyed over 11,500 homes, killed at least 30 people, displaced over 150,000, and caused economic losses exceeding US\$140 billion (including insured losses of US\$20-75 billion). Fires also disrupted water supplies, worsened the housing crisis, and led to mass evacuations and air quality emergencies.
    - **Western Canada:** Northwest Territories, British Columbia, Alberta and Saskatchewan experienced their second-highest emissions year on record with a combined emissions anomaly of +191 Tg C and provincial anomalies in the range of +184-441%
    - **Mexico:** According to national statistics, Mexico experienced its worst wildfire season on record with over 8,000 wildfires and more than 16,500 km<sup>2</sup> burned. Particularly severe activity occurred in March-May, reportedly driven by drought and elevated temperatures. This record is not captured in our analyses based on global satellite products, warranting further investigation of the differences.
    - **Alberta, Canada:** Extreme wildfires in summer 2024 destroyed 358 structures and led to \$1.23 billion in damages, second only to the Fort McMurray fire of 2016. The town of Jasper was evacuated. Two firefighter fatalities occurred.
    - **New York, USA:** In an unusual late-season outbreak, every borough experienced multiple wildfires during a two-week span in October-November 2024, an unprecedented fire signal in a densely populated urban environment.
  - **Africa:** For the second consecutive year, fire extent in Africa was well below average, with BA in the African savannah biome 12% below average, the third lowest on record. However, several regions experienced notable fire anomalies, particularly the Congo Basin, northern Angola, and South Africa. Record-setting BA and C emissions were recorded in some regions of the Republic of Congo and the Democratic Republic of Congo. Despite the extent of these events, many went



- under-reported in the media, reinforcing the importance of Earth observation-based monitoring. Highlights:
- **Congo Basin (Focal Event):** Record fire activity and C emissions in the Republic of Congo and Democratic Republic of the Congo. Fires contributed to the region's highest primary forest loss since 2015 and caused hazardous air pollution, with DRC reporting PM<sub>2.5</sub> levels 11 times the WHO standards. Fires in western ecoregions such as the Atlantic Equatorial and Central Congolian lowland forests were particularly intense.
  - **South Africa:** Fires killed 34 people, including 6 firefighters, and destroyed thousands of livestock and homes. KwaZulu-Natal Province was particularly affected. High fuel loads from previous wet years reportedly contributed to the intensity.
  - **Côte d'Ivoire:** Fires in Séguéla (Worodougou region) burned 50,000 ha, destroyed homes and plantations, and killed 23 people. Other fatal incidents occurred in Bouna, Bongouanou, and Taabo.
- **Asia:** Overall, Asia experienced a below-average fire season, with BA 26% below average and C emissions 28% below average. However, significant regional extremes were observed. Highlights:
    - **Nepal:** Nepal endured its second-worst fire season since 2002, with over 1,000 wildfires. Wildfires killed more than 100 people, with significant destruction of forests and homes. In the Lumbini Province, wildfires devastated 11,448 ha of forests and destroyed more than 230 houses and livestock shelters.
    - **Northern India:** Uttar Pradesh experienced its most severe wildfire season on record, reportedly driven by crop burning, heatwaves, and dry fuel accumulation. Regional fires contributed to severe haze episodes in New Delhi in November 2024, with PM<sub>2.5</sub> concentrations exceeding 200 µg/m<sup>3</sup> across large parts of Northern India (13 times the WHO daily standard).
    - **Iran:** Worst fire season since 2002. Fires burned key national parks and forest areas. Carbon emissions, fire counts, and BA all reached record highs, reportedly driven by a combination of climate stress and human pressures.
    - **South Korea and Japan:** Japan's largest wildfire in over 50 years took place in Iwate Prefecture in February 2025, destroying 221 buildings. South Korea's deadliest wildfires occurred in March 2025 (just outside of the 2024-25 fire season), killing 31 and damaging 4,000 homes.
    - **Sichuan and Guizhou, China:** A fire in Sichuan lasted 14 days, displaced 3,000 people, and impacted multiple villages. Strong winds and dry spring conditions reportedly drove unusually large wildfires.
    - **Heilongjiang and Jilin, China:** Record BA occurred in both provinces. Though not widely reported, these events underscore rising fire activity in northeast Asia, which has been linked to agricultural burning and shifting policy enforcement.
    - **Republic of Sakha and Zabaikalsky krai, Russia:** Fires in these regions accounted for 65% of total forest area burned across Russia and forced 58 redeployments of firefighting resources involving 1,861 firefighters.
  - **Europe:** Europe recorded its fourth lowest BA since 2002, with 30,000 km<sup>2</sup> burned (49% below average) and C emissions 22% below average. However, there were stark regional contrasts. Highlights:
    - **Portugal:** Most destructive fire season since 2017. Over 137,000 ha burned, with 16 fatalities and €180 million in damages. Fires in September affected wildland-urban interface areas in the northwest. A 5,000 ha fire in Madeira entered the laurel forest, a rare cloud forest and UNESCO World Heritage



- 3483 site. This incident highlighted the vulnerability of non-fire-adapted ecosystems  
 3484 under increasing fire pressure.
- 3485 ○ **Serbia, North Macedonia, and Bulgaria:** Worst wildfire seasons in two  
 3486 decades. Large-scale fires led to EUCPM activations and widespread  
 3487 evacuations, including four fires >10,000 ha in North Macedonia alone.
  - 3488 ○ **Ukraine:** Nearly 1 million ha burned during 2024-25, mostly in  
 3489 conflict-affected eastern areas. Fires were likely exacerbated by warfare, with  
 3490 higher-than-usual forest losses reported.
  - 3491 ○ **Romanian Danube Delta:** An unusually dry winter led to 45,000 ha of  
 3492 wetlands burning in February 2025. Though a recurring phenomenon, this  
 3493 was one of the most extensive burn events yet, and emblematic of changing  
 3494 fire regimes in sensitive wetland ecosystems.
  - 3495 ○ **Turkey (Mardin Province):** A rapidly spreading fire in June 2024 burned  
 3496 farmland and villages, killing 15 people and injuring at least 70. It was one of  
 3497 the deadliest fire events in the Eastern Mediterranean this season.
  - 3498 ○ **Austria and Germany:** While Central Europe had a quiet fire year overall,  
 3499 Austria recorded its highest number of fires and largest BA since 2012, and  
 3500 Germany had a slightly above-average season, consistent with a slow but  
 3501 steady upward trend.
- 3502 ● **Oceania:** Oceania experienced a moderate fire season overall, but numerous  
 3503 high-impact events were recorded. Highlights:
  - 3504 ○ **Western Australia:** Over 1,000 large fires burned ~470,000 ha amid record  
 3505 heat and severe dryness between Perth and Carnarvon. The Skeleton Rocks  
 3506 fire (44,000 ha) impacted long fire-interval ecosystems and a lithium mine,  
 3507 while the largest fire near Cervantes burned 80,000 ha and disrupted regional  
 3508 honey production. Manjimup fires affected over 42,000 ha of native forest and  
 3509 required interstate response.
  - 3510 ○ **Central Australia:** Over 5.7 million ha burned by October 2024, including a  
 3511 450,000 ha fire near Devil's Marbles that forced closures of major  
 3512 infrastructure. In January, 80,000 ha burned in the West MacDonnell Ranges,  
 3513 including national parks and Aboriginal land trusts.
  - 3514 ○ **Victoria and Tasmania:** Severe dry lightning outbreaks triggered major fires  
 3515 in culturally sensitive landscapes. Victoria's Grampians National Park saw  
 3516 two-thirds of its area burned, and the Little Desert fire burned 90,000 ha in  
 3517 under 8 hours. Tasmania's northwest fires burned 100,000 ha, affecting the  
 3518 Tarkine and Cradle Mountain.
  - 3519 ○ **Queensland:** Firefighters responded to 40 incidents at Mount Isa, with one  
 3520 fire burning over 100,000 ha for nearly two months. Smoke exposure caused  
 3521 hospital admissions and endangered species such as the Carpentarian  
 3522 Grasswren were threatened.
  - 3523 ○ **New Zealand:** Peat fires at Whangamarino Wetland and Tiwai Peninsula  
 3524 each burned ~1,000 ha, likely generating significant CO<sub>2</sub> emissions after  
 3525 similar events in 2022 emitted 0.6 million tonnes CO<sub>2</sub>.

## 3527 7.2. Focal Regions

3528  
 3529 In this year's report, our detailed analyses target three tropical regions and Southern  
 3530 California. The extreme nature of events in these focal regions are given in Section 2..

- 3531 ● **Northeast Amazonia** saw record forest fire activity, with burned area +332% above  
 3532 average, the highest since records began. Fires severely impacted Indigenous  
 3533 communities, displacing thousands and degrading air and water access.
- 3534 ● The **Pantanal-Chiquitano** experienced its worst fire season on record, with burned  
 3535 areas nearly triple the average and carbon emissions six times above average. Fires





3536 affected both the Pantanal wetlands, the world's largest tropical wetland, and the  
 3537 Chiquitano dry forests of Bolivia. PM<sub>2.5</sub> pollution reached hazardous levels of  
 3538 900 µg/m<sup>3</sup>, carrying strong potential for detrimental health and economic impacts.  
 3539 • **Southern California** recorded catastrophic wildfire losses, with 30 deaths, 11,500  
 3540 homes destroyed, and US\$140 billion in total damages. PM<sub>2.5</sub> levels peaked at  
 3541 483 µg/m<sup>3</sup>, triggering a regional housing and insurance crisis.  
 3542 • The **Congo Basin** had its highest recorded fire activity at 28% above the annual  
 3543 mean, contributing to a +150% increase in primary forest loss in 2024 versus 2023.  
 3544 Fires were the main driver of deforestation but received minimal media or institutional  
 3545 attention, highlighting a broader lack of media coverage of fires affecting equatorial  
 3546 Africa.

3547

### 3548 7.3. Impact Assessments

3549

3550 In this year's report, we incorporate new assessments of the impact of fires on society,  
 3551 specifically via the exposure of populations, physical assets, and carbon projects to fire and  
 3552 via smoke degrading air quality. Key findings from our analyses were as follows.

#### 3553 Population exposure:

- 3554 • We estimate that ~100 million people were exposed to wildfire activity globally during  
 3555 the 2024-25 fire season, with the highest exposures in India and the Democratic  
 3556 Republic of the Congo (15 million each).  
 3557 ○ Uttar Pradesh (India) recorded the highest subnational exposure at 4.6 million  
 3558 people, a 146% increase over average, followed by Heilongjiang (China, 3.7  
 3559 million) and Punjab (India, 3.6 million).  
 3560 ○ Despite severe fire seasons, Canada, Brazil, and Bolivia contributed modestly  
 3561 to global population exposure due to the remoteness of areas burned.  
 3562 ○ Other countries experiencing large *relative* anomalies in population exposure  
 3563 included: Jordan, Peru and Ecuador (Andes); Venezuela, Guyana, and  
 3564 Suriname (northern South America), Nepal and Niger.  
 3565 • 20 thousand people were officially displaced according to IDMC displacement  
 3566 records, or 0.02% of those exposed according to our analysis. This reflects a gap  
 3567 between exposure and formal displacement, though true disruption is likely higher  
 3568 than in the IDMC records due to known issues with underreporting.  
 3569 • Exposed communities may still suffer serious health, economic, and psychological  
 3570 consequences (e.g., missed income, increased debt, long-term health declines),  
 3571 even if they are not formally displaced.

#### 3572 Physical asset exposure:

- 3573 • According to our analysis, an estimated US\$215 billion in physical assets were  
 3574 exposed to wildfires in 2024-25. Top countries by asset exposure were India (US\$44  
 3575 billion), United States (US\$26 billion), China (US\$17 billion), South Africa (US\$14  
 3576 billion).  
 3577 ○ Other countries with high absolute asset exposure were: Mexico, Turkey, and  
 3578 Russia (~US\$8 billion each).  
 3579 ○ Other countries experiencing large *relative* anomalies in physical asset  
 3580 exposure were: Pakistan, Sudan, Chad, Albania, Greece, Iraq, Syria, and  
 3581 Eritrea.  
 3582 • US\$57 billion in direct losses were recorded in the international disaster database  
 3583 EM-DAT, including \$53 billion caused by fires affecting LA and southern California.  
 3584 ○ Direct financial losses are generally smaller than our estimates of physical  
 3585 asset exposure (the detection of fire in proximity to the built environment)  
 3586 because exposure is a measure of potential for loss, and not of loss itself.



- 3587 ○ In the case of southern California, recorded direct financial losses from fires
- 3588 were three times larger than our estimates of exposed physical assets due to
- 3589 the underestimation of asset density in our analysis. A lesson from this work
- 3590 is that analyses of exposure must account for the significant variation in the
- 3591 density of real estate value across states of the USA, and likely in other
- 3592 countries as well.

#### 3593 Carbon project exposure:

- 3594 ● The 2024 fire season saw record BA across forestry projects in the Voluntary Carbon
- 3595 Market (VCM): 169 of 927 projects (18%) experienced fire, the highest on record
- 3596 since 2001, with burned area in 2024 affecting 1.6% of project areas on average.
- 3597 ● 72% of projects experienced above-average drought contributing to elevated risk of
- 3598 fire, with 13% exceeding extreme drought thresholds (SPEI < -2).
- 3599 ● The 2024 fire season had an above average impact on carbon projects in Latin and
- 3600 northern America, average BA was recorded in Eurasia and below average in Africa.
- 3601 In addition to climate, land use and land cover changes and project activities also
- 3602 contributed to regional differences in observed extremes.
- 3603 ● Despite elevated BA in the latest fire season, 46% of all carbon projects experienced
- 3604 no fire in the entire period since 2001, while 67% experienced little fire (defined as
- 3605 <0.5% burned annually in the surrounding 50-km buffer).
- 3606 ● The 2024 season underscores that while high-integrity forest carbon projects remain
- 3607 a key climate change mitigation tool, the permanence of carbon stored or avoided is
- 3608 increasingly threatened by extreme fire years, especially under worsening climate
- 3609 extremes.

#### 3610 Air quality:

- 3611 ● Our analysis of air quality impact in this report focuses exclusively on the
- 3612 Pantanal-Chiquitano focal region, where population-weighted PM<sub>2.5</sub> exceeded the
- 3613 WHO daily standard (15 µg/m<sup>3</sup>) on 43 days between July to October (over a third of
- 3614 all days in the period) from July to October and peaked at a regional
- 3615 population-weighted average of 61 µg/m<sup>3</sup> in September, with fires accounting for
- 3616 ~58% of the pollution. Smoke emissions from fires were the sole cause of
- 3617 exceedances of the WHO daily standard on 50 days in the period July-October.
- 3618 ● Wildfire smoke emissions exposed communities to extremely harmful air quality in
- 3619 various world regions, according to direct measurements (**Appendix A**). For
- 3620 example, communities in the Brazilian Pantanal, Southern California, Bolivia, and
- 3621 northern India were exposed to PM<sub>2.5</sub> concentrations of over 60, 30, 30, and 13 times
- 3622 the WHO daily standard of 15 µg/m<sup>3</sup>, respectively.
- 3623

#### 3624 7.4. Diagnosing Causes and Assessing Predictability

- 3625
- 3626 ● **Weather was the dominant driver of fire activity during all of the 2024-25 focal**
- 3627 **events** targeted in this report, contributing 40% to 70% of the explainable cause.
- 3628 ○ **Fuel** availability and dryness increased in importance during the most severe
- 3629 fires (up to 40% of explainability) and determined the final extent of BA.
- 3630 ○ **Ignitions** were consistently dominated by human influence, but they did not
- 3631 emerge as a primary cause of fire activity during the 2024-25 focal events
- 3632 (only around 10% of explainability).
- 3633 ● In **Northeast Amazonia** fire activity was predominantly driven by persistent,
- 3634 large-scale drought conditions that depleted deep soil moisture reserves. These
- 3635 droughts suppressed fuel moisture recovery for extended periods, even during rain
- 3636 periods. Soil moisture anomalies reached up to 3 standard deviations below the
- 3637 climatological mean, with values dropping to as little as 2% of average. The



- prolonged drought significantly increased fuel dryness and, during the period of most intense burning, fuel importance rose up to 20% above its annual baseline. Fuel also determined the final burned area extent, contributing significantly to the observed anomalies in BA, accounting for up to 50% in the sub-regions where BA anomalies were most extreme. Human-caused ignitions were present but did not emerge as a leading cause of fire (10-20%). Their contribution remained limited and at times negative compared to what is considered usual (thus reducing the total extent), likely reflecting limited ignition opportunities or active suppression efforts to limit BA.
- In the **Pantanal-Chiquitano**, extreme fire activity was primarily driven by antecedent drought persisting since 2023. Deep soil moisture remained in the driest 15% of records, 1-2 standard deviations below average, despite wetter conditions in early 2024. Although February-April rains moistened surface fuels, they failed to recharge deeper layers. Weather dominated fire activity (71% average contribution), with fuel importance rising to 40% during the peak burning week in early August and explaining over 50% of final BA anomalies. Lightning played a minimal ignition role, often occurring in association with convective downpour. Human-caused ignitions, though still dominant, were lower than in previous years and at times limited burned area extent.
  - In the **Congo Basin** extreme fire activity was driven by prolonged and severe drought persisting over recent years. The usual spring wet season (March-May) failed to occur, and the second wet season later in the year provided limited relief, leaving deep soil moisture up to 2 standard deviations below climatological norms. Weather was the dominant driver of fire activity, with rainfall 67% below and temperatures 90% above climatological averages, placing vegetation and soil dryness among the driest 1-2% of records (2003-2023). Human activity accounted for most fire ignitions but as for the other 2 tropical regions they were not the main causes of the fire severity and actually acted to reduce the final BA
  - In **Southern California**, the 2024-25 fire season was marked by atypical seasonality, with extreme fire activity occurring in January well outside the usual summer peak. The Palisades and Eaton fires were driven by a rare convergence of weather, fuel, and ignition factors, each contributing significantly (weather: 40%, fuel: 30%, ignition: 20%). Despite preceding years of exceptional wetness, a short-lived but extreme drying of surface fuels (3 standard deviation below normal) and intense winds (3 standard deviation above normal) created highly flammable conditions. These fires ignited and spread rapidly at the wildland-urban interface, highlighting how brief windows of extreme weather can override generally moist background conditions and trigger major off-season events in these parts of the world.
  - There were **distinct challenges to the forecasting of all focal events**:
    - In **Northeast Amazonia**, our models correctly identified two high-risk fire seasons, but most of the burning occurred during the first (February-April), not the second (August-November), despite similar fire danger forecasts. This disconnect highlights a key limitation: high fire danger does not always lead to high fire activity. Human factors, such as suppression, fire bans, or shifts in land use, likely played a role and are currently underrepresented in fire prediction systems.
    - In the **Pantanal and Chiquitano**, fires were closely linked to long-term drought conditions that dried out fuels months before the fire season peaked. Fire activity rose only after this slow build-up, meaning accurate forecasts required capturing both drought and fuel dynamics. While the general heightening of fire danger was picked up by the FWI, the machine-learning-based PoF model, which includes fuel conditions, better predicted when and where fires would actually occur.
    - In **Southern California**, fire prediction remains difficult without accounting for the 'whiplash effect' that arises from extreme fire weather following on from



3692 wet periods with high vegetation productivity. A wet period led to vegetation  
 3693 growth, followed by rapid drying and strong winds that enabled the January  
 3694 fires. As in the Pantanal-Chiquitano, including fuel information helped the PoF  
 3695 model identify higher-risk areas more accurately than the FWI.  
 3696 ○ In the **Congo Basin**, both FWI and PoF tended to overpredict fire danger.  
 3697 While drought increased flammability, ignition remained limited, possibly due  
 3698 to cultural practices, suppression efforts, or fewer ignition sources (though  
 3699 reporting on such activities in this region is extremely limited). Here, human  
 3700 activity and fuel moisture, more than fire weather, shaped outcomes. The FWI  
 3701 system, which unlike PoF does not include these factors, was less effective in  
 3702 predicting fire activity in the Congo Basin.  
 3703

## 3704 7.5. Attribution to Global Change

- 3705
- 3706 ● **Climate change has increased the likelihood of extreme fire events across all**  
 3707 **focal regions studied.** The high fire weather and extreme levels of burning seen in  
 3708 2024-25 were significantly more likely in a world with human-induced climate change.  
 3709
  - 3710 ● In **Northeast Amazonia**, we find that the extreme fire weather during January-March  
 3711 2024 was 30-70 times more likely due to anthropogenic climate forcing, while the risk  
 3712 of regional BA totals being as observed in the period was 2.1 times greater due to  
 3713 anthropogenic climate forcing and the area burned by fires was four times greater.  
 3714 ○ Our attribution analysis shows high confidence that climate change played a  
 3715 major role in Northeast Amazonia's record fire season. We are virtually  
 3716 certain (>99%) that anthropogenic climate forcing increased the risk of  
 3717 extreme fire weather, very likely (96%) that it amplified the area affected, and  
 3718 likely (89%) that it increased the chance of the extreme burned area  
 3719 observed.  
 3720 ○ While climate change has clearly enhanced the probability of extreme events  
 3721 in the region, such as that seen in 2024, there was conversely no robust  
 3722 evidence that climate change increased average annual BA totals in  
 3723 Northeast Amazonia during 2003-2019.  
 3724 ○ An increase in annual average BA during 2003–2019 of up to 17% was  
 3725 attributed to socioeconomic changes since 1900-1917, indicating that  
 3726 long-term human activities have elevated typical fire levels in the region.  
 3727 ○ Overall, our attribution analyses suggest that climate change has enhanced  
 3728 the likelihood of extreme fire events in the region, against a backdrop of  
 3729 increased annual BA levels driven by socioeconomic change such as land  
 3730 use/land cover change and human ignitions.  
 3731
  - 3732 ● In the **Pantanal and Chiquitano**, we find that the extreme fire weather  
 3733 August-September 2024 was 4-5 times more likely due to anthropogenic climate  
 3734 forcing, while the risk of regional BA totals being as observed in the period was 3.3  
 3735 times greater due to anthropogenic climate forcing and the area burned by fires was  
 3736 around 34 times greater.  
 3737 ○ Our attribution of extreme fire weather to climate change was made virtually  
 3738 certain (>99%, IPCC definition), while the amplification of both extreme  
 3739 burned area and region-wide burned area extent was attributed with likely  
 3740 confidence (87%). Taken together, these findings provide strong evidence that  
 3741 anthropogenic climate change raised the odds of the largest fire season on  
 3742 record in the Pantanal-Chiquitano region.  
 3743 ○ In addition to the enhanced odds of extreme BA events, a 10% increase in  
 3744 annual average BA during 2003-2019 was attributed to climate change.  
 3745 ○ At least a two-fold increase in BA during years with 2024-like fire conditions



- 3746 was attributed to socioeconomic change, indicating that human activities have  
 3747 substantially increased the risk of widespread fire under extreme conditions.  
 3748 However, other analyses focusing on long-term annual average burned area  
 3749 suggest that some human-driven changes may have reduced typical annual  
 3750 fire activity. While these findings are not strictly contradictory since they  
 3751 examine different aspects of the fire regime, the contrast between them  
 3752 reduces confidence in attributing overall fire trends to socioeconomic drivers  
 3753 alone and points to the need for further investigation.
- 3754 ○ Overall, extreme BA events in the Pantanal-Chiquitano, such as those seen in  
 3755 August-September 2024, are made more likely by climate change and are  
 3756 superimposed on broader background increases in fire extent related to  
 3757 climate change and possibly socioeconomic changes in the region.  
 3758
  - 3759 ● In **Southern California**, we find that the risk of regional BA totals being as observed  
 3760 during January 2025 was 2.3 times greater due to anthropogenic climate change and  
 3761 the area burned by fires was 25 times greater.
    - 3762 ○ Our attributions of amplified BA extent during the event to climate change  
 3763 were all made with at least 89% confidence. It is therefore *likely* (per IPCC  
 3764 definitions) that anthropogenic climate change raised the odds of the costly  
 3765 wildfires in Southern California during January 2025.
    - 3766 ○ The meteorological conditions during the event were previously studied by the  
 3767 World Weather Attribution (WWA) group, who reported that extreme fire  
 3768 weather conditions were also made more likely, by around 40%, with other  
 3769 indicators such as prolonged drought and delayed seasonal drying also  
 3770 showing climate influence (Barnes et al., 2025). We did not perform an  
 3771 independent attribution of fire weather here due to a lack of data required for  
 3772 construction of a counterfactual scenario in our attribution protocol.
    - 3773 ○ In addition to the enhanced odds of extreme BA events, a 7% increase in  
 3774 annual average BA during 2003-2019 was attributed to climate change.
    - 3775 ○ Our BA attribution approaches did not provide robust evidence that  
 3776 socioeconomic change affected average annual BA, though this is possibly  
 3777 due to the difference between the coarse model resolution and the fine scale  
 3778 over which effects would be expected at the wildland-urban interface in this  
 3779 region.
    - 3780 ○ Overall, extreme BA events in Southern California, such as those seen in  
 3781 January 2025, are made more likely by climate change and are superimposed  
 3782 on broader background increases in fire extent related to climate change.  
 3783
  - 3784 ● In the **Congo Basin**, we find that the extreme fire weather July-August 2024 was 3-8  
 3785 times more likely due to anthropogenic climate change, while the risk of regional BA  
 3786 totals being as observed in the period was 60% greater due to anthropogenic climate  
 3787 change and the area burned by fires was three times greater.
    - 3788 ○ It is virtually certain that anthropogenic climate change contributed to the  
 3789 extreme fire weather observed during the 2024 season in the Congo Basin.  
 3790 The widespread extent of burned area was very likely influenced by climate  
 3791 change (92% likelihood), while the most extreme sub-regional burned area  
 3792 events were likely influenced (78% likelihood). Together, these findings  
 3793 indicate that climate change increased the odds of the largest fire season on  
 3794 record in the region.
    - 3795 ○ In addition to the enhanced odds of extreme BA events, a more than 45%  
 3796 increase in annual average BA during 2003-2019 was attributed to climate  
 3797 change.
    - 3798 ○ Our BA attribution approaches did not provide robust evidence that  
 3799 socioeconomic change affected average annual BA during 2003-2019 versus  
 3800 a pre-industrial counterfactual.





3801 ○ Overall, extreme burned area events in the Congo Basin, such as those seen  
 3802 in July–August 2024, are made more likely by climate change and are  
 3803 superimposed on broader background increases in fire extent attributable to  
 3804 climate change, with no robust evidence that socioeconomic changes  
 3805 significantly altered recent fire activity.  
 3806

## 3807 7.6. Seasonal and Multi-Decadal Outlook

- 3808 ● **Fire weather and BA forecasts for boreal summer 2025 highlight several areas**  
 3809 **with elevated probability of anomalous fire danger.** Probabilities for anomalous  
 3810 fire prone seasons are high across Canada, northeast Europe (including the UK),  
 3811 and parts of Siberia. These conditions following the second-warmest May on record  
 3812 globally (1.4 °C above pre-industrial levels), with exceptional dryness and the lowest  
 3813 northwestern European rainfall since 1871.  
 3814 ○ In equatorial regions, forecasts show a more than 60% chance of anomalous  
 3815 fire weather conditions in Northeast Amazonia, the Congo Basin, and the  
 3816 Himalayan foothills.  
 3817 ○ In the US, severe drought conditions in Arizona and Texas are already  
 3818 leading to elevated fire activity in line with predicted anomalies in fire weather.  
 3819 ○ Seasonal outlooks of burned area anomalies coincide with fire weather  
 3820 anomalies in western South America, southern California, central North  
 3821 America, and eastern Central Asia.  
 3822 ○ Chile and northern Australia stand out with >50% confidence for anomalous  
 3823 fire activity during the boreal summer of 2025.  
 3824 ○ Despite high FWI in central Europe, we could not confidently predict a BA  
 3825 anomaly due to insufficient historical fire-climate data for reliable modelling.  
 3826
- 3827 ● **In Northeast Amazonia, our climate model projections consistently indicate a**  
 3828 **rise in extreme wildfire risk by the end of the century.** Under a *middle-of-the-road*  
 3829 emissions pathway (SSP370), the frequency of regional BA totals on the scale of  
 3830 2024 are projected to increase by up to 57% by 2100.  
 3831 ○ Also under SSP370, the greatest rate of increase (factor of 2-3 rise) is  
 3832 projected in the sub-regions that burned most extensively in the extreme  
 3833 event of 2024 (5% of model cells with greatest BA).  
 3834 ○ Under a *no mitigation* scenario (SSP585), an even sharper rise is projected,  
 3835 with a near-doubling of the frequency of extreme (2024-like) events at the  
 3836 regional scale. Greater rates of increase (up to a four-fold rise) are projected  
 3837 in the sub-regions that burned most extensively in 2024.  
 3838 ○ In contrast, limiting warming under a *strong mitigation* scenario (SSP126)  
 3839 effectively contains future fire risk. By 2100, the increased frequency of an  
 3840 extreme (2024-like) event is limited to 9%, with the sub-regions that burned  
 3841 most extensively in 2024 showing no significant change. This demonstrates  
 3842 the strong potential of climate action to mitigate the risk of future extreme fires  
 3843 in Northeast Amazonia.  
 3844 ○ Projections of future increased risks are not spatially uniform in any scenario.  
 3845 In some areas, such as Amapá and northern Pará in Brazil, and southern  
 3846 Suriname, increased extreme fire activity is projected as early as the 2030s  
 3847 under higher-emissions scenarios (SSP370 and SSP585). Even under  
 3848 SSP126, rises in extreme BA are projected for parts of the moist forest zone.  
 3849 ○ The frequency of extreme (2024-like) events is projected to rise only modestly  
 3850 in all scenarios through 2050, however by 2100 the increased risk under  
 3851 higher emissions scenarios (SSP370 and SSP585) clearly emerges from that  
 3852 of SSP126.  
 3853  
 3854





- 3855 • In the **Pantanal and Chiquitano**, our climate model projections indicate further  
 3856 **increases in extreme wildfire risk by the end of the century**. Under a  
 3857 *middle-of-the-road* emissions pathway (SSP370), the frequency of regional BA totals  
 3858 on the scale of 2024 are projected to increase by up to 34% by 2100.  
 3859     ○ Also under SSP370, the greatest rate of increase (21-45% rise) is projected in  
 3860 the sub-regions that burned most extensively in the extreme event of 2024  
 3861 (5% of model cells with greatest BA).  
 3862     ○ Under a *no mitigation* scenario (SSP585), an even sharper rise is projected,  
 3863 with a 44% rise in the frequency of extreme (2024-like) events at the regional  
 3864 scale. Greater rates of increase (up to a 75% rise) are projected in the  
 3865 sub-regions that burned most extensively in 2024.  
 3866     ○ In contrast, limiting warming under a *strong mitigation* scenario (SSP126)  
 3867 effectively contains future fire risk. By 2100, the increased frequency of an  
 3868 extreme (2024-like) event is limited to 13% and is not significant, while the  
 3869 sub-regions that burned most extensively in 2024 experience minimal  
 3870 increases in frequency (up to 24% rise). This demonstrates the strong  
 3871 potential of climate action to mitigate the risk of future extreme fires in the  
 3872 Pantanal-Chiquitano.  
 3873     ○ At the regional scale, only modest increases in the frequency of extreme  
 3874 (2024-like) fire seasons are projected by mid-century across all scenarios.  
 3875 However, by 2100, the increased risk becomes more pronounced under  
 3876 higher emissions pathways, with clear divergence between scenarios.  
 3877     ○ At the sub-regional level in the areas that burned most extensively, earlier  
 3878 increases in extreme fire risk could begin as soon as 2030.  
 3879     ○ Projections of future increased risks are not spatially uniform in any scenario.  
 3880 Geographically, widespread increases in BA are projected across most of the  
 3881 Pantanal-Chiquitano by 2100, though the response is considerably more  
 3882 uncertain in the Pantanal than in the Chiquitano. Some areas of increased  
 3883 extreme (2024-like) fire frequency may still emerge in the Pantanal even  
 3884 under SSP126.  
 3885     ○ It is important to note that these projections do not fully incorporate local *in*  
 3886 *situ* drivers, such as wetland degradation, which have already contributed to  
 3887 more frequent fires in recent years. Increases in fire activity might be  
 3888 expected to occur earlier than the models indicate, especially along the  
 3889 wetlands and adjacent drainage areas.  
 3890  
 3891 • In **Southern California**, our climate model projections of future change in  
 3892 **extreme (2024-like) fire events are highly uncertain**.  
 3893     ○ While high-emissions simulations under SSP585 and SSP370 suggest that  
 3894 extreme fire events could become less frequent over time, this strongly  
 3895 depends on how vegetation responds to rising CO<sub>2</sub> and a changing climate.  
 3896     ○ In particular, simulations suggest that increased tree cover driven by CO<sub>2</sub>  
 3897 fertilisation under higher-emissions scenarios (SSP585 and SSP370) may  
 3898 raise fuel loads while simultaneously increasing fuel moisture, with the overall  
 3899 effect being to reduce the likelihood of extreme fire events in our models.  
 3900     ○ However, when removing changes in tree cover, the projected future  
 3901 frequencies of extreme (2024-like) events become highly uncertain with no  
 3902 consistent direction of change under future scenarios.  
 3903     ○ There is a critical need for improved observation and modelling of how  
 3904 vegetation structure, fuel moisture, and local ecological processes shape fire  
 3905 behaviour in Southern California. Nonetheless, Southern California remains  
 3906 highly exposed to fire risk. Even under scenarios that suggest a decline in fire  
 3907 extremes, most residents alive today are still likely to experience multiple  
 3908 extreme fire seasons like 2025 in their lifetime. Stronger local adaptation and  
 3909 more regionally tailored research on climate-vegetation-fire interactions will



- 3910 be essential to manage risk in the coming decades.
- 3911 • In the **Congo Basin**, our climate model projections indicate that further  
 3912 **increases in extreme wildfire risk are likely by the end of the century**. Under a  
 3913 *middle-of-the-road* emissions pathway (SSP370), the frequency of regional BA totals  
 3914 on the scale of 2024 are projected to increase by up to 50% by 2100.
- 3915 ○ Also under SSP370, far greater rates of increase (up to a 5-fold rise) are  
 3916 projected in the sub-regions that burned most extensively in the extreme  
 3917 event of 2024 (5% of model cells with greatest BA).
- 3918 ○ Projections under SSP370 and SSP585 show similar levels of elevated risk,  
 3919 indicating that mitigation efforts stronger than those implied by SSP370 are  
 3920 likely needed to meaningfully reduce future fire risk.
- 3921 ○ In contrast, limiting warming under a *strong mitigation* scenario (SSP126)  
 3922 effectively contains future fire risk. By 2100, the increased frequency of an  
 3923 extreme (2024-like) event is limited to at most 11%, while the sub-regions that  
 3924 burned most extensively in 2024 experience a far smaller increase in  
 3925 frequency (up to 42% rise) than under higher emissions scenarios. This  
 3926 demonstrates the strong potential of climate action to mitigate the risk of  
 3927 future extreme fires in the Congo Basin.
- 3928 ○ Projections of future increased risks are not spatially uniform in any scenario.  
 3929 Some of the largest projected increases, seen in Gabon, Equatorial Guinea,  
 3930 and central DRC, may begin as early as the 2030s, with the frequency of  
 3931 extreme (2024-like) events is projected to increase 2 to 4-fold by 2100. This  
 3932 increase is driven largely by declining fuel moisture as climate change  
 3933 reduces rainfall and increases dry spells across much of the region.
- 3934 • **Anthropogenic climate change has the potential to significantly increase future**  
 3935 **fire risk for living generations, turning previously exceptional events into**  
 3936 **events that are experienced several times in a generation.**
- 3937 ○ **Northeast Amazonia:** Our projections show that a person born in this region  
 3938 today has a 41-55% likelihood of experiencing at least one extreme fire  
 3939 episode on the scale of January-March 2024 in their lifetime under *strong*  
 3940 *mitigation* scenario (SSP126). This likelihood rises to 52-69% under a  
 3941 *middle-of-the-road* scenario (SSP370), and 55-76% under a *no mitigation*  
 3942 scenario (SSP585). The odds of experiencing two or more such events are  
 3943 considerably higher under *no mitigation* (19-42%) than under *strong*  
 3944 *mitigation* (10-19%).
- 3945 ○ **Pantanal-Chiquitano:** Our projections indicate that a person born in this  
 3946 region during the 1940s already had a ~78-85% likelihood of experiencing at  
 3947 least one fire season like 2024. For someone born today, this likelihood rises  
 3948 to 86-91% even under SSP126. Under SSP370, the likelihood of experiencing  
 3949 at least two 2024-scale fire seasons rises to 62-74%, compared to 45-57% for  
 3950 someone born in the 1940s, but even under low emissions, the chance of two  
 3951 such events exceeds 58%. These findings highlight that while climate change  
 3952 mitigation can reduce future fire risk, it is not sufficient on its own. Early  
 3953 adaptation, ecosystem management, and stronger fire governance will be  
 3954 essential to reduce future impacts.
- 3955 ○ **Congo Basin:** Our projections show that a person born in this region today  
 3956 has a 49-63% likelihood of experiencing at least one fire season like July  
 3957 2024 under SSP126. This likelihood rises to 61-87% under SSP370 and  
 3958 67-91% under SSP585. The likelihood of experiencing multiple events differs  
 3959 starkly across SSPs, with up to a likelihood of 43% for three events under  
 3960 SSP585, compared to just 3-8% under SSP126.
- 3961



## 3962 **7.7. Progress in the State of Wildfires Report**

3963

3964 This report incorporates a number of major advances in our annual reporting on the State of  
 3965 Wildfires in the prior fire season. In **Section 2**, we added a new analysis of fire intensity to  
 3966 our extreme event identification variables, and we evaluated the dependence of our extreme  
 3967 event identification on the source of BA observation by incorporating data for 2019-2025  
 3968 from two additional BA datasets (FireCCIS311 and VIRS VNP64A1), supplementing our  
 3969 consistent multi-decade analysis based on the MODIS BA dataset (MCD64A1). The  
 3970 contribution of regional expert knowledge was also formally recognised through the  
 3971 establishment of regional expert panels for each continent, with these panels consulted for  
 3972 their interpretation of results across all aspects of the report. We added **Section 3**, which  
 3973 presents an entirely new set of impact assessments relating to population exposure, asset  
 3974 exposure, carbon project exposure and air quality degradation. In **Section 4**, we expanded  
 3975 the analysis of the predictability of the focal event to include seasonal predictions of burned  
 3976 area, complementing the fire danger seasonal forecasts already provided. In **Section 5**, our  
 3977 main advancement was a new approach to attributing both extreme regional BA totals *and*  
 3978 sub-regional BA extremes directly to the 2024-25 focal events, made possible by developing  
 3979 near real-time counterfactuals and employing methodologies for aggregating probabilities  
 3980 across space. This represents a step-change versus our first report, which focussed on  
 3981 attributing sub-regional BA extremes only and substituted near real-time counterfactuals with  
 3982 less targeted counterfactuals for the 2003-2019 period. By creating more robust  
 3983 counterfactuals with observed events, and accounting for the stochastic nature of fire  
 3984 anomalies locations, we were able to more directly and confidently assess whether human  
 3985 influence made these specific fires more likely on regional scales. In **Section 6**, we extended  
 3986 our forward-looking capabilities by providing seasonal forecasts of BA, complementing the  
 3987 fire danger forecasts already presented in previous reports. We also added future  
 3988 projections of FWI at future global warming levels of 1.5-4.0°C, providing a clearer picture of  
 3989 how extreme wildfire risk may evolve in the coming decades.

3990

3991 This new report documents the progress made in the observation, diagnosis, modelling and  
 3992 attribution of extreme wildfire events and their impacts. As a community, our work is both  
 3993 driving innovation in the methods under use and prompting the development of new  
 3994 capabilities for the routine analysis of extreme wildfire events and their impacts. This new  
 3995 report builds on our inaugural report (Jones et al., 2024b) and documents the progress being  
 3996 made by the fire science community.

3997

3998 By combining cutting edge techniques in fire forecasting, prediction and modelling across the  
 3999 sections of our report, we compile multiple lines of evidence for a clear climate signal in  
 4000 recent fire extremes. Our complementary analyses consistently point to a strong role for  
 4001 climate change in driving extreme fire conditions, showing that human influence, both  
 4002 through climate change through socioeconomic change factors, are increasing fire risk and  
 4003 producing extreme wildfires. While individual methods sometimes diverge, particularly in  
 4004 regions like the Pantanal, where local socioeconomic factors emerge more clearly as drivers  
 4005 in some analyses, the overall convergence across independent lines of evidence builds  
 4006 confidence in the conclusion that climate changes exerts significant upwards pressure on the  
 4007 likelihood of extreme fire events.

4008

4009 These multiple lines of evidence show that human influence, often through climate change  
 4010 though sometimes through socioeconomic factors, are increasing fire risk and driving higher  
 4011 burned areas. Across every region analysed, we find clear signals that recent extreme  
 4012 wildfires are not purely natural events, but increasingly shaped by human-driven changes to  
 4013 climate and ecosystems.

4014

4015 A key strength of this report lies in its systematic evaluation of model performance across  
 4016 diverse regions of the globe. In this edition, for instance, we identify limitations in the



capacity of coarse-resolution air quality models to assess smoke exposure in small regions (Section 3), and show how projections of future fire activity can be strongly influenced by how models represent sensitive vegetation responses to uncertain climate changes (Section 6). In regions such as California, long-term projections are particularly sensitive to changes in tree cover, which can be affected by uncertainties in both climate inputs and modelled vegetation responses.

A rich body of observations, such as land surface and meteorological data are available to observe and model the effects of climatic change and variability on extreme fire likelihood, in particular following important advances in the modelling of fuel load and moisture dynamics during recent decades. However, a major outstanding barrier that consistently limits the effectiveness of our analyses, and those of the broader fire science community, is a severe lack of information regarding *in situ* human activities. Funding of projects that overcome this barrier is paramount and carries the greatest potential to drive a step-change in performance of fire models and predictive systems. Often, prediction and modelling analyses rely on basic indicators of human effects such as population density, which cannot sufficiently represent the diversity of relationships between people, their land uses, and the outcomes for fire ignitions and spread dynamics. Our work, and that of many others, highlights the need to develop global datasets that effectively represent the range of human-fire interactions that occur on Earth but with sufficient scalability to support regional and global analyses. Inevitably, there will be a trade-off between the geographical scalability and nuance of these datasets as they are developed.

Overall, our international collaboration routine catalogues fire extremes and annually evaluates the most extreme fire events of international relevance using state-of-the-art fire science tools. We provide a consistent stream of actionable information to policymakers, disaster management services, firefighting agencies, and land managers, informing action on enhancing society's resilience to wildfires through investment in preparedness, mitigation, and adaptation.



4047

## 4048 Appendix A: Year in Review by Continent

4049

4050 This appendix includes the review completed by regional expert panels to supplement our  
 4051 quantitative analyses of extremes in the 2024-25 fire season (**Section 2**). Details of the  
 4052 assembled panel are provided in **Table A1**, below.

4053

4054 **Table A1:** Experts contributing to the identification of extreme events and characterisation of  
 4055 the global fire season during March 2024-February 2025.

Region	Co-authoring Experts	Country of Organisation / Nationality	Professional Background(s)	Supporting Expert Panellists	Others Consulted
Africa	Kebonye Dintwe	Botswana		Lucy Amisshah (Ghana), Sally Archibald (South Africa), Natasha Ribeiro (Mozambique), Tercia Strydom (South Africa)	
	Aya Brigitte N'Dri	Ivory Coast			
Asia	Cong Gao	China		Bambang Saharjo (Indonesia), Sundar Sharma (Nepal), Raman Sukumar (India), Veerachai Tanpipat (Thailand), Bo Zheng (China)	
	Elena Kukavskaya	Russia	Research		
Europe	Paulo Fernandes	Portugal	Research	Davide Ascoli (Italy), Stefan Doerr (UK), Julien Ruffault (France), Gavriil Xanthopoulos (Greece)	
	Cristina Santín	Spain	Research		
	Johan Sjöström	Sweden	Research		
North America	Crystal Kolden	USA	Research, Firefighting	Jacqueline Shuman (USA), Matt Jolly (USA), Piyush Jain (Canada), Chelene Hanes (Canada)	
	Mathieu Boubonnais	Canada			
	Victoria Donovan	USA			
Oceania	Hamish Clarke	Australia	Research, Environmental Management		Simeon Telfer, South Australian Country Fire Service; Rui Feix, Western Australian Department of Fire and Emergency Services; Chris Collins, Tasmania Fire Service; Grant Pearce, Fire and Emergency New Zealand; David Field, New South Wales Rural Fire Service; Russell Stephens Peacock, Queensland Fire and Emergency Services; Maggie Towers, Northern Territory Police, Fire and Emergency Services
	Sarah Harris	Australia	Research, Emergency Management		
South America	Liana Anderson	Brazil	Research	Dolores Armenteras (Colombia), Francisco de la Barrera (Chile), Mauro Gonzalez (Chile), Celso H.L. Silva-Junior (Brasil)	
	Carlos M. Di Bella	Argentina	Agronomist/Research		
	Bibiana Bilbao	Colombia			
	Galia Selaya	Bolivia	Tropical Ecology/Research and action		

4056



## 4057 **A1. Africa**

4058

4059 National and regional fire monitoring statistics are rarely recorded or made publicly available  
 4060 by fire agencies in Africa, meaning that our assessment of the latest global fire season  
 4061 largely focuses on the insights provided by global data analyses. According to these data,  
 4062 the total BA in Africa was approximately 2.4 million km<sup>2</sup> during the 2024-2025 fire season,  
 4063 11.6% below the mean annual BA since 2002 (2.7 million km<sup>2</sup>). Most of the BA occurred in  
 4064 non-forest (2 million km<sup>2</sup>), with the remaining portion in the forest. Non-forest and forest BAs  
 4065 were 12% and 7% lower than the mean annual BA, respectively. The BA anomaly was  
 4066 notably larger in NHA (-14.6%) than in SHA (-9.1%). The relatively low BA in many parts of  
 4067 the continent could be a result of a combination of factors, though it aligns with a trend that  
 4068 has been attributed to the continued suppression of fire from expanding croplands (Andela et  
 4069 al., 2017) and to changing rainfall patterns across the continent (Zubkova et al., 2019).

4070

4071 Africa's most pronounced positive anomalies in BA and fire C emissions of the 2024-25 fire  
 4072 season were seen in the Congo basin and northern parts of Angola (**Figure 1, Figure 2;**  
 4073 **Table 2, Table 3**). BA in the Republic of Congo was 25% above average, the highest on  
 4074 record, and similarly fire C emissions were 25% above average (**Table 2, Table 3, Figure**  
 4075 **S43**). In the Democratic Republic of the Congo, the Mai-Ndombe and Sankuru provinces  
 4076 each experienced record levels of BA or fire C emissions with anomalies in the range of  
 4077 36-58% (**Table 2, Table 3**). These anomalies were centred on several western ecoregions of  
 4078 the Congo Basin, including the Atlantic Equatorial coastal forests where BA was more than  
 4079 triple the annual mean, Western Congolian swamp forests where BA was twice the annual  
 4080 average and the Central Congolian lowland forests where BA was 77% above average, and  
 4081 the Northwestern Congolian lowland forests where BA was 55% above average. These  
 4082 results align with the recent report of the Global Forest Watch (World Resources Institute,  
 4083 2025) which found that the Democratic Republic of the Congo (DRC) and the Republic of the  
 4084 Congo experienced their highest rates of primary forest loss since 2015. While loss to  
 4085 wildfire is a minor component of overall forest loss in the region (below 15%), for instance  
 4086 compared to the expansion of shifting cultivation, wildfires were the major explanation for the  
 4087 more than doubling (+150%) increase in forest loss in 2024 versus 2023.

4088

4089 The uptick in fires in the Congo basin can be linked in part to the enabling effect of  
 4090 record-breaking fire weather caused by drought in the region (**Section 2.2.2.1**), however a  
 4091 range of socioeconomic changes have also been underway and likely influenced the events  
 4092 of last year. Use and degradation of the forests for resources, often linked to an increase in  
 4093 related wildfire ignitions, is growing due to the extraction of timber to produce charcoal,  
 4094 clearing of land for the expansion of cash crops, and shortening or cessation of fallow  
 4095 periods in smallholder shifting cultivation systems (World Resources Institute, 2025). The  
 4096 potential effects of fires in this region on forest carbon stocks are globally significant (though  
 4097 they are yet to be quantified), with the region's swamp forests harbouring 30 billion metric  
 4098 tonnes of C in peat (Garcin et al., 2023). The 2024 IQAir World Air Quality Report highlighted  
 4099 that the Democratic Republic of the Congo had an annual average PM<sub>2.5</sub> concentration of  
 4100 58.2 µg/m<sup>3</sup>, over 11 times higher than the World Health Organization's annual standard  
 4101 (IQAir, 2025). This indicates hazardous air quality levels, in part to the effects of elevated  
 4102 wildfire smoke emissions (IQAir, 2025). Despite the potentially large impacts on society and  
 4103 the environment, there was very limited news coverage on the impacts of these fires by  
 4104 national news outlets across the region. This underscores the importance of projects such as  
 4105 ours and the Global Forest Watch (World Resources Institute, 2025) using Earth  
 4106 Observations to routinely trace environmental extremes and highlighting events that would  
 4107 otherwise have gone under-reported.

4108

4109 The high BA in the Congo Basin during 2024-25 has implications for various initiatives  
 4110 supported by non-governmental organisations in the region, which aim to promote protection  
 4111 and sustainable management of tropical forests. For example, UNEP's Congo Basin





4112 Sustainable Landscapes Programme (Green Policy Platform, 2025) supports action in  
 4113 Cameroon, Central African Republic (CAR), the Democratic Republic of the Congo (DRC),  
 4114 Equatorial Guinea, Gabon, and Republic of the Congo. In programmes such as this, wildfire  
 4115 can sometimes be considered a secondary disturbance factor compared to other factors  
 4116 such as clear-cut deforestation, but years such as 2024 demonstrate that large-scale  
 4117 intermittent fires in the region can have lasting consequences for forest loss.

4118  
 4119 In Angola, BA and fire C emissions were 15-49% above average in the provinces of Moxico,  
 4120 Huíla, and Bié and were either record-setting or high-ranking (**Figure S44; Figure 2, Figure**  
 4121 **3; Table 2**). As discussed in **Section 2.2.2** and investigated formally for the Congo Basin in  
 4122 **Section 4**, a particularly hot and dry fire season elevated the risk of fire in these regions and  
 4123 coincided with broader social and economic factors promoting fire ignitions. The poor  
 4124 economic situation in Angola over the past three years has prompted deregulation of the  
 4125 charcoal industry and the harvesting of trees for charcoal production has risen, driving up fire  
 4126 activity (Valor Económico, 2024; VisiteHuila, 2024). In addition, the government has been  
 4127 promoting agriculture through financial programs, leading to the clearing of land through  
 4128 shifting agriculture in Miombo woodlands (Fundo de Garantia de Crédito, 2024; World Bank,  
 4129 2024b). In certain provinces, particularly Moxico in Angola, burning for hunting purposes is  
 4130 also widespread and declining populations of prey have been linked to increased burning of  
 4131 areas that were previously hunted less regularly (Papelo, 2024). These are just some of the  
 4132 socioeconomic factors that may have contributed to the elevated availability of ignition  
 4133 sources during 2024-25 fire season, when fire weather was particularly conducive to fire.

4134  
 4135 In Algeria, fires have killed and injured dozens and caused significant loss of life and  
 4136 damage in recent years. At least 34 people were killed and several hundred were injured in  
 4137 Bejaia province during the 2023-24 fire season (Jones et al., 2024b). However, in 2024-25, a  
 4138 low number of fires were recorded and there were no casualties in Algeria, which could be  
 4139 attributed to various factors such as the availability of better firefighting equipment, new fire  
 4140 management policies, and a new law that was passed that imposes life imprisonment for  
 4141 those caught deliberately starting forest fires (Serrah, 2024; The Arab Weekly, 2024).  
 4142 Algerian authorities launched a wildfire prevention system that included 13 water-bombing  
 4143 aircraft and 100 drones for monitoring and tracking firefighting operations. For instance, 26  
 4144 fires were extinguished within 24 hours in the central and eastern regions of Algeria, with no  
 4145 injuries or casualties reported (Gabriel, 2024).

4146  
 4147 In South Africa, the total BA was over 46,000km<sup>2</sup>, which was 17% higher than the mean  
 4148 annual BA. According to a report by the organisation Working on Fire (2024), the increased  
 4149 intensity and frequency of these fires continue to challenge firefighting resources. The  
 4150 2024-25 fire season broke records, with 2,750 firefighting teams dispatched, with a record  
 4151 number of 34 people losing their lives, including firefighters. In KwaZulu-Natal Province, the  
 4152 wildfires claimed the lives of 14 people, of whom 6 were firefighters who were trapped in a  
 4153 blaze. In addition to the lost lives, thousands of people were displaced, over 2,050 livestock  
 4154 destroyed, and critical infrastructure damaged. The high intensity fires in South Africa could  
 4155 be due to a string of particularly high rainfall years that resulted in large accumulated grassy  
 4156 fuel loads.

4157  
 4158 In Côte d'Ivoire, the overall BA in 2024-2025 was lower than the historical average, contrary  
 4159 to what some national experts had expected following the long dry season which began  
 4160 earlier than usual in the savanna areas of the country where fire is most widespread (N'Dri et  
 4161 al., 2018, 2024; Soro et al., 2021). Nonetheless, the fire season was marked by an  
 4162 above-average fire size distribution and there were several deadly events in the country's  
 4163 main fire hotspots, with fires burning over 150,000 ha of forest, 2,800 ha of plantations, 109  
 4164 ha of reforestation projects, and 107 properties in 2025 (CNDFB, 2025). In the department of  
 4165 Séguéla (Worodougou region), wildfires in February 2024 destroyed 50,000 ha of natural  
 4166 vegetation, 261 ha of cropland, 236 ha of cashew plantations, 19 homes, and claimed the



lives of 23 individuals across the villages of Sélakoro, Djénigbé, Touna, Djoman and Kondogo. In Bouna (Bounkani region), fires affected around 12,387 ha, of which 7,528 ha were forested, leading to additional humanitarian impacts. Three further fatalities were recorded between February and March 2024 in Bongouanou (Moronou region) and Taabo (Agnéby-Tiassa region). These impacts occurred despite the continued efforts of the *Comité National de Défense de la Forêt et de lutte contre les feux de Brousse* (CNDFB), such as the construction of firebreaks during the dry season and awareness campaigns. This reflects the challenges posed by expanding agricultural land and ignition sources, fire suppression policies that focus on fire exclusion to protect valuable crops (e.g. cashew nuts) but promote fuel build-up, and a lack of prescribed burning in Côte d'Ivoire's savanna ecosystems (Ruf et al., 2010; Soro et al., 2020; Kouassi et al., 2022). Generally, fire activity and BA have been declining across all ecoregions of Côte d'Ivoire, which has been attributed to conversion of savannas to agricultural lands and also bush encroachment in savanna areas (N'Dri et al., 2022; Douffi et al., 2021; Kouassi et al., 2022).

## A2. Asia

The 2024-25 fire season in Asia was generally not an extreme one, with much of Asia experiencing typical or low BA. Nonetheless, there were regional extreme fire events in the fire season.

Iran emerged as a notable case, experiencing its most severe wildfire season since 2002, marked by record-breaking BA, number of fires, and carbon emissions at the national level (**Figure 2, Figure 3**). Ecologically sensitive regions were disproportionately affected, including Karkheh National Park in Khuzestan Province and the forests and rangelands of Ab Kenar and Khan Ahmad Basht in Kohgiluyeh and Boyer-Ahmad Province (Global Fire Monitoring Center, 2024). As one of the driest countries in the world, Iran experiences approximately 1,500 wildfire outbreaks annually, resulting in the burning of 15,000 ha of forest (Kheshti, 2020; Tavakoli Hafshejani et al., 2022). Human activities are the primary driver of wildfires nationwide, with deforestation, illegal logging, and accidental ignition contributing to the high incidence of fires (Masoudian et al., 2025). These anthropogenic pressures are compounded by systemic shortcomings against wildfires, including inadequate resource allocation and insufficient prevention measures, which challenge the protection of natural ecosystems (Iran International, 2024).

Nepal also endured its second-worst fire season since 2002 (**Figure S45**), with over 5,000 fires according to some sources (Bolakhe, 2024; and >1,000 individual fires in our analysis, **Figure S45**) causing more than 100 fatalities (Bolakhe, 2024). In Lumbini province, located in western Nepal, wildfires devastated 11,448 ha of forests and destroyed more than 230 houses and livestock shelters (Sanju Paudel, The Kathmandu Post, 2024). These catastrophic events were driven by extreme drought, prolonged heatwaves, and frequent lightning strikes (Karuna shechen, 2024). Concurrently, anthropogenic factors including agricultural residue burning, poachers' use of fires, and unintentional human negligence, have exacerbated wildfire occurrence (Shradha Khadka, Governance Monitoring Centre Nepal, 2024). Notably, Nepal's forest cover has doubled over the last three decades, increasing from 26% to 45% between 1992 and 2016 (Karan Deep Singh, The New York Times, 2022). While Nepal's afforestation initiatives represent a significant environmental achievement, addressing the escalating human-nature conflict and strengthening resilience to climate-induced disasters remain critical challenges for ensuring the sustainability of this fragile progress.

Northern India, bordering Nepal, also experienced extreme heatwave and drought in 2024, triggering unprecedented wildfire activity across several states (Reuters, 2024). Uttar Pradesh, for example, experienced its most severe wildfire season, marked by



record-breaking BA, carbon emissions, rate of growth, and fire size (**Figure A1**). Human activities, mainly land clearing and negligence, serve as the primary ignition source in Northern India, leading to uncontrolled wildfires. These fires are further exacerbated by the accumulation of dry pine needles in forests, which act as a ready fuel, and the steep Himalayan slopes, which accelerate the rate of fire growth (Vivek Saini, Climate Fact Checks, 2024). Agricultural practices in Northern India, a critical crop-producing region, have also contributed to the extreme wildfire season. Despite regulatory bans, post-harvest burning of crop residue has continued unabated in recent years (Arshad R. Zargar, CBS News, 2024). At the same time, temperature inversions coupled with Himalayan topographical blockages have trapped pollutants over Northern India. This phenomenon culminated in severe air haze episodes in New Delhi in November 2024, with  $\text{PM}_{2.5}$  concentrations exceeding  $200 \mu\text{g}/\text{m}^3$  across large parts of Northern India (CAMS, 2024).

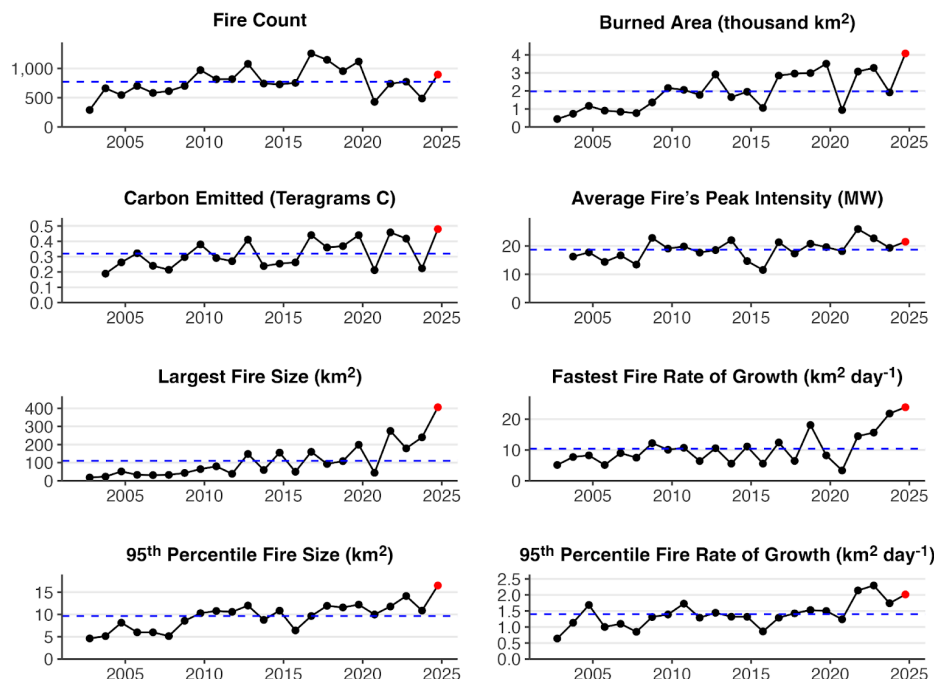


**Figure A1:** Summary of the 2024-2025 fire season in the Indian State of Uttar Pradesh. Time series show annual fire count, BA, C emissions totals within the region, as well as the average fire's peak fire intensity (95th percentile value of fire radiative power within fire perimeters), the 95th percentile fire size, fastest daily rate of growth, and 95th percentile fire daily rate of growth. Black dots show annual values prior to the latest fire season, red dots the values during the latest fire season, and blue dashed lines the average values across all fire seasons. Although Russia generally experienced a typical fire season, several regions in Siberia recorded extreme fire activity. Two regions (Republic of Sakha and Zabaikalsky krai) accounted for 65% of the total forest area burned in Russia (Avialesookhrana, 2024) with 97% of the fires recorded in hard-to-reach areas according to official data from the Federal Forestry Agency (Rosleshoz, 2024). The high fire activity was associated with intense heat, decreasing precipitation and dry thunderstorms (Rosleshoz, 2024), which have become more frequent phenomena in Siberia in recent decades (Huang et al., 2024). Firefighting was complicated by strong winds and mountainous terrain (Rosleshoz, 2024). To attract



additional fire-fighting forces, federal emergency regimes were introduced from May 31 to November 8 in the Zabaikalsky krai and from June 28 to September 13 in the more northern Republic of Sakha, including in the Arctic Circle. In total, 139 redeployments involving 3,500 firefighters were carried out in 2024. The main causes of forest fires were lightning (48%), local population (39%) and fire transitions from other land categories (10%) (Rosleshoz, 2024). While the area burned in 2024 in the Republic of Sakha was not the highest compared to fire activity in the previous years, there is an increasing trend of fire activity and severity in the region over the last decade (ISDM, 2024), associated with weather anomalies (Tomshin and Solovyev, 2022) resulting in an increase in the duration of the fire season and the average area burned (Kirillina et al., 2020; Narita et al., 2021). The estimated total emissions for June 2024 were the third highest in the past two decades, following those of 2019 and 2020 (AMAP, 2024). In the Zabaikalsky krai, the total area burned in 2024 was about 7% of the area of the region, which is the highest value since 2010 (ISDM, 2025). Overall, both regions are considered hotspot areas of fire-induced change, where anthropogenic patterns and climate change are increasing ecosystem damage from wildfires and inhibiting recovery of natural ecosystems (Kukavskaya et al., 2016; Burrell et al., 2022).

Persistent dry and warm spring conditions in southwest China, particularly in Sichuan and Guizhou provinces, resulted in high-ranking BA anomalies (Figure 2). Strong winds exacerbated fire risks by increasing regional fire size and rate of spread, leading to large and fast-moving wildfires (Global Times, 2024). One of the most severe wildfires in Sichuan lasted 14 days, displacing more than 3,000 civilians across 11 villages and one community (Dou et al., 2024). Northeast China, including Heilongjiang and Jilin provinces, also experienced widespread wildfire anomalies during the spring season (Figure 2; Table 2). Contrary to the climate-driven wildfires in southwest China, these wildfires were predominantly anthropogenic originating from crop residue burning. The Chinese government implemented policies in 2013 and 2018 to control straw burning, a major contributor to air pollution, which initially achieved measurable success (Huang et al., 2021; Song et al., 2024). However, due to financial strain on rural communities and administrative pressures on local officials, recent policy adjustments have shifted from a zero-tolerance approach to a more flexible framework. This revised strategy permits controlled crop residue burning in designated areas during periods of low air pollution risk (Ding, Sixth Tone, 2025).

Earth observations data showed high-ranking BA anomalies, frequent fires, fires with large sizes, and rates of growth during 2024-25 in several regions of Lebanon, Palestine, Jordan, Iraq, Syria, United Arab Emirates, Philippines, and Laos (Figure 2, Figure 4), consistent with reports of persistent heatwave in these regions (Zachariah et al., 2024).

A drought that persisted from the 2024-25 fire season to the 2025-26 fire season has resulted in several highly impactful events in Asia (Faranda et al., 2025). Thus, from March 21st 2025, South Korea experienced its deadliest wildfires on record with very strong wind, burning across 11 regions and resulting in 31 deaths, 44 injuries, more than 3.3 thousand displaced people, and at least 4 thousand homes damaged (Yonhap, 2025). The wildfire in Iwate Prefecture, Japan, which started on February 26th 2025, was the country's largest wildfire in over 50 years, killing one person, destroying 221 buildings and forcing evacuation of over 4,5 thousand people (NHK, 2025). These events are not reviewed at length here, however they will be featured in future editions of the State of Wildfires report.

4297

### 4298 A3. Europe

4299

In 2024, wildfire activity in the European Union was close to the long-term average in terms of total BA, but characterized by strong regional contrasts; approximately 420,000 ha were burned, slightly above the 18-year average (San-Miguel-Ayanz et al., 2025), with some countries experiencing record-breaking seasons and others seeing minimal fire activity.



4304 Across the continent, including in Turkey and Ukraine, a total of 1.82 million ha burned from  
 4305 March 2024 to February 2025 as recorded by the European Forest Fire Information System  
 4306 (2025), of which 48% pertain to large (>500 ha) fires. The EU Civil Protection Mechanism  
 4307 (EUCPM) was activated 16 times in response to wildfires, providing international assistance  
 4308 to Greece, Portugal, Cyprus, Bulgaria, Albania and North Macedonia (European  
 4309 Commission Emergency Response Coordination Centre, 2024).

4310  
 4311 The 2024 wildfire season in the Nordic and Baltic countries was the calmest in recent  
 4312 decades. While spring was drier and warmer than average in some areas, abundant summer  
 4313 precipitation limited fire spread. No major wildfire events were reported, and most incidents  
 4314 were confined to small wildfires caused by land-management activities (Swedish  
 4315 Firefighters, 2024). Likewise, wildfire activity in Western Europe during 2024 and early 2025  
 4316 was subdued, as precipitation during spring and summer limited fire occurrence and spread  
 4317 across the region. France experienced one of its quietest seasons in recent decades, and  
 4318 similar conditions were observed in Belgium, the Netherlands, Ireland, and the UK (Global  
 4319 Wildfire Information System, 2025). The fire season was insignificant in Central Europe,  
 4320 because of wetter-than-average conditions during spring, especially in the Czech Republic  
 4321 and in Slovakia. However, Austria saw the highest number of fires and the largest BA since  
 4322 2012 (Global Wildfire Information System, 2025) and Germany experienced a slightly  
 4323 above-average fire season, consistent with the trend of the previous five years. The most  
 4324 notable incident was a wildfire in Harz National Park in July, which led to the evacuation of  
 4325 approximately 500 people and involved 150 firefighters (Deutsche Welle, 2024).

4326  
 4327 In Southern Europe fire activity varied widely depending on seasonal precipitation and fire  
 4328 weather, with notable peaks in July-August (Balkans) and September (Portugal). In Portugal  
 4329 (**Figure S46**), 2024 was the most impactful year since 2017: 137,111 ha burned on the  
 4330 mainland, around 20% above the past decade's average, with 25 fires exceeding 1,000 ha,  
 4331 eight of which surpassed 5,000 ha (Instituto de Conservação da Natureza e Florestas,  
 4332 2024). Most of these fires occurred as a sudden burst in mid-September in the northwest  
 4333 and under exceptional fire weather conditions (Instituto Português do Mar e Atmosfera,  
 4334 2024). The Sever do Vouga complex and other major fires affected wildland-urban interface  
 4335 areas, resulting in 16 fatalities (Agência para a Gestão Integrada de Fogos Rurais, 2025),  
 4336 and €180 million in estimated losses across housing, infrastructure, forestry, and agriculture  
 4337 (Centro de Coordenação Regional Centro, 2024; Centro Pinus, 2024). Additionally, 48,272  
 4338 ha of protected areas and Natura 2000 habitats burned (Gonçalves and Marcos, 2024). In  
 4339 Madeira island, a fire burned over 5,000 ha, entering the non fire-adapted laurel forest, a  
 4340 UNESCO World Heritage Site (Público, 2024).

4341  
 4342 BA in Spain, Italy and Greece was respectively 41, 51 and 73% of the 2012-2023 average  
 4343 (Global Wildfire Information System, 2025). In Greece, the drought lasted until mid  
 4344 November, lengthening the fire season and enabling unusual high-elevation fires in the  
 4345 north. Nonetheless, strengthened preparedness and fire suppression hindered the spread of  
 4346 many potentially large fires. The most destructive fire occurred near Varnavas in August,  
 4347 entering the NE suburbs of Athens and killing one person (Giannaros et al., 2024).

4348  
 4349 The 2024 fire season in the Balkans and Southeastern Europe was among the most severe  
 4350 in recent decades for several countries. Wildfire activity was substantial in North Macedonia,  
 4351 Serbia, Albania, Kosovo and Bulgaria, including multiple large-scale events requiring  
 4352 international firefighting assistance. In Albania, the largest wildfire surpassed 4,000 ha in the  
 4353 Dropull i Poshtëm region and the EU Civil Protection Mechanism was activated in response,  
 4354 with aerial support from Greece and Italy (Directorate-General for European Civil Protection  
 4355 and Humanitarian Aid Operations, 2024). Evacuations were carried out near the coastal  
 4356 town of Shengjin. Bulgaria experienced its worst fire season since 2007, with two wildfires in  
 4357 July destroying houses, the Sakar Mountain fire (Radio Bulgaria, 2024) and the Gorska  
 4358 Polyana fire (Novinite, 2024). North Macedonia (**Figure A2**) and Serbia faced their worst fire





seasons in over two decades, and a state of emergency was declared in the former (Euronews, 2024), where four fires larger than 10,000 ha were recorded (European Forest Fire Information System, 2025). On 16 August, Serbian authorities reported 135 active wildfires within 24 hours (N1info, 2024). Other countries in the region, such as Croatia and Montenegro, had seasons closer to the norm. In the Romanian Danube delta, and during an unusually dry winter, 45,000 ha of wetlands burned in February 2025, a recurring phenomenon with increasing extent (Volodymyr and Andiy, 2025). BA in Turkey reached 270,000 ha, about 65% of the previous 12-years average (Global Wildfire Information System, 2025) but with noticeable societal consequences. Most large fires (up to 7000 ha) occurred in the province of Mardin (European Forest Fire Information System, 2025), including a rapidly spreading fire that burned farmland and impacted villages on 20 June, killing 15 and additionally injuring at least 70 people (The Nation, 2024). A fire that started near the coastal city of Izmir on 15 August brought havoc to the wildland-urban interface and ended up burning houses and injuring 78 people (Ozerkan, 2024). Long periods of high fire danger combined with intensified aggression and scarcity of firefighting resources set the scene in Ukraine. The fire season was severe in extent and nearly 1 million ha burned between March 2024 and February 2025 (European Forest Fire Information System, 2025). This is larger than the combined BA in all of Europe, Middle East and North Africa (San-Miguel-Ayanz et al., 2025). As the majority of these fires are located near the front line in the eastern part of the country, warfare was presumably a major driver of their ignition, with forests seemingly accounting for a larger share of BA than in the recent past (The Guardian, 2025). Nonetheless, higher BA had been recorded in the past, namely >2 million ha in both 2014 and 2015 (Global Wildfire Information System, 2025).

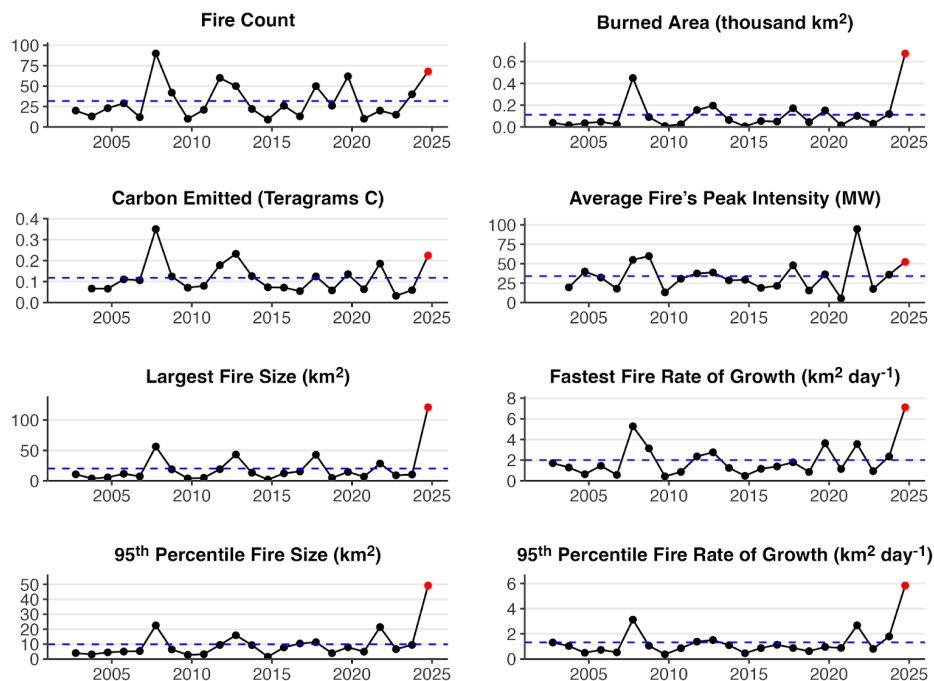


**Figure A2:** Summary of the 2024-2025 fire season in North Macedonia, as in **Figure A1**.

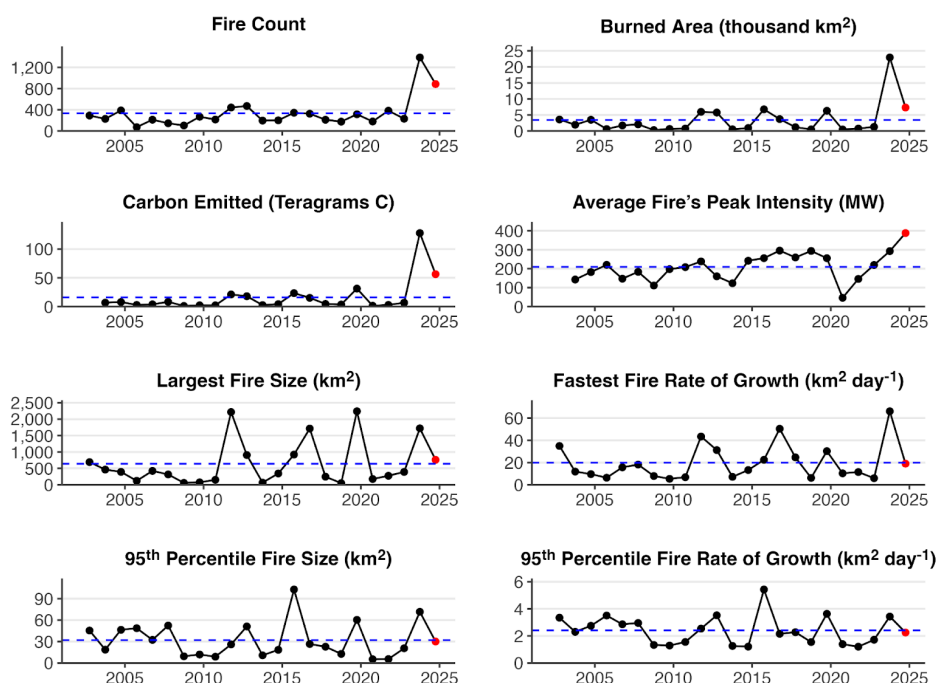




#### 4388 **A4. North America**

4389 Wildfires across North America were characterized by above average activity in Canada and  
4390 the United States and a record-breaking season in Mexico in 2024-2025. This included  
4391 multiple wildfires that resulted in substantial impacts to human communities, including the  
4392 Eaton and Palisades wildfires, which are among the most destructive in California, USA  
4393 history. Following a record breaking 2023 wildfire year, during which almost 150,000 km<sup>2</sup>  
4394 burned, Canada once again experienced an above average wildfire season in 2024. A total  
4395 of 5,686 wildfires burned approximately 46,000 km<sup>2</sup>, marking the six-highest area burned  
4396 since 1972 based on national records (Skakun et al. 2024). In the United States, over 64,000  
4397 wildfires burned over 36,000 km<sup>2</sup> in 2024, exceeding both the previous 5 and 10-year  
4398 averages (NICC, 2024). The USA also recorded the second-highest number of Level 4 and 5  
4399 National Fire Preparedness days since 1990, reflecting elevated national fire suppression  
4400 resource commitment associated with high potential for continued emerging wildfires (NICC,  
4401 2024). National fire records for Mexico suggest that the country experienced more than 8,000  
4402 wildfires in 2024, setting a record for area burned - over 16,500 km<sup>2</sup> - since record keeping  
4403 began in 1998 (Comisión Nacional Forestal, 2025), though this record is not reflected in the  
4404 global datasets compiled as part of this report.

4405 Much of Canada experienced earlier-than-normal snowmelt in 2024, resulting in an early  
4406 onset of the wildfire season. For example, parts of Alberta experienced snowmelt up to 30  
4407 days earlier than average. Drought conditions, which were prevalent across the country in  
4408 2023, persisted into 2024 in much of western Canada. Holdover fires from 2023, which  
4409 smouldered through the winter in northern British Columbia, Alberta (**Figure A3**), and parts  
4410 of the Northwest Territories, reignited in early spring due to warm and dry conditions (Kolden  
4411 et al. 2025). This contributed to above average area burned and wildfire emissions in May  
4412 (Copernicus Atmosphere Monitoring Service, 2024). Wildfires in May led to evacuations of  
4413 Fort Nelson, British Columbia and Fort McMurray, Alberta - an area previously affected by  
4414 Canada's costliest wildfire in 2016 (Canadian Forest Service, 2025).



4415

4416 **Figure A3:** Summary of the 2024-2025 fire season in Alberta, Canada, as in **Figure A1**.

4417 Most of the USA was characterized by normal to high precipitation at the start of 2024, with  
 4418 minimal wildfire activity (NICC, 2024). A heat wave at the end of February 2024 in the  
 4419 southern plains combined with strong winds and high fine fuel loads led to multiple large  
 4420 wildfires, including the record-breaking Smokehouse Creek Wildfire in the Texas Panhandle  
 4421 and western Oklahoma that burned over 4000 km<sup>2</sup> and resulted in two fatalities before  
 4422 reaching 100% containment in March (Texas House of Representatives Investigative  
 4423 Committee on the Panhandle Wildfires, 2024). Wildfire risk in the southern plains remained  
 4424 elevated for several weeks. Warm and dry conditions in March led to an increase in activity  
 4425 in the central Appalachians region of the eastern US, with the Virginia Department of  
 4426 Forestry reporting over 100 wildfires in 48 hours. By early April, fire activity peaked for the  
 4427 spring fire season in the southern and eastern US. Dry and windy conditions prompted  
 4428 significant growth of large wildfires burning in New Mexico; however, fire activity remained  
 4429 below average in the USA in May (NICC, 2024).

4430 Wildfires in Mexico started increasing in March during Mexico's typical wildfire season.  
 4431 Warm and dry conditions helped to fuel hundreds of wildfires (Comisión Nacional Forestal,  
 4432 2025; NASA Earth Observatory, 2024b) contributing to Mexico's record breaking wildfire  
 4433 season with anomalously high carbon emissions. Wildfire numbers peaked by mid-March  
 4434 through early May (Comisión Nacional Forestal, 2025).

4435 Wildfire activity remained high across Canada during the summer of 2024, with many  
 4436 regions experiencing above-average area burned. Areas including New Brunswick in the  
 4437 east, and the Northwest Territories, recorded area burned totals among the top five highest  
 4438 since 1972 (Skakun et al., 2024). Hot and dry conditions in July resulted in wildfires forcing  
 4439 the evacuation of Labrador City in Newfoundland and Labrador and John D'Or Prairie and



4440 Fox Lake in Alberta (Canadian Forest Service, 2025). In late July during a period of extreme  
 4441 99<sup>th</sup> percentile fire weather, a fast-moving wildfire resulted in the evacuation of the town of  
 4442 Jasper, Alberta and destroyed 358 structures resulting in an estimated \$1.23 billion in  
 4443 damages - the second costliest wildfire in Canadian history (Kolden et al. 2025; Insurance  
 4444 Bureau of Canada, 2025). There were two fatalities in July related to fire suppression  
 4445 operations in Alberta and the Yukon.

4446 Large fires continued to burn in northern regions of British Columbia, Alberta, and  
 4447 throughout the Northwest Territories throughout August and into the fall, resulting in the  
 4448 fourth, sixth, fifth highest area burned for these areas, respectively, since 1972 (Skakun et  
 4449 al., 2024). Significant fire activity also developed in Saskatchewan, Manitoba, and Ontario in  
 4450 August, and New Brunswick experienced the second highest area burned since 1972  
 4451 (Skakun et al. 2024). In total, 91 wildfire-related evacuations took place across Canada  
 4452 during the 2024 season, affecting 56,000 people (Canadian Forest Service, 2025).  
 4453 According to estimates from the Copernicus Atmosphere Monitoring System, the 2024  
 4454 wildfire season in Canada produced the second-highest total emissions recorded since 2003  
 4455 - surpassed only by the record-breaking 2023 season (Parrington & Di Tomaso, 2024).

4456 Wildfire activity began to pick up in the USA during the later part of June, with multiple fires  
 4457 in New Mexico resulting in several hundred structures burned (NICC, 2024), two fatalities,  
 4458 and over \$1 billion in damages (NCEI, 2025). By July, an extreme and long-lasting heatwave  
 4459 across the western US spurred numerous large wildfires, including the Park Fire in Northern  
 4460 California that drove thousands to evacuate and destroyed over 700 structures (CALFIRE,  
 4461 2025). Record breaking dry conditions in Oregon and Washington led to over 100  
 4462 human-caused wildfires by early July (US Forest Service, 2024), contributing to a record  
 4463 setting year in BA and anomalously high carbon emissions in Oregon (**Figure S47**). Through  
 4464 July and August, hot and dry weather drove numerous large wildfires in the northwestern  
 4465 front range, including the Stone Canyon wildfire in Colorado that resulted in one fatality and  
 4466 multiple burned homes and the Remington wildfire in Wyoming that killed hundreds of cattle.  
 4467 During September, numerous dry lightning strike wildfires occurred in the northwestern US  
 4468 along with multiple wildfires in southern California associated with extreme heat, including  
 4469 the Airport Fire that resulted in 22 injuries and 194 damaged structures (CALFIRE, 2025).

4470 Fall was anomalously warm and dry across much of the continental US, with 87% classified  
 4471 as abnormally dry or in drought by early November (NICC, 2024). The northeast US  
 4472 experienced hundreds of wildfires that interacted with densely populated regions in October  
 4473 and November coincident with record-dry conditions and warm temperatures across multiple  
 4474 states. For instance, New York City experienced its highest number of recorded wildfires  
 4475 during a two-week period, with every borough experiencing multiple wildfires. The conditions  
 4476 were unseasonable, with Connecticut, Massachusetts, and Rhode Island setting record red  
 4477 flag days, despite typical peaks for red flag days occurring in spring (NOAA, 2024).  
 4478 Massachusetts experienced its most active fall fire season in over 40 years (NICC, 2024).  
 4479 Two fatalities and hundreds of structures were destroyed before rainfall associated with an  
 4480 extratropical cyclone halted the fall fire season in the northeast in late November.

4481 Wildfire activity remained low at the end of 2024 and beginning of 2025, except in southern  
 4482 California. Southern California is climatically prone to experiencing a downslope (katabatic)  
 4483 wind during the late autumn and winter months known locally as Santa Ana winds.  
 4484 Historically, the most devastating wildfires in California have occurred when a delayed onset  
 4485 of autumn precipitation coincides with a Santa Ana wind event (Kolden and Abatzoglou,  
 4486 2018), but such concurrences are increasing in frequency with climate change (Goss et al.,  
 4487 2020). In November and December, Santa Ana wind events produced wildfires that burned  
 4488 nearly 10,000 ha and destroyed over 250 structures, however, this was just a precursor. In  
 4489 January 2025, the most disastrous wildfire event in modern US history occurred in Los  
 4490 Angeles County, California. Prolonged drought conditions, unseasonably warm winter



temperatures, and exceptionally powerful Santa Ana winds exceeding 140 km/h created extreme fire weather conditions (Barnes et al., 2025; CNN, 2025). Fire potential was also exacerbated by anomalously wet winters for two years prior, which increased the fine fuel load in the region. The potential for extreme wildfires to develop under dry downslope winds was predicted several days in advance, including by the National Interagency Fire Center (NIFC), the National Weather Service (NWS), and the Storm Prediction Center (SPC; see summary by Wikipedia, 2025) as well as by specialist commentators (e.g. Swain, 2025).

The two most destructive fires-Palisades and Eaton-that burned during the event occurred in the same general locations as destructive fires in 1961 and 1993 during other Santa Ana wind events. These two fires resulted in numerous outcomes with widespread and severe consequences. Among the most devastating were the high fatalities and extensive structure loss. Over 11,500 homes were destroyed across Los Angeles County, and at least 30 lives were lost, according to the Los Angeles County Coroner (2025). Specifically, the Palisades Fire damaged or destroyed nearly 8,000 structures, while the Eaton Fire impacted over 10,000 (CALFIRE, 2025; Wikipedia, 2025). The fires also triggered mass evacuations. At the peak of the crisis, at least 153,000 people were forced to evacuate, with up to 200,000 under evacuation warnings or orders (USGS, 2025b; NPR, 2025; Wikipedia, 2025).

In addition to human displacement and infrastructure damage, the fires severely affected both air and water quality. Air pollution reached hazardous levels, contributing to negative health outcomes for thousands. During the fires, peak  $PM_{2.5}$  levels reached  $483 \mu g/m^3$ , an order of magnitude greater than the  $35 \mu g/m^3$  daily standard set by the US Environmental Protection Agency, resulting in a prolonged period of hazardous air quality (California Air Resources Board, 2025). Municipal water supplies were similarly impacted, with water considered unsafe for tens of thousands of residents in the burned areas for several weeks following the fires (City of Pasadena, 2025). Beyond Los Angeles, the political fallout from the crisis led to federal orders to release over 8.3 million cubic meters of water from federal reservoirs further north in California. However, this water did not flow to southern California and was instead vital for irrigating crops in the state's heavily agricultural Central Valley (Levin et al., 2025).

The economic consequences were equally severe. Total economic losses were estimated at US\$140 billion, factoring in property destruction, health costs, business disruption, and infrastructure damage, making this one of the most costly wildfire events in US history (LAEDC, 2025; UCLA Anderson School of Management, 2025). Wider economic disruption is also projected, with estimated losses of US\$4.6-8.9 billion in economic output over five years, 25,000-50,000 job-years lost, and reductions in labour income of US\$1.9-3.7 billion (LAEDC, 2025). The Palisades and Eaton fires directly affected nearly 2,000 businesses (LAEDC, 2025). Moreover, as Los Angeles hosts the largest port on the US Pacific coast, these fires disrupted broader supply chains connected to the Port of LA (ASU, 2025).

Insured losses added another layer of financial strain, with industry estimates ranging from \$20 billion to \$75 billion (PreventionWeb, 2025; Morningstar DBRS, 2025; Insurance Insider, 2025; UCLA Anderson, 2025). This placed substantial pressure on the already volatile home insurance market in California, as well as on most global re-insurers.

The fires also deepened Southern California's ongoing housing and affordability crisis. Thousands of affordable housing units were lost, worsening the existing housing shortage, displacing large numbers of low-income residents, and exacerbating the region's homelessness problem (Urban Land Institute, 2025; UCLA Anderson, 2025; Vox, 2025). This led to ripple effects, with mass displacement into surrounding communities and beyond in the months that followed (NYT, 2025).



Finally, the aftermath of the fires brought additional physical hazards in the form of debris flows. Given southern California's geology, the region is highly susceptible to erosion and debris flows following wildfires. Several such events occurred after high-intensity rainfall in the weeks following the fires, causing further damage and prompting hundreds of additional evacuations in and near the recently burned areas (USGSa, 2025).

## A5. Oceania

Oceania experienced relatively moderate levels of fire during the 2024-25 fire season, although there were still a series of high profile and high impact events across the region. Overall, however, the season did not reach the magnitude of the previous year, which ranked among the top 5 years for BA in Australia since 2002. Where fires occurred and had impacts, lightning and sustained dryness were prominent drivers (Bureau of Meteorology, 2024; Dowdy and Brown, 2025).

The 2024-25 fire season in Western Australia was characterised by record-high temperatures, variable rainfall, and significant soil moisture deficits in coastal areas of the South, Southwest, and West. Over 1,000 large fires burned about 470,000 ha, many in coastal shrubland and woodland over the ~800 km stretch from Gingin, north of Perth, to Carnarvon. The largest fire by area burned occurred near Cervantes in November, where fire ignited by a car crash went on to burn more than 80,000 ha and severely impact local honey production. In the inland Goldfields region at Skeleton Rocks, more than 44,000 ha of Mallee-heath vegetation of the Great Western Woodlands were burned (according to the Department of Fire Emergency Services (DFES), Rui Feix, pers. comm.). This fire reached extreme intensity, impacting fire-sensitive species and post-fire regeneration cycles in an ecosystem that requires long intervals to recover. A lithium mine in the area was also directly impacted by the fire. Four other large incidents were recorded in the shrublands of the Great Western Woodlands, further affecting these vulnerable ecosystems. Between December and March, numerous fires occurred in the grasslands of the Wheatbelt and Esperance, as well as in the forests of the Perth Hills. These included fires that collectively destroyed seven residential properties in areas east of Mundaring, Arthur River, Wooroloo, and Waroona. In February and March, lightning ignited several large bushfires in native forests and coastal shrubland around Manjimup. Some of these fires burned for up to five weeks and affected more than 42,000 ha, including areas of Shannon and D'Entrecasteaux National Parks (DFES, Rui Feix, pers. comm.). These incidents required significant aerial support and personnel deployments, including interstate assistance.

Above average rainfall was recorded in Central Australia, leading to expectations of strong grass fuel growth and another period of increased fire activity, after last year's above average season (Verhoeven et al. 2020; Ruscalleda-Alvarez et al. 2023). By the end of October 2024, over 5.7 million ha had burned, much of it stemming from an intense band of dry lightning stretching from the Northern Territory into Queensland in October (according to Northern Territory Fire and Emergency Services, Maggie Towers, pers. comm.). Many of these fires combined with a particularly large fire complex near Devil's Marbles Conservation Reserve (450,000 ha) (NTFES, Maggie Towers, pers. comm.). The fire threatened hotels and other infrastructure and caused temporary closure of a major highway. In late January 2025, a bushfire swept through the West MacDonnell Ranges, affecting approximately 80,000 ha across the Tjoritja/West MacDonnell National Park, Standley Chasm, the Tyurretye and Iwupataka Aboriginal Land Trusts, as well as nearby pastoral properties (NTFES, Maggie Towers, pers. comm.). Standley Chasm and sections of the Larapinta Trail were closed for several days while a 10-day multi-agency effort worked to contain the fire.

Queensland's north west saw heightened fire activity during Spring, with fire fighters responding to 40 incidents in Mount Isa alone. One of these fires burned for nearly two months, reaching over 100,000 ha according to Queensland Fire Department, (Russell





Stephens-Peacock, pers. comm.). The fires caused an increase in hospital admissions due to respiratory illnesses and impacted mining operations, pastoral property and Lawn Hill National Park. The fires affected the habitat and food sources of endangered species such as the Carpenterian Grass wren, found only in north-western Queensland.

In 2024-25, eastern Australia, comprising southern Queensland, New South Wales (NSW), and the Australian Capital Territory (ACT), experienced a notably warm period, with significant rainfall variation across regions and seasons. Although temperatures were above average in the austral spring, many areas received above average rainfall, thereby reducing fire occurrence and impacts. Repeated dry lightning started a number of complexes of fires in remote and difficult to access terrain across NSW, including areas like Lithgow, the Hawkesbury, Bulga and around Tamworth. Despite the number of fires, NSW saw more moderate fire weather than other parts of the country and Emergency Warnings were only issued for three fires (according to New South Wales Rural Fire Service, David Field, pers. comm.).

The south to south east of Australia (including the states of South Australia, Victoria and Tasmania) experienced record dryness in the leadup to the fire season. Fires in Chappelvale and Casterton-Edenhope in late spring signaled an early start to the fire season in Victoria. In December a band of dry lightning ignited a number of fires including several in the Grampians National Park. About 75,000 ha burned in the Grampians, affecting culturally and ecologically sensitive areas. The coincidence of the fire with Christmas and the peak holiday season led to major tourism losses and extensive community evacuations. This fire was contained by January 6 but later in January another band of dry lightning passed through the west of the state, this time affecting the western side of the Grampians burning another almost 60,000 ha (according to Country Fire Authority, Sarah Harris, pers. comm.). By season's end over two thirds of this important National Park was impacted by fire. Another significant fire occurred on December 26, a public holiday, in Little Desert National Park in the state's west. This fire was an extremely fast-moving fire with approximately 65,000 ha burning in less than eight hours and a final area burned of 90,000 ha (according to Country Fire Authority, Sarah Harris, pers. comm.). These fires required interstate deployments to assist in the fire fight. The fire season concluded with challenging fires that burned through rugged terrain in the Gippsland area, impacting the World Heritage-listed Budjim National Park with its significant cultural heritage. Several planned burns escaped during the season, highlighting the significant dryness of the area.

In South Australia dry lightning storms in early February combined with severe drought conditions to cause the Wilmington fire, which burned approximately half of Mount Remarkable National Park. Firefighting efforts reduced the impact to human, ecological and cultural assets. Lightning storms in February and March also caused an above average number of fires in eastern parts of South Australia. While impacts were limited, firefighting resources were strained. (South Australia, Country Fire Service, Simeon Telfer pers. comm.)

Tasmania faced a significant bushfire season, with up to 100,000 ha burned in the state's northwest, including sensitive ecosystems such as the Tarkine rainforest and the alpine vegetation around Cradle Mountain (according to Tasmania Fire Service, Chris Collins, pers. comm.). Sparked by intense lightning storms in remote and rugged terrain, the fires required interstate support to assist with firefighting efforts. The blazes led to evacuations, threatened heritage sites and caused major disruptions to local businesses and the tourism industry.

In New Zealand the 2024-2025 fire season was moderate, with a couple of minor fires at the end of the 2023/24 fire season (Mar-Jun 2024) and a few more significant fires during the 2024/25 fire season (Jul 2024-Feb 2025). A key feature was the occurrence of a couple of significant wetland fires that burned large areas of peatland (2,271 ha) and damaged flora and fauna habitat. These fires occurred at Whangamarino Wetland, Waikato (central North





Island) in October 2024 and Tiwai Peninsula, Southland (southern South Island) in late January 2025, with both fires just over 1,000 ha. The fires followed two major peatland fires in 2022 at Kaimaumu in the far north (2,434 ha), and Awarua in the south (890 ha and close to this season's Tiwai fire) (according to Fire and Emergency New Zealand, Grant Pearce, pers. comm.). Carbon emissions are likely to be high, given the 2022 fires were estimated to release more than 620,000 t CO<sub>2</sub> (Pronger et al., 2024). There were a number of other noted fires in a mixture of vegetation types including in Canterbury, Northland and North Otago. However, unlike recent years, there were no major house loss incidents, with just a few homes and outbuildings lost across the multiple fires.

## A6. South America

The 2024-25 fire season was a remarkable year for fire in South America, with seven of its 13 countries reaching new records in BA since 2002 and widespread records in the fire size, growth rate and intensity distributions (Figure 3; Figure 4). Anomalies in BA commenced early in 2024 and persisted through November in some regions (Figure S4). As discussed in Section 2.2.2 and Sections 4-6, intense drought and fire weather affected much of South America during the 2024-25 fire season and this drought occurred at a time when socioeconomic factors are increasingly cited as drivers of shifting fire regimes and timing. The event is part of a trend towards an earlier onset of the fire season since 2020, with new record fire counts set for the months of March to May in 2020 and for January in 2022, based on monitoring by Brazil's National Institute for Space Research (INPE) since 1998 (INPE, 2025). During 2024, January, February and June presented the second highest value on record (previous record during 2003 for January and 2007 for the other months, respectively). Fires have expanded into new territories, driven by a combination of climate variability, shifting land-use practices, and governance challenges, as discussed in the study cases, below.

Across South America, the number of fire hotspots recorded by the Queimadas/INPE system (511 thousand hotspots in 2024) rivalled the previous record set in 2010 (523 thousand hotspots) (INPE, 2025). Compounding climate and human drivers likely led to a widespread extreme fire year across the continent in 2024-2025. The land use fire dependent practices, associated with new deforestation frontiers during an extreme drought year amplified the fire crisis. Amidst rising socioeconomic and environmental impacts of fires in the region, researchers have been calling on governments across the globe to rethink strategies for combating the root causes of extreme wildfires, from climate change to fire-free agricultural practices (UNEP, 2022). Increases in extreme droughts with already vulnerable forest due to extreme climatological events are expected and therefore controlling ignition sources are the only immediate measure for preventing 2024-like scenarios. In this context, major fire events in terms of largest fire size emerged in many parts of Brazil, in Peru, Ecuador and Bolivia during the 2024-25 fire season, with unprecedented levels of BA and exceptional fire weather (Figure S2).

In Brazil, one of the most intense droughts in decades, combined with the expansion of the agricultural frontier in Amazonas and Pará states (Santos et al., 2023), caused fires to persist nearly year-round (Figure S2.4). In northern Brazil, including much of the Amazon biome, several states such as Amazonas and Pará experienced their largest BA on record. Other states, including Mato Grosso, São Paulo, and Paraná, recorded their highest fire extent in a single year. In the Pantanal biome, Mato Grosso do Sul experienced the second-largest BA extent on record, the fourth in rank in fire size and fifth regarding the fastest growth. This resulted in estimated losses to agribusiness caused by the fires amounting to R\$ 1.2 billion (~ \$222 million) (Câmara, 2024). In addition, Pantanal recorded particulate matter concentrations of 903.2 µg/m<sup>3</sup> in September 2024 (Viana et al., 2024), which is 60 times higher than the World Health Organization (WHO) standards. Efforts to contain the flames lasted 78 days and involved the National Force, local communities,



environmental organizations, and state fire brigades (Nunes, 2025). The response faced significant challenges, particularly in remote border areas with difficult access and complex logistics. Providing support to isolated populations was especially difficult, with reported cases of respiratory illnesses worsened by smoke exposure, as well as emotional distress, including stress and anxiety (Nunes, 2025).

São Paulo and Mato Grosso state, both centres of large-scale crop production, experienced the fourth-largest BA extent on record. Regarding fire intensity, 2024 was the record for São Paulo, Paraná, Mato Grosso do Sul, Rio de Janeiro and Roraima, and the second in the rank for Amazonas and Goiás. All together, from the southeast to the north of the country, records in one or more fire metrics were observed during this period, placing Brazil in a state of fire emergency.

In general, early fire season onset and long duration occurred across most Brazilian regions, with the first month of anomalous fire ranging from March in most of the Amazonian states and extending through to December. In fact, more fire hotspots were detected in February and March 2024 than in any year since 1998 (INPE, 2025). Record fire counts were observed across states covering more than half of Brazil's territory, and represented a threat almost during the entire year, posing challenges for managing the wildfires response and combat. By August 2024, the National Centre for Early Warning of Natural Disasters (CEMADEN, 2024) pointed out that the drought, covering Amazonia to the southeast, initiated in the second half of 2023, was already one of the strongest in decades. Data from the National Secretariat for Civil Protection and Defence (S2ID, 2024), in December 2024 pointed out that there were 21 of the 27 states with a recognized decree either in state of emergency or calamity due to the drought, affecting more than 520 municipalities in the country. These conditions brought widespread devastation across Brazil in 2024, impacting urban and rural communities and affecting an estimated 18.9 million people nationwide (CNM, 2024). Fire disaster forced 10,700 people from their homes, resulting in housing instability and severe disruptions to livelihoods. Thousands more were affected by the breakdown of essential services, such as school closures (CNM, 2024). Although Brazil does not have an official database on wildfire-related fatalities, existing records point to a rising death toll (Carvalho et al., 2025). Estimates have identified 186 deaths between 2020 and 2024, with 38 in 2024 alone. However, the actual number is likely higher due to underreporting.

Notably, the state of São Paulo in Brazil recorded 8,712 hotspot fires, the highest number since 1998 (INPE, 2025). August and September together accounted for approximately 70 % of these detections (6,134), roughly four times the 1998-2023 August average (914 hotspot fires) and three times the corresponding September average (848 hotspot fires). According to a study by the Amazon Environmental Research Institute (IPAM, 2024), of the 2,600 hotspot fires recorded in the state of São Paulo between August 22 and 24, 81% were in areas of agricultural use - drawing attention to the fact that the state recorded, on the 23rd August alone, more hotspots than the entire Amazon biome. In an even more alarming interval, analysed images from the geostationary satellite indicate that the smoke columns in western São Paulo appeared in just 90 minutes, between 10:30 AM and 12:00 PM on the 23rd August, and, on that same day, the number of fires jumped from 25 to 1,886 hotspot fires, reinforcing the hypothesis of orchestrated action and the unprecedented intensity of these fires.

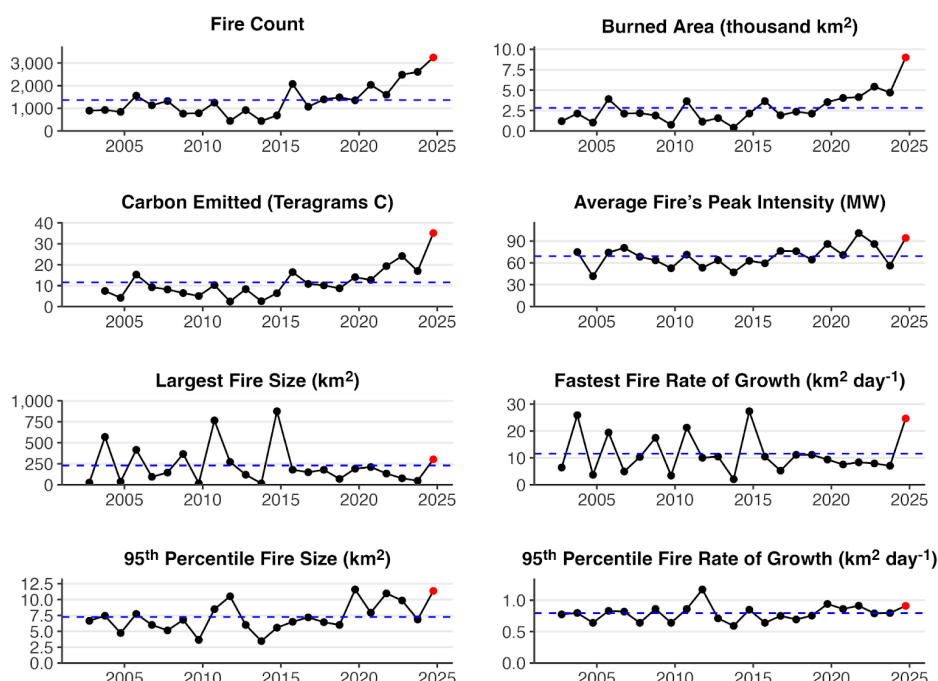
Amazonas state, the largest of Brazil's Amazonian states, can be pointed out as an epicentre of wildfires and its impacts. During 2024, it was ranked as first in number of fires (Figure 4) and presented a historical record of fire occurrence in June, July and August, consecutively, since the monitoring began in 1998 (INPE, 2025). Moreover, it was the 3rd year with the fastest fire growth rates, with a fire season lasting for 8 months. It has been estimated that fires affected over 790,000 ha of forests, approximately 39% of the affected area, especially in the southern region of the state (Alencar et al., 2022). The Amazonas



state has been facing an increase in the deforestation rate since 2021, mainly in the southern region, following the pressure and political speech of Brazil's BR-319 Highway paving. The lack of governance, associated with illegal logging, land grabbing and public lands invasion, are some of the drivers of the fire peaks observed in the region (Fearnside, 2022). Moreover, it has been estimated that the population from this region has been exposed to aerosols emitted from the wildfires causing a pollution of up to  $113 \mu\text{g}/\text{m}^3$ , 653% above the  $15 \mu\text{g}/\text{m}^3$  standard set by the WHO, according to the data from the Atmosphere Monitoring Service (CAMS) and Copernicus Climate Change Service (C3S).

A recent report from the Global Forest Watch (World Resources Institute, 2025) also showed widespread high levels of forest loss (stand-replacing fire extent) to wildfire in 2024 in the Amazon biome (including both Brazil and neighbouring Amazonian countries). The highest rates of forest loss since 2016 was observed, with total forest loss more than doubling in 2024 versus 2023 and 60% of those losses were attributed to wildfires. Note that Global Forest Watch data define "forest loss" as the complete removal of tree canopy, including areas affected by stand-replacing fires, but do not capture more subtle or partial fire-related degradation. As a result, the data may overestimate deforestation while underestimating degradation, limiting understanding of the broader ecological impacts of wildfires on forests. Moreover, Indigenous communities were disproportionately affected by wildfires in 2024, a year that recorded the highest number of fires in territories inhabited by isolated Indigenous peoples (COIAB, 2024). In 2024, fires in Indigenous lands in Brazil increased by 81% compared to 2023, accounting for the largest share of Amazonia fires at 24% (Alencar et al., 2024). In Roraima, uncontrolled fires in indigenous lands have degraded air quality, ravaged crops, homes, and native vegetation leading to food and water insecurity (ISA, 2024). The fires have further worsened the ongoing humanitarian crisis in the Yanomami Territory, Brazil's largest Indigenous land. Local organizations estimate that at least 70,000 people across urban and rural communities were affected by the lack of access to clean water, a result of the compounded impacts of drought and fire (WWF-Brazil, 2024).

The implications of extreme fire activity in Amazonia extend beyond immediate ecological damage. As a globally significant carbon sink and a key part of the terrestrial hydrological cycle, the Amazon stores an estimated 100-120 Pg of carbon (Malhi et al., 2006). Intensified fire regimes risk accelerating forest degradation, potentially triggering a biome-scale shift from net carbon sink to a significant carbon source, releasing several petagrams of carbon and exacerbating global warming through positive feedbacks (Gatti et al., 2021). Fire-driven environmental degradation also poses public health risks and economic instability. Biomass burning increases respiratory illness, especially among populations exposed to prolonged smoke (Campanharo et al., 2019, 2021). Economically, fire reduces agricultural productivity, damages infrastructure, and undermines regional development, compounding poverty and inequality. Costs extend to firefighting programmes and personnel (Morello et al., 2020), as well as hospitalisations from respiratory or other fire-related conditions (Machado-Silva et al., 2020). Rising fire activity may also weaken the effectiveness of forest conservation and restoration policies, including those tied to international climate agreements, threatening long-term mitigation and adaptation efforts.



4785

4786 **Figure A4:** Summary of the 2024-2025 fire season in Brazil's Amazonas State, as in **Figure**  
 4787 **A1.**

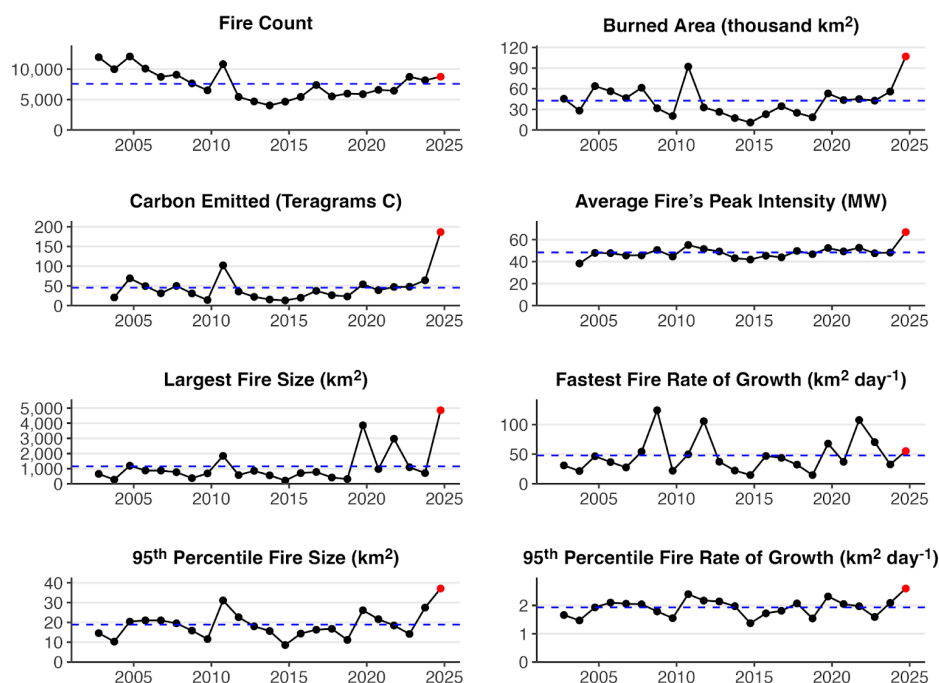
4788 Bolivia endured one of its worst fire seasons on record by many measures, intensified by the  
 4789 El Niño phenomenon, record temperatures, and accelerating deforestation and contributing  
 4790 significant carbon emissions to the atmosphere (**Figure A5**). These conditions intensified fire  
 4791 outbreaks, especially in ecologically vulnerable regions such as the Chiquitania and  
 4792 Amazonian lowlands (Ruiz, 2025). The cumulative number of fire hotspots in 2024 was  
 4793 923,464, with 77% occurring in Santa Cruz (Chiquitano dry forest), 19% in Beni (Amazonian  
 4794 lowlands), 1.6% in La Paz, and the rest in other departments including Pando (north  
 4795 Amazonia) (CEJIS, 2024). A recent report from Global Forest Watch (World Resources  
 4796 Institute, 2025), found that forest loss in Bolivia tripled in 2024 versus 2023 and was many  
 4797 times over the annual mean since 2002, with 60% of those losses related to wildfires. The  
 4798 forest fires have been attributed to a combination of one of the most severe droughts on  
 4799 record as well as a number of socioeconomic factors and government policies that  
 4800 encourage agricultural expansion, such as the lifting of soy and beef export quotas, removal  
 4801 of import taxes on agrochemicals and machinery (World Resources Institute, 2025).

4802 The number of ha burned was a contentious issue in the country. According to the NGO  
 4803 Fundación Tierra (2024), in September 2024 about 10 million ha were burned. The wildfires  
 4804 extended up to November. In early January 2025 an independent group of experts of the  
 4805 national journal (El Deber, 2025) reported that 14 million ha burned based on the MODIS  
 4806 Terra sensor. In April 2025, the ministry of environment officially reported 12.6 million ha  
 4807 burned in 2024, 12% of the country's territory, with 57% corresponding to primary forest and  
 4808 43% pastures and agricultural lands (Ministerio de Medio Ambiente y Agua, 2025). Although  
 4809 wildfires have been occurring regularly in Bolivia over the past decade, the events of 2024  
 4810 have been the most catastrophic to date. The event is considered the second megafire after



the one that occurred in 2019. Indigenous lands, protected areas, and fiscal lands were among the most impacted categories. The Global Forest Watch cited a lack of early warning systems and adequate firefighting resources as a factor contributing to high rural exposure to fire and urban exposure to wildfire smoke (World Resources Institute, 2025). An investigation by Fundación Tierra (2025) reports that wildfires in Bolivia are mostly intentional, with 66% being maliciously set and 34% resulting from out-of-control slash-and-burn agricultural practices.

The Bolivian Air Contamination Index reached 537 in the city of Cobija, northern Bolivia (Silva Trigo, 2024), corresponding to a  $PM_{2.5}$  concentration of over  $500 \mu g/m^3$  (24-hour average), a level considered extremely harmful and impactful to the health of millions of people in the region and beyond. As a result, the government declared a sanitary emergency. In addition to the extensive environmental destruction and incomparable biodiversity loss, these fires have significantly increased atmospheric carbon emissions, exacerbating regional and global climate challenges. It is important to note that laws and regulations in Bolivia encourage agricultural and livestock expansion and are lenient towards the use of fire (Yifan He et al. 2025). Encroachment and illegal land occupation are also pointed to as causes of provoked wildfires in Bolivia. Efforts in the legislative branch to prohibit or amend these regulations have not been successful thus far. Therefore, there is a looming risk that similar events may occur again in the near future.



4830

4831 **Figure A5:** Summary of the 2024-2025 fire season in Bolivia, as in **Figure A1**.

4832 In early 2024, Venezuela experienced its most intense wildfire season on record, with over  
 4833 30,000 active fires between January and March (NASA FIRMS, 2025). Unlike Brazil,  
 4834 Venezuela's peak fire season runs from December to April, driven by the northward shift of  
 4835 the Intertropical Convergence Zone (ITCZ; Katz & Giannini, 2010; Ramírez & Gómez, 2021),





which were intensified by the 2023-2024 El Niño, one of the strongest in decades, creating an extreme fire weather window (NOAA CPC, 2024). Fires have historically been concentrated in the Orinoco Llanos, a savanna-dominated region covering approximately one-third of Venezuela, where fire is used for agricultural purposes and grazing (Bilbao et al., 2020). More recently, deforestation in tropical forests south of the Orinoco has fueled large fires, like those seen in 2019 (Lizundia-Loiola et al., 2020). In 2024, wildfires impacted nearly all ecosystems, from Amazonian humid forests in Bolívar and Amazonas (5,600+ fires, including Canaima National Park), to flooded savannas in Apure, cloud forests in Henri Pittier, and an estimated 36,000 ha of Caribbean pine lost in Uverito, Latin America's largest plantation (Ciudad CCS, 2024; Lozada, 2024). Since 2019, Venezuela's National Parks Institute (INPARQUES) has promoted an intercultural Integrated Fire Management (IFM) strategy, coordinated by an intersectoral team involving government agencies, local communities, and researchers (Bilbao et al., 2022). With support from FAO and RAMIF (under ACTO), this national IFM system aims to strengthen fire management efforts in response to Venezuela's vast ecological and territorial complexity, as well as to the increasing extreme fire weather conditions projected for the region, including higher temperatures, prolonged dryness, and lower humidity (Feron et al., 2024).

A fundamental challenge in the wildfire crisis affecting Bolivia and Venezuela is the complexity of managing fires in border regions. Many of the most affected areas are located along international boundaries, where coordination between neighboring countries is often inadequate or inefficient. The lack of standardized protocols, difficulties in sharing real-time information, and disparities in firefighting capacities create significant logistical and operational challenges. Fires in these areas are particularly difficult to control due to overlapping jurisdictions and administrative barriers that delay response efforts. This is also the case in other regions in south america, such as the trinational frontier with Acre, Peru and Bolivia (Pismel et al., 2023) and at the Pantanal region. Without improved cross-border collaboration, enhanced communication channels, and harmonized fire management strategies, these transboundary wildfire zones will remain highly vulnerable, exacerbating the broader crisis in South America.

Ecuador presented the peak in BA during 2024, with an anomaly of 166%, the highest on record. Official governmental reports from the National secretariat of risk management, there were almost 6,000 wildfires, 83 thousand ha of burned vegetation, 1,663 affected people, 47 people hurt, 6 deaths, 45,000 animals killed and over 5,000 animals affected, according to the National Secretariat for Risk Management (SitRep., 2024). These events were attributed to the extreme drought and land use and land cover conversion fire dependent practices.

In 2024, there were 13,400 hotspots in Peru, which was 1,000 more than in 2023 (Caceres et al. 2024). Of the total, 49% were in natural areas such as forests or other natural covers, 35% in non-forest vegetation types, and 12% in anthropogenic areas. The maximum number of hotspots occurred in September. According to Caceres et al. (2024), in August and September, the regions most impacted by fire were Ucayali, Madre de Dios, Huánuco, San Martín, and Loreto, all belonging to the Amazonia region. In November 2024, the number of wildfires totaled 1,798, with over 80,000 ha burned, 35 people and a countless number of animals died in the events (Castillo, 2024, Informe Defensorial n.º 225). The severity of the wildfires was reflected by Castillo (2024) using information from INDECI (Institute of Civil Defense).

In the extreme south of South America, fires in Patagonia started in early 2025, continuing a recent trend that aligns with an 80% increase in BA since 2002. In Argentina, the 2024-25 fire season was the most destructive in decades for northern Patagonia. By late February 2025, more than 30,000 ha had burned across Río Negro and Neuquén provinces, primarily affecting Lanín and Nahuel Huapi National Parks (Greenpeace, 2025). Extreme fire behavior was driven by prolonged drought, anomalously high temperatures, and intense westerly





winds. Nearly all ignition sources were anthropogenic, amid conditions of critical fuel dryness (Greenpeace, 2025). The Patagonia 2024-25 fire campaign represents the most extensive and intense in decades, underscoring the combined influence of climate extremes and human pressures.

In Chile, fire occurrence and BA were lower during the 2024-25 fire season than in recent years. The 2024 season reached a BA of 73,834 ha compared to the 429,103 ha burned in 2023. However, in February 2024, the Valparaíso Region experienced a record-setting catastrophic fire associated with extreme weather conditions (high temperatures and strong winds), affecting wildland-urban interface areas with significant material losses and more than 30 deaths (González et al. 2024). Central and south-central Chile have experienced an intense and uninterrupted megadrought since 2010, which has increased the size and severity of wildfires (Garreaud et al 2017; González et al. 2018; Bowman et al. 2019). Priority steps to advance solving this problem are restoring and managing forest vegetation and removing highly flammable forest plantations to move towards less fire-prone landscapes.

## 8. Competing Interests Statement

SV is a member of the editorial board of Earth System Science Data. The authors declare no further conflict of interest.

## 9. Acknowledgements

The authors thank all contributing panellists of the regional expert panels (Table A1): Lucy Amissah, Dolores Armenteras, Davide Ascoli, Sally Archibald, Francisco de la Barrera, Stefan Doerr, Mauro Gonzalez, Chelene Hanes, Piyush Jain, Matt Jolly, Natasha Ribeiro, Julien Ruffault, Bambang Saharjo, Sundar Sharma, Celso Silva Junior, Jacqueline Shuman, Tercia Strydom, Raman Sukumar, Veerachai Tanpipat, Gavriil Xanthopoulos, Bo Zheng. The regional panel of Oceania thank the following for their contributions to the identification and description of key events in the 2024-25 fire season: Telmo António; Chris Collins; David Field; Rui Feix; Russell Stephens Peacock; Grant Pearce; Simeon Telfer; Maggie Towers. We thank the working groups “FLARE: Fire science Learning Across the Earth System” and “TerraFIRMA: Dummies Guide to using Fire Models” for contributing to defining the report scope and establishing contributor links. We thank Luca Minello for his assistance with the analyses of C project exposure to fire. We thank the CNDFF (Comité National de Défense de la Forêt et de lutte contre les Feux de Brousse) for their contribution to the characterisation of the fire season in West Africa. We acknowledge the use of GrammarlyGO ([www.grammarly.com](http://www.grammarly.com)) and ChatGPT-4 (<https://chatgpt.com/>) to identify improvements in language use and writing style only.

## 10. Author Contributions

**Conceptualisation and Project Administration:** DIK, CAB, FdG, MWJ.

**Data Curation, Resources, and Software:** DIK, CAB, FDG, MWJ, MLFB, EBr, JRM, ZL, ASIB, EBU, AC, EDT, JE, AJH, SL, GM, YQ, FRS, CBS, MAT-V, DvW, JBW, EW, NA, EC, LG, MP, MT, GRvdW, SV.

**Formal Analysis:** DIK, CAB, FDG, MWJ, MLFB, EBr, JRM, ZL, KB, IJMF, LF, AJH, SL, GM, YQ, FRS, CBS, MAT-V, RV, DvW, JBW.

**Visualisation:** DIK, CAB, FDG, MWJ, MLFB, JRM, ZL, KB, IJMF, LF, SL, AL, FRS, MAT-V, RV, JBW, NA.



4937

4938 **Writing - Original Draft Preparation:** DIK, CAB, FDG, MWJ, MLFB, EBr, JRM, ZL, ASIB,  
 4939 AC, EdT, IJMF, LF, AJH, TK, TRK, SL, YQ, PSS, FRS, CBS, MAT-V, RV, JBW, EW, BB, MB,  
 4940 GC, CMdB, KB, VMD, SHar, EAK, BN'D, CS, GS, JS, JA, NA, DSH, SHan, SM, MP, MT,  
 4941 LOA, HC, PMF, CAK.

4942

4943 **Writing - Review & Editing:** All authors.

## 4944 11. Data Availability

4945 **Section 2:** BA data from NASA's MODIS BA product (MCD64A1) are extended from Giglio  
 4946 et al. (2018) and are available at Giglio et al. (2021,  
 4947 <https://lpdaac.usgs.gov/products/mcd64a1v061/>, last access: 6 August 2025). GFED4.1s fire  
 4948 C emissions data are extended from van der Werf and are available at  
 4949 <https://globalfiredata.org/> (last access: 6 August 2025). GFAS fire C emissions data are  
 4950 extended from Kaiser et al. (2012) and are available at  
 4951 [https://confluence.ecmwf.int/display/CKB/CAMS+global+biomass+burning+emissions+base](https://confluence.ecmwf.int/display/CKB/CAMS+global+biomass+burning+emissions+base+d+on+fire+radiative+power+%28GFAS%29%3A+data+documentation)  
 4952 [d+on+fire+radiative+power+%28GFAS%29%3A+data+documentation](https://confluence.ecmwf.int/display/CKB/CAMS+global+biomass+burning+emissions+base+d+on+fire+radiative+power+%28GFAS%29%3A+data+documentation) (last access: 6 August  
 4953 2025). Global Fire Atlas are extended from Andela et al. (2019) and are available at Andela  
 4954 and Jones (2025, <https://doi.org/10.5281/zenodo.11400061>, last access: 6 August 2025).  
 4955 Regional summaries of the MODIS BA, GFED4.1s, GFAS, and the Global Fire Atlas are  
 4956 presented here and are available at Jones et al. (2025,  
 4957 <https://doi.org/10.5281/zenodo.15525674>, last access: 6 August 2025). Regional summaries  
 4958 of FWI anomalies are available from Turco et al. (2025,  
 4959 <https://doi.org/10.5281/zenodo.15538595>, last access: 6 August 2025). Studies utilising our  
 4960 regional summaries should cite both the current article and the primary reference for the  
 4961 variable(s) of interest: Giglio et al. (2018) for the MODIS MCD64A1 BA product; Andela et al.  
 4962 (2019) for the Global Fire Atlas; Giglio et al. (2016) for active fire observations of FRP from  
 4963 MOD14A1 and MYD14A1; Lizundia-Loiola et al. (2022) for the FireCCIS311 BA product; van  
 4964 der Werf et al. (2017) for GFED4.1s fire C emissions; Kaiser et al. (2012) for GFAS fire C  
 4965 emissions; Vitolo et al. (2020) for FWI from the ECMWF ERA5 reanalysis. **Section 3:**  
 4966 Regional summaries of population and physical asset exposure are available from  
 4967 Steinmann et al. (2025a, <https://doi.org/10.5281/zenodo.15755007>, last access: 6 August  
 4968 2025). **Section 4 (and subsequent sections):** The input meteorological data used for  
 4969 training the PoF model, listed in Table S1, are taken from the ERA5-Land dataset, openly  
 4970 available through the Copernicus Climate Change Service (C3S, 2019;  
 4971 <https://doi.org/10.24381/cds.e2161bac>; accessed 6 August 2025). The fuel characteristic  
 4972 dataset, updated from McNorton and Di Giuseppe (2024), is available from the ECMWF  
 4973 (2025; <https://doi.org/10.24381/378d1497>, last access: 6 August 2025). Model driving data  
 4974 and re-gridded BA target data for ConFLAME, for section 4, 5 and 6, are available from  
 4975 Barbosa et al. (2025a; <https://doi.org/10.5281/zenodo.15721434>, last access: 6 August  
 4976 2025), with ConFLAME driver assessment data for Northeastern Amazonia and Pantanal &  
 4977 Chiquitano available from Barbosa et al. (2025c; <https://doi.org/10.5281/zenodo.16786041>,  
 4978 last access: 6 August 2025) and Southern California and Congo Basin from Kelley et al.  
 4979 (2025a; <https://doi.org/10.5281/zenodo.16789657>, last access: 6 August 2025). Data for the  
 4980 FWI seasonal forecast used in Section 4 and 6 are available from the Copernicus  
 4981 Emergency Management Service (CEMS, 2025; <https://doi.org/10.24381/cds.b9c753f1>, last  
 4982 access: 6 August 2025). **Section 5 (and subsequent sections):** Historical (1960-2013)  
 4983 HadGEM3-A are available from the Met Office (2025;  
 4984 <http://catalogue.ceda.ac.uk/uuid/99b29b4bfeae470599fb96243e90cde3>, last access: 6  
 4985 August 2025). ConFLAME NRT attribution outputs are available from (Kelley et al. 2025c;  
 4986 <https://doi.org/10.5281/zenodo.15641876>, last access: 6 August 2025). FireMIP / ISIMIP  
 4987 driving and output data is available from the Inter-Sectoral Impact Model Intercomparison  
 4988 Project (ISIMIP; <https://data.ISIMIP.org/>, last access: 6 August 2025). **Section 6 (and**  
 4989 **subsequent sections):** ConFLAME future burned area projections are available from



(Kelley et al., 2025b; <https://doi.org/10.5281/zenodo.15807587>, last access: 10 August 2025). Data and scripts used to produce Fire Weather Index (FWI) projections at different global warming levels are available from Liu & Eden (2025; <https://doi.org/10.5281/zenodo.15790287>, last access: 6 August 2025).

## 12. Code Availability

**Section 3:** Code for regional summaries of population and physical asset exposure have been made available by Steinmann et al. (2025b; <https://doi.org/10.5281/zenodo.15831766>, last access: 6 August 2025). **Section 4 (and subsequent sections):** ConFLAME attribution and future projections framework (Kelley et al., 2021; Barbosa et al., 2025b) is available from Barbosa et al. (2025a; <https://doi.org/10.5281/zenodo.16790787>, last access: 6 August 2025). The PoF model used in Section 4 is from ECMWF implementation. A simplified version with the main scripts for data processing, model training, and analysis are archived in a publicly accessible repository <https://doi.org/10.24433/CO.8570224.v1> with documentation to facilitate replication of the results. **Section 5 (and subsequent sections):** The code used to produce the FWI attribution results is available from Kelley et al., 2024 (<https://doi.org/10.5281/zenodo.11460379>, last access: 6 August 2025). The FWI code used to generate the figures in section 4 can be accessed via the ECMWF GitHub (<https://github.com/ecmwf-projects/geff>; last access: 6 August 2025). Code used for the FireMIP attribution results, along with processed ISIMIP data, can be found at <https://doi.org/10.5281/zenodo.16779167> (Lampe & Burton 2025), with methods documented in Burton, Lampe et al. (2024). The current version of ibicus, used for JULES-ES bias correction, is available from PyPI (<https://pypi.org/project/ibicus/>, last access: 6 August 2025) and is described in detail in <https://ibicus.readthedocs.io/en/latest/> (last access: 6 August 2025). Model code and evaluation for bias-correction of JULES-ES model output can be found at Spuler and Wessel (2025, <https://doi.org/10.5281/zenodo.15792440>, last access: 6 August 2025).

## 13. Financial Support

DIK and MLFB were funded by the UK Natural Environment Research Council (NERC) as part of the LTSM2 TerraFIRMA project and NC-International programme (NE/X006247/1) delivering National Capability. CAB and EW were funded by the UK Department for Science (DSIT) Met Office Hadley Centre Climate Programme and the DSIT Innovation & Technology International Science Partnerships Fund (ISPF; UK Met Office Climate Science for Service Partnership [CSSP] Brazil). FDG and JRM were funded by a service contract (n 942604) issued by the Joint Research Center on behalf of the European Commission. MWJ was funded by the UK NERC (NE/V01417X/1). ASIB was funded by the DSIT Innovation & Technology International Science Partnerships Fund (ISPF; UK Met Office Climate Science for Service Partnership [CSSP] Brazil). CBS was funded by the Swiss Innovation Agency Innosuisse (53733.1 IP-SBM). EAK was funded by the State Assignment Project (FWES-2024-0040). EBr was funded by the UK NERC ARIES Doctoral Training Partnership (NE/S007334/1). GM was funded by the FAPESP (2019/25701-8 and 2023/03206-0). HC was funded by the Westpac Scholars Trust via a Westpac Research Fellowship and by the Australian Research Council via an Industry Fellowship with the Victorian Department of Energy, Environment, and Climate Action, the Victorian Country Fire Authority and Natural Hazards Research Australia (IM240100046). JBW was funded by the UK Engineering and Physical Sciences Research Council (EPSRC; 2696930). LOA was funded by the São Paulo Research Foundation (FAPESP; 2021/07660-2 and 2020/16457-3), and the Brazilian National Council for Scientific and Technological Development (CNPq; 409531/2021-9 and 314473/2020-3). MAT-V and MT were funded by the Spanish Ministry of Science and Innovation (MCIN; MCIN/AEI/10.13039/501100011033; ONFIRE PID2021-123193OB-I00) and by the European Regional Development Fund (ERDF; project “A way of making Europe”). MP and EDT are part of the Copernicus Atmosphere Monitoring Service, which is



operated by the European Centre for Medium-Range Weather Forecasts (ECMWF) on behalf of the European Commission as part of the Copernicus Programme. MT was funded by the Spanish Ministry of Science, Innovation and Universities through the Ramón y Cajal (RYC2019-027115-I). PF was supported by the Portuguese Foundation for Science and Technology (FCT; UID/04033/2023 [Centre for the Research and Technology of Agro-Environmental and Biological Sciences] and LA/P/0126/2020 [https://doi.org/10.54499/LA/P/0126/2020]). RV was funded by the Brazilian National Council for Scientific and Technological Development (CNPq; #443285/2023-3) and the Brazilian Institute of Environment and Renewable Natural Resources (IBAMA) / Federal University of Rio de Janeiro (UFRJ; #968711). SM was funded by the Dragon Capital Chair on Biodiversity Economics. SV and YQ were funded by a European Research Council Consolidator Grant (101000987). TRK was funded by Schmidt Sciences, LLC.

## 14. References

- Abatzoglou, J. T. and Kolden, C. A.: Climate Change in Western US Deserts: Potential for Increased Wildfire and Invasive Annual Grasses, *Rangeland Ecology & Management*, 64, 471–478, <https://doi.org/10.2111/REM-D-09-00151.1>, 2011.
- Abatzoglou, J. T., Williams, A. P., Boschetti, L., Zubkova, M., and Kolden, C. A.: Global patterns of interannual climate–fire relationships, *Glob Change Biol*, 24, 5164–5175, <https://doi.org/10.1111/gcb.14405>, 2018.
- Abatzoglou, J. T., Williams, A. P., and Barbero, R.: Global Emergence of Anthropogenic Climate Change in Fire Weather Indices, *Geophys. Res. Lett.*, 46, 326–336, <https://doi.org/10.1029/2018GL080959>, 2019.
- Abatzoglou, J. T., Smith, C. M., Swain, D. L., Ptak, T., and Kolden, C. A.: Population exposure to pre-emptive de-energization aimed at averting wildfires in Northern California, *Environ. Res. Lett.*, 15, 094046, <https://doi.org/10.1088/1748-9326/aba135>, 2020.
- Abatzoglou, J. T., Juang, C. S., Williams, A. P., Kolden, C. A., and Westerling, A. L.: Increasing Synchronous Fire Danger in Forests of the Western United States, *Geophysical Research Letters*, 48, e2020GL091377, <https://doi.org/10.1029/2020GL091377>, 2021.
- Abatzoglou, J. T., Kolden, C. A., Williams, A. P., Sadegh, M., Balch, J. K., and Hall, A.: Downslope Wind-Driven Fires in the Western United States, *Earth's Future*, 11, e2022EF003471, <https://doi.org/10.1029/2022EF003471>, 2023.
- Abatzoglou, J. T., Kolden, C. A., Cullen, A. C., Sadegh, M., Williams, E. L., Turco, M., and Jones, M. W.: Climate change has increased the odds of extreme regional forest fire years globally, *Nat Commun*, 16, 6390, <https://doi.org/10.1038/s41467-025-61608-1>, 2025.
- Abram, N. J., Henley, B. J., Sen Gupta, A., Lippmann, T. J. R., Clarke, H., Dowdy, A. J., Sharples, J. J., Nolan, R. H., Zhang, T., Wooster, M. J., Wurtzel, J. B., Meissner, K. J., Pitman, A. J., Ukkola, A. M., Murphy, B. P., Tapper, N. J., and Boer, M. M.: Connections of climate change and variability to large and extreme forest fires in southeast Australia, *Commun Earth Environ*, 2, 8, <https://doi.org/10.1038/s43247-020-00065-8>, 2021.
- Adzhar, R., Kelley, D. I., Dong, N., George, C., Torello Raventos, M., Veenendaal, E., Feldpausch, T. R., Phillips, O. L., Lewis, S. L., Sonké, B., Taedoumg, H., Schwantes Marimon, B., Domingues, T., Arroyo, L., Djagbletey, G., Saiz, G., and Gerard, F.: MODIS Vegetation Continuous Fields tree cover needs calibrating in tropical savannas, *Biogeosciences*, 19, 1377–1394, <https://doi.org/10.5194/bg-19-1377-2022>, 2022.



- 5086 Africa News: Wildfires force evacuations of South African coastal towns  
 5087 <https://www.africanews.com/2024/01/31/wildfires-force-evacuations-of-south-african-coastal-towns/> (last  
 5088 access: 6th August 2025), 2024.
- 5089 Agência para a Gestão Integrada de Fogos Rurais: Relatório de Atividades 2024 Relatório anual de atividades  
 5090 do Sistema de Gestão Integrada de Fogos Rurais (SGIFR),  
 5091 [https://www.agif.pt/app/uploads/2025/06/Relat%C3%B3rio-de-Atividades-2024\\_SGIFR\\_pg-34-corrigida.](https://www.agif.pt/app/uploads/2025/06/Relat%C3%B3rio-de-Atividades-2024_SGIFR_pg-34-corrigida.pdf)  
 5092 pdf (last access: 6th August 2025), 2024.
- 5093 Aguilera, R., Corringham, T., Gershunov, A., and Benmarhnia, T.: Wildfire smoke impacts respiratory health more  
 5094 than fine particles from other sources: observational evidence from Southern California, *Nat Commun*,  
 5095 12, 1493, <https://doi.org/10.1038/s41467-021-21708-0>, 2021a.
- 5096 Aguilera, R., Corringham, T., Gershunov, A., and Benmarhnia, T.: Wildfire smoke impacts respiratory health more  
 5097 than fine particles from other sources: observational evidence from Southern California, *Nat Commun*,  
 5098 12, 1493, <https://doi.org/10.1038/s41467-021-21708-0>, 2021b.
- 5099 Agustí-Panareda, A., Diamantakis, M., Massart, S., Chevallier, F., Muñoz-Sabater, J., Barré, J., Curcoll, R.,  
 5100 Engelen, R., Langerock, B., Law, R. M., Loh, Z., Morguí, J. A., Parrington, M., Peuch, V.-H., Ramonet,  
 5101 M., Roehl, C., Vermeulen, A. T., Warneke, T., and Wunch, D.: Modelling CO<sub>2</sub> weather – why horizontal  
 5102 resolution matters, *Atmospheric Chemistry and Physics*, 19, 7347–7376,  
 5103 <https://doi.org/10.5194/acp-19-7347-2019>, 2019.
- 5104 Alencar, A., Arruda, V., Martenexen, F., Rosa, E. R., Velez-Martin, E., Guedes Pinto, L. F., Duverger, S. G.,  
 5105 Monteiro, N., and Silva, W.: Fogo no Brasil em 2024: o retrato fundiário da área queimada nos biomas,  
 5106 <https://ipam.org.br/bibliotecas/fogo-no-brasil-em-2024-o-retrato-fundiario-da-area-queimada-nos-biomas/>  
 5107 / (last access: 6th August 2025), IPAM Amazônia, 2024.
- 5108 Alencar, A. A., Brando, P. M., Asner, G. P., and Putz, F. E.: Landscape fragmentation, severe drought, and the  
 5109 new Amazon forest fire regime, *Ecological Applications*, 25, 1493–1505,  
 5110 <https://doi.org/10.1890/14-1528.1>, 2015.
- 5111 Alencar et al.: Long-Term Landsat-Based Monthly Burned Area Dataset for the Brazilian Biomes Using Deep  
 5112 Learning [data set], [https://doi.org/DOI: 10.3390/rs14112510](https://doi.org/DOI:10.3390/rs14112510), 2022.
- 5113 Almeida, C. T., Oliveira-Júnior, J. F., Delgado, R. C., Cubo, P., and Ramos, M. C.: Spatiotemporal rainfall and  
 5114 temperature trends throughout the Brazilian Legal Amazon, 1973–2013, *Intl Journal of Climatology*, 37,  
 5115 2013–2026, <https://doi.org/10.1002/joc.4831>, 2017.
- 5116 Alvarado, S. T., Andela, N., Silva, T. S. F., and Archibald, S.: Thresholds of fire response to moisture and fuel load  
 5117 differ between tropical savannas and grasslands across continents, *Global Ecol Biogeogr*, 29, 331–344,  
 5118 <https://doi.org/10.1111/geb.13034>, 2020.
- 5119 Anand, P., Mina, U., Khare, M., Kumar, P., and Kota, S. H.: Air pollution and plant health response-current status  
 5120 and future directions, *Atmospheric Pollution Research*, 13, 101508,  
 5121 <https://doi.org/10.1016/j.apr.2022.101508>, 2022.
- 5122 Andela, N. and Jones, M. W.: Update of: The Global Fire Atlas of individual fire size, duration, speed and  
 5123 direction, Zenodo [Data set], <https://doi.org/10.5281/zenodo.11400061>, 2025.
- 5124 Andela, N. and Van Der Werf, G. R.: Recent trends in African fires driven by cropland expansion and El Niño to  
 5125 La Niña transition, *Nature Clim Change*, 4, 791–795, <https://doi.org/10.1038/nclimate2313>, 2014.





- 5126 Andela, N., Morton, D. C., Giglio, L., Chen, Y., van der Werf, G. R., Kasibhatla, P. S., DeFries, R. S., Collatz, G.  
 5127 J., Hantson, S., Kloster, S., Bachelet, D., Forrest, M., Lasslop, G., Li, F., Mangeon, S., Melton, J. R.,  
 5128 Yue, C., and Randerson, J. T.: A human-driven decline in global burned area, *Science*, 356, 1356–1362,  
 5129 <https://doi.org/10.1126/science.aal4108>, 2017.
- 5130 Andela, N., Morton, D. C., Giglio, L., and Randerson, J. T.: Global Fire Atlas with Characteristics of Individual  
 5131 Fires, 2003-2016, ORNL DAAC, <https://doi.org/10.3334/ORNLDAAAC/1642>, 2019a.
- 5132 Andela, N., Morton, D. C., Giglio, L., Paugam, R., Chen, Y., Hantson, S., van der Werf, G. R., and Randerson, J.  
 5133 T.: The Global Fire Atlas of individual fire size, duration, speed and direction, *Earth System Science*  
 5134 *Data*, 11, 529–552, <https://doi.org/10.5194/essd-11-529-2019>, 2019b.
- 5135 Andela, N., Morton, D. C., Schroeder, W., Chen, Y., Brando, P. M., and Randerson, J. T.: Tracking and classifying  
 5136 Amazon fire events in near real time, *Science Advances*, 8, eabd2713,  
 5137 <https://doi.org/10.1126/sciadv.abd2713>, 2022.
- 5138 Anderegg, W. R. L., Trugman, A. T., Badgley, G., Anderson, C. M., Bartuska, A., Ciais, P., Cullenward, D., Field,  
 5139 C. B., Freeman, J., Goetz, S. J., Hicke, J. A., Huntzinger, D., Jackson, R. B., Nickerson, J., Pacala, S.,  
 5140 and Randerson, J. T.: Climate-driven risks to the climate mitigation potential of forests, *Science*, 368,  
 5141 <https://doi.org/10.1126/science.aaz7005>, 2020.
- 5142 Andreae, M. O.: Emission of trace gases and aerosols from biomass burning – an updated assessment,  
 5143 *Atmospheric Chemistry and Physics*, 19, 8523–8546, <https://doi.org/10.5194/acp-19-8523-2019>, 2019.
- 5144 Aragão, L. E. O. C., Anderson, L. O., Fonseca, M. G., Rosan, T. M., Vedovato, L. B., Wagner, F. H., Silva, C. V.  
 5145 J., Silva Junior, C. H. L., Arai, E., Aguiar, A. P., Barlow, J., Berenguer, E., Deeter, M. N., Domingues, L.  
 5146 G., Gatti, L., Gloor, M., Malhi, Y., Marengo, J. A., Miller, J. B., Phillips, O. L., and Saatchi, S.: 21st  
 5147 Century drought-related fires counteract the decline of Amazon deforestation carbon emissions, *Nat*  
 5148 *Commun*, 9, 536, <https://doi.org/10.1038/s41467-017-02771-y>, 2018.
- 5149 Archibald, S. and Roy, D. P.: Identifying individual fires from satellite-derived burned area data, in: 2009 IEEE  
 5150 International Geoscience and Remote Sensing Symposium, 2009 IEEE International Geoscience and  
 5151 Remote Sensing Symposium, III-160-III-163, <https://doi.org/10.1109/IGARSS.2009.5417974>, 2009.
- 5152 Archibald, S., Roy, D. P., van Wilgen, B. W., and Scholes, R. J.: What limits fire? An examination of drivers of  
 5153 burnt area in Southern Africa, *Global Change Biology*, 15, 613–630,  
 5154 <https://doi.org/10.1111/j.1365-2486.2008.01754.x>, 2009.
- 5155 Arctic Monitoring and Assessment Programme (AMAP): AMAP Arctic Climate Change Update 2024: Key Trends  
 5156 and Impacts, available at:  
 5157 [https://www.amap.no/documents/doc/amap-arctic-climate-change-update-2024-key-trends-and-impacts/](https://www.amap.no/documents/doc/amap-arctic-climate-change-update-2024-key-trends-and-impacts/3851)  
 5158 3851, (last access: 6th August 2025), 2024.
- 5159 Ardyna, M., Hamilton, D. S., Harmel, T., Lacour, L., Bernstein, D. N., Laliberté, J., Horvat, C., Laxenaire, R., Mills,  
 5160 M. M., van Dijken, G., Polyakov, I., Claustre, H., Mahowald, N., and Arrigo, K. R.: Wildfire aerosol  
 5161 deposition likely amplified a summertime Arctic phytoplankton bloom, *Commun Earth Environ*, 3, 1–8,  
 5162 <https://doi.org/10.1038/s43247-022-00511-9>, 2022.
- 5163 Arino, O., Rosaz, J.-M., and Goloub, P.: The ATSR World Fire Atlas A synergy with ‘Polder’ aerosol products,  
 5164 *Earth Observation Quarterly*, 64, 30, 1999.





- 5165 Artés, T., Oom, D., de Rigo, D., Durrant, T. H., Maianti, P., Libertà, G., and San-Miguel-Ayanz, J.: A global wildfire  
 5166 dataset for the analysis of fire regimes and fire behaviour, *Sci Data*, 6, 296,  
 5167 <https://doi.org/10.1038/s41597-019-0312-2>, 2019.
- 5168 Athanasiou, M.: Preliminary findings on the behaviour and spread of the wildfire of August 2023 in Evros, Greece.  
 5169 Project “Learning from the Evros wildfire: Firefighting effectiveness evaluation and proposals”, WWF  
 5170 Greece, Athens, 76 pp. WWF Greece, Athens,  
 5171 [https://wwfeu.awsassets.panda.org/downloads/fire\\_lessons-learnt\\_evros.pdf](https://wwfeu.awsassets.panda.org/downloads/fire_lessons-learnt_evros.pdf) (last access: 6th August  
 5172 2025), 2024.
- 5173 Avialesookhrana (Aerial Forest Protection Service): Information on forest fire situation in the territory of the RF  
 5174 subjects as of 31.12.2024, [https://aviales.ru/files/documents/2024/fds\\_svedeniya/сведения о](https://aviales.ru/files/documents/2024/fds_svedeniya/сведения о лесопожарной обстановке на территории субъектов рф на 31.12.2024.pdf)  
 5175 [лесопожарной обстановке на территории субъектов рф на 31.12.2024.pdf](https://aviales.ru/files/documents/2024/fds_svedeniya/сведения о лесопожарной обстановке на территории субъектов рф на 31.12.2024.pdf) (last access: 6th August  
 5176 2025), 2024.
- 5177 Aznar-Siguan, G. and Bresch, D. N.: CLIMADA v1: a global weather and climate risk assessment platform,  
 5178 *Geoscientific Model Development*, 12, 3085–3097, <https://doi.org/10.5194/gmd-12-3085-2019>, 2019.
- 5179 Badgley, G., Chay, F., Chegwidan, O. S., Hamman, J. J., Freeman, J., and Cullenward, D.: California’s forest  
 5180 carbon offsets buffer pool is severely undercapitalized, *Front. For. Glob. Change*, 5,  
 5181 <https://doi.org/10.3389/ffgc.2022.930426>, 2022a.
- 5182 Badgley, G., Freeman, J., Hamman, J. J., Haya, B., Trugman, A. T., Anderegg, W. R. L., and Cullenward, D.:  
 5183 Systematic over-crediting in California’s forest carbon offsets program, *Global Change Biology*, 28,  
 5184 1433–1445, <https://doi.org/10.1111/gcb.15943>, 2022b.
- 5185 Baltzer, J. L., Day, N. J., Walker, X. J., Greene, D., Mack, M. C., Alexander, H. D., Arseneault, D., Barnes, J.,  
 5186 Bergeron, Y., Boucher, Y., Bourgeau-Chavez, L., Brown, C. D., Carrière, S., Howard, B. K., Gauthier, S.,  
 5187 Parisien, M.-A., Reid, K. A., Rogers, B. M., Roland, C., Sirois, L., Stehn, S., Thompson, D. K., Turetsky,  
 5188 M. R., Veraverbeke, S., Whitman, E., Yang, J., and Johnstone, J. F.: Increasing fire and the decline of  
 5189 fire adapted black spruce in the boreal forest, *Proceedings of the National Academy of Sciences*, 118,  
 5190 e2024872118, <https://doi.org/10.1073/pnas.2024872118>, 2021.
- 5191 Barbero, R., Abatzoglou, J. T., Steel, E. A., and K Larkin, N.: Modeling very large-fire occurrences over the  
 5192 continental United States from weather and climate forcing, *Environ. Res. Lett.*, 9, 124009,  
 5193 <https://doi.org/10.1088/1748-9326/9/12/124009>, 2014.
- 5194 Barbosa, M. L., Haddad, I., da Silva Nascimento, A. L., Máximo da Silva, G., Moura da Veiga, R., Hoffmann, T.  
 5195 B., Rosane de Souza, A., Dalagnol, R., Susin Streher, A., Souza Pereira, F. R., Oliveira e Cruz de  
 5196 Aragão, L. E., and Oighenstein Anderson, L.: Compound impact of land use and extreme climate on the  
 5197 2020 fire record of the Brazilian Pantanal, *Global Ecology and Biogeography*, 31, 1960–1975,  
 5198 <https://doi.org/10.1111/geb.13563>, 2022.
- 5199 Barbosa, M. L., Kelley, D., Moura da Veiga, R., Dong, N., and Burton, C.: State of Wildfires 2024-25 ConFLAME:  
 5200 [douglass3/Bayesian\\_fire\\_models \[Code\]](https://doi.org/10.5281/ZENODO.16790787), , <https://doi.org/10.5281/ZENODO.16790787>, 2025a.
- 5201 Barbosa, M. L. F.: Tracing the Ashes: Uncovering Burned Area Patterns and Drivers Over the Brazilian Biomes,  
 5202 PhD Thesis, available at:  
 5203 <http://mtc-m21d.sid.inpe.br/col/sid.inpe.br/mtc-m21d/2024/04.04.17.26/doc/publicacao.pdf> (last access:  
 5204 6th August 2025), Instituto Nacional de Pesquisas Espaciais, 2024.



- 5205 Barbosa, M. L. F., Kelley, D. I., Burton, C. A., Ferreira, I. J. M., da Veiga, R. M., Bradley, A., Molin, P. G., and  
 5206 Anderson, L. O.: FLAME 1.0: a novel approach for modelling burned area in the Brazilian biomes using  
 5207 the maximum entropy concept, *Geoscientific Model Development*, 18, 3533–3557,  
 5208 <https://doi.org/10.5194/gmd-18-3533-2025>, 2025b.
- 5209 Barbosa, M. L. F., Kelley, D., Hartley, A., Spuler, F., Wessel, J., Ciavarella, A., McNorton, J., Burton, C., Ferreira,  
 5210 I., and Fiedler, L.: State of Wildfires 2024/25 – ConFLAME Driver Assessment - Northeastern  
 5211 Amazonia/Pantanal-Chiquitano [Data set], <https://doi.org/10.5281/ZENODO.16786041>, 2025c.
- 5212 Barbosa, M. L. F., Kelley, D., Ciavarella, A., Hartley, A., McNorton, J., Di Giuseppe, F., Jones, M., Spuler, F.,  
 5213 Wessel, J., and Burton, C.: State of Wildfires 2024-25 ConFLAME driving data [Data set] (v0.1.0),  
 5214 <https://doi.org/10.5281/ZENODO.15721434>, 2025d.
- 5215 Barichivich, J., Gloor, E., Peylin, P., Brien, R. J. W., Schöngart, J., Espinoza, J. C., and Pattnayak, K. C.:  
 5216 Recent intensification of Amazon flooding extremes driven by strengthened Walker circulation, *Sci. Adv.*,  
 5217 4, <https://doi.org/10.1126/sciadv.aat8785>, 2018.
- 5218 Barlow, J., Parry, L., Gardner, T. A., Ferreira, J., Aragão, L. E. O. C., Carmenta, R., Berenguer, E., Vieira, I. C. G.,  
 5219 Souza, C., and Cochrane, M. A.: The critical importance of considering fire in REDD+ programs,  
 5220 *Biological Conservation*, 154, 1–8, <https://doi.org/10.1016/j.biocon.2012.03.034>, 2012.
- 5221 Barlow, J., França, F., Gardner, T. A., Hicks, C. C., Lennox, G. D., Berenguer, E., Castello, L., Economo, E. P.,  
 5222 Ferreira, J., Guénard, B., Gontijo Leal, C., Isaac, V., Lees, A. C., Parr, C. L., Wilson, S. K., Young, P. J.,  
 5223 and Graham, N. A. J.: The future of hyperdiverse tropical ecosystems, *Nature*, 559, 517–526,  
 5224 <https://doi.org/10.1038/s41586-018-0301-1>, 2018.
- 5225 Barlow, J., Berenguer, E., Carmenta, R., and França, F.: Clarifying Amazonia's burning crisis, *Glob Change Biol*,  
 5226 26, 319–321, <https://doi.org/10.1111/gcb.14872>, 2020.
- 5227 Barnes, C., Boulanger, Y., Keeping, T., Gachon, P., Gillett, N., Boucher, J., Roberge, F., Kew, S., Haas, O.,  
 5228 Heinrich, D., Vahlberg, M., Singh, R., Elbe, M., Sivanu, S., Arrighi, J., van Aalst, M., Otto, F., Zachariah,  
 5229 M., Krikken, F., and Wang, X.: Climate change more than doubled the likelihood of extreme fire weather  
 5230 conditions in Eastern Canada., <https://doi.org/10.25561/105981>, 2023.
- 5231 Barnes, C., Santos, F. L., Libonati, R., Keeping, T., Rodrigues, R., Alves, L. M., Sivanu, S., Vahlberg, M., Alcayna,  
 5232 T., Otto, F., Zachariah, M., Singh, R., Mugge, M., Biehl, J., Petryna, A., Dias, M., Reis, E., and Uzquiano,  
 5233 S.: Hot, dry and windy conditions that drove devastating Pantanal wildfires 40% more intense due to  
 5234 climate change, <https://doi.org/10.25561/113726>, 2024.
- 5235 Barnes, C., Keeping, T., Madakumbura, G., Abatzoglou, J., Williams, P., AghaKhouchak, A., Pinto, I., Thompson,  
 5236 V., Vautard, R., Lampe, S., Thiery, W., Pietrousti, R., Otto, F., Vahlberg, M., Singh, R., Lambrou, N.,  
 5237 Blakely, E., Zhu, Y., Li, J., Benmarhnia, T., Longcore, T., Marlier, M., Raju, E., Baumgart, N., and Arrighi,  
 5238 J.: Climate change increased the likelihood of wildfire disaster in highly exposed Los Angeles area,  
 5239 <https://www.worldweatherattribution.org/wp-content/uploads/WWA-scientific-report-LA-wildfires-1.pdf>,  
 5240 2025.
- 5241 Bedia, J., Herrera, S., Gutiérrez, J. M., Benali, A., Brands, S., Mota, B., and Moreno, J. M.: Global patterns in the  
 5242 sensitivity of burned area to fire-weather: Implications for climate change, *Agricultural and Forest  
 5243 Meteorology*, 214–215, 369–379, <https://doi.org/10.1016/j.agrformet.2015.09.002>, 2015.



- 5244 Bedia, J., Golding, N., Casanueva, A., Iturbide, M., Buontempo, C., and Gutiérrez, J. M.: Seasonal predictions of  
 5245 Fire Weather Index: Paving the way for their operational applicability in Mediterranean Europe, *Climate*  
 5246 Services, 9, 101–110, <https://doi.org/10.1016/j.cliser.2017.04.001>, 2018.
- 5247 Bélo Carvalho, R., Oliveras Menor, I., Schmidt, I. B., Berlinck, C. N., Genes, L., and Dirzo, R.: Brazil on fire:  
 5248 Igniting awareness of the 2024 wildfire crisis, *Journal of Environmental Management*, 389, 126190,  
 5249 <https://doi.org/10.1016/j.jenvman.2025.126190>, 2025.
- 5250 Betts, R. A., Belcher, S. E., Hermanson, L., Klein Tank, A., Lowe, J. A., Jones, C. D., Morice, C. P., Rayner, N. A.,  
 5251 Scaife, A. A., and Stott, P. A.: Approaching 1.5 °C: how will we know we've reached this crucial warming  
 5252 mark?, *Nature*, 624, 33–35, <https://doi.org/10.1038/d41586-023-03775-z>, 2023.
- 5253 Beverly, J. L. and Bothwell, P.: Wildfire evacuations in Canada 1980–2007, *Nat Hazards*, 59, 571–596,  
 5254 <https://doi.org/10.1007/s11069-011-9777-9>, 2011.
- 5255 Bilbao, B., Mistry, J., Millán, A., and Berardi, A.: Sharing Multiple Perspectives on Burning: Towards a  
 5256 Participatory and Intercultural Fire Management Policy in Venezuela, Brazil, and Guyana, *Fire*, 2, 39,  
 5257 <https://doi.org/10.3390/fire2030039>, 2019.
- 5258 Bilbao, B., Steil, L., Urbiet, I. R., Anderson, L., Pinto, C., González, M. E., Millán, A., Falleiro, R. M., Morici, E.,  
 5259 Ibarnegaray, V., Pérez-Saliciup, D. R., Pereira, J. M., and Moreno, J. M.: Wildfires. Adaptation to  
 5260 Climate Change Risks in Ibero-American Countries-RIOCCADAPT., in: *ResearchGate*, 435–496, 2020.
- 5261 Bilbao, B. A., Millán, A., Luque, M. M., Mistry, J., Gómez-Martínez, R., Rivera-Lombardi, R., Méndez-Vallejo, C.,  
 5262 León, E., Biskis, J., Gutiérrez, G., León, E., and Ancidey, B.: An intercultural vision for integrated fire  
 5263 management in Venezuela, *Tropical Forest Issues*, <https://doi.org/10.55515/CNUU7417>, 2022.
- 5264 Billmire, M., French, N., Loboda, T., Owen, R., and Tyner, M.: Santa Ana winds and predictors of wildfire  
 5265 progression in Southern California, *International Journal of Wildland Fire*, 23, 1119–1129,  
 5266 <https://doi.org/10.1071/WF13046>, 2014.
- 5267 Bistinas, I., Harrison, S. P., Prentice, I. C., and Pereira, J. M. C.: Causal relationships versus emergent patterns in  
 5268 the global controls of fire frequency, *Biogeosciences*, 11, 5087–5101,  
 5269 <https://doi.org/10.5194/bg-11-5087-2014>, 2014.
- 5270 Bodí, M. B., Martín, D. A., Balfour, V. N., Santín, C., Doerr, S. H., Pereira, P., Cerdà, A., and Mataix-Solera, J.:  
 5271 Wildland fire ash: Production, composition and eco-hydro-geomorphic effects, *Earth-Science Reviews*,  
 5272 130, 103–127, <https://doi.org/10.1016/j.earscirev.2013.12.007>, 2014.
- 5273 Bolakhe, S.: Wildfires are raging in Nepal — climate change isn't the only culprit, *Nature*,  
 5274 <https://doi.org/10.1038/d41586-024-01758-2>, 2024.
- 5275 Booth, R. C.: It's a make-or-break moment for housing in California (last access: 6th August 2025), *Vox*, 2025.
- 5276 Borgschulte, M., Molitor, D., and Zou, E. Y.: Air Pollution and the Labor Market: Evidence from Wildfire Smoke,  
 5277 The Review of Economics and Statistics, 106(6), 1558–1575, [https://doi.org/10.1162/rest\\_a\\_01243](https://doi.org/10.1162/rest_a_01243),  
 5278 2024.
- 5279 Boschetti, L. and Roy, D. P.: Defining a fire year for reporting and analysis of global interannual fire variability,  
 5280 Journal of Geophysical Research: Biogeosciences, 113, G03020,  
 5281 <https://doi.org/10.1029/2008JG000686>, 2008.



- 5282 Botzen, W. J. W., Deschenes, O., and Sanders, M.: The Economic Impacts of Natural Disasters: A Review of  
 5283 Models and Empirical Studies, *Review of Environmental Economics and Policy*, 13,  
 5284 167–188, <https://doi.org/10.1093/reep/rez004>, 2019.
- 5285 Boucher, O., Servonnat, J., Albright, A. L., Aumont, O., Balkanski, Y., Bastrikov, V., Bekki, S., Bonnet, R., Bony,  
 5286 S., Bopp, L., Braconnot, P., Brockmann, P., Cadule, P., Caubel, A., Cheruy, F., Codron, F., Cozic, A.,  
 5287 Cugnet, D., D'Andrea, F., Davini, P., de Lavergne, C., Denvil, S., Deshayes, J., Devilliers, M., Ducharne,  
 5288 A., Dufresne, J.-L., Dupont, E., Éthé, C., Fairhead, L., Falletti, L., Flavoni, S., Foujols, M.-A., Gardoll, S.,  
 5289 Gastineau, G., Ghattas, J., Grandpeix, J.-Y., Guenet, B., Guez, E., Lionel, Guilyardi, E., Guimberteau,  
 5290 M., Hauglustaine, D., Hourdin, F., Idelkadi, A., Joussaume, S., Kageyama, M., Khodri, M., Krinner, G.,  
 5291 Lebas, N., Levassasseur, G., Lévy, C., Li, L., Lott, F., Lurton, T., Luyssaert, S., Madec, G., Madeleine,  
 5292 J.-B., Maignan, F., Marchand, M., Marti, O., Mellul, L., Meurdesoif, Y., Mignot, J., Musat, I., Ottlé, C.,  
 5293 Peylin, P., Planton, Y., Polcher, J., Rio, C., Rochetin, N., Rousset, C., Sepulchre, P., Sima, A.,  
 5294 Swingedouw, D., Thiéblemont, R., Traore, A. K., Vancoppenolle, M., Vial, J., Vialard, J., Viovy, N., and  
 5295 Vuichard, N.: Presentation and Evaluation of the IPSL-CM6A-LR Climate Model, *Journal of Advances in*  
 5296 *Modelling Earth Systems*, 12, e2019MS002010, <https://doi.org/10.1029/2019MS002010>, 2020.
- 5297 Boussetta, S., Balsamo, G., Arduini, G., Dutra, E., McNorton, J., Choulga, M., Agustí-Panareda, A., Beljaars, A.,  
 5298 Wedi, N., Muñoz-Sabater, J., de Rosnay, P., Sandu, I., Hadade, I., Carver, G., Mazzetti, C., Prudhomme,  
 5299 C., Yamazaki, D., and Zsoter, E.: ECLand: The ECMWF Land Surface Modelling System, *Atmosphere*,  
 5300 12, 723, <https://doi.org/10.3390/atmos12060723>, 2021.
- 5301 Bowman, D., Williamson, G., Yebra, M., Lizundia-Loiola, J., Pettinari, M. L., Shah, S., Bradstock, R., and  
 5302 Chuvieco, E.: Wildfires: Australia needs national monitoring agency, *Nature*, 584, 188–191,  
 5303 <https://doi.org/10.1038/d41586-020-02306-4>, 2020.
- 5304 Bowman, D. M. J. S., Moreira-Muñoz, A., Kolden, C. A., Chávez, R. O., Muñoz, A. A., Salinas, F.,  
 5305 González-Reyes, Á., Rocco, R., de la Barrera, F., Williamson, G. J., Borchers, N., Cifuentes, L. A.,  
 5306 Abatzoglou, J. T., and Johnston, F. H.: Human–environmental drivers and impacts of the globally  
 5307 extreme 2017 Chilean fires, *Ambio*, 48, 350–362, <https://doi.org/10.1007/s13280-018-1084-1>, 2019.
- 5308 Bradshaw, L. S., Deeming, J., Burgan, R., and Cohen, J.: The 1978 National Fire-Danger Rating System:  
 5309 Technical Documentation, U.S. Department of Agriculture, Forest Service, Intermountain Forest and  
 5310 Range Experiment Station, 52 pp., 1984a.
- 5311 Bradshaw, L. S., Deeming, J. E., Burgan, R. E., and Cohen, J. D.: The 1978 National Fire-Danger Rating System:  
 5312 technical documentation, General Technical Report INT-169. Ogden, UT: U.S. Department of  
 5313 Agriculture, Forest Service, Intermountain Forest and Range Experiment Station,  
 5314 <https://doi.org/10.2737/INT-GTR-169>, 1984b.
- 5315 Brando, P. M., Soares-Filho, B., Rodrigues, L., Assunção, A., Morton, D., Tuchsneider, D., Fernandes, E. C.  
 5316 M., Macedo, M. N., Oliveira, U., and Coe, M. T.: The gathering firestorm in southern Amazonia, *Science*  
 5317 *Advances*, 6, eaay1632, <https://doi.org/10.1126/sciadv.aay1632>, 2020.
- 5318 Breiman, L.: Random Forests, *Machine Learning*, 45, 5–32, <https://doi.org/10.1023/A:1010933404324>, 2001.
- 5319 Briscoe, T. and Rainey, J.: Hazardous wildfire smoke is making L.A. air hard to breathe, available at:  
 5320 <https://www.latimes.com/california/story/2025-01-08/wildfire-smoke-la-air-quality> (last access: 6th  
 5321 August 2025), 2025.



- 5322 Bureau of Meteorology: Annual Australian Climate Statement 2023, Australian Government - Bureau of  
 5323 Meteorology, <http://www.bom.gov.au/climate/current/annual/aus/2023/> (last access: 6th August 2025),  
 5324 2024.
- 5325 Bureau of Meteorology: Annual Australian Climate Statement 2024  
 5326 <http://www.bom.gov.au/climate/current/annual/aus/2024/> (last access: 6th August 2025), Australian  
 5327 Government Bureau of Meteorology, 2025.
- 5328 Burrell, A. L., Sun, Q., Baxter, R., Kukavskaya, E. A., Zhila, S., Shestakova, T., Rogers, B. M., Kaduk, J., and  
 5329 Barrett, K.: Climate change, fire return intervals and the growing risk of permanent forest loss in boreal  
 5330 Eurasia, *Science of The Total Environment*, 831, 154885,  
 5331 <https://doi.org/10.1016/j.scitotenv.2022.154885>, 2022.
- 5332 Burton, C., Lampe, S., Kelley, D. I., Thiery, W., Hantson, S., Christidis, N., Gudmundsson, L., Forrest, M., Burke,  
 5333 E., Chang, J., Huang, H., Ito, A., Kou-Giesbrecht, S., Lasslop, G., Li, W., Nieradzik, L., Li, F., Chen, Y.,  
 5334 Randerson, J., Reyer, C. P. O., and Mengel, M.: Global burned area increasingly explained by climate  
 5335 change, *Nat. Clim. Chang.*, 14, 1186–1192, <https://doi.org/10.1038/s41558-024-02140-w>, 2024.
- 5336 Byrne, B., Liu, J., Bowman, K. W., Pascolini-Campbell, M., Chatterjee, A., Pandey, S., Miyazaki, K., van der Werf,  
 5337 G. R., Wunch, D., Wennberg, P. O., Roehl, C. M., and Sinha, S.: Carbon emissions from the 2023  
 5338 Canadian wildfires, *Nature*, 633, 835–839, <https://doi.org/10.1038/s41586-024-07878-z>, 2024.
- 5339 Cáceres, Z., Shimbo, J., Cáceres, S. R., da Silva, W. V., Arruda, V., and Alencar, A.: Nota técnica: Incendios  
 5340 forestales en el Perú 2002-2024 (last access: 6th August 2025), 2024.
- 5341 Cai, W., Cowan, T., and Raupach, M.: Positive Indian Ocean Dipole events precondition southeast Australia  
 5342 bushfires, *Geophysical Research Letters*, 36, L19710, <https://doi.org/10.1029/2009GL039902>, 2009.
- 5343 Calfire: California Department of Forestry and Fire Protection <https://www.fire.ca.gov/> (last access: 6th August  
 5344 2025), 2025.
- 5345 California Department of Forestry and Fire Protection: Statistics, available at:  
 5346 <https://www.fire.ca.gov/our-impact/statistics> (last access date: 6th August 2025), 2025.
- 5347 Calkin, D. E., Barrett, K., Cohen, J. D., Finney, M. A., Pyne, S. J., and Quarles, S. L.: Wildland-urban fire  
 5348 disasters aren't actually a wildfire problem, *Proceedings of the National Academy of Sciences*, 120,  
 5349 e2315797120, <https://doi.org/10.1073/pnas.2315797120>, 2023a.
- 5350 Calkin, D. E., Barrett, K., Cohen, J. D., Finney, M. A., Pyne, S. J., and Quarles, S. L.: Wildland-urban fire  
 5351 disasters aren't actually a wildfire problem, *Proc. Natl. Acad. Sci. U.S.A.*, 120, e2315797120,  
 5352 <https://doi.org/10.1073/pnas.2315797120>, 2023b.
- 5353 Câmara, J. and Moreira, R.: Pantanal em chamas: prejuízo causado pelo fogo no agronegócio de MS chega a  
 5354 R\$ 1,2 bilhão,  
 5355 [https://g1.globo.com/ms/mato-grosso-do-sul/noticia/2024/09/18/pantanal-em-chamas-prejuizo-causado-](https://g1.globo.com/ms/mato-grosso-do-sul/noticia/2024/09/18/pantanal-em-chamas-prejuizo-causado-pelo-fogo-no-agronegocio-de-ms-chega-a-r-12-bilhao-aponta-famasul.ghtml)  
 5356 [pelo-fogo-no-agronegocio-de-ms-chega-a-r-12-bilhao-aponta-famasul.ghtml](https://g1.globo.com/ms/mato-grosso-do-sul/noticia/2024/09/18/pantanal-em-chamas-prejuizo-causado-pelo-fogo-no-agronegocio-de-ms-chega-a-r-12-bilhao-aponta-famasul.ghtml) (last access: 6th August  
 5357 2025), G1, 2024.
- 5358 Canada, N. R.: Canadian Forest Service. Canadian Wildland Fire Information System (CWFIS), Natural  
 5359 Resources Canada, Canadian Forest Service, Northern Forestry Centre, Edmonton, Alberta, available  
 5360 at: <http://cwfis.cfs.nrcan.gc.ca> (last access: 6th August 2025), 2025.



- 5361 Canadell, J. G., Meyer, C. P., Cook, G. D., Dowdy, A., Briggs, P. R., Knauer, J., Pepler, A., and Haverd, V.:  
 5362 Multi-decadal increase of forest burned area in Australia is linked to climate change, *Nat Commun*, 12,  
 5363 6921, <https://doi.org/10.1038/s41467-021-27225-4>, 2021.
- 5364 Canadian Environmental Protection Act Federal-Provincial Working Group on Air Quality: National ambient air  
 5365 quality objectives for particulate matter. Part 1, Science assessment document: A report by the  
 5366 Canadian Environmental Protection Act (CEPA)/Federal-Provincial Advisory Committee (FPAC) Working  
 5367 Group on Air Quality Objectives and Guidelines, Health Canada, Environmental Health Directorate,  
 5368 Ottawa, Ontario, 22 pp., available at:  
 5369 <https://publications.gc.ca/collections/Collection/H46-2-98-220-1-1E.pdf> (last access: 6th August 2025),  
 5370 1998.
- 5371 Canelles, Q., Aquilué, N., James, P. M. A., Lawler, J., and Brotons, L.: Global review on interactions between  
 5372 insect pests and other forest disturbances, *Landscape Ecol*, 36, 945–972,  
 5373 <https://doi.org/10.1007/s10980-021-01209-7>, 2021.
- 5374 Cardil, A., Rodrigues, M., Tapia, M., Barbero, R., Ramírez, J., Stoof, C. R., Silva, C. A., Mohan, M., and  
 5375 de-Miguel, S.: Climate teleconnections modulate global burned area, *Nat Commun*, 14, 427,  
 5376 <https://doi.org/10.1038/s41467-023-36052-8>, 2023.
- 5377 Carmenta, R., Coudel, E., and Steward, A. M.: Forbidden fire: Does criminalising fire hinder conservation efforts  
 5378 in swidden landscapes of the Brazilian Amazon?, *Geographical Journal*, 185, 23–37,  
 5379 <https://doi.org/10.1111/geoj.12255>, 2019.
- 5380 Carmenta, R., Cammelli, F., Dressler, W., Verbicaro, C., and Zaehring, J. G.: Between a rock and a hard place:  
 5381 The burdens of uncontrolled fire for smallholders across the tropics, *World Development*, 145, 105521,  
 5382 <https://doi.org/10.1016/j.worlddev.2021.105521>, 2021.
- 5383 Carmenta, R., Albuquerque, A., Anderson, L. A., Barlow, J., Caneiro, R., da Costa Dias, T., Ferreira, J., França,  
 5384 F., Nóbrega, J., Parry, L., Power, G., Steward, A. M., Taveres, P., and Estrada-Carmona, N.: Changes in  
 5385 forest food collection and hunter perceptions of Amazonian fire impacts, in press, *Ecology and Society*,  
 5386 2025.
- 5387 Carter, T. S., Heald, C. L., Jimenez, J. L., Campuzano-Jost, P., Kondo, Y., Moteki, N., Schwarz, J. P., Wiedinmyer,  
 5388 C., Darmenov, A. S., Da Silva, A. M., and Kaiser, J. W.: How emissions uncertainty influences the  
 5389 distribution and radiative impacts of smoke from fires in North America, *Atmos. Chem. Phys.*, 20,  
 5390 2073–2097, <https://doi.org/10.5194/acp-20-2073-2020>, 2020.
- 5391 Carvalho, A., Flannigan, M. D., Logan, K., Miranda, A. I., and Borrego, C.: Fire activity in Portugal and its  
 5392 relationship to weather and the Canadian Fire Weather Index System, *Int. J. Wildland Fire*, 17, 328–338,  
 5393 <https://doi.org/10.1071/WF07014>, 2008.
- 5394 Casanueva, A., Herrera, S., Iturbide, M., Lange, S., Jury, M., Dosio, A., Maraun, D., and Gutiérrez, J. M.: Testing  
 5395 bias adjustment methods for regional climate change applications under observational uncertainty and  
 5396 resolution mismatch, *Atmospheric Science Letters*, 21, e978, <https://doi.org/10.1002/asl.978>, 2020.
- 5397 Castillo, G.: 2024: el año en que se incrementaron los incendios forestales en el Perú  
 5398 <https://rpp.pe/peru/actualidad/2024-el-ano-en-que-se-incrementaron-los-incendios-forestales-en-el-peru>  
 5399 -noticia-1606773, RPP (last access: 6th August 2025), 2024.





- 5400 Cecil, D. J., Buechler, D. E., and Blakeslee, R. J.: Gridded lightning climatology from TRMM-LIS and OTD:  
 5401 Dataset description, Atmospheric Research, 135–136, 404–414,  
 5402 <https://doi.org/10.1016/j.atmosres.2012.06.028>, 2014.
- 5403 CEMADEN: SEI/MCTI - 12227428 - Nota Técnica  
 5404 <https://www.gov.br/ceaden/pt-br/assuntos/monitoramento/monitoramento-de-seca-para-o-brasil/monito>  
 5405 ramento-de-secas-e-impactos-no-brasil-agosto-2024/NOTATECNICAN529202SEICEMADENSECAS.pdf  
 5406 f (last access: 6th August 2025), 2024.
- 5407 Center for International Earth Science Information Network (CIESIN): Gridded Population of the World, Version 4  
 5408 (GPWv4): Population Count, Revision 11 [Data set]. NASA Socioeconomic Data and Applications  
 5409 Center (SEDAC), available at:  
 5410 <https://www.earthdata.nasa.gov/data/catalog/esdis-ciesin-sedac-gpwv4-popcount-r11-4.11> (last access:  
 5411 6th August 2025), 2025.
- 5412 Centro de Coordenação Regional Centro: Inventariação e valorização de danos e perdas decorrentes dos  
 5413 incêndios rurais em 2024, 2024.
- 5414 Centro Pinus: Impacto económico dos incêndios de 2024 na Fileira do Pinho,  
 5415 <https://www.centropinus.org/files/upload/noticias/relatorio-centropinus-impacto-incendios-2024-fileira-pin>  
 5416 ho.pdf (last access: 6th August 2025), 2024.
- 5417 Ceppi, P. and Nowack, P.: Observational evidence that cloud feedback amplifies global warming, Proceedings of  
 5418 the National Academy of Sciences, 118, e2026290118, <https://doi.org/10.1073/pnas.2026290118>, 2021.
- 5419 Chakraborty, R. and Menghal, P. S.: Equatorial African Lightning: Past. Present and Future,  
 5420 <https://doi.org/10.48550/arXiv.2505.00392>, 2025.
- 5421 Chen, B., Wu, S., Jin, Y., Song, Y., Wu, C., Venevsky, S., Xu, B., Webster, C., and Gong, P.: Wildfire risk for  
 5422 global wildland–urban interface areas, Nat Sustain, 7, 474–484,  
 5423 <https://doi.org/10.1038/s41893-024-01291-0>, 2024.
- 5424 Chen, G., Guo, Y., Yue, X., Tong, S., Gasparrini, A., Bell, M. L., Armstrong, B., Schwartz, J., Jaakkola, J. J. K.,  
 5425 Zanobetti, A., Lavigne, E., Saldiva, P. H. N., Kan, H., Royé, D., Milojevic, A., Overcenco, A., Urban, A.,  
 5426 Schneider, A., Entezari, A., Vicedo-Cabrera, A. M., Zeka, A., Tobias, A., Nunes, B., Alahmad, B.,  
 5427 Forsberg, B., Pan, S.-C., Íñiguez, C., Ameling, C., Valencia, C. D. la C., Åström, C., Houthuijs, D., Dung,  
 5428 D. V., Samoli, E., Mayvaneh, F., Sera, F., Carrasco-Escobar, G., Lei, Y., Orru, H., Kim, H., Holobaca,  
 5429 I.-H., Kyselý, J., Teixeira, J. P., Madureira, J., Katsouyanni, K., Hurtado-Díaz, M., Maasikmets, M.,  
 5430 Ragettli, M. S., Hashizume, M., Stafoggia, M., Pascal, M., Scortichini, M., Coêlho, M. de S. Z. S.,  
 5431 Ortega, N. V., Rytí, N. R. I., Scovronick, N., Matus, P., Goodman, P., Garland, R. M., Abrutsky, R.,  
 5432 Garcia, S. O., Rao, S., Fratianni, S., Dang, T. N., Colistro, V., Huber, V., Lee, W., Seposo, X., Honda, Y.,  
 5433 Guo, Y. L., Ye, T., Yu, W., Abramson, M. J., Samet, J. M., and Li, S.: Mortality risk attributable to  
 5434 wildfire-related PM2.5 pollution: a global time series study in 749 locations, The Lancet Planetary  
 5435 Health, 5, e579–e587, [https://doi.org/10.1016/S2542-5196\(21\)00200-X](https://doi.org/10.1016/S2542-5196(21)00200-X), 2021.
- 5436 Chen, T. and Guestrin, C.: XGBoost: A Scalable Tree Boosting System, in: Proceedings of the 22nd ACM  
 5437 SIGKDD International Conference on Knowledge Discovery and Data Mining, New York, NY, USA,  
 5438 785–794, <https://doi.org/10.1145/2939672.2939785>, 2016.
- 5439 Chen, Y., Morton, D. C., Andela, N., van der Werf, G. R., Giglio, L., and Randerson, J. T.: A pan-tropical cascade  
 5440 of fire driven by El Niño/Southern Oscillation, Nature Clim Change, 7, 906–911,  
 5441 <https://doi.org/10.1038/s41558-017-0014-8>, 2017.



- 5442 Chen, Y., Hantson, S., Andela, N., Coffield, S. R., Graff, C. A., Morton, D. C., Ott, L. E., Fofoula-Georgiou, E.,  
 5443 Smyth, P., Goulden, M. L., and Randerson, J. T.: California wildfire spread derived using VIIRS satellite  
 5444 observations and an object-based tracking system, *Sci Data*, 9, 249,  
 5445 <https://doi.org/10.1038/s41597-022-01343-0>, 2022.
- 5446 Chen, Y., Hall, J., van Wees, D., Andela, N., Hantson, S., Giglio, L., van der Werf, G. R., Morton, D. C., and  
 5447 Randerson, J. T.: Multi-decadal trends and variability in burned area from the fifth version of the Global  
 5448 Fire Emissions Database (GFED5), *Earth System Science Data*, 15, 5227–5259,  
 5449 <https://doi.org/10.5194/essd-15-5227-2023>, 2023.
- 5450 Christidis, N., Stott, P. A., Scaife, A. A., Arribas, A., Jones, G. S., Copsey, D., Knight, J. R., and Tennant, W. J.: A  
 5451 New HadGEM3-A-Based System for Attribution of Weather- and Climate-Related Extreme Events,  
 5452 *Journal of Climate*, 26, 2756–2783, <https://doi.org/10.1175/JCLI-D-12-00169.1>, 2013.
- 5453 Chu, L., Grafton, R. Q., and Nelson, H.: Accounting for forest fire risks: global insights for climate change  
 5454 mitigation, *Mitig Adapt Strateg Glob Change*, 28, 48, <https://doi.org/10.1007/s11027-023-10087-0>, 2023.
- 5455 Chuvieco, E., Mouillot, F., van der Werf, G. R., San Miguel, J., Tanase, M., Koutsias, N., García, M., Yebra, M.,  
 5456 Padilla, M., Gitas, I., Heil, A., Hawbaker, T. J., and Giglio, L.: Historical background and current  
 5457 developments for mapping burned area from satellite Earth observation, *Remote Sensing of*  
 5458 *Environment*, 225, 45–64, <https://doi.org/10.1016/j.rse.2019.02.013>, 2019.
- 5459 Chuvieco, E., Roteta, E., Sali, M., Stroppiana, D., Boettcher, M., Kirches, G., Storm, T., Khairoun, A., Pettinari, M.  
 5460 L., Franquesa, M., and Albergel, C.: Building a small fire database for Sub-Saharan Africa from  
 5461 Sentinel-2 high-resolution images, *Science of The Total Environment*, 845, 157139,  
 5462 <https://doi.org/10.1016/j.scitotenv.2022.157139>, 2022.
- 5463 Chuvieco, E., Yebra, M., Martino, S., Thonicke, K., Gómez-Giménez, M., San-Miguel, J., Oom, D., Velea, R.,  
 5464 Mouillot, F., Molina, J. R., Miranda, A. I., Lopes, D., Salis, M., Bugaric, M., Sofiev, M., Kadantsev, E.,  
 5465 Gitas, I. Z., Stavrakoudis, D., Eftychidis, G., Bar-Massada, A., Neidermeier, A., Pampanoni, V., Pettinari,  
 5466 M. L., Arrogante-Funes, F., Ochoa, C., Moreira, B., and Viegas, D.: Towards an Integrated Approach to  
 5467 Wildfire Risk Assessment: When, Where, What and How May the Landscapes Burn, *Fire*, 6, 215,  
 5468 <https://doi.org/10.3390/fire6050215>, 2023.
- 5469 Ciais, P., Bastos, A., Chevallier, F., Lauerwald, R., Poulter, B., Canadell, J. G., Hugelius, G., Jackson, R. B., Jain,  
 5470 A., Jones, M., Kondo, M., Lujckx, I. T., Patra, P. K., Peters, W., Pongratz, J., Petrescu, A. M. R., Piao, S.,  
 5471 Qiu, C., Von Randow, C., Regnier, P., Saunio, M., Scholes, R., Shvidenko, A., Tian, H., Yang, H.,  
 5472 Wang, X., and Zheng, B.: Definitions and methods to estimate regional land carbon fluxes for the  
 5473 second phase of the REgional Carbon Cycle Assessment and Processes Project (RECCAP-2),  
 5474 *Geoscientific Model Development*, 15, 1289–1316, <https://doi.org/10.5194/gmd-15-1289-2022>, 2022.
- 5475 Ciavarella, A., Christidis, N., Andrews, M., Groenendijk, M., Rostron, J., Elkington, M., Burke, C., Lott, F. C., and  
 5476 Stott, P. A.: Upgrade of the HadGEM3-A based attribution system to high resolution and a new  
 5477 validation framework for probabilistic event attribution, *Weather and Climate Extremes*, 20, 9–32,  
 5478 <https://doi.org/10.1016/j.wace.2018.03.003>, 2018.
- 5479 Ciudad CCS: Venezuela combate incendios forestales sin precedentes, <https://ciudadccs.info/publicacion/16957>  
 5480 (last access: 6th August 2025), 2024.
- 5481 CNM: Boletim de outubro 2024: Situação de emergência municipal por incêndios florestais Confederação  
 5482 Nacional de Municípios,



- 5483 [https://cnm.org.br/storage/biblioteca/2024/Boletins/202410\\_BOL\\_DEF\\_outubro\\_2024.pdf](https://cnm.org.br/storage/biblioteca/2024/Boletins/202410_BOL_DEF_outubro_2024.pdf) (last access  
 5484 date: 6th August 2025), 2024.
- 5485 Collins, L., Clarke, H., Clarke, M. F., McColl Gausden, S. C., Nolan, R. H., Penman, T., and Bradstock, R.:  
 5486 Warmer and drier conditions have increased the potential for large and severe fire seasons across  
 5487 south-eastern Australia, *Global Ecology and Biogeography*, 31, 1933–1948,  
 5488 <https://doi.org/10.1111/geb.13514>, 2022.
- 5489 Comisión Nacional Forestal: Cierre Estadístico 2024: Coordinación General de Conservación y Restauración  
 5490 Gerencia de Manejo del Fuego 01 de enero al 31 de diciembre de 2024, available at:  
 5491 <https://www.gob.mx/conafor/documentos/reporte-semanal-de-incendios> (last access: 6th August 2025),  
 5492 2025.
- 5493 Comité National de Défense de la Forêt et de lutte contre les feux de Brousse (CNDFB): Rapport 2024 et  
 5494 mi-2025, available at:  
 5495 [https://afriksoir.net/feux-de-brousse-en-cote-divoire-de-janvier-a-avril-2025-le-bilan-de-4-mois-est-sans-](https://afriksoir.net/feux-de-brousse-en-cote-divoire-de-janvier-a-avril-2025-le-bilan-de-4-mois-est-sans-appel/#~:text=Pour%20cette%20ann%C3%A9e%202025%20,%20au,feux%20de%20brousse%20dres s%20C3%A9%20par)  
 5496 [appel/#~:text=Pour%20cette%20ann%C3%A9e%202025%20,%20au,feux%20de%20brousse%20dres](https://afriksoir.net/feux-de-brousse-en-cote-divoire-de-janvier-a-avril-2025-le-bilan-de-4-mois-est-sans-appel/#~:text=Pour%20cette%20ann%C3%A9e%202025%20,%20au,feux%20de%20brousse%20dres s%20C3%A9%20par)  
 5497 [s%20C3%A9%20par](https://afriksoir.net/feux-de-brousse-en-cote-divoire-de-janvier-a-avril-2025-le-bilan-de-4-mois-est-sans-appel/#~:text=Pour%20cette%20ann%C3%A9e%202025%20,%20au,feux%20de%20brousse%20dres s%20C3%A9%20par) (last access: 6th August 2025), 2024.
- 5498 Conte, M. N. and Kotchen, M. J.: EXPLAINING THE PRICE OF VOLUNTARY CARBON OFFSETS, *Clim.*  
 5499 *Change Econ.*, 01, 93–111, <https://doi.org/10.1142/s2010007810000091>, 2010.
- 5500 Coop, J. D., Parks, S. A., Stevens-Rumann, C. S., Crausbay, S. D., Higuera, P. E., Hurteau, M. D., Tepley, A.,  
 5501 Whitman, E., Assal, T., Collins, B. M., Davis, K. T., Dobrowski, S., Falk, D. A., Fornwalt, P. J., Fulé, P. Z.,  
 5502 Harvey, B. J., Kane, V. R., Littlefield, C. E., Margolis, E. Q., North, M., Parisien, M.-A., Prichard, S., and  
 5503 Rodman, K. C.: Wildfire-Driven Forest Conversion in Western North American Landscapes, *BioScience*,  
 5504 70, 659–673, <https://doi.org/10.1093/biosci/biaa061>, 2020.
- 5505 Copernicus: Canada wildfire season begins with major British Columbia blaze (last access: 6th August 2025),  
 5506 2024.
- 5507 Copernicus Atmospheric Monitoring Services (CAMS): CAMS global system tracks exceptional air pollution  
 5508 episode in South Asia, available at:  
 5509 <https://atmosphere.copernicus.eu/cams-global-system-tracks-exceptional-air-pollution-episode-south-asia>  
 5510 (last access: 6th August 2025), 2024.
- 5511 Copernicus Climate Change Service: ERA5-Land hourly data from 1950 to present [Data set],  
 5512 <https://doi.org/10.24381/CDS.E2161BAC>, 2019.
- 5513 Copernicus Climate Change Service (C3S): Surface air temperature for May 2025, available at:  
 5514 <https://climate.copernicus.eu/surface-air-temperature-may-2025> (last access: 6th August 2025), 2025.
- 5515 Copernicus Emergency Management Service: Copernicus EMS Fire danger indices historical data from the  
 5516 Copernicus Emergency Management Service, Copernicus Climate Change Service (C3S) Climate Data  
 5517 Store (CDS) [data set], <https://doi.org/10.24381/cds.0e89c522>, 2019.
- 5518 Copernicus Emergency Management Service: Seasonal forecast of fire danger indices from the Copernicus  
 5519 Emergency Management Service [Data set], <https://doi.org/10.24381/CDS.B9C753F1>, 2025.
- 5520 County of Los Angeles Medical Examiner: WILDFIRES UPDATE | 30th Death Related to the January Wildfires  
 5521 Confirmed (last access: 6th August 2025), 2025.



- 5522 Croker, A. R., Woods, J., and Kountouris, Y.: Community-Based Fire Management in East and Southern African  
 5523 Savanna-Protected Areas: A Review of the Published Evidence, *Earth's Future*, 11, e2023EF003552,  
 5524 <https://doi.org/10.1029/2023EF003552>, 2023.
- 5525 Csiszar, I., Schroeder, W., Giglio, L., Ellicott, E., Vadrevu, K. P., Justice, C. O., and Wind, B.: Active fires from the  
 5526 Suomi NPP Visible Infrared Imaging Radiometer Suite: Product status and first evaluation results,  
 5527 *Journal of Geophysical Research: Atmospheres*, 119(2), 803–816,  
 5528 <https://doi.org/10.1002/2013JD020453>, 2014.
- 5529 Cunningham, C., Abatzoglou, J., Kolden, C., Williamson, G. J., Steuer, M., and Bowman, D.: Climate-linked  
 5530 escalation of societally disastrous wildfires [preprint], 2024b, <https://doi.org/10.32942/X22622>, 18  
 5531 October 2024a.
- 5532 Cunningham, C. X., Williamson, G. J., and Bowman, D. M. J. S.: Increasing frequency and intensity of the most  
 5533 extreme wildfires on Earth, *Nat Ecol Evol*, 1–6, <https://doi.org/10.1038/s41559-024-02452-2>, 2024b.
- 5534 Cunningham, C. X., Williamson, G. J., Nolan, R. H., Teckentrup, L., Boer, M. M., and Bowman, D. M. J. S.:  
 5535 Pyrogeography in flux: Reorganization of Australian fire regimes in a hotter world, *Global Change*  
 5536 *Biology*, 30, e17130, <https://doi.org/10.1111/gcb.17130>, 2024c.
- 5537 Cunningham, D., Cunningham, P., and Fagan, M. E.: Evaluating Forest Cover and Fragmentation in Costa Rica  
 5538 with a Corrected Global Tree Cover Map, *Remote Sensing*, 12, 3226,  
 5539 <https://doi.org/10.3390/rs12193226>, 2020.
- 5540 Daeli, W., Carmenta, R., Monroe, M. C., and Adams, A. E.: Where Policy and Culture Collide: Perceptions and  
 5541 Responses of Swidden Farmers to the Burn Ban in West Kalimantan, Indonesia, *Hum Ecol*, 49,  
 5542 159–170, <https://doi.org/10.1007/s10745-021-00227-y>, 2021.
- 5543 Dalton, R., Bury, L., Robertson, F., and Perkins, R.: LA wildfire insured loss estimates creep to \$40bn+  
 5544 [https://www.insuranceinsider.com/article/2efppeico48uc4c23xts/all-topics/catastrophe-losses/la-wildfire-i](https://www.insuranceinsider.com/article/2efppeico48uc4c23xts/all-topics/catastrophe-losses/la-wildfire-insured-loss-estimates-creep-to-40bn?zephrr_sso_ott=MpvfKs)  
 5545 [nsured-loss-estimates-creep-to-40bn?zephrr\\_sso\\_ott=MpvfKs](https://www.insuranceinsider.com/article/2efppeico48uc4c23xts/all-topics/catastrophe-losses/la-wildfire-insured-loss-estimates-creep-to-40bn?zephrr_sso_ott=MpvfKs) (last access: 6th August 2025), 2025.
- 5546 Damasceno-Junior, G. A., Pereira, A. de M. M., Oldeland, J., Parolin, P., and Pott, A.: Fire, Flood and Pantanal  
 5547 Vegetation, in: *Flora and Vegetation of the Pantanal Wetland*, edited by: Damasceno-Junior, G. A. and  
 5548 Pott, A., Springer International Publishing, Cham, 661–688,  
 5549 [https://doi.org/10.1007/978-3-030-83375-6\\_18](https://doi.org/10.1007/978-3-030-83375-6_18), 2021.
- 5550 Deber, E.: En 2024 se quemaron 14 millones de hectáreas en el país; más de la mitad en bosque  
 5551 [https://eldeber.com.bo/pais/en-2024-se-quemaron-14-millones-de-ha-en-el-pais-mas-de-la-mitad-en-bos](https://eldeber.com.bo/pais/en-2024-se-quemaron-14-millones-de-ha-en-el-pais-mas-de-la-mitad-en-bosque_501689)  
 5552 [que\\_501689](https://eldeber.com.bo/pais/en-2024-se-quemaron-14-millones-de-ha-en-el-pais-mas-de-la-mitad-en-bosque_501689) (last access: 6th August 2025), 2025.
- 5553 Deeming, J. E., Burgan, R. E., and Cohen, J. D.: The National Fire-Danger Rating System - 1978, Gen. Tech.  
 5554 Rep. INT-GTR-39. Ogden, UT: U.S. Department of Agriculture, Forest Service, Intermountain Forest and  
 5555 Range Experiment Station. 63 p., 39, 1977.
- 5556 Delforge, D., Wathelet, V., Below, R., Sofia, C. L., Tonnelier, M., van Loenhout, J. A. F., and Speybroeck, N.:  
 5557 EM-DAT: the Emergency Events Database, *International Journal of Disaster Risk Reduction*, 124,  
 5558 105509, <https://doi.org/10.1016/j.ijdrr.2025.105509>, 2025.
- 5559 Deutsche Welle: Germany: Hundreds evacuated due to Harz Mountains fire (last access date: 6th August 2025),  
 5560 [dw.com](https://www.dw.com), 2024.



- 5561 Di Giuseppe, F.: Accounting for fuel in fire danger forecasts: the fire occurrence probability index (FOPI), Environ.  
 5562 Res. Lett., 18, 064029, <https://doi.org/10.1088/1748-9326/acd2ee>, 2023.
- 5563 Di Giuseppe, F., Pappenberger, F., Wetterhall, F., Krzeminski, B., Camia, A., Libertá, G., and San Miguel, J.: The  
 5564 Potential Predictability of Fire Danger Provided by Numerical Weather Prediction, J. Appl. Meteorol.  
 5565 Clim., 55, 2469–2491, <https://doi.org/10.1175/JAMC-D-15-0297.1>, 2016.
- 5566 Di Giuseppe, F., Vitolo, C., Krzeminski, B., Barnard, C., Maciel, P., and San-Miguel, J.: Fire Weather Index: the  
 5567 skill provided by the European Centre for Medium-Range Weather Forecasts ensemble prediction  
 5568 system, Natural Hazards and Earth System Sciences, 20, 2365–2378,  
 5569 <https://doi.org/10.5194/nhess-20-2365-2020>, 2020.
- 5570 Di Giuseppe, F., Benedetti, A., Coughlan, R., Vitolo, C., and Vuckovic, M.: A Global Bottom-Up Approach to  
 5571 Estimate Fuel Consumed by Fires Using Above Ground Biomass Observations, Geophysical Research  
 5572 Letters, 48, e2021GL095452, <https://doi.org/10.1029/2021GL095452>, 2021.
- 5573 Di Giuseppe, F., Vitolo, C., Barnard, C., Libertá, G., Maciel, P., San-Miguel-Ayanz, J., Villaume, S., and  
 5574 Wetterhall, F.: Global seasonal prediction of fire danger, Sci Data, 11, 128,  
 5575 <https://doi.org/10.1038/s41597-024-02948-3>, 2024.
- 5576 Di Giuseppe, F., McNorton, J., Lombardi, A., and Wetterhall, F.: Global data-driven prediction of fire activity, Nat  
 5577 Commun, 16, 2918, <https://doi.org/10.1038/s41467-025-58097-7>, 2025.
- 5578 DiMiceli, C., Carroll, M., Sohlberg, R., Kim, D.-H., Kelly, M., and Townshend, J.: MOD44B MODIS/Terra  
 5579 Vegetation Continuous Fields Yearly L3 Global 250m SIN Grid V006, NASA EOSDIS Land Processes  
 5580 Distributed Active Archive Center [data set], <https://doi.org/10.5067/MODIS/MOD44B.006>, 2015.
- 5581 DiMiceli, C., Carroll, M., Sohlberg, R., Huang, C., Hansen, M., and Townshend, J.: Annual Global Automated  
 5582 MODIS Vegetation Continuous Fields (MOD44B) at 250 m Spatial Resolution for Data Years Beginning  
 5583 Day 65, 2000-2010, Collection 5 Percent Tree Cover, University of Maryland, 2017.
- 5584 DiMiceli, C., Sohlberg, R., and Townshend, J.: MODIS/Terra Vegetation Continuous Fields Yearly L3 Global 250m  
 5585 SIN Grid V061, NASA EOSDIS Land Processes Distributed Active Archive Center [data set],  
 5586 <https://doi.org/10.5067/MODIS/MOD44B.061>, 2022.
- 5587 Ding, R.: Let it burn: Why China is looking the other way on farm fires, Sixth Tone,  
 5588 <https://www.sixthtone.com/news/1016586> (last access: 6th August 2025), 2025.
- 5589 Dong, X., Li, F., Lin, Z., Harrison, S. P., Chen, Y., and Kug, J.-S.: Climate influence on the 2019 fires in Amazonia,  
 5590 Science of The Total Environment, 794, 148718, <https://doi.org/10.1016/j.scitotenv.2021.148718>, 2021.
- 5591 Dou, C., Tang, Y., Jiang, N., Yan, L., and Ding, H.: Analysis of Sichuan wildfire based on the first synergetic  
 5592 observation from three payloads of SDGSAT-1, The Innovation, 5, 100707,  
 5593 <https://doi.org/10.1016/j.xinn.2024.100707>, 2024.
- 5594 Douffi, K. G., Yao, A. C., Koffi, K. J., Traore, A. S., and Kone, M.: Afforestation in Response to Thermal Change  
 5595 in the Forest-Savannah Transition of the Lamto Scientific Reserve, Côte d'Ivoire, Eur J Forest Eng, 7,  
 5596 45–56, <https://doi.org/10.33904/ejfe.978520>, 2021.
- 5597 Dowdy, A. and Brown, A.: Broadscale thunderstorm environment dataset intended for climate analysis, Front.  
 5598 Clim., 7, <https://doi.org/10.3389/fclim.2025.1539873>, 2025.



- 5599 Dowdy, A. J.: Seamless climate change projections and seasonal predictions for bushfires in Australia, *J. South.*  
 5600 *Hemisph. Earth Syst. Sci.*, 70, 120–138, <https://doi.org/10.1071/ES20001>, 2020.
- 5601 Doxsey-Whitfield, E., MacManus, K., Adamo, S., Pistolesi, L., Squires, J., Borkovska, O., and Baptista, S. R.: Taking Advantage of the Improved Availability of Census Data: A First Look at  
 5602 the Gridded Population of the World, Version 4, *Papers in Applied Geography*, 1, 226–234,  
 5603 <https://doi.org/10.1080/23754931.2015.1014272>, 2015.
- 5605 Driscoll, D. A., Macdonald, K. J., Gibson, R. K., Doherty, T. S., Nimmo, D. G., Nolan, R. H., Ritchie, E. G.,  
 5606 Williamson, G. J., Heard, G. W., Tasker, E. M., Bilney, R., Porch, N., Collett, R. A., Crates, R. A., Hewitt,  
 5607 A. C., Pendall, E., Boer, M. M., Gates, J., Boulton, R. L., Mclean, C. M., Groffen, H., Maisey, A. C.,  
 5608 Beranek, C. T., Ryan, S. A., Callen, A., Hamer, A. J., Stauber, A., Daly, G. J., Gould, J., Klop-Toker, K.  
 5609 L., Mahony, M. J., Kelly, O. W., Wallace, S. L., Stock, S. E., Weston, C. J., Volkova, L., Black, D., Gibb,  
 5610 H., Grubb, J. J., McGeoch, M. A., Murphy, N. P., Lee, J. S., Dickman, C. R., Neldner, V. J., Ngugi, M. R.,  
 5611 Miritis, V., Köhler, F., Perri, M., Denham, A. J., Mackenzie, B. D. E., Reid, C. A. M., Rayment, J. T.,  
 5612 Arriaga-Jiménez, A., Hewins, M. W., Hicks, A., Melbourne, B. A., Davies, K. F., Bitters, M. E., Linley, G.  
 5613 D., Greenville, A. C., Webb, J. K., Roberts, B., Letnic, M., Price, O. F., Walker, Z. C., Murray, B. R.,  
 5614 Verhoeven, E. M., Thomsen, A. M., Keith, D., Lemmon, J. S., Ooi, M. K. J., Allen, V. L., Decker, O. T.,  
 5615 Green, P. T., Moussalli, A., Foon, J. K., Bryant, D. B., Walker, K. L., Bruce, M. J., Madani, G., Tschärke,  
 5616 J. L., Wagner, B., Nitschke, C. R., Gosper, C. R., Yates, C. J., Dillon, R., Barrett, S., Spencer, E. E.,  
 5617 Wardle, G. M., Newsome, T. M., Pulsford, S. A., Singh, A., Roff, A., Marsh, K. J., McDonald, K., Howell,  
 5618 L. G., Lane, M. R., Cristescu, R. H., Witt, R. R., et al.: Biodiversity impacts of the 2019–2020 Australian  
 5619 megafires, *Nature*, 635, 898–905, <https://doi.org/10.1038/s41586-024-08174-6>, 2024.
- 5620 Earth.org: Drought Baking the Southern United States, available at:  
 5621 <https://www.climate.gov/news-features/features/drought-baking-southern-united-states> (last access: 6th  
 5622 August 2025), 2011.
- 5623 Eberenz, S., Stocker, D., Rösli, T., and Bresch, D. N.: Asset exposure data for global physical risk assessment,  
 5624 *Earth System Science Data*, 12, 817–833, <https://doi.org/10.5194/essd-12-817-2020>, 2020.
- 5625 ECMWF: Observation and ERA5-Land derived 9 km global daily fire fuel characteristics since 2003 [Data set],  
 5626 <https://doi.org/10.24381/378D1497>, 2025.
- 5627 Eden, J. M., Wolter, K., Otto, F. E. L., and Jan Van Oldenborgh, G.: Multi-method attribution analysis of extreme  
 5628 precipitation in Boulder, Colorado, *Environ. Res. Lett.*, 11, 124009,  
 5629 <https://doi.org/10.1088/1748-9326/11/12/124009>, 2016.
- 5630 Eden, J. M., Kew, S. F., Bellprat, O., Lenderink, G., Manola, I., Omrani, H., and Van Oldenborgh, G. J.: Extreme  
 5631 precipitation in the Netherlands: An event attribution case study, *Weather and Climate Extremes*, 21,  
 5632 90–101, <https://doi.org/10.1016/j.wace.2018.07.003>, 2018.
- 5633 Efron, B. and Tibshirani, R.: The problem of regions, *Ann. Statist.*, 26, <https://doi.org/10.1214/aos/1024691353>,  
 5634 1998.
- 5635 Eschenbacher, S.: Brazil's Amazon rainforest fires in August reach 14-year high, available at:  
 5636 [https://www.reuters.com/world/americas/brazils-amazon-rainforest-fires-august-reach-14-year-high-2024](https://www.reuters.com/world/americas/brazils-amazon-rainforest-fires-august-reach-14-year-high-2024-09-01/)  
 5637 -09-01/ (last access: 6th August 2025), 2024.
- 5638 Espinoza, J.-C., Jimenez, J. C., Marengo, J. A., Schongart, J., Ronchail, J., Lavado-Casimiro, W., and Ribeiro, J.  
 5639 V. M.: The new record of drought and warmth in the Amazon in 2023 related to regional and global  
 5640 climatic features, *Sci Rep*, 14, 8107, <https://doi.org/10.1038/s41598-024-58782-5>, 2024.





- 5641 Euronews: At least 20 wildfires burn across parts of North Macedonia's south,  
 5642 <https://www.euronews.com/my-europe/2024/07/20/battle-against-flames-ongoing-in-north-macedonia-wi>  
 5643 [th-international-support](https://www.euronews.com/my-europe/2024/07/20/battle-against-flames-ongoing-in-north-macedonia-wi) (last access: 6th August 2025), euronews, 2024.
- 5644 European Civil Protection and Humanitarian Aid Operations: European Civil Protection and Humanitarian Aid  
 5645 Operations (last access: 6th August 2025), 2024.
- 5646 European Commission Emergency Response Coordination Centre: Maps, available at:  
 5647 <https://ercportal.jrc.ec.europa.eu/ECHO-Products/Maps#/maps/latest> (last access date: 6th August  
 5648 2025), 2025.
- 5649 European Commission Joint Research Centre: Forest fires in Europe, Middle East and North Africa 2022  
 5650 [JRC135226], Publications Office of the European Union, Luxembourg, <https://doi.org/10.2760/348120>,  
 5651 2023.
- 5652 European Commission Joint Research Centre: Forest fires in Europe, Middle East and North Africa 2023  
 5653 [JRC139704], Publications Office of the European Union, Luxembourg, <https://doi.org/10.2760/8027062>,  
 5654 2024.
- 5655 European Commission Joint Research Centre: Drought over large parts of Europe raises concern, available at:  
 5656 [https://joint-research-centre.ec.europa.eu/jrc-news-and-updates/drought-over-large-parts-europe-raises-](https://joint-research-centre.ec.europa.eu/jrc-news-and-updates/drought-over-large-parts-europe-raises-concern-2025-05-05_en)  
 5657 [concern-2025-05-05\\_en](https://joint-research-centre.ec.europa.eu/jrc-news-and-updates/drought-over-large-parts-europe-raises-concern-2025-05-05_en) (last access: 6th August 2025), 2025.
- 5658 European Forest Fire Information System: <https://forest-fire.emergency.copernicus.eu/> (last access: 6th August  
 5659 2025), 2024.
- 5660 Fang, T., Hwang, B. C. H., Kapur, S., Hopstock, K. S., Wei, J., Nguyen, V., Nizkorodov, S. A., and Shiraiwa, M.:  
 5661 Wildfire particulate matter as a source of environmentally persistent free radicals and reactive oxygen  
 5662 species, *Environ. Sci.: Atmos.*, 3, 581–594, <https://doi.org/10.1039/D2EA00170E>, 2023.
- 5663 Faranda, D., Alvarez-Castro, M. C., Alberti, T., and Cazzaniga, G.: March 2025 Japan and South Korea wildfires  
 5664 have been fueled by meteorological conditions likely strengthened by human-driven climate change.  
 5665 *ClimaMeter*, Institut Pierre Simon Laplace, CNRS, available at:  
 5666 <https://doi.org/10.5281/zenodo.15083384> (last access: 6th August 2025), 2025.
- 5667 Fearnside, P. M.: Amazon environmental services: Why Brazil's Highway BR-319 is so damaging, *Ambio*, 51,  
 5668 1367–1370, <https://doi.org/10.1007/s13280-022-01718-y>, 2022.
- 5669 Feng, M., Sexton, J. O., Huang, C., Anand, A., Channan, S., Song, X.-P., Song, D.-X., Kim, D.-H., Noojipady, P.,  
 5670 and Townshend, J. R.: Earth science data records of global forest cover and change: Assessment of  
 5671 accuracy in 1990, 2000, and 2005 epochs, *Remote Sensing of Environment*, 184, 73–85,  
 5672 <https://doi.org/10.1016/j.rse.2016.06.012>, 2016.
- 5673 Fernandes, P. M. and Botelho, H. S.: A review of prescribed burning effectiveness in fire hazard reduction, *Int. J.*  
 5674 *Wildland Fire*, 12, 117–128, <https://doi.org/10.1071/wf02042>, 2003.
- 5675 Feron, S., Cordero, R. R., Damiani, A., MacDonell, S., Pizarro, J., Goubanova, K., Valenzuela, R., Wang, C.,  
 5676 Rester, L., and Beaulieu, A.: South America is becoming warmer, drier, and more flammable, *Commun*  
 5677 *Earth Environ*, 5, 501, <https://doi.org/10.1038/s43247-024-01654-7>, 2024.



- 5678 Ferreira, N.: Corremos o risco de estar a fazer desaparecer espécies ainda não descritas, last access:  
 5679 <https://www.publico.pt/2024/08/20/azul/noticia/laurissilva-madeira-corremos-risco-estar-desaparecer-es>  
 5680 [pecies-nao-descritas-2101375](https://www.publico.pt/2024/08/20/azul/noticia/laurissilva-madeira-corremos-risco-estar-desaparecer-es) (last access: 6th August 2025), PÚBLICO, 2024.
- 5681 Field, R. D., van der Werf, G. R., Fanin, T., Fetzer, E. J., Fuller, R., Jethva, H., Levy, R., Livesey, N. J., Luo, M.,  
 5682 Torres, O., and Worden, H. M.: Indonesian fire activity and smoke pollution in 2015 show persistent  
 5683 nonlinear sensitivity to El Niño-induced drought, *Proceedings of the National Academy of Sciences*, 113,  
 5684 9204–9209, <https://doi.org/10.1073/pnas.1524888113>, 2016.
- 5685 Finney, D. L., Doherty, R. M., Wild, O., Stevenson, D. S., MacKenzie, I. A., and Blyth, A. M.: A projected  
 5686 decrease in lightning under climate change, *Nature Clim Change*, 8, 210–213,  
 5687 <https://doi.org/10.1038/s41558-018-0072-6>, 2018.
- 5688 Finney, M. A., Cohen, J. D., McAllister, S. S., and Jolly, W. M.: On the need for a theory of wildland fire spread,  
 5689 *Int. J. Wildland Fire*, 22, 25–36, <https://doi.org/10.1071/WF11117>, 2012.
- 5690 Fiore, A. M., Naik, V., Spracklen, D. K., Steiner, A., Unger, N., Prather, M., Bergmann, D., Cameron-Smith, P. J.,  
 5691 Cionni, I., Collins, W. J., Dalsøren, S., Eyring, V., Folberth, G. A., Ginoux, P., Horowitz, L. W., Josse, B.,  
 5692 Lamarque, J.-F., A. MacKenzie, I., Nagashima, T., O'Connor, F. M., Righi, M., Rumbold, S. T., Shindell,  
 5693 D. T., Skeie, R. B., Sudo, K., Szopa, S., Takemura, T., and Zeng, G.: Global air quality and climate,  
 5694 *Chemical Society Reviews*, 41, 6663–6683, <https://doi.org/10.1039/C2CS35095E>, 2012.
- 5695 Fire Hub - The Global Fire Management Hub: 1st Technical Workshop – Summary Report, FAO Headquarters,  
 5696 <https://openknowledge.fao.org/server/api/core/bitstreams/491e9112-8106-4b02-97f1-0a27f3e1f6d6/content>  
 5697 (last access: 6th August 2025), 2023.
- 5698 Flemming, J., Huijnen, V., Arteta, J., Bechtold, P., Beljaars, A., Blechschmidt, A.-M., Diamantakis, M., Engelen, R.  
 5699 J., Gaudel, A., Inness, A., Jones, L., Josse, B., Katragkou, E., Marecal, V., Peuch, V.-H., Richter, A.,  
 5700 Schultz, M. G., Stein, O., and Tsikerdekis, A.: Tropospheric chemistry in the Integrated Forecasting  
 5701 System of ECMWF, *Geoscientific Model Development*, 8, 975–1003,  
 5702 <https://doi.org/10.5194/gmd-8-975-2015>, 2015.
- 5703 Foley, J. A., DeFries, R., Asner, G. P., Barford, C., Bonan, G., Carpenter, S. R., Chapin, F. S., Coe, M. T., Daily,  
 5704 G. C., Gibbs, H. K., Helkowski, J. H., Holloway, T., Howard, E. A., Kucharik, C. J., Monfreda, C., Patz, J.  
 5705 A., Prentice, I. C., Ramankutty, N., and Snyder, P. K.: Global Consequences of Land Use, *Science*, 309,  
 5706 570–574, <https://doi.org/10.1126/science.1111772>, 2005.
- 5707 Fonseca Morello, T., Marchetti Ramos, R., O. Anderson, L., Owen, N., Rosan, T. M., and Steil, L.: Predicting fires  
 5708 for policy making: Improving accuracy of fire brigade allocation in the Brazilian Amazon, *Ecological*  
 5709 *Economics*, 169, 106501, <https://doi.org/10.1016/j.ecolecon.2019.106501>, 2020.
- 5710 Ford, A. E. S., Harrison, S. P., Kountouris, Y., Millington, J. D. A., Mistry, J., Perkins, O., Rabin, S. S., Rein, G.,  
 5711 Schreckenberger, K., Smith, C., Smith, T. E. L., and Yadav, K.: Modelling Human-Fire Interactions:  
 5712 Combining Alternative Perspectives and Approaches, *Frontiers in Environmental Science*, 9, 418,  
 5713 <https://doi.org/10.3389/fenvs.2021.649835>, 2021.
- 5714 Forster, P. M., Smith, C., Walsh, T., Lamb, W. F., Lamboll, R., Cassou, C., Hauser, M., Hausfather, Z., Lee, J.-Y.,  
 5715 Palmer, M. D., Von Schuckmann, K., Slangen, A. B. A., Szopa, S., Trewin, B., Yun, J., Gillett, N. P.,  
 5716 Jenkins, S., Matthews, H. D., Raghavan, K., Ribes, A., Rogelj, J., Rosen, D., Zhang, X., Allen, M.,  
 5717 Aleluia Reis, L., Andrew, R. M., Betts, R. A., Borger, A., Broersma, J. A., Burgess, S. N., Cheng, L.,  
 5718 Friedlingstein, P., Domingues, C. M., Gambarini, M., Gasser, T., Gütschow, J., Ishii, M., Kadow, C.,  
 5719 Kennedy, J., Killick, R. E., Krummel, P. B., Liné, A., Monselesan, D. P., Morice, C., Mühle, J., Naik, V.,



- 5720 Peters, G. P., Pirani, A., Pongratz, J., Minx, J. C., Rigby, M., Rohde, R., Savita, A., Seneviratne, S. I.,  
 5721 Thorne, P., Wells, C., Western, L. M., Van Der Werf, G. R., Wijffels, S. E., Masson-Delmotte, V., and  
 5722 Zhai, P.: Indicators of Global Climate Change 2024: annual update of key indicators of the state of the  
 5723 climate system and human influence, *Earth Syst. Sci. Data*, 17, 2641–2680,  
 5724 <https://doi.org/10.5194/essd-17-2641-2025>, 2025.
- 5725 Forsyth, T.: Public concerns about transboundary haze: A comparison of Indonesia, Singapore, and Malaysia,  
 5726 *Global Environmental Change*, 25, 76–86, <https://doi.org/10.1016/j.gloenvcha.2014.01.013>, 2014.
- 5727 Frazier, A. E. and Hemingway, B. L.: A Technical Review of Planet Smallsat Data: Practical Considerations for  
 5728 Processing and Using PlanetScope Imagery, *Remote Sensing*, 13, 3930,  
 5729 <https://doi.org/10.3390/rs13193930>, 2021.
- 5730 Friedlingstein, P., O'Sullivan, M., Jones, M. W., Andrew, R. M., Bakker, D. C. E., Hauck, J., Landschützer, P., Le  
 5731 Quéré, C., Luijkx, I. T., Peters, G. P., Peters, W., Pongratz, J., Schwingshackl, C., Sitch, S., Canadell, J.  
 5732 G., Ciais, P., Jackson, R. B., Alin, S. R., Anthoni, P., Barbero, L., Bates, N. R., Becker, M., Bellouin, N.,  
 5733 Decharme, B., Bopp, L., Brasika, I. B. M., Cadule, P., Chamberlain, M. A., Chandra, N., Chau, T.-T.-T.,  
 5734 Chevallier, F., Chini, L. P., Cronin, M., Dou, X., Enyo, K., Evans, W., Falk, S., Feely, R. A., Feng, L.,  
 5735 Ford, D. J., Gasser, T., Ghattas, J., Gkritzalis, T., Grassi, G., Gregor, L., Gruber, N., Gürses, Ö., Harris,  
 5736 I., Hefner, M., Heinke, J., Houghton, R. A., Hurtt, G. C., Iida, Y., Ilyina, T., Jacobson, A. R., Jain, A.,  
 5737 Jarníková, T., Jersild, A., Jiang, F., Jin, Z., Joos, F., Kato, E., Keeling, R. F., Kennedy, D., Klein  
 5738 Goldewijk, K., Knauer, J., Korsbakken, J. I., Körtzinger, A., Lan, X., Lefèvre, N., Li, H., Liu, J., Liu, Z.,  
 5739 Ma, L., Marland, G., Mayot, N., McGuire, P. C., McKinley, G. A., Meyer, G., Morgan, E. J., Munro, D. R.,  
 5740 Nakaoka, S.-I., Niwa, Y., O'Brien, K. M., Olsen, A., Omar, A. M., Ono, T., Paulsen, M., Pierrot, D.,  
 5741 Pocock, K., Poulter, B., Powis, C. M., Rehder, G., Resplandy, L., Robertson, E., Rödenbeck, C., Rosan,  
 5742 T. M., Schwinger, J., Séférian, R., et al.: Global Carbon Budget 2023, *Earth System Science Data*, 15,  
 5743 5301–5369, <https://doi.org/10.5194/essd-15-5301-2023>, 2023.
- 5744 Friedlingstein, P., O'Sullivan, M., Jones, M. W., Andrew, R. M., Hauck, J., Landschützer, P., Le Quéré, C., Li, H.,  
 5745 Luijkx, I. T., Olsen, A., Peters, G. P., Peters, W., Pongratz, J., Schwingshackl, C., Sitch, S., Canadell, J.  
 5746 G., Ciais, P., Jackson, R. B., Alin, S. R., Arnet, A., Arora, V., Bates, N. R., Becker, M., Bellouin, N.,  
 5747 Berghoff, C. F., Bittig, H. C., Bopp, L., Cadule, P., Campbell, K., Chamberlain, M. A., Chandra, N.,  
 5748 Chevallier, F., Chini, L. P., Colligan, T., Decayeux, J., Djeutchouang, L. M., Dou, X., Duran Rojas, C.,  
 5749 Enyo, K., Evans, W., Fay, A. R., Feely, R. A., Ford, D. J., Foster, A., Gasser, T., Gehlen, M., Gkritzalis,  
 5750 T., Grassi, G., Gregor, L., Gruber, N., Gürses, Ö., Harris, I., Hefner, M., Heinke, J., Hurtt, G. C., Iida, Y.,  
 5751 Ilyina, T., Jacobson, A. R., Jain, A. K., Jarníková, T., Jersild, A., Jiang, F., Jin, Z., Kato, E., Keeling, R. F.,  
 5752 Klein Goldewijk, K., Knauer, J., Korsbakken, J. I., Lan, X., Lauvset, S. K., Lefèvre, N., Liu, Z., Liu, J., Ma,  
 5753 L., Maksyutov, S., Marland, G., Mayot, N., McGuire, P. C., Metzl, N., Monacci, N. M., Morgan, E. J.,  
 5754 Nakaoka, S.-I., Neill, C., Niwa, Y., Nützel, T., Olivier, L., Ono, T., Palmer, P. I., Pierrot, D., Qin, Z.,  
 5755 Resplandy, L., Roobaert, A., Rosan, T. M., Rödenbeck, C., Schwinger, J., Smallman, T. L., Smith, S. M.,  
 5756 Sospedra-Alfonso, R., Steinhoff, T., et al.: Global Carbon Budget 2024, *Earth System Science Data*,  
 5757 17(3), 965–1039, <https://doi.org/10.5194/essd-17-965-2025>, 2025.
- 5758 Frieler, K., Volkholz, J., Lange, S., Schewe, J., Mengel, M., del Rocio Rivas López, M., Otto, C., Reyer, C. P. O.,  
 5759 Karger, D. N., Malle, J. T., Treu, S., Menz, C., Blanchard, J. L., Harrison, C. S., Petrik, C. M., Eddy, T. D.,  
 5760 Ortega-Cisneros, K., Novaglio, C., Rousseau, Y., Watson, R. A., Stock, C., Liu, X., Heneghan, R.,  
 5761 Tittensor, D., Maury, O., Büchner, M., Vogt, T., Wang, T., Sun, F., Sauer, I. J., Koch, J., Vanderkelen, I.,  
 5762 Jägermeyr, J., Müller, C., Rabin, S., Klar, J., Vega del Valle, I. D., Lasslop, G., Chadburn, S., Burke, E.,  
 5763 Gallego-Sala, A., Smith, N., Chang, J., Hantson, S., Burton, C., Gädeke, A., Li, F., Gosling, S. N., Müller  
 5764 Schmied, H., Hattermann, F., Wang, J., Yao, F., Hickler, T., Marcé, R., Pierson, D., Thiery, W.,  
 5765 Mercado-Bettín, D., Ladwig, R., Ayala-Zamora, A. I., Forrest, M., and Bechtold, M.: Scenario setup and



- 5766 forcing data for impact model evaluation and impact attribution within the third round of the  
5767 Inter-Sectoral Impact Model Intercomparison Project (ISIMIP3a), Geoscientific Model Development, 17,  
5768 1–51, <https://doi.org/10.5194/gmd-17-1-2024>, 2024.
- 5769 Frieler, K., Lange, S., Schewe, J., Mengel, M., Treu, S., Otto, C., Volkholz, J., Reyer, C. P. O., Heinicke, S.,  
5770 Jones, C., Blanchard, J. L., Harrison, C. S., Petrik, C. M., Eddy, T. D., Ortega-Cisneros, K., Novaglio, C.,  
5771 Heneghan, R., Tittensor, D. P., Maury, O., Büchner, M., Vogt, T., Quesada Chacón, D., Emanuel, K.,  
5772 Lee, C.-Y., Camargo, S. J., Jägermeyr, J., Rabin, S., Klar, J., Vega del Valle, I. D., Novak, L., Sauer, I. J.,  
5773 Lasslop, G., Chadburn, S., Burke, E., Gallego-Sala, A., Smith, N., Chang, J., Hantson, S., Burton, C.,  
5774 Gädeke, A., Li, F., Gosling, S. N., Müller Schmied, H., Hattermann, F., Hickler, T., Marcé, R., Pierson, D.,  
5775 Thiery, W., Mercado-Bettín, D., Ladwig, R., Ayala-Zamora, A. I., Forrest, M., Bechtold, M., Reinecke, R.,  
5776 de Graaf, I., Kaplan, J. O., Koch, A., and Lengaigne, M.: Scenario set-up and the new CMIP6-based  
5777 climate-related forcings provided within the third round of the Inter-Sectoral Model Intercomparison  
5778 Project (ISIMIP3b, group I and II) [preprint], <https://doi.org/10.5194/egusphere-2025-2103>, 2025.
- 5779 Frölicher, T. L. and Laufkötter, C.: Emerging risks from marine heat waves, Nat Commun, 9, 650,  
5780 <https://doi.org/10.1038/s41467-018-03163-6>, 2018.
- 5781 Fuller, D. O. and Murphy, K.: The ENSO-Fire Dynamic in Insular Southeast Asia, Climatic Change, 74, 435–455,  
5782 <https://doi.org/10.1007/s10584-006-0432-5>, 2006.
- 5783 Fundación Tierra: Reporte de incendios 2024, available at:  
5784 <https://www.ftierra.org/index.php/publicacion/documentos-de-trabajo/attachment/254/52> (last access:  
5785 6th August 2025), 2024.
- 5786 Fundación Tierra: Incendios forestales 2024 .Tras las huellas del fuego, available at:  
5787 <https://ftierra.org/index.php/publicacion/libro/258-incendios-forestales-2024-tras-las-huellas-del-fuego>  
5788 (last access: 6th August 2025), TIERRA, 2025.
- 5789 Fundo de Garantia de Crédito: Fundo de Garantia de Crédito, available at:  
5790 [https://www.fgc.gov.ao/noticia.aspx?id=5189&noticia=Secretario\\_de\\_Estado\\_considera\\_PDAC\\_como\\_a](https://www.fgc.gov.ao/noticia.aspx?id=5189&noticia=Secretario_de_Estado_considera_PDAC_como_a_lavanca_da_producao_agricola)  
5791 [lavanca\\_da\\_producao\\_agricola](https://www.fgc.gov.ao/noticia.aspx?id=5189&noticia=Secretario_de_Estado_considera_PDAC_como_a_lavanca_da_producao_agricola) (last access: 6th August 2025), 2024.
- 5792 Fuzzi, S., Baltensperger, U., Carslaw, K., Decesari, S., Denier van der Gon, H., Facchini, M. C., Fowler, D.,  
5793 Koren, I., Langford, B., Lohmann, U., Nemitz, E., Pandis, S., Riipinen, I., Rudich, Y., Schaap, M., Slowik,  
5794 J. G., Spracklen, D. V., Vignati, E., Wild, M., Williams, M., and Gilardoni, S.: Particulate matter, air  
5795 quality and climate: lessons learned and future needs, Atmospheric Chemistry and Physics, 15,  
5796 8217–8299, <https://doi.org/10.5194/acp-15-8217-2015>, 2015.
- 5797 Gabriel, H.: Algeria extinguishes 26 fires in past 24 hours, available at:  
5798 <https://www.aa.com.tr/en/africa/algeria-extinguishes-26-fires-in-past-24-hours/3282209> (last access: 6th  
5799 August 2025), Anadolu Ajansi, 2024.
- 5800 Garcin, Y., Schefuß, E., Dargie, G. C., Hawthorne, D., Lawson, I. T., Sebag, D., Biddulph, G. E., Crezee, B.,  
5801 Bocko, Y. E., Ifo, S. A., Mampouya Wenina, Y. E., Mbemba, M., Ewango, C. E. N., Emba, O., Bola, P.,  
5802 Kanyama Tabu, J., Tyrrell, G., Young, D. M., Gassier, G., Girkin, N. T., Vane, C. H., Adatte, T., Baird, A.  
5803 J., Boom, A., Gulliver, P., Morris, P. J., Page, S. E., Sjögersten, S., and Lewis, S. L.: Hydroclimatic  
5804 vulnerability of peat carbon in the central Congo Basin, Nature, 612, 277–282,  
5805 <https://doi.org/10.1038/s41586-022-05389-3>, 2022.
- 5806 Garnett, S. T., Burgess, N. D., Fa, J. E., Fernández-Llamazares, Á., Molnár, Z., Robinson, C. J., Watson, J. E. M.,  
5807 Zander, K. K., Austin, B., Brondizio, E. S., Collier, N. F., Duncan, T., Ellis, E., Geyle, H., Jackson, M. V.,



- 5808 Jonas, H., Malmer, P., McGowan, B., Sivongxay, A., and Leiper, I.: A spatial overview of the global  
 5809 importance of Indigenous lands for conservation, *Nat Sustain*, 1, 369–374,  
 5810 <https://doi.org/10.1038/s41893-018-0100-6>, 2018.
- 5811 Garreaud, R. D., Alvarez-Garretón, C., Barichivich, J., Boisier, J. P., Christie, D., Galleguillos, M., LeQuesne, C.,  
 5812 McPhee, J., and Zambrano-Bigiarini, M.: The 2010–2015 megadrought in central Chile: impacts on  
 5813 regional hydroclimate and vegetation, *Hydrology and Earth System Sciences*, 21, 6307–6327,  
 5814 <https://doi.org/10.5194/hess-21-6307-2017>, 2017.
- 5815 Garrett, M. G., Monica: Wildfires are breaking out in Southern California as the ‘most destructive windstorm’ in  
 5816 over a decade hits, available at:  
 5817 <https://www.cnn.com/2025/01/07/weather/california-windstorm-fire-los-angeles-climate>, CNN (last  
 5818 access: 6th August 2025), 2025.
- 5819 Garrido, B.: Mais de 80% dos focos de calor em SP foram em áreas produtivas, available at:  
 5820 <https://ipam.org.br/focos-de-calor-sp/> (last access: 6th August 2025), IPAM Amazônia, 2024.
- 5821 Gatti, L. V., Basso, L. S., Miller, J. B., Gloor, M., Gatti Domingues, L., Cassol, H. L. G., Tejada, G., Aragão, L. E.  
 5822 O. C., Nobre, C., Peters, W., Marani, L., Arai, E., Sanches, A. H., Corrêa, S. M., Anderson, L., Von  
 5823 Randow, C., Correia, C. S. C., Crispim, S. P., and Neves, R. A. L.: Amazonia as a carbon source linked  
 5824 to deforestation and climate change, *Nature*, 595, 388–393,  
 5825 <https://doi.org/10.1038/s41586-021-03629-6>, 2021a.
- 5826 Gatti, L. V., Basso, L. S., Miller, J. B., Gloor, M., Gatti Domingues, L., Cassol, H. L. G., Tejada, G., Aragão, L. E.  
 5827 O. C., Nobre, C., Peters, W., Marani, L., Arai, E., Sanches, A. H., Corrêa, S. M., Anderson, L., Von  
 5828 Randow, C., Correia, C. S. C., Crispim, S. P., and Neves, R. A. L.: Amazonia as a carbon source linked  
 5829 to deforestation and climate change, *Nature*, 595, 388–393,  
 5830 <https://doi.org/10.1038/s41586-021-03629-6>, 2021b.
- 5831 Gayle, D.: Forest fires push up greenhouse gas emissions from war in Ukraine, *The Guardian*, available at:  
 5832 [https://www.theguardian.com/world/2025/feb/24/forest-fires-push-up-greenhouse-gas-emissions-from-w](https://www.theguardian.com/world/2025/feb/24/forest-fires-push-up-greenhouse-gas-emissions-from-war-in-ukraine)  
 5833 [ar-in-ukraine](https://www.theguardian.com/world/2025/feb/24/forest-fires-push-up-greenhouse-gas-emissions-from-war-in-ukraine) (last access: 6th August 2025), *The Guardian*, 2025.
- 5834 Gelman, A., Carlin, J. B., Stern, H. S., Dunson, D. B., Vehtari, A., and Rubin, D. B.: Bayesian Data Analysis,  
 5835 Chapman and Hall/CRC, <https://doi.org/10.1201/b16018>, 2013.
- 5836 Giannaros, T., Papavasileiou, G., Lagouvardos, K., Georgiadis, N., Athanassakis, G., and Tziritis, E.: 2024 Fire  
 5837 Season Report – Greece, available at:  
 5838 [https://wwfeu.awsassets.panda.org/downloads/202412\\_fire\\_season\\_annual\\_report\\_noa\\_wwf.pdf](https://wwfeu.awsassets.panda.org/downloads/202412_fire_season_annual_report_noa_wwf.pdf) (last  
 5839 access: 6th August 2025), 2025.
- 5840 Giglio, L. and Roy, D. P.: Assessment of satellite orbit-drift artifacts in the long-term AVHRR FireCCI11 global  
 5841 burned area data set, *Science of Remote Sensing*, 5, 100044,  
 5842 <https://doi.org/10.1016/j.srs.2022.100044>, 2022.
- 5843 Giglio, L., Van Der Werf, G. R., Randerson, J. T., Collatz, G. J., and Kasibhatla, P.: Global estimation of burned  
 5844 area using MODIS active fire observations, *Atmos. Chem. Phys.*, 6, 957–974,  
 5845 <https://doi.org/10.5194/acp-6-957-2006>, 2006.
- 5846 Giglio, L., Randerson, J. T., and van der Werf, G. R.: Analysis of daily, monthly, and annual burned area using the  
 5847 fourth-generation global fire emissions database (GFED4), *Journal of Geophysical Research:*  
 5848 *Biogeosciences*, 118, 317–328, <https://doi.org/10.1002/jgrg.20042>, 2013.



- 5849 Giglio, L., Schroeder, W., and Justice, C. O.: The collection 6 MODIS active fire detection algorithm and fire  
 5850 products, *Remote Sensing of Environment*, 178, 31–41, <https://doi.org/10.1016/j.rse.2016.02.054>, 2016.
- 5851 Giglio, L., Boschetti, L., Roy, D. P., Humber, M. L., and Justice, C. O.: The Collection 6 MODIS burned area  
 5852 mapping algorithm and product, *Remote Sensing of Environment*, 217, 72–85,  
 5853 <https://doi.org/10.1016/j.rse.2018.08.005>, 2018.
- 5854 Giglio, L., Justice, C., Boschetti, L., and Roy, D.: MODIS/Terra+Aqua Burned Area Monthly L3 Global 500m SIN  
 5855 Grid V061, NASA EOSDIS Land Processes Distributed Active Archive Center [Data set],  
 5856 <https://doi.org/10.5067/MODIS/MCD64A1.061>, 2021.
- 5857 Giglio, Louis: VIIRS/NPP Burned Area Monthly L4 Global 500m SIN Grid V002 [data set],  
 5858 <https://doi.org/10.5067/VIIRS/VNP64A1.002>, 2024.
- 5859 Gill, B. and Britz-McKibbin, P.: Biomonitoring of smoke exposure in firefighters: A review, *Current Opinion in*  
 5860 *Environmental Science & Health*, 15, 57–65, <https://doi.org/10.1016/j.coesh.2020.04.002>, 2020.
- 5861 Gincheva, A., Pausas, J. G., Edwards, A., Provenzale, A., Cerdà, A., Hanes, C., Royé, D., Chuvieco, E., Mouillot,  
 5862 F., Vissio, G., Rodrigo, J., Bedía, J., Abatzoglou, J. T., Senciales González, J. M., Short, K. C., Baudena,  
 5863 M., Llasat, M. C., Magnani, M., Boer, M. M., González, M. E., Torres-Vázquez, M. Á., Fiorucci, P.,  
 5864 Jacklyn, P., Libonati, R., Trigo, R. M., Herrera, S., Jerez, S., Wang, X., and Turco, M.: A monthly gridded  
 5865 burned area database of national wildland fire data, *Sci Data*, 11, 352,  
 5866 <https://doi.org/10.1038/s41597-024-03141-2>, 2024.
- 5867 Global Fire Emissions Database (GFED): Global Fire Emissions Database: Data Pages, available at:  
 5868 <https://www.globalfiredata.org/index.html> (last access: 6th August 2025), 2024.
- 5869 Global Fire Monitoring Center: Iran News: Wildfires ravage Iran's forests amidst drought and systemic  
 5870 negligence, available at:  
 5871 [https://gfmcc.online/2024/06-2024/iran-news-wildfires-ravage-irans-forests-amidst-drought-and-systemic-](https://gfmcc.online/2024/06-2024/iran-news-wildfires-ravage-irans-forests-amidst-drought-and-systemic-negligence.html)  
 5872 [negligence.html](https://gfmcc.online/2024/06-2024/iran-news-wildfires-ravage-irans-forests-amidst-drought-and-systemic-negligence.html) (last access: 6th August 2025), 2024.
- 5873 Global Times: China initiates Level-IV emergency response to wildfire in SW China's Sichuan, available at:  
 5874 <https://www.globaltimes.cn/page/202403/1308958.shtml> (last access: 6th August 2025), 2024.
- 5875 Global Wildfire Information System: Global Wildfire Information System, available at:  
 5876 <https://gwis.jrc.ec.europa.eu/> (last access: 6th August 2025), 2025.
- 5877 Goldman, E., Carter, S., and Sims, M.: Fires Drove Record-breaking Tropical Forest Loss in 2024 | World  
 5878 Resources Institute Research, 2025.
- 5879 Gonçalves, J. and Marcos, B.: Análise da área ardida em Portugal continental no ano de 2024, available at:  
 5880 <https://severuspt.github.io/AnaliseAreaArdida2024/> (last access: 6th August 2025), 2024.
- 5881 González, M. E., Gómez-González, S., Lara, A., Garreaud, R., and Díaz-Hormazábal, I.: The 2010–2015  
 5882 Megadrought and its influence on the fire regime in central and south-central Chile, *Ecosphere*, 9,  
 5883 e02300, <https://doi.org/10.1002/ecs2.2300>, 2018.
- 5884 González, M. E., Syphard, A. D., Fischer, A. P., Muñoz, A. A., and Miranda, A.: Chile's Valparaíso hills on fire,  
 5885 *Science*, 383, 1424–1424, <https://doi.org/10.1126/science.ado5411>, 2024.





- 5886 Good, P., Sellar, A., Tang, Y., Rumbold, S., Ellis, R., Kelley, D., and Kuhlbrodt, T.: MOHC UKESM1.0-LL model  
 5887 output prepared for CMIP6 ScenarioMIP ssp126, ssp245, ssp370, and ssp585, WDC-Climate [data set],  
 5888 <https://doi.org/10.22033/ESGF/CMIP6.6333>, 2019.
- 5889 Goss, M., Swain, D. L., Abatzoglou, J. T., Sarhadi, A., Kolden, C. A., Williams, A. P., and Diffenbaugh, N. S.:  
 5890 Climate change is increasing the likelihood of extreme autumn wildfire conditions across California,  
 5891 *Environ. Res. Lett.*, 15, 094016, <https://doi.org/10.1088/1748-9326/ab83a7>, 2020.
- 5892 Gould, C. F., Heft-Neal, S., Johnson, M., Aguilera, J., Burke, M., and Nadeau, K.: Health Effects of Wildfire  
 5893 Smoke Exposure, *Annual Review of Medicine*, 75, 277–292,  
 5894 <https://doi.org/10.1146/annurev-med-052422-020909>, 2024.
- 5895 Grau-Andrés, R., Moreira, B., and Pausas, J. G.: Global plant responses to intensified fire regimes, *Global*  
 5896 *Ecology and Biogeography*, 33, e13858, <https://doi.org/10.1111/geb.13858>, 2024.
- 5897 Green Policy Platform: Congo Basin Sustainable Landscapes Programme, available at:  
 5898 <https://www.greenpolicyplatform.org/initiatives/GefCongoBasin/about> (last access: 6th August 2025),  
 5899 2025.
- 5900 Greenpeace: La Patagonia argentina sufre los peores incendios forestales de las últimas tres décadas, available  
 5901 at:  
 5902 [https://www.greenpeace.org/argentina/story/problemas/bosques/la-patagonia-argentina-sufre-los-peores](https://www.greenpeace.org/argentina/story/problemas/bosques/la-patagonia-argentina-sufre-los-peores-incendios-forestales-de-las-ultimas-tres-decadas/)  
 5903 [-incendios-forestales-de-las-ultimas-tres-decadas/](https://www.greenpeace.org/argentina/story/problemas/bosques/la-patagonia-argentina-sufre-los-peores-incendios-forestales-de-las-ultimas-tres-decadas/) (last access: 6th August 2025), Fundación  
 5904 Greenpeace Argentina, 2025.
- 5905 Gussman, D.: Forged in fire: Understanding the regional relationship between fire and deforestation in the  
 5906 Guiana Shield, University of Exeter, PhD Thesis,  
 5907 [https://www.researchgate.net/profile/Dylan-Gussman/publication/361581512\\_Forged\\_in\\_fire\\_Understan](https://www.researchgate.net/profile/Dylan-Gussman/publication/361581512_Forged_in_fire_Understanding_the_regional_relationship_between_fire_and_deforestation_in_the_Guiana_Shield/links/62baa62960e77b7db838b70e/Forged-in-fire-Understanding-the-regional-relationship-between-fire-and-deforestation-in-the-Guiana-Shield.pdf)  
 5908 [ding\\_the\\_regional\\_relationship\\_between\\_fire\\_and\\_deforestation\\_in\\_the\\_Guiana\\_Shield/links/62baa629](https://www.researchgate.net/profile/Dylan-Gussman/publication/361581512_Forged_in_fire_Understanding_the_regional_relationship_between_fire_and_deforestation_in_the_Guiana_Shield/links/62baa62960e77b7db838b70e/Forged-in-fire-Understanding-the-regional-relationship-between-fire-and-deforestation-in-the-Guiana-Shield.pdf)  
 5909 [60e77b7db838b70e/Forged-in-fire-Understanding-the-regional-relationship-between-fire-and-deforestati](https://www.researchgate.net/profile/Dylan-Gussman/publication/361581512_Forged_in_fire_Understanding_the_regional_relationship_between_fire_and_deforestation_in_the_Guiana_Shield/links/62baa62960e77b7db838b70e/Forged-in-fire-Understanding-the-regional-relationship-between-fire-and-deforestation-in-the-Guiana-Shield.pdf)  
 5910 [on-in-the-Guiana-Shield.pdf](https://www.researchgate.net/profile/Dylan-Gussman/publication/361581512_Forged_in_fire_Understanding_the_regional_relationship_between_fire_and_deforestation_in_the_Guiana_Shield/links/62baa62960e77b7db838b70e/Forged-in-fire-Understanding-the-regional-relationship-between-fire-and-deforestation-in-the-Guiana-Shield.pdf) (last access 1 June 2025), 2022.
- 5911 Guzman-Morales, J. and Gershunov, A.: Climate Change Suppresses Santa Ana Winds of Southern California  
 5912 and Sharpens Their Seasonality, *Geophysical Research Letters*, 46, 2772–2780,  
 5913 <https://doi.org/10.1029/2018GL080261>, 2019.
- 5914 Haas, O., Prentice, I. C., and Harrison, S. P.: Global environmental controls on wildfire burnt area, size, and  
 5915 intensity, *Environ. Res. Lett.*, 17, 065004, <https://doi.org/10.1088/1748-9326/ac6a69>, 2022.
- 5916 Hamilton, D. S., Perron, M. M. G., Bond, T. C., Bowie, A. R., Buchholz, R. R., Guieu, C., Ito, A., Maenhaut, W.,  
 5917 Myriokefalitakis, S., Olgun, N., Rathod, S. D., Schepanski, K., Tagliabue, A., Wagner, R., and Mahowald,  
 5918 N. M.: Earth, Wind, Fire, and Pollution: Aerosol Nutrient Sources and Impacts on Ocean  
 5919 Biogeochemistry, *Annual Review of Marine Science*, 14, 303–330,  
 5920 <https://doi.org/10.1146/annurev-marine-031921-013612>, 2022a.
- 5921 Hamilton, D. S., Perron, M. M. G., Bond, T. C., Bowie, A. R., Buchholz, R. R., Guieu, C., Ito, A., Maenhaut, W.,  
 5922 Myriokefalitakis, S., Olgun, N., Rathod, S. D., Schepanski, K., Tagliabue, A., Wagner, R., and Mahowald,  
 5923 N. M.: Earth, Wind, Fire, and Pollution: Aerosol Nutrient Sources and Impacts on Ocean  
 5924 Biogeochemistry, *Annual Review of Marine Science*, 14, 303–330,  
 5925 <https://doi.org/10.1146/annurev-marine-031921-013612>, 2022b.



- 5926 Hantson, S., Padilla, M., Corti, D., and Chuvieco, E.: Strengths and weaknesses of MODIS hotspots to  
 5927 characterize global fire occurrence, *Remote Sensing of Environment*, 131, 152–159,  
 5928 <https://doi.org/10.1016/j.rse.2012.12.004>, 2013.
- 5929 Hantson, S., Arneth, A., Harrison, S. P., Kelley, D. I., Prentice, I. C., Rabin, S. S., Archibald, S., Mouillot, F.,  
 5930 Arnold, S. R., Artaxo, P., Bachelet, D., Ciais, P., Forrest, M., Friedlingstein, P., Hickler, T., Kaplan, J. O.,  
 5931 Kloster, S., Knorr, W., Lasslop, G., Li, F., Mangeon, S., Melton, J. R., Meyn, A., Sitch, S., Spessa, A.,  
 5932 van der Werf, G. R., Voulgarakis, A., and Yue, C.: The status and challenge of global fire modelling,  
 5933 *Biogeosciences*, 13, 3359–3375, <https://doi.org/10.5194/bg-13-3359-2016>, 2016.
- 5934 Hantson, S., Kelley, D. I., Arneth, A., Harrison, S. P., Archibald, S., Bachelet, D., Forrest, M., Hickler, T., Lasslop,  
 5935 G., Li, F., Mangeon, S., Melton, J. R., Nieradzki, L., Rabin, S. S., Prentice, I. C., Sheehan, T., Sitch, S.,  
 5936 Teckentrup, L., Voulgarakis, A., and Yue, C.: Quantitative assessment of fire and vegetation properties  
 5937 in simulations with fire-enabled vegetation models from the Fire Model Intercomparison Project,  
 5938 *Geoscientific Model Development*, 13, 3299–3318, <https://doi.org/10.5194/gmd-13-3299-2020>, 2020.
- 5939 Hantson, S., Andela, N., Goulden, M. L., and Randerson, J. T.: Human-ignited fires result in more extreme fire  
 5940 behavior and ecosystem impacts, *Nat Commun*, 13, 2717, <https://doi.org/10.1038/s41467-022-30030-2>,  
 5941 2022.
- 5942 Harris, S. and Lucas, C.: Understanding the variability of Australian fire weather between 1973 and 2017, *PLOS*  
 5943 *ONE*, 14, e0222328, <https://doi.org/10.1371/journal.pone.0222328>, 2019.
- 5944 Harrison, S. P., Bartlein, P. J., Brovkin, V., Houweling, S., Kloster, S., and Prentice, I. C.: The biomass burning  
 5945 contribution to climate–carbon-cycle feedback, *Earth Syst. Dynam.*, 9, 663–677,  
 5946 <https://doi.org/10.5194/esd-9-663-2018>, 2018.
- 5947 Hawkins, L. R., Abatzoglou, J. T., Li, S., and Rupp, D. E.: Anthropogenic Influence on Recent Severe Autumn  
 5948 Fire Weather in the West Coast of the United States, *Geophysical Research Letters*, 49,  
 5949 e2021GL095496, <https://doi.org/10.1029/2021GL095496>, 2022.
- 5950 Haynes, K., Short, K., Xanthopoulos, G., Viegas, D., Ribeiro, L. M., and Blanchi, R.: Wildfires and WUI Fire  
 5951 Fatalities, in: *Encyclopedia of Wildfires and Wildland-Urban Interface (WUI) Fires*, edited by: Manzello,  
 5952 S. L., Springer International Publishing, Cham, 1–16, [https://doi.org/10.1007/978-3-319-51727-8\\_92-1](https://doi.org/10.1007/978-3-319-51727-8_92-1),  
 5953 2019.
- 5954 Hazra, D. and Gallagher, P.: Role of insurance in wildfire risk mitigation, *Economic Modelling*, 108, 105768,  
 5955 <https://doi.org/10.1016/j.econmod.2022.105768>, 2022.
- 5956 He, Y., Czaplicki Cabezas, S., Maillard, O., Müller, R., Romero-Muñoz, A., Romero Pimentel, L. F., Vadillo, A.,  
 5957 and Vos, V. A.: Enact reforms to protect Bolivia's forests from fire, *Science*, 387, 255–255,  
 5958 <https://doi.org/10.1126/science.adt8304>, 2025.
- 5959 Hegerl, G. C., Hoegh-Guldberg, O., Casassa, G., Hoerling, M., Kovats, S., Parmesan, C., Pierce, D., and Stott,  
 5960 P.: IPCC WGI Expert Meeting on Detection and Attribution Related to Anthropogenic Climate Change:  
 5961 Good Practice Guidance Paper on Detection and Attribution Related to Anthropogenic Climate Change,  
 5962 Intergovernmental Panel on Climate Change, Geneva, available at:  
 5963 [https://archive.ipcc.ch/pdf/supporting-material/ipcc\\_good\\_practice\\_guidance\\_paper\\_anthropogenic.pdf](https://archive.ipcc.ch/pdf/supporting-material/ipcc_good_practice_guidance_paper_anthropogenic.pdf)  
 5964 (last access: 6th August 2025), edited by: Stocker, T., Field, C., Dahe, Q., Barros, V., Plattner, G.-K.,  
 5965 Tignor, M., Midgley, P., and Ebi, K., 2009.



- 5966 Held, I. M., Guo, H., Adcroft, A., Dunne, J. P., Horowitz, L. W., Krasting, J., Shevliakova, E., Winton, M., Zhao, M.,  
 5967 Bushuk, M., Wittenberg, A. T., Wyman, B., Xiang, B., Zhang, R., Anderson, W., Balaji, V., Donner, L.,  
 5968 Dunne, K., Durachta, J., Gauthier, P. P. G., Ginoux, P., Golaz, J.-C., Griffies, S. M., Hallberg, R., Harris,  
 5969 L., Harrison, M., Hurlin, W., John, J., Lin, P., Lin, S.-J., Malyshev, S., Menzel, R., Milly, P. C. D., Ming, Y.,  
 5970 Naik, V., Paynter, D., Paulot, F., Ramaswamy, V., Reichl, B., Robinson, T., Rosati, A., Seman, C.,  
 5971 Silvers, L. G., Underwood, S., and Zadeh, N.: Structure and Performance of GFDL's CM4.0 Climate  
 5972 Model, *Journal of Advances in Modeling Earth Systems*, 11, 3691–3727,  
 5973 <https://doi.org/10.1029/2019MS001829>, 2019.
- 5974 Hersbach, H., Bell, B., Berrisford, P., Biavati, G., Horányi, A., Muñoz Sabater, J., Nicolas, J., Peubey, C., Radu,  
 5975 R., Rozum, I., Sheppers, D., Simmons, A., Soci, C., Dee, D., and Thépaut, J.-N.: ERA5 hourly data on  
 5976 single levels from 1940 to present, Copernicus Climate Change Service (C3S) Climate Data Store  
 5977 (CDS) [data set], <https://doi.org/10.24381/CDS.ADBB2D47>, 2023.
- 5978 Higuera, P. E. and Abatzoglou, J. T.: Record-setting climate enabled the extraordinary 2020 fire season in the  
 5979 western United States, *Glob. Change Biol.*, 27, 1–2, <https://doi.org/10.1111/gcb.15388>, 2021.
- 5980 Higuera, P. E., Cook, M. C., Balch, J. K., Stavros, E. N., Mahood, A. L., and St. Denis, L. A.: Shifting  
 5981 social-ecological fire regimes explain increasing structure loss from Western wildfires, *PNAS Nexus*, 2,  
 5982 pgad005, <https://doi.org/10.1093/pnasnexus/pgad005>, 2023.
- 5983 Ho, A. T. Y., Huynh, K. P., Jacho-Chávez, D. T., and Vallée, G.: We didn't start the fire: Effects of a natural  
 5984 disaster on consumers' financial distress, *Journal of Environmental Economics and Management*, 119,  
 5985 102790, <https://doi.org/10.1016/j.jeem.2023.102790>, 2023.
- 5986 Holbrook, N. J., Scannell, H. A., Sen Gupta, A., Benthuyssen, J. A., Feng, M., Oliver, E. C. J., Alexander, L. V.,  
 5987 Burrows, M. T., Donat, M. G., Hobday, A. J., Moore, P. J., Perkins-Kirkpatrick, S. E., Smale, D. A.,  
 5988 Straub, S. C., and Wernberg, T.: A global assessment of marine heatwaves and their drivers, *Nat*  
 5989 *Commun*, 10, 2624, <https://doi.org/10.1038/s41467-019-10206-z>, 2019.
- 5990 Holl, K. D. and Brancalion, P. H. S.: Tree planting is not a simple solution, *Science*, 368, 580–581,  
 5991 <https://doi.org/10.1126/science.aba8232>, 2020.
- 5992 Hollis, J. J., Matthews, S., Fox-Hughes, P., Grootemaat, S., Heemstra, S., Kenny, B. J., and Sauvage, S.:  
 5993 Introduction to the Australian Fire Danger Rating System†, *Int. J. Wildland Fire*, 33, NULL-NULL,  
 5994 <https://doi.org/10.1071/WF23140>, 2024.
- 5995 Horton, H.: Drought fears in Europe amid reports May was world's second hottest ever, available at:  
 5996 [https://www.theguardian.com/environment/2025/jun/11/drought-fears-in-europe-amid-reports-may-was-](https://www.theguardian.com/environment/2025/jun/11/drought-fears-in-europe-amid-reports-may-was-worlds-second-hottest-ever)  
 5997 [worlds-second-hottest-ever](https://www.theguardian.com/environment/2025/jun/11/drought-fears-in-europe-amid-reports-may-was-worlds-second-hottest-ever) (last access: 6th August 2025), 2025.
- 5998 Hsu, A., Jones, M. W., Thurgood, J. R., Smith, A. J. P., Carmenta, R., Abatzoglou, J. T., Anderson, L. O., Clarke,  
 5999 H., Doerr, S. H., Fernandes, P. M., Kolden, C. A., Santín, C., Strydom, T., Le Quéré, C., Ascoli, D.,  
 6000 Castellnou, M., Goldammer, J. G., Guiomar, N. R. G. N., Kukavskaya, E. A., Rigolot, E., Tanpipat, V.,  
 6001 Varner, M., Yamashita, Y., Baard, J., Barreto, R., Becerra, J., Brunn, E., Bergius, N., Carlsson, J.,  
 6002 Cheney, C., Druce, D., Elliot, A., Evans, J., De Moraes Falleiro, R., Prat-Guitart, N., Hiers, J. K., Kaiser,  
 6003 J. W., Macher, L., Morris, D., Park, J., Robles, C., Román-Cuesta, R. M., Rücker, G., Senra, F., Steil, L.,  
 6004 Valverde, J. A. L., and Zerr, E.: A global assemblage of regional prescribed burn records — GlobalRx,  
 6005 *Sci Data*, 12, 1083, <https://doi.org/10.1038/s41597-025-04941-w>, 2025.



- 6006 Huang, L., Zhu, Y., Wang, Q., Zhu, A., Liu, Z., Wang, Y., Allen, D. T., and Li, L.: Assessment of the effects of  
 6007 straw burning bans in China: Emissions, air quality, and health impacts, *Science of The Total*  
 6008 *Environment*, 789, 147935, <https://doi.org/10.1016/j.scitotenv.2021.147935>, 2021.
- 6009 Huang, X., Xue, L., Wang, Z., Liu, Y., Ding, K., and Ding, A.: Escalating Wildfires in Siberia Driven by Climate  
 6010 Feedbacks Under a Warming Arctic in the 21st Century, *AGU Advances*, 5, e2023AV001151,  
 6011 <https://doi.org/10.1029/2023AV001151>, 2024.
- 6012 Huang, Z. and Skidmore, M.: The Impact of Wildfires and Wildfire-Induced Air Pollution on House Prices in the  
 6013 United States, *Land Economics*, 100, 22–50, <https://doi.org/10.3368/le.100.1.102322-0093R>, 2024.
- 6014 Huijnen, V., Flemming, J., Chabrillat, S., Errera, Q., Christophe, Y., Blechschmidt, A.-M., Richter, A., and Eskes,  
 6015 H.: C-IFS-CB05-BASCOE: stratospheric chemistry in the Integrated Forecasting System of ECMWF,  
 6016 *Geoscientific Model Development*, 9, 3071–3091, <https://doi.org/10.5194/gmd-9-3071-2016>, 2016.
- 6017 Humphreys, A., Walker, E. G., Bratman, G. N., and Errett, N. A.: What can we do when the smoke rolls in? An  
 6018 exploratory qualitative analysis of the impacts of rural wildfire smoke on mental health and wellbeing,  
 6019 and opportunities for adaptation, *BMC Public Health*, 22, <https://doi.org/10.1186/s12889-021-12411-2>,  
 6020 2022.
- 6021 Hunka, N., Santoro, M., Armston, J., Dubayah, R., McRoberts, R. E., Næsset, E., Quegan, S., Urbazhev, M.,  
 6022 Pascual, A., May, P. B., Minor, D., Leitold, V., Basak, P., Liang, M., Melo, J., Herold, M., Málaga, N.,  
 6023 Wilson, S., Montesinos, P. D., Arana, A., Paiva, R. E. D. L. C., Ferrand, J., Keoka, S.,  
 6024 Guerra-Hernández, J., and Duncanson, L.: On the NASA GEDI and ESA CCI biomass maps: aligning  
 6025 for uptake in the UNFCCC global stocktake, *Environ. Res. Lett.*, 18, 124042,  
 6026 <https://doi.org/10.1088/1748-9326/ad0b60>, 2023.
- 6027 Inness, A., Ades, M., Agustí-Panareda, A., Barré, J., Benedictow, A., Blechschmidt, A.-M., Dominguez, J. J.,  
 6028 Engelen, R., Eskes, H., Flemming, J., Huijnen, V., Jones, L., Kipling, Z., Massart, S., Parrington, M.,  
 6029 Peuch, V.-H., Razinger, M., Remy, S., Schulz, M., and Suttie, M.: The CAMS reanalysis of atmospheric  
 6030 composition, *Atmospheric Chemistry and Physics*, 19, 3515–3556,  
 6031 <https://doi.org/10.5194/acp-19-3515-2019>, 2019.
- 6032 INPE: Banco de Dados de queimadas, available at:  
 6033 [https://terrabrasilis.dpi.inpe.br/queimadas/situacao-atual/estatisticas/estatisticas\\_paises/](https://terrabrasilis.dpi.inpe.br/queimadas/situacao-atual/estatisticas/estatisticas_paises/) (last access:  
 6034 6th August 2025), 2025.
- 6035 Instituto Brasileiro de Geografia e Estatística (IBGE): Coordenação de Recursos Naturais e Estudos Ambientais.  
 6036 Bacias e divisões hidrográficas do Brasil - Rio de Janeiro [data set], 2021.
- 6037 Instituto da Conservação da Natureza e das Florestas: 8º relatório provisório de incêndios rurais - 2024 - 1 de  
 6038 janeiro a 15 de outubro, available at:  
 6039 <https://www.icnf.pt/florestas/gfr/gfrgestaoinformacao/grfrelatorios/areasardidaseocorrencias> (last access:  
 6040 6th August 2025), 2024.
- 6041 Instituto Português do Mar e Atmosfera: Instituto Português do Mar e Atmosfera: Relatório incêndios rurais –  
 6042 análise meteorológica e índices de perigo, available at:  
 6043 [https://www.ipma.pt/resources/www/docs/im.publicacoes/edicoes.online/20241129/IPVgKYBfuawamtSM](https://www.ipma.pt/resources/www/docs/im.publicacoes/edicoes.online/20241129/IPVgKYBfuawamtSMzMgL/met_20240901_20240930_fog_mm_co_pt.pdf)  
 6044 [zMgL/met\\_20240901\\_20240930\\_fog\\_mm\\_co\\_pt.pdf](https://www.ipma.pt/resources/www/docs/im.publicacoes/edicoes.online/20241129/IPVgKYBfuawamtSMzMgL/met_20240901_20240930_fog_mm_co_pt.pdf) (last access: 6th August 2025), 2024.
- 6045 Instituto Socioambiental: “Roraima está queimando”: recorde de calor gera incêndios em Terras Indígenas e  
 6046 deixa capital coberta pela fumaça, available at:



- 6047 <https://www.socioambiental.org/noticias-socioambientais/roraima-esta-queimando-recorde-de-calor-gera>  
 6048 -incendios-em-terras-indigenas (last access: 6th August 2025), 2024.
- 6049 Insurance Bureau of Canada: Insurance Bureau of Canada provides Jasper wildfire recovery update, available  
 6050 at:  
 6051 <https://www.ibc.ca/news-insights/news/insurance-bureau-of-canada-provides-jasper-wildfire-recovery-up>  
 6052 date (last access: 6th August 2025), 2025.
- 6053 Intergovernmental Panel on Climate Change (IPCC) (Ed.): Changing State of the Climate System, 2023a, in:  
 6054 Climate Change 2021 – The Physical Science Basis: Working Group I Contribution to the Sixth  
 6055 Assessment Report of the Intergovernmental Panel on Climate Change, Cambridge University Press,  
 6056 Cambridge, 287–422, <https://doi.org/10.1017/9781009157896.004>, 2023a.
- 6057 Intergovernmental Panel on Climate Change (IPCC) (Ed.): Key Risks across Sectors and Regions, 2023b, in:  
 6058 Climate Change 2022 – Impacts, Adaptation and Vulnerability: Working Group II Contribution to the  
 6059 Sixth Assessment Report of the Intergovernmental Panel on Climate Change, Cambridge University  
 6060 Press, Cambridge, 2411–2538, <https://doi.org/10.1017/9781009325844.025>, 2023b.
- 6061 Intergovernmental Panel on Climate Change (IPCC) (Ed.): Point of Departure and Key Concepts, 2023c, in:  
 6062 Climate Change 2022 – Impacts, Adaptation and Vulnerability: Working Group II Contribution to the  
 6063 Sixth Assessment Report of the Intergovernmental Panel on Climate Change, Cambridge University  
 6064 Press, Cambridge, 121–196, <https://doi.org/10.1017/9781009325844.003>, 2023c.
- 6065 Intergovernmental Panel on Climate Change (IPCC): Summary for Policymakers. In: Climate Change 2023:  
 6066 Synthesis Report. Contribution of Working Groups I, II and III to the Sixth Assessment Report of the  
 6067 Intergovernmental Panel on Climate Change [Core Writing Team, H. Lee and J. Romero (eds.)]. IPCC,  
 6068 Geneva, Switzerland, pp. 1–34, doi: 10.59327/IPCC/AR6-9789291691647.001, 2023d.
- 6069 Intergovernmental Panel on Climate Change (IPCC) (Ed.): Weather and Climate Extreme Events in a Changing  
 6070 Climate, in: Climate Change 2021 – The Physical Science Basis: Working Group I Contribution to the  
 6071 Sixth Assessment Report of the Intergovernmental Panel on Climate Change, Cambridge University  
 6072 Press, Cambridge, 1513–1766, <https://doi.org/10.1017/9781009157896.013>, 2023e.
- 6073 Internal Displacement Monitoring Centre (IDMC): 2025 Global Report on Internal Displacement (GRID),  
 6074 <https://doi.org/10.55363/IDMC.XTGW2833>, 2025.
- 6075 Inter-Sectoral Impact Model Intercomparison Project (ISIMIP): ISIMIP Repository, available at:  
 6076 <https://data.ISIMIP.org/> (last access: 6th August 2025), 2025.
- 6077 IQAir: 2024 World Air Quality Report, available at: <https://www.iqair.com/newsroom/waqr-2024-pr> (last access:  
 6078 6th August 2025), 2025.
- 6079 Iran International: Fires in Iran's protected wildlife area expose governance failures, available at:  
 6080 <https://www.iranintl.com/en/202407110417> (last access: 6th August 2025), 2024.
- 6081 ISDM (Informational System of Forest Fire Remote Monitoring): Wildfires Monitoring Information System of the  
 6082 Federal Forestry Agency, available at: [https://pushkino.aviales.ru/main\\_pages/index.shtml](https://pushkino.aviales.ru/main_pages/index.shtml) (last access:  
 6083 6th August 2025), 2025.
- 6084 Iturbide, M., Gutiérrez, J. M., Alves, L. M., Bedia, J., Cerezo-Mota, R., Gimadevilla, E., Cofiño, A. S., Di Luca, A.,  
 6085 Faria, S. H., Gorodetskaya, I. V., Hauser, M., Herrera, S., Hennessy, K., Hewitt, H. T., Jones, R. G.,  
 6086 Krakovska, S., Manzananas, R., Martínez-Castro, D., Narisma, G. T., Nurhati, I. S., Pinto, I., Seneviratne,



- 6087 S. I., van den Hurk, B., and Vera, C. S.: An update of IPCC climate reference regions for subcontinental  
 6088 analysis of climate model data: definition and aggregated datasets, *Earth System Science Data*, 12,  
 6089 2959–2970, <https://doi.org/10.5194/essd-12-2959-2020>, 2020.
- 6090 Jain, P., Coogan, S. C. P., Subramanian, S. G., Crowley, M., Taylor, S., and Flannigan, M. D.: A review of  
 6091 machine learning applications in wildfire science and management, *Environ. Rev.*, 28, 478–505,  
 6092 <https://doi.org/10.1139/er-2020-0019>, 2020.
- 6093 Jain, P., Barber, Q. E., Taylor, S., Whitman, E., Castellanos Acuna, D., Boulanger, Y., Chavardès, R. D., Chen, J.,  
 6094 Englefield, P., Flannigan, M., Girardin, M. P., Hanes, C. C., Little, J., Morrison, K., Skakun, R. S.,  
 6095 Thompson, D. K., Wang, X., and Parisien, M.-A.: Drivers and Impacts of the Record-Breaking 2023  
 6096 Wildfire Season in Canada, *Nature Communications*, 15, 6764,  
 6097 <https://doi.org/10.1038/s41467-024-51154-7>, 2024.
- 6098 Jiang, Y., Zhou, L., Tucker, C. J., Raghavendra, A., Hua, W., Liu, Y. Y., and Joiner, J.: Widespread increase of  
 6099 boreal summer dry season length over the Congo rainforest, *Nat. Clim. Chang.*, 9, 617–622,  
 6100 <https://doi.org/10.1038/s41558-019-0512-y>, 2019.
- 6101 Jiménez-Muñoz, J. C., Mattar, C., Barichivich, J., Santamaría-Artigas, A., Takahashi, K., Malhi, Y., Sobrino, J. A.,  
 6102 and Schrier, G. van der: Record-breaking warming and extreme drought in the Amazon rainforest during  
 6103 the course of El Niño 2015–2016, *Sci Rep*, 6, 33130, <https://doi.org/10.1038/srep33130>, 2016.
- 6104 Johnson, S. J., Stockdale, T. N., Ferranti, L., Balmaseda, M. A., Molteni, F., Magnusson, L., Tietsche, S.,  
 6105 Decremmer, D., Weisheimer, A., Balsamo, G., Keeley, S. P. E., Mogensen, K., Zuo, H., and Monge-Sanz,  
 6106 B. M.: SEAS5: the new ECMWF seasonal forecast system, *Geoscientific Model Development*, 12,  
 6107 1087–1117, <https://doi.org/10.5194/gmd-12-1087-2019>, 2019a.
- 6108 Johnson, S. J., Stockdale, T. N., Ferranti, L., Balmaseda, M. A., Molteni, F., Magnusson, L., Tietsche, S.,  
 6109 Decremmer, D., Weisheimer, A., Balsamo, G., Keeley, S. P. E., Mogensen, K., Zuo, H., and Monge-Sanz,  
 6110 B. M.: SEAS5: the new ECMWF seasonal forecast system, *Geosci. Model Dev.*, 12, 1087–1117,  
 6111 <https://doi.org/10.5194/gmd-12-1087-2019>, 2019b.
- 6112 Johnston, F. H., Henderson, S. B., Chen, Y., Randerson, J. T., Marlier, M., DeFries, R. S., Kinney, P., Bowman, D.  
 6113 M. J. S., and Brauer, M.: Estimated Global Mortality Attributable to Smoke from Landscape Fires,  
 6114 *Environmental Health Perspectives*, 120, 695–701, <https://doi.org/10.1289/ehp.1104422>, 2012.
- 6115 Johnston, F. H., Borchers-Arriagada, N., Morgan, G. G., Jalaludin, B., Palmer, A. J., Williamson, G. J., and  
 6116 Bowman, D. M. J. S.: Unprecedented health costs of smoke-related PM<sub>2.5</sub> from the 2019–20 Australian  
 6117 megafires, *Nat Sustain*, 4, 42–47, <https://doi.org/10.1038/s41893-020-00610-5>, 2021.
- 6118 Johnston, F. H., Williamson, G., Borchers-Arriagada, N., Henderson, S. B., and Bowman, D. M. J. S.: Climate  
 6119 Change, Landscape Fires, and Human Health: A Global Perspective, *Annual Review of Public Health*,  
 6120 45, 295–314, <https://doi.org/10.1146/annurev-publhealth-060222-034131>, 2024.
- 6121 Johnstone, J. F., Allen, C. D., Franklin, J. F., Frelich, L. E., Harvey, B. J., Higuera, P. E., Mack, M. C.,  
 6122 Meentemeyer, R. K., Metz, M. R., Perry, G. L., Schoennagel, T., and Turner, M. G.: Changing  
 6123 disturbance regimes, ecological memory, and forest resilience, *Frontiers in Ecology and the*  
 6124 *Environment*, 14, 369–378, <https://doi.org/10.1002/fee.1311>, 2016.
- 6125 Jolly, W. M., Cochrane, M. A., Freeborn, P. H., Holden, Z. A., Brown, T. J., Williamson, G. J., and Bowman, D. M.  
 6126 J. S.: Climate-induced variations in global wildfire danger from 1979 to 2013, *Nat Commun*, 6,  
 6127 <https://doi.org/10.1038/ncomms8537>, 2015.





- 6128 Jones, M. W., Abatzoglou, J. T., Veraverbeke, S., Andela, N., Lasslop, G., Forkel, M., Smith, A. J. P., Burton, C.,  
 6129 Betts, R. A., van der Werf, G. R., Sitch, S., Canadell, J. G., Santin, C., Kolden, C., Doerr, S. H., and Le  
 6130 Quéré, C.: Global and Regional Trends and Drivers of Fire Under Climate Change, *Reviews of*  
 6131 *Geophysics*, 60, e2020RG000726, <https://doi.org/10.1029/2020RG000726>, 2022.
- 6132 Jones, M. W., Veraverbeke, S., Andela, N., Doerr, S. H., Kolden, C., Mataveli, G., Pettinari, M. L., Le Quéré, C.,  
 6133 Rosan, T. M., van der Werf, G. R., van Wees, D., and Abatzoglou, J. T.: Global rise in forest fire  
 6134 emissions linked to climate change in the extratropics, *Science*, 386, ead15889,  
 6135 <https://doi.org/10.1126/science.ad15889>, 2024a.
- 6136 Jones, M. W., Kelley, D. I., Burton, C. A., Di Giuseppe, F., Barbosa, M. L. F., Brambleby, E., Hartley, A. J.,  
 6137 Lombardi, A., Mataveli, G., McNorton, J. R., Spuler, F. R., Wessel, J. B., Abatzoglou, J. T., Anderson, L.  
 6138 O., Andela, N., Archibald, S., Armenteras, D., Burke, E., Carmenta, R., Chuvieco, E., Clarke, H., Doerr,  
 6139 S. H., Fernandes, P. M., Giglio, L., Hamilton, D. S., Hantson, S., Harris, S., Jain, P., Kolden, C. A.,  
 6140 Kurvits, T., Lampe, S., Meier, S., New, S., Parrington, M., Perron, M. M. G., Qu, Y., Ribeiro, N. S.,  
 6141 Saharjo, B. H., San-Miguel-Ayán, J., Shuman, J. K., Tanpipat, V., van der Werf, G. R., Veraverbeke, S.,  
 6142 and Xanthopoulos, G.: State of Wildfires 2023–2024, *Earth System Science Data*, 16, 3601–3685,  
 6143 <https://doi.org/10.5194/essd-16-3601-2024>, 2024b.
- 6144 Jones, M. W., Andela, N., Brambleby, E., Chuvieco, E., Giglio, L., Kaiser, J. W., Parrington, M., Qu, Y.,  
 6145 Torres-Vázquez, M. Á., van der Werf, G. R., and Veraverbeke, S.: State of Wildfires 2024-25: Anomalies  
 6146 in Burned Area, Fire Emissions, and Individual Fire Characteristics by Continent, Biome, Country, and  
 6147 Administrative Region, *Zenodo* [Data set], <https://doi.org/10.5281/zenodo.15525674>, 2025.
- 6148 Jones, R. L., Kharb, A., and Tubeuf, S.: The untold story of missing data in disaster research: a systematic  
 6149 review of the empirical literature utilising the Emergency Events Database (EM-DAT), *Environ. Res.*  
 6150 *Lett.*, 18, 103006, <https://doi.org/10.1088/1748-9326/acfd42>, 2023.
- 6151 Jorge, A. L., Abatzoglou, J. T., Fleishman, E., Williams, E. L., Rupp, D. E., Jenkins, J. S., Sadegh, M., Kolden, C.  
 6152 A., and Short, K. C.: COVID-19 Fueled an Elevated Number of Human-Caused Ignitions in the Western  
 6153 United States During the 2020 Wildfire Season, *Earth's Future*, 13, e2024EF005744,  
 6154 <https://doi.org/10.1029/2024EF005744>, 2025.
- 6155 Kaiser, J. W., Heil, A., Andreae, M. O., Benedetti, A., Chubarova, N., Jones, L., Morcrette, J.-J., Razinger, M.,  
 6156 Schultz, M. G., Suttie, M., and van der Werf, G. R.: Biomass burning emissions estimated with a global  
 6157 fire assimilation system based on observed fire radiative power, *Biogeosciences*, 9, 527–554,  
 6158 <https://doi.org/10.5194/bg-9-527-2012>, 2012.
- 6159 Kam, P. M., Aznar-Siguan, G., Schewe, J., Milano, L., Ginnetti, J., Willner, S., McCaughey, J. W., and Bresch, D.  
 6160 N.: Global warming and population change both heighten future risk of human displacement due to river  
 6161 floods, *Environ. Res. Lett.*, 16, 044026, <https://doi.org/10.1088/1748-9326/abd26c>, 2021.
- 6162 Kam, P. M., Ciccone, F., Kropf, C. M., Riedel, L., Fairless, C., and Bresch, D. N.: Impact-based forecasting of  
 6163 tropical cyclone-related human displacement to support anticipatory action, *Nat Commun*, 15, 8795,  
 6164 <https://doi.org/10.1038/s41467-024-53200-w>, 2024.
- 6165 Karan, D. and Bhadra, S.: How Nepal Grew Back Its Forests, *The New York Times*, available at:  
 6166 <https://www.nytimes.com/2022/11/11/world/asia/nepal-reforestation-climate.html> (last access: 6th  
 6167 August 2025), 2022.



- 6168 Karuna Schechen: Extreme heat and wildfire in Nepal, available at:  
 6169 <https://karuna-shechen.org/en/extreme-heat-and-wildfires-in-nepal/> (last access: 6th August 2025),  
 6170 2024.
- 6171 Katz, R. W. and Giannini, A.: Climate Variability and Change in South America, in: Climate Change and  
 6172 Biodiversity in the Tropical Andes, Inter-American Institute for Global Change Research, 2010.
- 6173 Keeley, J. E.: Fire intensity, fire severity and burn severity: a brief review and suggested usage, *Int. J. Wildland*  
 6174 *Fire*, 18, 116–126, <https://doi.org/10.1071/WF07049>, 2009.
- 6175 Kelley, D., Burton, C., Barbosa, M. L. F., Jones, M., Di Giuseppe, F., Hartley, A., McNorton, J., Spuler, F., Wessel,  
 6176 J., and Lampe, S.: douglask3/State\_of\_Wildfires\_report: Final code used in published version of the first  
 6177 State of Wildfires report [Code] (v1.0), <https://doi.org/10.5281/ZENODO.11460379>, 2024.
- 6178 Kelley, D., Ferreira Barbosa, M. L., Hartley, A., Spuler, F., Wessel, J., Ciavarella, A., McNorton, J., Burton, C.,  
 6179 Ferreira, I., and Fiedler, L.: State of Wildfires 2024/25 – ConFLAME Driver Assessment - Congo  
 6180 Basin/Southern California [Data set], <https://doi.org/10.5281/ZENODO.16789657>, 2025a.
- 6181 Kelley, D., Ferreira Barbosa, M. L., Bradley, A., Burke, E., Burton, C., Hartley, A., Ferreira, I., and Hantson, S.:  
 6182 State of Wildfires 2024-25: ConFLAME Future Projections [Data set],  
 6183 <https://doi.org/10.5281/ZENODO.15807587>, 2025b.
- 6184 Kelley, D., Ferreira Barbosa, M. L., Hartley, A., Spuler, F., Wessel, J., Ciavarella, A., McNorton, J., Burton, C.,  
 6185 Ferreira, I., and Fiedler, L.: State of Wildfires 2024-25: ConFLAME NRT Attribution Results [Data set],  
 6186 <https://doi.org/10.5281/ZENODO.15641876>, 2025c.
- 6187 Kelley, D. I., Harrison, S. P., and Prentice, I. C.: Improved simulation of fire–vegetation interactions in the Land  
 6188 surface Processes and eXchanges dynamic global vegetation model (LPX-Mv1), *Geoscientific Model*  
 6189 *Development*, 7, 2411–2433, <https://doi.org/10.5194/gmd-7-2411-2014>, 2014.
- 6190 Kelley, D. I., Bistinas, I., Whitley, R., Burton, C., Marthews, T. R., and Dong, N.: How contemporary bioclimatic  
 6191 and human controls change global fire regimes, *Nat. Clim. Chang.*, 9, 690–696,  
 6192 <https://doi.org/10.1038/s41558-019-0540-7>, 2019.
- 6193 Kelley, D. I., Burton, C., Huntingford, C., Brown, M. A. J., Whitley, R., and Dong, N.: Technical note: Low  
 6194 meteorological influence found in 2019 Amazonia fires, *Biogeosciences*, 18, 787–804,  
 6195 <https://doi.org/10.5194/bg-18-787-2021>, 2021.
- 6196 Khankeh, H., Mazhin, S., Farrokhi, M., Noroozi, M., Roudini, J., Hosseini, S., Motlagh, M., and Kolivand, P.:  
 6197 Worldwide disaster loss and damage databases: A systematic review, *J Edu Health Promot*, 10, 329,  
 6198 [https://doi.org/10.4103/jehp.jehp\\_1525\\_20](https://doi.org/10.4103/jehp.jehp_1525_20), 2021.
- 6199 Kheshti, M.: Protect Iran's Zagros forests from wildfires, *Science*, 369, 1066–1066,  
 6200 <https://doi.org/10.1126/science.abd2967>, 2020.
- 6201 Kim, J., Wise, A., and Bowman, E.: Strong winds pick up, increasing fire danger as firefighters battle LA blazes,  
 6202 available at: <https://www.npr.org/2025/01/11/g-s1-42247/la-wildfires-california-containment-evacuation>  
 6203 (last access: 6th August 2025), 2025.
- 6204 Kirillina, K., Shvetsov, E. G., Protopopova, V. V., Thiesmeyer, L., and Yan, W.: Consideration of anthropogenic  
 6205 factors in boreal forest fire regime changes during rapid socio-economic development: case study of



- 6206 forestry districts with increasing burnt area in the Sakha Republic, Russia, *Environ. Res. Lett.*, 15,  
 6207 035009, <https://doi.org/10.1088/1748-9326/ab6c6e>, 2020.
- 6208 Kolden, C.: Wildfires: count lives and homes, not hectares burnt, *Nature*, 586, 9–9,  
 6209 <https://doi.org/10.1038/d41586-020-02740-4>, 2020.
- 6210 Kolden, C. A. and Abatzoglou, J. T.: Spatial Distribution of Wildfires Ignited under Katabatic versus Non-Katabatic  
 6211 Winds in Mediterranean Southern California USA, *Fire*, 1, 19, <https://doi.org/10.3390/fire1020019>, 2018.
- 6212 Kolden, C. A. and Henson, C.: A Socio-Ecological Approach to Mitigating Wildfire Vulnerability in the Wildland  
 6213 Urban Interface: A Case Study from the 2017 Thomas Fire, *Fire*, 2, 9,  
 6214 <https://doi.org/10.3390/fire2010009>, 2019.
- 6215 Kolden, C. A., Abatzoglou, J. T., Jones, M. W., and Jain, P.: Wildfires in 2023, *Nat Rev Earth Environ*, 5,  
 6216 238–240, <https://doi.org/10.1038/s43017-024-00544-y>, 2024.
- 6217 Kolden, C. A., Abatzoglou, J. T., Jones, M. W., and Jain, P.: Wildfires in 2024, *Nat Rev Earth Environ*, 6,  
 6218 237–239, <https://doi.org/10.1038/s43017-025-00663-0>, 2025.
- 6219 Kouassi, J.-L., Wandan, N., and Mbow, C.: Exploring spatio-temporal trends and environmental drivers of wildfire  
 6220 occurrence and impacts in Côte d'Ivoire, West Africa, *African Journal of Ecology*, 60, 1218–1236,  
 6221 <https://doi.org/10.1111/aje.13066>, 2022.
- 6222 Kramer, S. J., Bisson, K. M., and Fischer, A. D.: Observations of Phytoplankton Community Composition in the  
 6223 Santa Barbara Channel During the Thomas Fire, *Journal of Geophysical Research: Oceans*, 125,  
 6224 e2020JC016851, <https://doi.org/10.1029/2020JC016851>, 2020.
- 6225 Krikken, F., Lehner, F., Haustein, K., Drobyshev, I., and Van Oldenborgh, G. J.: Attribution of the role of climate  
 6226 change in the forest fires in Sweden 2018, *Nat. Hazards Earth Syst. Sci.*, 21, 2169–2179,  
 6227 <https://doi.org/10.5194/nhess-21-2169-2021>, 2021.
- 6228 Kudláčková, L., Bartošová, L., Linda, R., Bláhová, M., Poděbradská, M., Fischer, M., Balek, J., Žalud, Z., and  
 6229 Trnka, M.: Assessing fire danger classes and extreme thresholds of the Canadian Fire Weather Index  
 6230 across global environmental zones: a review, *Environ. Res. Lett.*, 20, 013001,  
 6231 <https://doi.org/10.1088/1748-9326/ad97cf>, 2024.
- 6232 Kukavskaya, E. A., Buryak, L. V., Shvetsov, E. G., Conard, S. G., and Kalenskaya, O. P.: The impact of  
 6233 increasing fire frequency on forest transformations in southern Siberia, *Forest Ecology and*  
 6234 *Management*, 382, 225–235, <https://doi.org/10.1016/j.foreco.2016.10.015>, 2016.
- 6235 Ladd, T. M., Catlett, D., Maniscalco, M. A., Kim, S. M., Kelly, R. L., John, S. G., Carlson, C. A., and  
 6236 Iglesias-Rodríguez, M. D.: Food for all? Wildfire ash fuels growth of diverse eukaryotic plankton,  
 6237 *Proceedings of the Royal Society B: Biological Sciences*, 290, 20231817,  
 6238 <https://doi.org/10.1098/rspb.2023.1817>, 2023.
- 6239 Lafferty, D. C. and Sriver, R. L.: Downscaling and bias-correction contribute considerable uncertainty to local  
 6240 climate projections in CMIP6, *npj Clim Atmos Sci*, 6, 1–13, <https://doi.org/10.1038/s41612-023-00486-0>,  
 6241 2023.
- 6242 Lampe, S. and Burton, C.: State of Wildfires 2024–2025: FireMIP Burned Area Attribution [Code], ,  
 6243 <https://doi.org/10.5281/ZENODO.16779167>, 2025.



- 6244 Lange, S.: Trend-preserving bias adjustment and statistical downscaling with ISIMIP3BASD (v1.0), Geoscientific  
 6245 Model Development, 12, 3055–3070, <https://doi.org/10.5194/gmd-12-3055-2019>, 2019.
- 6246 Lapola, D. M., Pinho, P., Barlow, J., Aragão, L. E. O. C., Berenguer, E., Carmenta, R., Liddy, H. M., Seixas, H.,  
 6247 Silva, C. V. J., Silva-Junior, C. H. L., Alencar, A. A. C., Anderson, L. O., Armenteras, D., Brovkin, V.,  
 6248 Calders, K., Chambers, J., Chini, L., Costa, M. H., Faria, B. L., Fearnside, P. M., Ferreira, J., Gatti, L.,  
 6249 Gutierrez-Velez, V. H., Han, Z., Hibbard, K., Koven, C., Lawrence, P., Pongratz, J., Portela, B. T. T.,  
 6250 Rounsevell, M., Ruane, A. C., Schaldach, R., da Silva, S. S., von Randow, C., and Walker, W. S.: The  
 6251 drivers and impacts of Amazon forest degradation, *Science*, 379, eabp8622,  
 6252 <https://doi.org/10.1126/science.abp8622>, 2023.
- 6253 Lareau, N. P., Nauslar, N. J., and Abatzoglou, J. T.: The Carr Fire Vortex: A Case of Pyrotornadogenesis?,  
 6254 *Geophysical Research Letters*, 45, 13107–13115, <https://doi.org/10.1029/2018GL080667>, 2018.
- 6255 Latif, M., Anderson, D., Barnett, T., Cane, M., Kleeman, R., Leetmaa, A., O'Brien, J., Rosati, A., and Schneider,  
 6256 E.: A review of the predictability and prediction of ENSO, *Journal of Geophysical Research: Oceans*,  
 6257 103, 14375–14393, <https://doi.org/10.1029/97JC03413>, 1998.
- 6258 Laurent, P., Mouillot, F., Yue, C., Ciais, P., Moreno, M. V., and Nogueira, J. M. P.: FRY, a global database of fire  
 6259 patch functional traits derived from space-borne burned area products, *Sci Data*, 5, 180132,  
 6260 <https://doi.org/10.1038/sdata.2018.132>, 2018.
- 6261 van Leeuwen, S. and Miller-Sabbioni, C.: Australia's Megafires: Biodiversity Impacts and Lessons from  
 6262 2019–2020, in: *Australia's Megafires: Biodiversity Impacts and Lessons from 2019–20, Rumpff, L.,*  
 6263 *Legge, S. M.; van Leeuwen, S.; Wintle, B. A.; Woinarski, J. C. Z.*, 2023.
- 6264 Lehmann, C. E. R., Anderson, T. M., Sankaran, M., Higgins, S. I., Archibald, S., Hoffmann, W. A., Hanan, N. P.,  
 6265 Williams, R. J., Fensham, R. J., Felfili, J., Hutley, L. B., Ratnam, J., San Jose, J., Montes, R., Franklin,  
 6266 D., Russell-Smith, J., Ryan, C. M., Durigan, G., Hiernaux, P., Haidar, R., Bowman, D. M. J. S., and  
 6267 Bond, W. J.: Savanna Vegetation-Fire-Climate Relationships Differ Among Continents, *Science*, 343,  
 6268 548–552, <https://doi.org/10.1126/science.1247355>, 2014.
- 6269 Lemos, M. C., Kirchhoff, C. J., and Ramprasad, V.: Narrowing the climate information usability gap, *Nature Clim*  
 6270 *Change*, 2, 789–794, <https://doi.org/10.1038/nclimate1614>, 2012.
- 6271 Levin, M., Huffman, J., and Friedman, L.: Rep. Mike Levin Leads Letter Demanding Answers on US Army Corps  
 6272 of Engineers' Wasteful Water Release, available at:  
 6273 [https://levin.house.gov/media/press-releases/rep-mike-levin-leads-letter-demanding-answers-on-us-army-](https://levin.house.gov/media/press-releases/rep-mike-levin-leads-letter-demanding-answers-on-us-army-corps-of-engineers-wasteful-water-release)  
 6274 [corps-of-engineers-wasteful-water-release](https://levin.house.gov/media/press-releases/rep-mike-levin-leads-letter-demanding-answers-on-us-army-corps-of-engineers-wasteful-water-release) (last access: 6th August 2025), 2025.
- 6275 Li, S., Sparrow, S. N., Otto, F. E. L., Rifai, S. W., Oliveras, I., Krikken, F., Anderson, L. O., Malhi, Y., and Wallom,  
 6276 D.: Anthropogenic climate change contribution to wildfire-prone weather conditions in the Cerrado and  
 6277 Arc of deforestation, *Environ. Res. Lett.*, 16, 094051, <https://doi.org/10.1088/1748-9326/ac1e3a>, 2021a.
- 6278 Li, Y., Sulla-Menashe, D., Motesharrei, S., Song, X.-P., Kalnay, E., Ying, Q., Li, S., and Ma, Z.: Inconsistent  
 6279 estimates of forest cover change in China between 2000 and 2013 from multiple datasets: differences in  
 6280 parameters, spatial resolution, and definitions, *Sci Rep*, 7, 8748,  
 6281 <https://doi.org/10.1038/s41598-017-07732-5>, 2017.
- 6282 Li, Y., Yuan, S., Fan, S., Song, Y., Wang, Z., Yu, Z., Yu, Q., and Liu, Y.: Satellite Remote Sensing for Estimating  
 6283 PM2.5 and Its Components, *Curr Pollution Rep*, 7, 72–87, <https://doi.org/10.1007/s40726-020-00170-4>,  
 6284 2021b.



- 6285 Li, Y., Janssen, T. A. J., Chen, R., He, B., and Veraverbeke, S.: Trends and drivers of Arctic-boreal fire intensity  
 6286 between 2003 and 2022, *Science of The Total Environment*, 926, 172020,  
 6287 <https://doi.org/10.1016/j.scitotenv.2024.172020>, 2024.
- 6288 Li, Z. and Yu, W.: Economic Impact of the Los Angeles Wildfires, available at:  
 6289 [https://www.anderson.ucla.edu/about/centers/ucla-anderson-forecast/economic-impact-los-angeles-wildf](https://www.anderson.ucla.edu/about/centers/ucla-anderson-forecast/economic-impact-los-angeles-wildfires)  
 6290 ires (last access: 6th August 2025), 2025.
- 6291 Liang, Y., Sengupta, D., Campmier, M. J., Lunderberg, D. M., Apte, J. S., and Goldstein, A. H.: Wildfire smoke  
 6292 impacts on indoor air quality assessed using crowdsourced data in California, *Proc. Natl. Acad. Sci.*  
 6293 U.S.A., 118, e2106478118, <https://doi.org/10.1073/pnas.2106478118>, 2021.
- 6294 Libonati, R., Geirinhas, J. L., Silva, P. S., Russo, A., Rodrigues, J. A., Belém, L. B. C., Nogueira, J., Roque, F. O.,  
 6295 DaCamara, C. C., Nunes, A. M. B., Marengo, J. A., and Trigo, R. M.: Assessing the role of compound  
 6296 drought and heatwave events on unprecedented 2020 wildfires in the Pantanal, *Environ. Res. Lett.*, 17,  
 6297 015005, <https://doi.org/10.1088/1748-9326/ac462e>, 2022.
- 6298 Lin, Y. C., Jenkins, S. F., Chow, J. R., Biass, S., Woo, G., and Lallemand, D.: Modeling Downward Counterfactual  
 6299 Events: Unrealized Disasters and why they Matter, *Front. Earth Sci.*, 8, 575048,  
 6300 <https://doi.org/10.3389/feart.2020.575048>, 2020.
- 6301 Linley, G. D., Jolly, C. J., Doherty, T. S., Geary, W. L., Armenteras, D., Belcher, C. M., Bliege Bird, R., Duane, A.,  
 6302 Fletcher, M.-S., Giorgis, M. A., Haslem, A., Jones, G. M., Kelly, L. T., Lee, C. K. F., Nolan, R. H., Parr, C.  
 6303 L., Pausas, J. G., Price, J. N., Regos, A., Ritchie, E. G., Ruffault, J., Williamson, G. J., Wu, Q., and  
 6304 Nimmo, D. G.: What do you mean, 'megafire'?, *Global Ecology and Biogeography*, 31, 1906–1922,  
 6305 <https://doi.org/10.1111/geb.13499>, 2022.
- 6306 Linley, G. D., Jolly, C. J., Doherty, T. S., Geary, W. L., Armenteras, D., Belcher, C. M., Bliege Bird, R., Duane, A.,  
 6307 Fletcher, M.-S., Giorgis, M. A., Haslem, A., Jones, G. M., Kelly, L. T., Lee, C. K. F., Nolan, R. H., Parr, C.  
 6308 L., Pausas, J. G., Price, J. N., Regos, A., Ritchie, E. G., Ruffault, J., Williamson, G. J., Wu, Q., and  
 6309 Nimmo, D. G.: 'Megafire'—You May Not Like It, But You Cannot Avoid It, *Global Ecology and*  
 6310 *Biogeography*, 34, e70032, <https://doi.org/10.1111/geb.70032>, 2025.
- 6311 Littell, J. S., Peterson, D. L., Riley, K. L., Liu, Y., and Luce, C. H.: A review of the relationships between drought  
 6312 and forest fire in the United States, *Glob Chang Biol*, 22, 2353–2369, <https://doi.org/10.1111/gcb.13275>,  
 6313 2016.
- 6314 Liu, Z. and Eden, J.: State of Wildfires 2024-25 - GWL FWI projections [Data set], Zenodo,  
 6315 <https://doi.org/10.5281/ZENODO.15790287>, 2025.
- 6316 Liu, Z., Eden, J. M., Dieppois, B., and Blackett, M.: A global view of observed changes in fire weather extremes:  
 6317 uncertainties and attribution to climate change, *Climatic Change*, 173, 14,  
 6318 <https://doi.org/10.1007/s10584-022-03409-9>, 2022a.
- 6319 Liu, Z., Eden, J. M., Dieppois, B., Drobyshev, I., Gallo, C., and Blackett, M.: Were Meteorological Conditions  
 6320 Related to the 2020 Siberia Wildfires Made More Likely by Anthropogenic Climate Change? [in  
 6321 "Explaining Extreme Events in 2020 from a Climate Perspective"], *Bulletin of the American*  
 6322 *Meteorological Society*, 103, S44–S49, 2022b.
- 6323 Liu, Z., Eden, J., Dieppois, B., Drobyshev, I., Conradie, S., Gallo, C., and Blackett, M.: Collective attribution and  
 6324 future risk assessment of recent high-impact wildfire events, *EGU23*,  
 6325 <https://doi.org/10.5194/egusphere-egu23-14441>, 2023a.



- 6326 Liu, Z., Eden, J. M., Dieppo, B., Conradie, W. S., and Blackett, M.: The April 2021 Cape Town Wildfire: Has  
 6327 Anthropogenic Climate Change Altered the Likelihood of Extreme Fire Weather?,  
 6328 <https://doi.org/10.1175/BAMS-D-22-0204.1>, 2023b.
- 6329 Lizundia-Loiola, J., Otón, G., Ramo, R., and Chuvieco, E.: A spatio-temporal active-fire clustering approach for  
 6330 global burned area mapping at 250 m from MODIS data, *Remote Sensing of Environment*, 236, 111493,  
 6331 <https://doi.org/10.1016/j.rse.2019.111493>, 2020a.
- 6332 Lizundia-Loiola, J., Pettinari, M. L., and Chuvieco, E.: Temporal Anomalies in Burned Area Trends: Satellite  
 6333 Estimations of the Amazonian 2019 Fire Crisis, *Remote Sensing*, 12, 151,  
 6334 <https://doi.org/10.3390/rs12010151>, 2020b.
- 6335 Lizundia-Loiola, J., Franquesa, M., Khairoun, A., and Chuvieco, E.: Global burned area mapping from Sentinel-3  
 6336 Synergy and VIIRS active fires, *Remote Sensing of Environment*, 282, 113298,  
 6337 <https://doi.org/10.1016/j.rse.2022.113298>, 2022.
- 6338 Los Angeles County Economic Development Corporation: Impact of 2025 Los Angeles Wildfires and  
 6339 Comparative Study  
 6340 <https://laedc.org/wp-content/uploads/2025/02/LAEDC-2025-LA-Wildfires-Study.pdf>, 2025.
- 6341 Luque, M. A. M., Leon, E., Ardila, J. G. B., Gutiérrez, G., Bilbao, B., Rivera-Lombardi, R., and Milán, A.:  
 6342 Community Forest Brigades and their implementation as part of a new vision in the integrated fire  
 6343 management in the Bolivarian Republic of Venezuela, *Biodiversidade Brasileira*, 10, 49–49,  
 6344 <https://doi.org/10.37002/biodiversidadebrasileira.v10i1.1624>, 2020.
- 6345 Lüthi, S., Aznar-Siguan, G., Fairless, C., and Bresch, D. N.: Globally consistent assessment of economic impacts  
 6346 of wildfires in CLIMADA v2.2, *Geoscientific Model Development*, 14, 7175–7187,  
 6347 <https://doi.org/10.5194/gmd-14-7175-2021>, 2021.
- 6348 Machado-Silva, F., Libonati, R., Melo De Lima, T. F., Bittencourt Peixoto, R., De Almeida França, J. R., De Avelar  
 6349 Figueiredo Mafra Magalhães, M., Lemos Maia Santos, F., Abrantes Rodrigues, J., and DaCamara, C.  
 6350 C.: Drought and fires influence the respiratory diseases hospitalizations in the Amazon, *Ecological*  
 6351 *Indicators*, 109, 105817, <https://doi.org/10.1016/j.ecolind.2019.105817>, 2020.
- 6352 Maher, N., Milinski, S., and Ludwig, R.: Large ensemble climate model simulations: introduction, overview, and  
 6353 future prospects for utilising multiple types of large ensemble, *Earth Syst. Dynam.*, 12, 401–418,  
 6354 <https://doi.org/10.5194/esd-12-401-2021>, 2021.
- 6355 Majasalmi, T. and Rautiainen, M.: Representation of tree cover in global land cover products: Finland as a case  
 6356 study area, *Environ Monit Assess*, 193, 121, <https://doi.org/10.1007/s10661-021-08898-2>, 2021.
- 6357 Malhi, Y., Wood, D., Baker, T. R., Wright, J., Phillips, O. L., Cochrane, T., Meir, P., Chave, J., Almeida, S., Arroyo,  
 6358 L., Higuchi, N., Killeen, T. J., Laurance, S. G., Laurance, W. F., Lewis, S. L., Monteagudo, A., Neill, D.  
 6359 A., Vargas, P. N., Pitman, N. C. A., Quesada, C. A., Salomão, R., Silva, J. N. M., Lezama, A. T.,  
 6360 Terborgh, J., Martínez, R. V., and Vinceti, B.: The regional variation of aboveground live biomass in  
 6361 old-growth Amazonian forests, *Global Change Biology*, 12, 1107–1138,  
 6362 <https://doi.org/10.1111/j.1365-2486.2006.01120.x>, 2006.
- 6363 Maraun, D., Shepherd, T. G., Widmann, M., Zappa, G., Walton, D., Gutiérrez, J. M., Hagemann, S., Richter, I.,  
 6364 Soares, P. M. M., Hall, A., and Mearns, L. O.: Towards process-informed bias correction of climate  
 6365 change simulations, *Nature Clim Change*, 7, 764–773, <https://doi.org/10.1038/nclimate3418>, 2017.





- 6366 Mariani, M., Fletcher, M.-S., Holz, A., and Nyman, P.: ENSO controls interannual fire activity in southeast  
 6367 Australia, *Geophysical Research Letters*, 43, 10,891–10,900, <https://doi.org/10.1002/2016GL070572>,  
 6368 2016.
- 6369 Marques, J. F., Alves, M. B., Silveira, C. F., Amaral e Silva, A., Silva, T. A., dos Santos, V. J., and Calijuri, M. L.:  
 6370 Fires dynamics in the Pantanal: Impacts of anthropogenic activities and climate change, *Journal of*  
 6371 *Environmental Management*, 299, 113586, <https://doi.org/10.1016/j.jenvman.2021.113586>, 2021.
- 6372 Masoudian, E., Mirzaei, A., and Bagheri, H.: Assessing wildfire susceptibility in Iran: Leveraging machine learning  
 6373 for geospatial analysis of climatic and anthropogenic factors, *Trees, Forests and People*, 19, 100774,  
 6374 <https://doi.org/10.1016/j.tfp.2025.100774>, 2025.
- 6375 Mastrandrea, M. D., Field, C. B., Stocker, T. F., Edenhofer, O., Ebi, K. L., Frame, D. J., Held, H., Kriegler, E.,  
 6376 Mach, K. J., Matschoss, P. R., Plattner, G.-K., Yohe, G. W., and Zwiers, F. W.: Guidance note for lead  
 6377 authors of the IPCC fifth assessment report on consistent treatment of uncertainties. Intergovernmental  
 6378 Panel on Climate Change (IPCC), <http://www.ipcc.ch>, 2010.
- 6379 Mataveli, G., Jones, M. W., Carmenta, R., Sanchez, A., Dutra, D. J., Chaves, M., de Oliveira, G., Anderson, L. O.,  
 6380 and Aragão, L. E. O. C.: Deforestation falls but rise of wildfires continues degrading Brazilian Amazon  
 6381 forests, *Global Change Biology*, 30, e17202, <https://doi.org/10.1111/gcb.17202>, 2024.
- 6382 Mataveli, G., Maure, L. A., Sanchez, A., Dutra, D. J., de Oliveira, G., Jones, M. W., Amaral, C., Artaxo, P., and  
 6383 Aragão, L. E. O. C.: Forest Degradation Is Undermining Progress on Deforestation in the Amazon,  
 6384 *Global Change Biology*, 31, e70209, <https://doi.org/10.1111/gcb.70209>, 2025.
- 6385 Mathison, C., Burke, E., Hartley, A. J., Kelley, D. I., Burton, C., Robertson, E., Gedney, N., Williams, K., Wiltshire,  
 6386 A., Ellis, R. J., Sellar, A. A., and Jones, C. D.: Description and evaluation of the JULES-ES set-up for  
 6387 ISIMIP2b, *Geoscientific Model Development*, 16, 4249–4264,  
 6388 <https://doi.org/10.5194/gmd-16-4249-2023>, 2023.
- 6389 Matthews, S.: A comparison of fire danger rating systems for use in forests, *Australian Meteorological and*  
 6390 *Oceanographic Journal*, 58, 41–48, <https://doi.org/10.22499/2.5801.005>, 2009.
- 6391 Mattson-Teig, B.: January 2025 Economist Snapshot: Los Angeles Wildfires Recovery Will Be Costly and  
 6392 Lengthy, available at:  
 6393 [https://urbanland.uli.org/capital-markets-and-finance/january-economist-snapshot-los-angeles-wildfires-r](https://urbanland.uli.org/capital-markets-and-finance/january-economist-snapshot-los-angeles-wildfires-recovery-will-be-costly-and-lengthy)  
 6394 [ecovery-will-be-costly-and-lengthy](https://urbanland.uli.org/capital-markets-and-finance/january-economist-snapshot-los-angeles-wildfires-recovery-will-be-costly-and-lengthy) (last access: 6th August 2025), Urban Land, 2025.
- 6395 Mauritsen, T., Bader, J., Becker, T., Behrens, J., Bittner, M., Brokopf, R., Brovkin, V., Claussen, M., Crueger, T.,  
 6396 Esch, M., Fast, I., Fiedler, S., Fläschner, D., Gayler, V., Giorgetta, M., Goll, D. S., Haak, H., Hagemann,  
 6397 S., Hedemann, C., Hohenegger, C., Ilyina, T., Jahns, T., Jimenez-de-la-Cuesta, D., Jungclaus, J.,  
 6398 Kleinen, T., Kloster, S., Kracher, D., Kinne, S., Kleberg, D., Lasslop, G., Kornblueh, L., Marotzke, J.,  
 6399 Matei, D., Meraner, K., Mikolajewicz, U., Modali, K., Möbis, B., Müller, W. A., Nabel, J. E. M. S., Nam, C.  
 6400 C. W., Notz, D., Nyawira, S.-S., Paulsen, H., Peters, K., Pincus, R., Pohlmann, H., Pongratz, J., Popp,  
 6401 M., Raddatz, T. J., Rast, S., Redler, R., Reick, C. H., Rohrschneider, T., Schemann, V., Schmidt, H.,  
 6402 Schnur, R., Schulzweida, U., Six, K. D., Stein, L., Stemmler, I., Stevens, B., von Storch, J.-S., Tian, F.,  
 6403 Voigt, A., Vrese, P., Wieners, K.-H., Wilkenskjaeld, S., Winkler, A., and Roeckner, E.: Developments in the  
 6404 MPI-M Earth System Model version 1.2 (MPI-ESM1.2) and Its Response to Increasing CO<sub>2</sub>, *Journal of*  
 6405 *Advances in Modeling Earth Systems*, 11, 998–1038, <https://doi.org/10.1029/2018MS001400>, 2019.



- 6406 McCulloch, M. T., Winter, A., Sherman, C. E., and Trotter, J. A.: 300 years of sclerosponge thermometry shows  
 6407 global warming has exceeded 1.5 °C, *Nat. Clim. Chang.*, 14, 171–177,  
 6408 <https://doi.org/10.1038/s41558-023-01919-7>, 2024.
- 6409 McNorton, J., Agustí-Panareda, A., Arduini, G., Balsamo, G., Bousserez, N., Boussetta, S., Chericoni, M.,  
 6410 Choulga, M., Engelen, R., and Guevara, M.: An Urban Scheme for the ECMWF Integrated Forecasting  
 6411 System: Global Forecasts and Residential CO<sub>2</sub> Emissions, *Journal of Advances in Modeling Earth*  
 6412 *Systems*, 15, e2022MS003286, <https://doi.org/10.1029/2022MS003286>, 2023.
- 6413 McNorton, J. R. and Di Giuseppe, F.: A global fuel characteristic model and dataset for wildfire prediction,  
 6414 *Biogeosciences*, 21, 279–300, <https://doi.org/10.5194/bg-21-279-2024>, 2024.
- 6415 McNorton, J. R., Giuseppe, F. D., Pinnington, E. M., Chantry, M., and Barnard, C.: A Global Probability-of-Fire  
 6416 (PoF) Forecast, *Geophysical Research Letters*, 51, e2023GL107929,  
 6417 <https://doi.org/10.1029/2023GL107929>, 2024.
- 6418 McPhaden, M. J., Jarugula, S., Aroucha, L. C., and Lübbecke, J. F.: Indian Ocean Dipole intensifies Benguela  
 6419 Niño through Congo River discharge, *Commun Earth Environ*, 5, 779,  
 6420 <https://doi.org/10.1038/s43247-024-01955-x>, 2024.
- 6421 Meier, S., Strobl, E., Elliott, R. J. R., and Kettridge, N.: Cross-country risk quantification of extreme wildfires in  
 6422 Mediterranean Europe, 2023b, *Risk Analysis*, 43, 1745–1762, <https://doi.org/10.1111/risa.14075>, 2023a.
- 6423 Meier, S., Elliott, R. J. R., and Strobl, E.: The regional economic impact of wildfires: Evidence from Southern  
 6424 Europe, 2023a, *Journal of Environmental Economics and Management*, 118, 102787,  
 6425 <https://doi.org/10.1016/j.jeem.2023.102787>, 2023b.
- 6426 Meier, S., Strobl, E., and Elliott, R. J. R.: The impact of wildfire smoke exposure on excess mortality and later-life  
 6427 socioeconomic outcomes: the Great Fire of 1910, *Cliometrica*, 19, 279–342,  
 6428 <https://doi.org/10.1007/s11698-024-00297-0>, 2025.
- 6429 Menezes, L. S., De Oliveira, A. M., Santos, F. L. M., Russo, A., De Souza, R. A. F., Roque, F. O., and Libonati,  
 6430 R.: Lightning patterns in the Pantanal: Untangling natural and anthropogenic-induced wildfires, *Science*  
 6431 *of The Total Environment*, 820, 153021, <https://doi.org/10.1016/j.scitotenv.2022.153021>, 2022.
- 6432 Mengel, M., Treu, S., Lange, S., and Frieler, K.: ATTRICI v1.1 – counterfactual climate for impact attribution,  
 6433 *Geoscientific Model Development*, 14, 5269–5284, <https://doi.org/10.5194/gmd-14-5269-2021>, 2021.
- 6434 Michaelowa, A., Michaelowa, K., Shishlov, I., and Brescia, D.: Catalysing private and public action for climate  
 6435 change mitigation: the World Bank’s role in international carbon markets, *Climate Policy*, 21, 120–132,  
 6436 <https://doi.org/10.1080/14693062.2020.1790334>, 2021.
- 6437 Mills, G., Salkin, O., Fearon, M., Harris, S., Brown, T., and Reinbold, H.: Meteorological drivers of the eastern  
 6438 Victorian Black Summer (2019–2020) fires, *J. South. Hemisph. Earth Syst. Sci.*, 72, 139–163,  
 6439 <https://doi.org/10.1071/ES22011>, 2022.
- 6440 Mindlin, J., Vera, C. S., Shepherd, T. G., and Osman, M.: Plausible Drying and Wetting Scenarios for Summer in  
 6441 Southeastern South America, *Journal of Climate*, 36, 7973–7991,  
 6442 <https://doi.org/10.1175/JCLI-D-23-0134.1>, 2023.
- 6443 Ministerio de Medio Ambiente y agua: Ministerio de Medio Ambiente Lleva Adelante su Rendición Pública de  
 6444 Cuentas Inicial, available at:



- 6445 <https://www.mmaya.gob.bo/2025/04/14/ministerio-de-medio-ambiente-lleva-adelante-su-rendicion-publica-de-cuentas-inicial-2025/> (last access: 6th August 2025), Ministerio de Medio Ambiente y Agua, 2025.
- 6446
- 6447 Modaresi Rad, A., Abatzoglou, J. T., Kreidler, J., Alizadeh, M. R., AghaKouchak, A., Hudyma, N., Nauslar, N. J.,  
 6448 and Sadegh, M.: Human and infrastructure exposure to large wildfires in the United States, *Nat Sustain*,  
 6449 6, 1343–1351, <https://doi.org/10.1038/s41893-023-01163-z>, 2023.
- 6450 Morcrette, J.-J., Boucher, O., Jones, L., Salmond, D., Bechtold, P., Beljaars, A., Benedetti, A., Bonet, A., Kaiser,  
 6451 J. W., Razinger, M., Schulz, M., Serrar, S., Simmons, A. J., Sofiev, M., Suttie, M., Tompkins, A. M., and  
 6452 Untch, A.: Aerosol analysis and forecast in the European Centre for Medium-Range Weather Forecasts  
 6453 Integrated Forecast System: Forward modeling, *Journal of Geophysical Research: Atmospheres*, 114,  
 6454 <https://doi.org/10.1029/2008JD011235>, 2009.
- 6455 Moreira, F., Ascoli, D., Safford, H., Adams, M. A., Moreno, J. M., Pereira, J. M. C., Catry, F. X., Armesto, J., Bond,  
 6456 W., González, M. E., Curt, T., Koutsias, N., McCaw, L., Price, O., Pausas, J. G., Rigolot, E., Stephens,  
 6457 S., Tavsanoğlu, C., Vallejo, V. R., Wilgen, B. W. V., Xanthopoulos, G., and Fernandes, P. M.: Wildfire  
 6458 management in Mediterranean-type regions: paradigm change needed, *Environ. Res. Lett.*, 15, 011001,  
 6459 <https://doi.org/10.1088/1748-9326/ab541e>, 2020.
- 6460 Morningstar DBRS: Aftermath of Los Angeles Wildfires: A Wake-Up Call for Property & Casualty Insurers and  
 6461 Regulators, available at:  
 6462 [https://dbrs.morningstar.com/research/451515/aftermath-of-los-angeles-wildfires-a-wake-up-call-for-prop](https://dbrs.morningstar.com/research/451515/aftermath-of-los-angeles-wildfires-a-wake-up-call-for-property-casualty-insurers-and-regulators)  
 6463 [erty-casualty-insurers-and-regulators](https://dbrs.morningstar.com/research/451515/aftermath-of-los-angeles-wildfires-a-wake-up-call-for-property-casualty-insurers-and-regulators) (last access: 6th August 2025), 2025.
- 6464 Muñoz-Sabater, J., Dutra, E., Agustí-Panareda, A., Albergel, C., Arduini, G., Balsamo, G., Boussetta, S.,  
 6465 Choulga, M., Harrigan, S., Hersbach, H., Martens, B., Miralles, D. G., Piles, M., Rodríguez-Fernández,  
 6466 N. J., Zsoter, E., Buontempo, C., and Thépaut, J.-N.: ERA5-Land: a state-of-the-art global reanalysis  
 6467 dataset for land applications, *Earth System Science Data*, 13, 4349–4383,  
 6468 <https://doi.org/10.5194/essd-13-4349-2021>, 2021.
- 6469 Murray, C. J. L., Aravkin, A. Y., Zheng, P., Abbafati, C., Abbas, K. M., Abbasi-Kangevari, M., Abd-Allah, F.,  
 6470 Abdelalim, A., Abdollahi, M., Abdollahpour, I., Abegaz, K. H., Abolhassani, H., Aboyans, V., Abreu, L. G.,  
 6471 Abrigo, M. R. M., Abualhasan, A., Abu-Raddad, L. J., Abushouk, A. I., Adabi, M., Adekanmbi, V.,  
 6472 Adeoye, A. M., Adetokunboh, O. O., Adham, D., Advani, S. M., Agarwal, G., Aghamir, S. M. K., Agrawal,  
 6473 A., Ahmad, T., Ahmadi, K., Ahmadi, M., Ahmadieh, H., Ahmed, M. B., Akalu, T. Y., Akinyemi, R. O.,  
 6474 Akinyemiju, T., Akombi, B., Akunna, C. J., Alahdab, F., Al-Aly, Z., Alam, K., Alam, S., Alam, T., Alanezi,  
 6475 F. M., Alanzi, T. M., Alemu, B. wassihun, Alhabib, K. F., Ali, M., Ali, S., Alicandro, G., Alinia, C., Alipour,  
 6476 V., Alizade, H., Aljunid, S. M., Alla, F., Allebeck, P., Almasi-Hashiani, A., Al-Mekhlafi, H. M., Alonso, J.,  
 6477 Altirkawi, K. A., Amini-Rarani, M., Amiri, F., Amugsi, D. A., Ancuceanu, R., Anderlini, D., Anderson, J. A.,  
 6478 Andrei, C. L., Andrei, T., Angus, C., Anjomshoa, M., Ansari, F., Ansari-Moghaddam, A., Antonazzo, I. C.,  
 6479 Antonio, C. A. T., Antony, C. M., Antriyandarti, E., Anvari, D., Anwer, R., Appiah, S. C. Y., Arabloo, J.,  
 6480 Arab-Zozani, M., Ariani, F., Armoon, B., Ärnlov, J., Arzani, A., Asadi-Aliabadi, M., Asadi-Pooya, A. A.,  
 6481 Ashbaugh, C., Assmus, M., Atafar, Z., Atnafu, D. D., Atout, M. M. W., Ausloos, F., Ausloos, M.,  
 6482 Quintanilla, B. P. A., Ayano, G., Ayanore, M. A., Azari, S., Azarian, G., Azene, Z. N., et al.: Global  
 6483 burden of 87 risk factors in 204 countries and territories, 1990–2019: a systematic analysis for the  
 6484 Global Burden of Disease Study 2019, *The Lancet*, 396, 1223–1249,  
 6485 [https://doi.org/10.1016/S0140-6736\(20\)30752-2](https://doi.org/10.1016/S0140-6736(20)30752-2), 2020.
- 6486 N1info: Serbia sees 135 wildfires in the past 24 hours, available at:  
 6487 <https://n1info.rs/english/news/serbia-sees-135-wildfires-in-the-past-24-hours/> (last access: 6th August  
 6488 2025), N1, 2024.



- 6489 Narita, D., Gavrilieva, T., and Isaev, A.: Impacts and management of forest fires in the Republic of Sakha,  
 6490 Russia: A local perspective for a global problem, *Polar Science*, 27, 100573,  
 6491 <https://doi.org/10.1016/j.polar.2020.100573>, 2021.
- 6492 NASA Earth Observatory: Early Fires in Brazil's Pantanal, available at:  
 6493 <https://earthobservatory.nasa.gov/images/152925/early-fires-in-brazils-pantanal> (last access: 6th August  
 6494 2025), 2024a.
- 6495 NASA Earth Observatory: Fire in Southern Mexico, available at:  
 6496 <https://earthobservatory.nasa.gov/images/152628/fire-in-southern-mexico> (last access: 6th August  
 6497 2025), 2024b.
- 6498 NASA Earth Observatory: Intense, Widespread Drought Grips South America, available at:  
 6499 <https://earthobservatory.nasa.gov/images/153447/intense-widespread-drought-grips-south-america> (last  
 6500 access: 6th August 2025), 2024c.
- 6501 NASA FIRMS: Fire Information for Resource Management System. MODIS and VIIRS Fire Data, available at:  
 6502 [https://firms.modaps.eosdis.nasa.gov/\[data set\]](https://firms.modaps.eosdis.nasa.gov/[data set]) (last access: 6 August 2025), 2025.
- 6503 National Centers for Environmental Information (NCEI): U.S. Drought: Monthly Changes and Impacts for June  
 6504 2025, available at: <https://www.ncei.noaa.gov/news/us-drought-monthly-report-june-2025> (last access:  
 6505 6th August 2025), 2025.
- 6506 National Interagency Coordination Center: National Interagency Coordination Center Wildland Fire Summary and  
 6507 Statistics Annual Report 2024  
 6508 [https://www.nifc.gov/sites/default/files/NICC/2-Predictive%20Services/Intelligence/Annual%20Reports/2](https://www.nifc.gov/sites/default/files/NICC/2-Predictive%20Services/Intelligence/Annual%20Reports/2024/annual_report_2024.pdf)  
 6509 [024/annual\\_report\\_2024.pdf](https://www.nifc.gov/sites/default/files/NICC/2-Predictive%20Services/Intelligence/Annual%20Reports/2024/annual_report_2024.pdf), 2024.
- 6510 National Interagency Fire Center (NIFC): National Significant Wildland Fire Potential Outlook, available at:  
 6511 [https://www.nifc.gov/nicc-files/predictive/outlooks/monthly\\_seasonal\\_outlook.pdf](https://www.nifc.gov/nicc-files/predictive/outlooks/monthly_seasonal_outlook.pdf) (last access: 6th  
 6512 August 2025), 2025.
- 6513 N'Dri, A. B., Soro, T. D., Gignoux, J., Dosso, K., Koné, M., N'Dri, J. K., Koné, N. A., and Barot, S.: Season affects  
 6514 fire behavior in annually burned humid savanna of West Africa, *Fire Ecology*, 14, 5,  
 6515 <https://doi.org/10.1186/s42408-018-0005-9>, 2018.
- 6516 N'Dri, A. B., Kpangba, K. P., Werner, P. A., Koffi, K. F., and Bakayoko, A.: The response of sub-adult savanna  
 6517 trees to six successive annual fires: An experimental field study on the role of fire season, *Journal of*  
 6518 *Applied Ecology*, 59, 1347–1361, <https://doi.org/10.1111/1365-2664.14149>, 2022.
- 6519 N'Dri, A. B., Kpré, A. J.-N., and Doumbia, A.: Managing fires in a woody encroachment context: Fine fuel load  
 6520 does not change across fire seasons in a Guinean savanna (West Africa), *Journal of Environmental*  
 6521 *Management*, 371, 123236, <https://doi.org/10.1016/j.jenvman.2024.123236>, 2024.
- 6522 NERC Environmental Data Service: EUCLEIA: European Climate and weather Events: Interpretation and  
 6523 Attribution [Data set], 2025.
- 6524 Neris, J., Santin, C., Lew, R., Robichaud, P. R., Elliot, W. J., Lewis, S. A., Sheridan, G., Rohlf, A.-M., Ollivier, Q.,  
 6525 Oliveira, L., and Doerr, S. H.: Designing tools to predict and mitigate impacts on water quality following  
 6526 the Australian 2019/2020 wildfires: Insights from Sydney's largest water supply catchment, *Integrated*  
 6527 *Environmental Assessment and Management*, 17, 1151–1161, <https://doi.org/10.1002/ieam.4406>, 2021.



- 6528 New York Times: Swept by the Fires, Away From Their Lives, available at:  
 6529 <https://www.nytimes.com/2025/05/16/realestate/la-fire-victims-altadena-palisades.html> (last access: 6th  
 6530 August 2025), The New York Times, 2025.
- 6531 Newton, P., Kinzer, A. T., Miller, D. C., Oldekop, J. A., and Agrawal, A.: The Number and Spatial Distribution of  
 6532 Forest-Proximate People Globally, *One Earth*, 3, 363–370, <https://doi.org/10.1016/j.oneear.2020.08.016>,  
 6533 2020.
- 6534 NHK (Japan Broadcasting Corporation): Wildfire declared extinguished in Japan's Ofunato City after 40 days,  
 6535 available at: [https://www3.nhk.or.jp/nhkworld/en/news/20250408\\_01/](https://www3.nhk.or.jp/nhkworld/en/news/20250408_01/) (last access: 6th August 2025),  
 6536 2025.
- 6537 Nielsen-Pincus, M., Moseley, C., and Gebert, K.: Job growth and loss across sectors and time in the western US:  
 6538 The impact of large wildfires, *Forest Policy and Economics*, 38, 199–206,  
 6539 <https://doi.org/10.1016/j.forpol.2013.08.010>, 2014.
- 6540 Nikolakis, W., Welham, C., and Greene, G.: Diffusion of indigenous fire management and carbon-credit  
 6541 programs: Opportunities and challenges for “scaling-up” to temperate ecosystems, *Front. For. Glob.*  
 6542 *Change*, 5, 967653, <https://doi.org/10.3389/ffgc.2022.967653>, 2022.
- 6543 NOAA Climate Prediction Center (CPC): ENSO: Recent Evolution, Current Status and Predictions, available at:  
 6544 <https://www.cpc.ncep.noaa.gov/> (last access: 6th August 2025), 2024.
- 6545 NOAA National Centers for Environmental Information: Monthly Global Climate Report for Annual 2024, available  
 6546 at: <https://www.ncei.noaa.gov/access/monitoring/monthly-report/global/202413> (last access: 6th August  
 6547 2025), 2025.
- 6548 Noble, I. R., Gill, A. M., and Bary, G. a. V.: McArthur's fire-danger meters expressed as equations, *Australian*  
 6549 *Journal of Ecology*, 5, 201–203, <https://doi.org/10.1111/j.1442-9993.1980.tb01243.x>, 1980.
- 6550 Nolan, R. H., Collins, L., Leigh, A., Ooi, M. K. J., Curran, T. J., Fairman, T. A., Resco de Dios, V., and Bradstock,  
 6551 R.: Limits to post-fire vegetation recovery under climate change, 2021a, *Plant, Cell & Environment*, 44,  
 6552 3471–3489, <https://doi.org/10.1111/pce.14176>, 2021a.
- 6553 Nolan, R. H., Bowman, D. M. J. S., Clarke, H., Haynes, K., Ooi, M. K. J., Price, O. F., Williamson, G. J.,  
 6554 Whittaker, J., Bedward, M., Boer, M. M., Cavanagh, V. I., Collins, L., Gibson, R. K., Griebel, A., Jenkins,  
 6555 M. E., Keith, D. A., McIlwee, A. P., Penman, T. D., Samson, S. A., Tozer, M. G., and Bradstock, R. A.:  
 6556 What Do the Australian Black Summer Fires Signify for the Global Fire Crisis?, 2021b, *Fire*, 4, 97,  
 6557 <https://doi.org/10.3390/fire4040097>, 2021b.
- 6558 Novinite: Bulgaria's Prime Minister Calls for Aid as Fires Threaten Yambol Villages, 2024.
- 6559 Nunes, J. P., Doerr, S. H., Sheridan, G., Neris, J., Santín, C., Emelko, M. B., Silins, U., Robichaud, P. R., Elliot,  
 6560 W. J., and Keizer, J.: Assessing water contamination risk from vegetation fires: Challenges,  
 6561 opportunities and a framework for progress, *Hydrological Processes*, 32, 687–694,  
 6562 <https://doi.org/10.1002/hyp.11434>, 2018.
- 6563 Nunes, V.: Pantanal em chamas: Incêndio na Serra do Amolar mobiliza forças e alerta sobre a preservação  
 6564 ambiental, available at:  
 6565 [https://www.capitalnews.com.br/retrospectiva/2024/pantanal-em-chamas-incendio-na-serra-do-amolar-](https://www.capitalnews.com.br/retrospectiva/2024/pantanal-em-chamas-incendio-na-serra-do-amolar-mobiliza-forcas-e-alerta-sobre-a-preservacao-ambiental/414842)  
 6566 [mobiliza-forcas-e-alerta-sobre-a-preservacao-ambiental/414842](https://www.capitalnews.com.br/retrospectiva/2024/pantanal-em-chamas-incendio-na-serra-do-amolar-mobiliza-forcas-e-alerta-sobre-a-preservacao-ambiental/414842) (last access: 6th August 2025),  
 6567 *Notícias de Campo Grande e MS - Capital News*, 2025.



- 6568 O'Dell, K., Ford, B., Fischer, E. V., and Pierce, J. R.: Contribution of Wildland-Fire Smoke to US PM<sub>2.5</sub> and Its  
 6569 Influence on Recent Trends, Environ. Sci. Technol., 53, 1797–1804,  
 6570 <https://doi.org/10.1021/acs.est.8b05430>, 2019.
- 6571 OECD: Taming Wildfires in the Context of Climate Change, OECD, <https://doi.org/10.1787/dd00c367-en>, 2023.
- 6572 Olson, D. M., Dinerstein, E., Wikramanayake, E. D., Burgess, N. D., Powell, G. V. N., Underwood, E. C., D'amico,  
 6573 J. A., Itoua, I., Strand, H. E., Morrison, J. C., Loucks, C. J., Allnutt, T. F., Ricketts, T. H., Kura, Y.,  
 6574 Lamoreux, J. F., Wettengel, W. W., Hedao, P., and Kassem, K. R.: Terrestrial Ecoregions of the World: A  
 6575 New Map of Life on Earth, BioScience, 51, 933,  
 6576 [https://doi.org/10.1641/0006-3568\(2001\)051\[0933:TEOTWA\]2.0.CO;2](https://doi.org/10.1641/0006-3568(2001)051[0933:TEOTWA]2.0.CO;2), 2001.
- 6577 Otón, G., Lizundia-Loiola, J., Pettinari, M. L., and Chuvieco, E.: Development of a consistent global long-term  
 6578 burned area product (1982–2018) based on AVHRR-LTDR data, International Journal of Applied Earth  
 6579 Observation and Geoinformation, 103, 102473, <https://doi.org/10.1016/j.jag.2021.102473>, 2021.
- 6580 Otto, F. E. L., Philip, S., Kew, S., Li, S., King, A., and Cullen, H.: Attributing high-impact extreme events across  
 6581 timescales—a case study of four different types of events, Climatic Change, 149, 399–412,  
 6582 <https://doi.org/10.1007/s10584-018-2258-3>, 2018a.
- 6583 Otto, F. E. L., Van Der Wiel, K., Van Oldenborgh, G. J., Philip, S., Kew, S. F., Uhe, P., and Cullen, H.: Climate  
 6584 change increases the probability of heavy rains in Northern England/Southern Scotland like those of  
 6585 storm Desmond—a real-time event attribution revisited, Environ. Res. Lett., 13, 024006,  
 6586 <https://doi.org/10.1088/1748-9326/aa9663>, 2018b.
- 6587 Ozerkan, F.: Turkey battles forest fires for third day, available at:  
 6588 <https://phys.org/news/2024-08-turkey-forest-day.html> (last access: 6th August 2025), Phys.org, 2024.
- 6589 Page, S. E., Siegert, F., Rieley, J. O., Boehm, H.-D. V., Jaya, A., and Limin, S.: The amount of carbon released  
 6590 from peat and forest fires in Indonesia during 1997, Nature, 420, 61–65,  
 6591 <https://doi.org/10.1038/nature01131>, 2002.
- 6592 Pai, S. J., Carter, T. S., Heald, C. L., and Kroll, J. H.: Updated World Health Organization Air Quality Guidelines  
 6593 Highlight the Importance of Non-anthropogenic PM<sub>2.5</sub>, Environ. Sci. Technol. Lett., 9, 501–506,  
 6594 <https://doi.org/10.1021/acs.estlett.2c00203>, 2022.
- 6595 Pan, X., Chin, M., Ichoku, C. M., and Field, R. D.: Connecting Indonesian Fires and Drought With the Type of El  
 6596 Niño and Phase of the Indian Ocean Dipole During 1979–2016, Journal of Geophysical Research:  
 6597 Atmospheres, 123, 7974–7988, <https://doi.org/10.1029/2018JD028402>, 2018.
- 6598 Pan, X., Ichoku, C., Chin, M., Bian, H., Darmenov, A., Colarco, P., Ellison, L., Kucsera, T., da Silva, A., Wang, J.,  
 6599 Oda, T., and Cui, G.: Six global biomass burning emission datasets: intercomparison and application in  
 6600 one global aerosol model, Atmospheric Chemistry and Physics, 20, 969–994,  
 6601 <https://doi.org/10.5194/acp-20-969-2020>, 2020.
- 6602 Papelo, J.: Desastre ambiental: implicações das queimadas e desmatamentos no interior do País, available at:  
 6603 [https://novojournal.co.ao/opinioao/detalhe/desastre-ambiental-implicacoes-das-queimadas-e-desmatamen](https://novojournal.co.ao/opinioao/detalhe/desastre-ambiental-implicacoes-das-queimadas-e-desmatamentos-no-interior-do-pais-36744.html)  
 6604 [tos-no-interior-do-pais-36744.html](https://novojournal.co.ao/opinioao/detalhe/desastre-ambiental-implicacoes-das-queimadas-e-desmatamentos-no-interior-do-pais-36744.html) (last access: 6th August 2025), Novo Jornal, 2024.
- 6605 Parks Canada: Jasper Wildfire 2024, available at:  
 6606 <https://parks.canada.ca/pn-np/ab/jasper/visit/feu-alert-fire/feudeforet-jasper-wildfire> (last access: 6th  
 6607 August 2025), 2024.





- 6608 Parrington, M. and Di Tomaso, E.: Monitoring the 2024 Canada wildfires in CAMS, available at:  
 6609 <https://www.ecmwf.int/en/newsletter/181/news/monitoring-2024-canada-wildfires-cams> (last access: 6th  
 6610 August 2025), ECMWF, 2024.
- 6611 Parrington, M. and Di Tomaso, E.: Monitoring the 2024 Canada wildfires in CAMS, available at:  
 6612 <https://www.ecmwf.int/en/newsletter/181/news/monitoring-2024-canada-wildfires-cams> (last access: 6th  
 6613 August 2025), 2025.
- 6614 Pasadena Office of the City Manager: Pasadena Drinking Water System Impacted by Eaton Fire, available at:  
 6615 [https://www.cityofpasadena.net/city-manager/news/pasadena-drinking-water-system-impacted-by-eaton](https://www.cityofpasadena.net/city-manager/news/pasadena-drinking-water-system-impacted-by-eaton-fire/)  
 6616 -fire/ (last access: 6th August 2025), 2025.
- 6617 Pascoe, J., Shanks, M., Pascoe, B., Clarke, J., Goolmeier, T., Moggridge, B., Williamson, B., Miller, M., Costello,  
 6618 O., and Fletcher, M.: Lighting a pathway: Our obligation to culture and Country, *Eco Management*  
 6619 *Restoration*, 24, 153–155, <https://doi.org/10.1111/emr.12592>, 2023.
- 6620 Perron, M. M. G., Meyerink, S., Corkill, M., Strzelec, M., Proemse, B. C., Gault-Ringold, M., Sanz Rodriguez, E.,  
 6621 Chase, Z., and Bowie, A. R.: Trace elements and nutrients in wildfire plumes to the southeast of  
 6622 Australia, *Atmospheric Research*, 270, 106084, <https://doi.org/10.1016/j.atmosres.2022.106084>, 2022.
- 6623 Perry, M. C., Vanvyve, E., Betts, R. A., and Palin, E. J.: Past and future trends in fire weather for the UK, *Natural*  
 6624 *Hazards and Earth System Sciences*, 22, 559–575, <https://doi.org/10.5194/nhess-22-559-2022>, 2022.
- 6625 Persson, F.: Large reduction in the number of forest fire operations in 2024, Swedish Firefighters, available at:  
 6626 <https://firefighters.se/2024/10/14/stor-minskning-i-antalet-skogsbrandsinsatser-2024/> (last access: 6th  
 6627 August 2025), 2024.
- 6628 Peuch, V.-H., Engelen, R., Rixen, M., Dee, D., Flemming, J., Suttie, M., Ades, M., Agustí-Panareda, A.,  
 6629 Ananasso, C., Andersson, E., Armstrong, D., Barré, J., Bousserez, N., Dominguez, J. J., Garrigues, S.,  
 6630 Inness, A., Jones, L., Kipling, Z., Letertre-Danczak, J., Parrington, M., Razinger, M., Ribas, R.,  
 6631 Vermoote, S., Yang, X., Simmons, A., Marcilla, J. G. de, and Thépaut, J.-N.: The Copernicus  
 6632 Atmosphere Monitoring Service: From Research to Operations,  
 6633 <https://doi.org/10.1175/BAMS-D-21-0314.1>, 2022.
- 6634 Philip, S., Kew, S., Van Oldenborgh, G. J., Otto, F., Vautard, R., Van Der Wiel, K., King, A., Lott, F., Arrighi, J.,  
 6635 Singh, R., and Van Aalst, M.: A protocol for probabilistic extreme event attribution analyses, *Adv. Stat.*  
 6636 *Clim. Meteorol. Oceanogr.*, 6, 177–203, <https://doi.org/10.5194/ascmo-6-177-2020>, 2020.
- 6637 Phillips, C. A., Rogers, B. M., Elder, M., Cooperdock, S., Moubarak, M., Randerson, J. T., and Frumhoff, P. C.:  
 6638 Escalating carbon emissions from North American boreal forest wildfires and the climate mitigation  
 6639 potential of fire management, *Science Advances*, 8, eabl7161, <https://doi.org/10.1126/sciadv.abl7161>,  
 6640 2022.
- 6641 Pismel, G. O., Marchezini, V., Selaya, G., de Paula, Y. A. P., Mendoza, E., and Anderson, L. O.: Wildfire  
 6642 governance in a tri-national frontier of southwestern Amazonia: Capacities and vulnerabilities,  
 6643 *International Journal of Disaster Risk Reduction*, 86, 103529, <https://doi.org/10.1016/j.ijdrr.2023.103529>,  
 6644 2023.
- 6645 Pivello, V. R., Vieira, I., Christianini, A. V., Ribeiro, D. B., da Silva Menezes, L., Berlinck, C. N., Melo, F. P. L.,  
 6646 Marengo, J. A., Tornquist, C. G., Tomas, W. M., and Overbeck, G. E.: Understanding Brazil's  
 6647 catastrophic fires: Causes, consequences and policy needed to prevent future tragedies, *Perspectives*  
 6648 *in Ecology and Conservation*, 19, 233–255, <https://doi.org/10.1016/j.pecon.2021.06.005>, 2021.



- 6649 Polade, S. D., Pierce, D. W., Cayan, D. R., Gershunov, A., and Dettinger, M. D.: The key role of dry days in  
 6650 changing regional climate and precipitation regimes, *Sci Rep*, 4, 4364,  
 6651 <https://doi.org/10.1038/srep04364>, 2014.
- 6652 Pronger, J., Price, R., Schindler, J., Robertson, H., and West, D.: Estimating carbon emissions from peatland fires  
 6653 at Kaimaumu–Motutangi and Awarua wetlands, available at:  
 6654 [https://www.doc.govt.nz/globalassets/documents/conservation/land-and-freshwater/wetlands/estimating-](https://www.doc.govt.nz/globalassets/documents/conservation/land-and-freshwater/wetlands/estimating-carbon-emissions-from-peatland-fires.pdf)  
 6655 [carbon-emissions-from-peatland-fires.pdf](https://www.doc.govt.nz/globalassets/documents/conservation/land-and-freshwater/wetlands/estimating-carbon-emissions-from-peatland-fires.pdf) (last access: 6th August 2025), Manaaki Whenua Landcare  
 6656 Research, 2024.
- 6657 Pullabhotla, H., Zahid, M., Heft-Neal, S., Rath, V., and Burke, M.: Reply to Giglio and Roy: Aggregate infant  
 6658 mortality estimates robust to choice of burned area product, *Proceedings of the National Academy of*  
 6659 *Sciences, USA*, 120, e2318188120, <https://doi.org/10.1073/pnas.2318188120>, 2023.
- 6660 Pyne, S. J.: *Fire in America: A Cultural History of Wildland and Rural Fire*, University of Washington Press, ISBN  
 6661 0295805218, 2017.
- 6662 Qu, Y., Jones, M. W., Brambley, E., Hunt, H. G. P., Pérez-Invernón, F. J., Yebra, M., Zhao, L., Moris, J. V.,  
 6663 Janssen, T., and Veraverbeke, S.: A new global gridded lightning dataset with high spatial and temporal  
 6664 resolution, , <https://doi.org/10.5194/egusphere-egu25-8351>, 2025.
- 6665 Quilcaille, Y., Batibeniz, F., Ribeiro, A. F. S., Padrón, R. S., and Seneviratne, S. I.: Fire weather index data under  
 6666 historical and shared socioeconomic pathway projections in the 6th phase of the Coupled Model  
 6667 Intercomparison Project from 1850 to 2100, *Earth System Science Data*, 15, 2153–2177,  
 6668 <https://doi.org/10.5194/essd-15-2153-2023>, 2023.
- 6669 Rabin, S. S., Melton, J. R., Lasslop, G., Bachelet, D., Forrest, M., Hantson, S., Kaplan, J. O., Li, F., Mangeon, S.,  
 6670 Ward, D. S., Yue, C., Arora, V. K., Hickler, T., Kloster, S., Knorr, W., Nieradzik, L., Spessa, A., Folberth,  
 6671 G. A., Sheehan, T., Voulgarakis, A., Kelley, D. I., Prentice, I. C., Sitch, S., Harrison, S., and Arneth, A.:  
 6672 The Fire Modeling Intercomparison Project (FireMIP), phase 1: experimental and analytical protocols  
 6673 with detailed model descriptions, *Geoscientific Model Development*, 10, 1175–1197,  
 6674 <https://doi.org/10.5194/gmd-10-1175-2017>, 2017.
- 6675 Radeloff, V. C., Helmers, D. P., Kramer, H. A., Mockrin, M. H., Alexandre, P. M., Bar-Massada, A., Butsic, V.,  
 6676 Hawbaker, T. J., Martinuzzi, S., Syphard, A. D., and Stewart, S. I.: Rapid growth of the US  
 6677 wildland-urban interface raises wildfire risk, *Proceedings of the National Academy of Sciences, USA*,  
 6678 115, 3314–3319, <https://doi.org/10.1073/pnas.1718850115>, 2018.
- 6679 Radi Bulgaria: Dangerous fire near Sakar mountain now under control, combating the flames in Slavyanka  
 6680 continues, available at:  
 6681 [https://bnr.bg/en/post/102030013/dangerous-fire-near-sakar-mountain-now-under-control-combating-the-](https://bnr.bg/en/post/102030013/dangerous-fire-near-sakar-mountain-now-under-control-combating-the-flames-in-slavyanka-continues)  
 6682 [flames-in-slavyanka-continues](https://bnr.bg/en/post/102030013/dangerous-fire-near-sakar-mountain-now-under-control-combating-the-flames-in-slavyanka-continues) (last access: 6th August 2025), 2024.
- 6683 Reddington, C. L., Butt, E. W., Ridley, D. A., Artaxo, P., Morgan, W. T., Coe, H., and Spracklen, D. V.: Air quality  
 6684 and human health improvements from reductions in deforestation-related fire in Brazil, *Nature Geosci*, 8,  
 6685 768–771, <https://doi.org/10.1038/ngeo2535>, 2015.
- 6686 Reddington, C. L., Spracklen, D. V., Artaxo, P., Ridley, D. A., Rizzo, L. V., and Arana, A.: Analysis of particulate  
 6687 emissions from tropical biomass burning using a global aerosol model and long-term surface  
 6688 observations, *Atmospheric Chemistry and Physics*, 16, 11083–11106,  
 6689 <https://doi.org/10.5194/acp-16-11083-2016>, 2016.



- 6690 Rémy, S., Veira, A., Paugam, R., Sofiev, M., Kaiser, J. W., Marengo, F., Burton, S. P., Benedetti, A., Engelen, R.  
 6691 J., Ferrare, R., and Hair, J. W.: Two global data sets of daily fire emission injection heights since 2003,  
 6692 Atmos. Chem. Phys., 17, 2921–2942, <https://doi.org/10.5194/acp-17-2921-2017>, 2017.
- 6693 Rémy, S., Kipling, Z., Huijnen, V., Flemming, J., Nabat, P., Michou, M., Ades, M., Engelen, R., and Peuch, V.-H.:  
 6694 Description and evaluation of the tropospheric aerosol scheme in the Integrated Forecasting System  
 6695 (IFS-AER, cycle 47R1) of ECMWF, Geoscientific Model Development, 15, 4881–4912,  
 6696 <https://doi.org/10.5194/gmd-15-4881-2022>, 2022.
- 6697 Rémy, S., Metzger, S., Huijnen, V., Williams, J. E., and Flemming, J.: An improved representation of aerosol in  
 6698 the ECMWF IFS-COMPO 49R1 through the integration of EQSAM4Climv12 – a first attempt at  
 6699 simulating aerosol acidity, Geoscientific Model Development, 17, 7539–7567,  
 6700 <https://doi.org/10.5194/gmd-17-7539-2024>, 2024.
- 6701 Ren, X., Zhang, L., Cai, W., and Wu, L.: Moderate Indian Ocean Dipole Dominates Spring Fire Weather  
 6702 Conditions in Southern Australia, Environ. Res. Lett., 19, 064056,  
 6703 <https://doi.org/10.1088/1748-9326/ad4fa5>, 2024.
- 6704 Reuters: Forest fires raze parts of India amid heat, dry weather, available at:  
 6705 <https://www.reuters.com/world/india/forest-fires-raze-parts-india-amid-heat-dry-weather-2024-04-30/>  
 6706 (last access: 6th August 2025), Reuters, 2024.
- 6707 Ribeiro, A. F. S., Brando, P. M., Santos, L., Rattis, L., Hirschi, M., Hauser, M., Seneviratne, S. I., and  
 6708 Zscheischler, J.: A compound event-oriented framework to tropical fire risk assessment in a changing  
 6709 climate, Environ. Res. Lett., 17, 065015, <https://doi.org/10.1088/1748-9326/ac7342>, 2022.
- 6710 Riedel, L., Schmid, T., Rössli, T., Steinmann, C. B., Schmid, E., Bresch, D. N., and Kropf, C. M.: Ensemble of  
 6711 tragedies: Climate risk model calibration under deep uncertainty [preprint],  
 6712 <https://doi.org/10.22541/essoar.174786012.24238776/v1>, 2025.
- 6713 Roads, J., Fujioka, F., Chen, S., and Burgan, R.: Seasonal fire danger forecasts for the USA, International  
 6714 Journal of Wildland Fire, 14, 1–18, 14, 1–18, <https://doi.org/10.1071/WF03052>, 2005a.
- 6715 Roads, J., Fujioka, F., Chen, S., and Burgan, R.: Seasonal fire danger forecasts for the USA, Int. J. Wildland Fire,  
 6716 14, 1–18, <https://doi.org/10.1071/WF03052>, 2005b.
- 6717 Roads, J., Tripp, P., Juang, H., Wang, J., Fujioka, F., and Chen, S.: NCEP-ECPC monthly to seasonal US fire  
 6718 danger forecasts, International Journal of Wildland Fire, 19, 399–414, <https://doi.org/10.1071/WF07079>,  
 6719 2010.
- 6720 Roberts, G. and Wooster, M. J.: Development of a multi-temporal Kalman filter approach to geostationary active  
 6721 fire detection & fire radiative power (FRP) estimation, Remote Sensing of Environment, 152, 392–412,  
 6722 <https://doi.org/10.1016/j.rse.2014.06.020>, 2014.
- 6723 Roberts, G., Wooster, M. J., Lauret, N., Gastellu-Etchegorry, J.-P., Lynham, T., and McRae, D.: Investigating the  
 6724 impact of overlying vegetation canopy structures on fire radiative power (FRP) retrieval through  
 6725 simulation and measurement, Remote Sensing of Environment, 217, 158–171,  
 6726 <https://doi.org/10.1016/j.rse.2018.08.015>, 2018.
- 6727 Rodríguez-Trejo, D. A., Ponce-Calderón, L. P., Tchikoué, H., Martínez-Domínguez, R., Martínez-Muñoz, P., and  
 6728 Pulido-Luna, J. A.: Towards integrated fire management in Mexico's Megalopolis region: a diagnosis,  
 6729 TFI, 61, 80–86, <https://doi.org/10.55515/NWAM8441>, 2022.



- 6730 Román, M. O., Wang, Z., Sun, Q., Kalb, V., Miller, S. D., Molthan, A., Schultz, L., Bell, J., Stokes, E. C., Pandey,  
 6731 B., Seto, K. C., Hall, D., Oda, T., Wolfe, R. E., Lin, G., Golpayegani, N., Devadiga, S., Davidson, C.,  
 6732 Sarkar, S., Praderas, C., Schmaltz, J., Boller, R., Stevens, J., Ramos González, O. M., Padilla, E.,  
 6733 Alonso, J., Detrés, Y., Armstrong, R., Miranda, I., Conte, Y., Marrero, N., MacManus, K., Esch, T., and  
 6734 Masuoka, E. J.: NASA's Black Marble nighttime lights product suite, *Remote Sensing of Environment*,  
 6735 210, 113–143, <https://doi.org/10.1016/j.rse.2018.03.017>, 2018.
- 6736 Román, M. O., Justice, C., Paynter, I., Boucher, P. B., Devadiga, S., Endsley, A., Erb, A., Friedl, M., Gao, H.,  
 6737 Giglio, L., Gray, J. M., Hall, D., Hulley, G., Kimball, J., Knyazikhin, Y., Lyapustin, A., Myneni, R. B.,  
 6738 Noojipady, P., Pu, J., Riggs, G., Sarkar, S., Schaaf, C., Shah, D., Tran, K. H., Vermote, E., Wang, D.,  
 6739 Wang, Z., Wu, A., Ye, Y., Shen, Y., Zhang, S., Zhang, S., Zhang, X., Zhao, M., Davidson, C., and Wolfe,  
 6740 R.: Continuity between NASA MODIS Collection 6.1 and VIIRS Collection 2 land products, *Remote*  
 6741 *Sensing of Environment*, 302, 113963, <https://doi.org/10.1016/j.rse.2023.113963>, 2024.
- 6742 Roms, D. M.: Evaluating the Future of Lightning in Cloud-Resolving Models, *Geophysical Research Letters*, 46,  
 6743 14863–14871, <https://doi.org/10.1029/2019GL085748>, 2019.
- 6744 Rosan, T. M., Sitch, S., Mercado, L. M., Heinrich, V., Friedlingstein, P., and Aragão, L. E. O. C.:  
 6745 Fragmentation-Driven Divergent Trends in Burned Area in Amazonia and Cerrado, *Front. For. Glob.*  
 6746 *Change*, 5, <https://doi.org/10.3389/ffgc.2022.801408>, 2022.
- 6747 Rosleskhoz: Operational data on the forest fire season in Russia, available at:  
 6748 [https://rosleshoz.gov.ru/news/federal/rosleskhoz-v-2024-kolichestvo-lesnykh-pozharov-sokratilos-v-1-5-r-](https://rosleshoz.gov.ru/news/federal/rosleskhoz-v-2024-kolichestvo-lesnykh-pozharov-sokratilos-v-1-5-r-aza-v-sravnenii-so-srednepyatiletnimi-znacheniyami-n11213/)  
 6749 [aza-v-sravnenii-so-srednepyatiletnimi-znacheniyami-n11213/](https://rosleshoz.gov.ru/news/federal/rosleskhoz-v-2024-kolichestvo-lesnykh-pozharov-sokratilos-v-1-5-r-aza-v-sravnenii-so-srednepyatiletnimi-znacheniyami-n11213/) (last access: 6th August 2025), 2024.
- 6750 Roteta, E., Bastarrika, A., Ibisate, A., and Chuvieco, E.: A Preliminary Global Automatic Burned-Area Algorithm at  
 6751 Medium Resolution in Google Earth Engine, *Remote Sensing*, 13, 4298,  
 6752 <https://doi.org/10.3390/rs13214298>, 2021.
- 6753 Roy, D. P., Boschetti, L., Justice, C. O., and Ju, J.: The collection 5 MODIS burned area product — Global  
 6754 evaluation by comparison with the MODIS active fire product, *Remote Sensing of Environment*, 112,  
 6755 3690–3707, <https://doi.org/10.1016/j.rse.2008.05.013>, 2008.
- 6756 Ruf, F., Kone, S., and Bebo, B.: Le boom de l'anacarde en Côte d'Ivoire : transition écologique et sociale des  
 6757 systèmes à base de coton et de cacao, *Cah. Agric.*, 28, 21, <https://doi.org/10.1051/cagri/2019019>, 2019.
- 6758 RUIZ, F. C.: MONITOREO ESPACIO-TEMPORAL DE COMPLEJOS DE INCENDIOS FORESTALES:  
 6759 INTEGRACIÓN DE FOCOS DE CALOR VIIRS  
 6760 [https://proceedings.science/sbsr-2025/trabalhos/monitoreo-espacio-temporal-de-complejos-de-incendio](https://proceedings.science/sbsr-2025/trabalhos/monitoreo-espacio-temporal-de-complejos-de-incendio-s-forestales-integracion-de-f?lang=en)  
 6761 [s-forestales-integracion-de-f?lang=en](https://proceedings.science/sbsr-2025/trabalhos/monitoreo-espacio-temporal-de-complejos-de-incendio-s-forestales-integracion-de-f?lang=en), 2025.
- 6762 Ruscalleda-Alvarez, J., Cliff, H., Catt, G., Holmes, J., Burrows, N., Paltridge, R., Russell-Smith, J., Schubert, A.,  
 6763 See, P., and Legge, S.: Right-way fire in Australia's spinifex deserts: An approach for measuring  
 6764 management success when fire activity varies substantially through space and time, *Journal of*  
 6765 *Environmental Management*, 331, 117234, <https://doi.org/10.1016/j.jenvman.2023.117234>, 2023.
- 6766 Russell-Smith, J., Yates, C. P., Edwards, A. C., Whitehead, P. J., Murphy, B. P., and Lawes, M. J.: Deriving  
 6767 Multiple Benefits from Carbon Market-Based Savanna Fire Management: An Australian Example, *PLoS*  
 6768 *ONE*, 10, e0143426, <https://doi.org/10.1371/journal.pone.0143426>, 2015.
- 6769 S2ID: Sistema Integrado de Informações sobre Desastres, available at: <https://s2id.mi.gov.br/> (last access: 6th  
 6770 August 2025), 2024.



- 6771 Safford, H. D., Paulson, A. K., Steel, Z. L., Young, D. J. N., and Wayman, R. B.: The 2020 California fire season:  
 6772 A year like no other, a return to the past or a harbinger of the future?, *Global Ecol Biogeogr*, 31,  
 6773 2005–2025, <https://doi.org/10.1111/geb.13498>, 2022.
- 6774 Saini, V.: A “Himalayan” Crisis: Understanding Wildfires in Uttarakhand and India, available at:  
 6775 <https://climatefactchecks.org/a-himalayan-crisis-understanding-wildfires-in-uttarakhand-and-india/> (last  
 6776 access: 6th August 2025), Climate Fact Checks, 2024.
- 6777 Sánchez-García, C., Santín, C., Neris, J., Sigmund, G., Otero, X. L., Manley, J., González-Rodríguez, G.,  
 6778 Belcher, C. M., Cerdà, A., Marcotte, A. L., Murphy, S. F., Rhoades, C. C., Sheridan, G., Strydom, T.,  
 6779 Robichaud, P. R., and Doerr, S. H.: Chemical characteristics of wildfire ash across the globe and their  
 6780 environmental and socio-economic implications, *Environment International*, 178, 108065,  
 6781 <https://doi.org/10.1016/j.envint.2023.108065>, 2023.
- 6782 Sanju, P., Gaganshila, K., and Mahesh, K.: Over 230 homes, animal sheds gutted in multiple fires across western  
 6783 Nepal since Saturday, *The Kathmandu Post*, available at:  
 6784 [https://kathmandupost.com/national/2024/04/22/over-230-homes-animal-sheds-gutted-in-multiple-fires-a](https://kathmandupost.com/national/2024/04/22/over-230-homes-animal-sheds-gutted-in-multiple-fires-a-cross-western-nepal-since-saturday)  
 6785 [cross-western-nepal-since-saturday](https://kathmandupost.com/national/2024/04/22/over-230-homes-animal-sheds-gutted-in-multiple-fires-a-cross-western-nepal-since-saturday) (last access: 6th August 2025), 2024.
- 6786 San-Miguel-Ayanz, J., Schulte, E., Schmuck, G., and Camia, A.: The European Forest Fire Information System in  
 6787 the context of environmental policies of the European Union, *Forest Policy and Economics*, 29, 19–25,  
 6788 <https://doi.org/10.1016/j.forpol.2011.08.012>, 2013.
- 6789 San-Miguel-Ayanz, J., Durrant, T., Boca, R., Maiani, P., Libertà, G., Jacome Felix Oom, D., Branco, A., De Rigo,  
 6790 D., Suarez-Moreno, M., Ferrari, D., Roglia, E., Scionti, N., Broglia, M., and Sedano, F.: Advance report  
 6791 on forest fires in Europe, Middle East and North Africa 2024, Publications Office of the European Union,  
 6792 <https://data.europa.eu/doi/10.2760/1264626>, 2025.
- 6793 Santoro, M. and Cartus, O.: ESA Biomass Climate Change Initiative (Biomass\_cci): Global datasets of forest  
 6794 above-ground biomass for the years 2010, 2017 and 2018, v3, CEDA Archive [data set],  
 6795 <https://doi.org/10.5285/5F331C418E9F4935B8EB1B836F8A91B8>, 2021.
- 6796 Santoro, M., Cartus, O., Wegmüller, U., Besnard, S., Carvalhais, N., Araza, A., Herold, M., Liang, J., Cavlovic, J.,  
 6797 and Engdahl, M. E.: Global estimation of above-ground biomass from spaceborne C-band scatterometer  
 6798 observations aided by LiDAR metrics of vegetation structure, *Remote Sensing of Environment*, 279,  
 6799 113114, <https://doi.org/10.1016/j.rse.2022.113114>, 2022.
- 6800 Santos, F. C., Chaves, F. M., Negri, R. G., and Massi, K. G.: Fires in Pantanal: The link to Agriculture,  
 6801 Conversions in Cerrado, and Hydrological Changes, *Wetlands*, 44, 75,  
 6802 <https://doi.org/10.1007/s13157-024-01832-5>, 2024.
- 6803 Santos, J. L., Yanai, A. M., Graça, P. M. L. A., Correia, F. W. S., and Fearnside, P. M.: Amazon deforestation:  
 6804 simulated impact of Brazil's proposed BR-319 highway project, *Environ Monit Assess*, 195, 1217,  
 6805 <https://doi.org/10.1007/s10661-023-11820-7>, 2023.
- 6806 Schaller, N., Otto, F. E. L., van Oldenborgh, G. J., Massey, N. R., Sparrow, S., and Allen, M. R.: The heavy  
 6807 precipitation event of May–June 2013 in the upper Danube and Elbe basins [in “Explaining Extreme  
 6808 Events of 2013 from a Climate Perspective”], *Bulletin of the American Meteorological Society*, 95,  
 6809 S69–S72, 2014.



- 6810 Schleicher, J., Schaafsma, M., Burgess, N. D., Sandbrook, C., Danks, F., Cowie, C., and Vira, B.: Poorer without  
 6811 It? The Neglected Role of the Natural Environment in Poverty and Wellbeing, Sustainable Development,  
 6812 26, 83–98, <https://doi.org/10.1002/sd.1692>, 2018.
- 6813 Scholten, R. C., Jandt, R., Miller, E. A., Rogers, B. M., and Veraverbeke, S.: Overwintering fires in boreal forests,  
 6814 Nature, 593, 399–404, <https://doi.org/10.1038/s41586-021-03437-y>, 2021.
- 6815 Scholten, R. C., Veraverbeke, S., Chen, Y., and Randerson, J. T.: Spatial variability in Arctic–boreal fire regimes  
 6816 influenced by environmental and human factors, Nat. Geosci., 17, 866–873,  
 6817 <https://doi.org/10.1038/s41561-024-01505-2>, 2024.
- 6818 Schroeder, W., Prins, E., Giglio, L., Csiszar, I., Schmidt, C., Morissette, J., and Morton, D.: Validation of GOES and  
 6819 MODIS active fire detection products using ASTER and ETM+ data, Remote Sensing of Environment,  
 6820 112, 2711–2726, <https://doi.org/10.1016/j.rse.2008.01.005>, 2008a.
- 6821 Schroeder, W., Prins, E., Giglio, L., Csiszar, I., Schmidt, C., Morissette, J., and Morton, D.: Validation of GOES and  
 6822 MODIS active fire detection products using ASTER and ETM+ data, Remote Sensing of Environment,  
 6823 112, 2711–2726, <https://doi.org/10.1016/j.rse.2008.01.005>, 2008b.
- 6824 Schroeder, W., Oliva, P., Giglio, L., and Csiszar, I. A.: The New VIIRS 375 m active fire detection data product:  
 6825 Algorithm description and initial assessment, Remote Sensing of Environment, 143, 85–96,  
 6826 <https://doi.org/10.1016/j.rse.2013.12.008>, 2014.
- 6827 Schroeder, W., Oliva, P., Giglio, L., Quayle, B., Lorenz, E., and Morelli, F.: Active fire detection using  
 6828 Landsat-8/OLI data, Remote Sensing of Environment, 185, 210–220,  
 6829 <https://doi.org/10.1016/j.rse.2015.08.032>, 2016.
- 6830 Schug, F., Bar-Massada, A., Carlson, A. R., Cox, H., Hawbaker, T. J., Helmers, D., Hostert, P., Kaim, D.,  
 6831 Kasraee, N. K., Martinuzzi, S., Mockrin, M. H., Pfoch, K. A., and Radeloff, V. C.: The global  
 6832 wildland–urban interface, Nature, 621, 94–99, <https://doi.org/10.1038/s41586-023-06320-0>, 2023.
- 6833 Seddon, N., Chausson, A., Berry, P., Girardin, C. A. J., Smith, A., and Turner, B.: Understanding the value and  
 6834 limits of nature-based solutions to climate change and other global challenges, Philosophical  
 6835 Transactions of the Royal Society B: Biological Sciences, 375, 20190120,  
 6836 <https://doi.org/10.1098/rstb.2019.0120>, 2020.
- 6837 Sellar, A. A., Jones, C. G., Mulcahy, J. P., Tang, Y., Yool, A., Wiltshire, A., O'Connor, F. M., Stringer, M., Hill, R.,  
 6838 Palmieri, J., Woodward, S., de Mora, L., Kuhlbrodt, T., Rumbold, S. T., Kelley, D. I., Ellis, R., Johnson, C.  
 6839 E., Walton, J., Abraham, N. L., Andrews, M. B., Andrews, T., Archibald, A. T., Berthou, S., Burke, E.,  
 6840 Blockley, E., Carslaw, K., Dalvi, M., Edwards, J., Folberth, G. A., Gedney, N., Griffiths, P. T., Harper, A.  
 6841 B., Hendry, M. A., Hewitt, A. J., Johnson, B., Jones, A., Jones, C. D., Keeble, J., Liddicoat, S.,  
 6842 Morgenstern, O., Parker, R. J., Predoi, V., Robertson, E., Siahann, A., Smith, R. S., Swaminathan, R.,  
 6843 Woodhouse, M. T., Zeng, G., and Zerroukat, M.: UKESM1: Description and Evaluation of the U.K. Earth  
 6844 System Model, Journal of Advances in Modeling Earth Systems, 11, 4513–4558,  
 6845 <https://doi.org/10.1029/2019MS001739>, 2019.
- 6846 Seok, M.-W., Ko, Y. H., Park, K.-T., and Kim, T.-W.: Possible enhancement in ocean productivity associated with  
 6847 wildfire-derived nutrient and black carbon deposition in the Arctic Ocean in 2019–2021, Marine Pollution  
 6848 Bulletin, 201, 116149, <https://doi.org/10.1016/j.marpolbul.2024.116149>, 2024.





- 6849 Serrah, M.: After years of wildfires, Algeria tames the flames, available at:  
 6850 <https://www.context.news/climate-risks/after-years-of-wildfires-algeria-tames-the-flames> (last access: 6th  
 6851 August 2025), Context News, 2024.
- 6852 Sexton, J. O., Noojipady, P., Song, X.-P., Feng, M., Song, D.-X., Kim, D.-H., Anand, A., Huang, C., Channan, S.,  
 6853 Pimm, S. L., and Townshend, J. R.: Conservation policy and the measurement of forests, *Nature Clim*  
 6854 *Change*, 6, 192–196, <https://doi.org/10.1038/nclimate2816>, 2016.
- 6855 Shaddick, G., Thomas, M. L., Amini, H., Broday, D., Cohen, A., Frostad, J., Green, A., Gumy, S., Liu, Y., Martin,  
 6856 R. V., Pruss-Ustun, A., Simpson, D., van Donkelaar, A., and Brauer, M.: Data Integration for the  
 6857 Assessment of Population Exposure to Ambient Air Pollution for Global Burden of Disease Assessment,  
 6858 *Environ. Sci. Technol.*, 52, 9069–9078, <https://doi.org/10.1021/acs.est.8b02864>, 2018.
- 6859 Shakesby, R. A. and Doerr, S. H.: Wildfire as a hydrological and geomorphological agent, *Earth-Science*  
 6860 *Reviews*, 74, 269–307, <https://doi.org/10.1016/j.earscirev.2005.10.006>, 2006.
- 6861 Shepherd, G., Warner, K., and Hogarth, N.: Forests and poverty: how has our understanding of the relationship  
 6862 been changed by experience?, *int. forest. rev.*, 22, 29–43,  
 6863 <https://doi.org/10.1505/146554820829523907>, 2020.
- 6864 Shepherd, T. G., Boyd, E., Calel, R. A., Chapman, S. C., Dessai, S., Dima-West, I. M., Fowler, H. J., James, R.,  
 6865 Maraun, D., Martius, O., Senior, C. A., Sobel, A. H., Stainforth, D. A., Tett, S. F. B., Trenberth, K. E., van  
 6866 den Hurk, B. J. J. M., Watkins, N. W., Wilby, R. L., and Zenghelis, D. A.: Storylines: an alternative  
 6867 approach to representing uncertainty in physical aspects of climate change, *Climatic Change*, 151,  
 6868 555–571, <https://doi.org/10.1007/s10584-018-2317-9>, 2018.
- 6869 Shmuel, A. and Heifetz, E.: A Machine-Learning Approach to Predicting Daily Wildfire Expansion Rate, *Fire*, 6,  
 6870 319, <https://doi.org/10.3390/fire6080319>, 2023.
- 6871 Shmuel, A., Lazebnik, T., Glickman, O., Heifetz, E., and Price, C.: Global lightning-ignited wildfires prediction and  
 6872 climate change projections based on explainable machine learning models, *Sci Rep*, 15, 7898,  
 6873 <https://doi.org/10.1038/s41598-025-92171-w>, 2025.
- 6874 Short, K. C.: A spatial database of wildfires in the United States, 1992-2011, *Earth System Science Data*, 6,  
 6875 1–27, <https://doi.org/10.5194/essd-6-1-2014>, 2014.
- 6876 Shradha, K. and Nitu, R.: Rampant forest fires ravaging Nepal, Governance Monitoring Centre Nepal, available  
 6877 at: <https://gmcnepal.org/publications/climate-window/rampant-forest-fires-ravaging-nepal/> (last access:  
 6878 6th August 2025), 2024.
- 6879 Shuman, J. K., Balch, J. K., Barnes, R. T., Higuera, P. E., Roos, C. I., Schwilk, D. W., Stavros, E. N., Banerjee, T.,  
 6880 Bela, M. M., Bendix, J., Bertolino, S., Billign, S., Bladon, K. D., Brando, P., Breidenthal, R. E., Buma, B.,  
 6881 Calhoun, D., Carvalho, L. M. V., Cattau, M. E., Cawley, K. M., Chandra, S., Chipman, M. L.,  
 6882 Cobian-Iñiguez, J., Conlisk, E., Coop, J. D., Cullen, A., Davis, K. T., Dayalu, A., De Sales, F., Dolman,  
 6883 M., Ellsworth, L. M., Franklin, S., Guiterman, C. H., Hamilton, M., Hanan, E. J., Hansen, W. D., Hantson,  
 6884 S., Harvey, B. J., Holz, A., Huang, T., Hurteau, M. D., Ilangakoon, N. T., Jennings, M., Jones, C.,  
 6885 Klimaszewski-Patterson, A., Kobziar, L. N., Kominoski, J., Kosovic, B., Krawchuk, M. A., Laris, P.,  
 6886 Leonard, J., Loria-Salazar, S. M., Lucash, M., Mahmoud, H., Margolis, E., Maxwell, T., McCarty, J. L.,  
 6887 McWethy, D. B., Meyer, R. S., Miesel, J. R., Moser, W. K., Nagy, R. C., Niyogi, D., Palmer, H. M.,  
 6888 Pellegrini, A., Poulter, B., Robertson, K., Rocha, A. V., Sadegh, M., Santos, F., Scordo, F., Sexton, J. O.,  
 6889 Sharma, A. S., Smith, A. M. S., Soja, A. J., Still, C., Swetnam, T., Syphard, A. D., Tingley, M. W., Tohidi,  
 6890 A., Trugman, A. T., Turetsky, M., Varner, J. M., Wang, Y., Whitman, T., Yelenik, S., and Zhang, X.:



- 6891 Reimagine fire science for the anthropocene, *PNAS Nexus*, 1, pgac115,  
 6892 <https://doi.org/10.1093/pnasnexus/pgac115>, 2022.
- 6893 Siciliano, B., Dantas, G., Silva, C. M. da, and Arbilla, G.: The Updated Brazilian National Air Quality Standards: A  
 6894 Critical Review, *J. Braz. Chem. Soc.*, 31, 523–535, <https://doi.org/10.21577/0103-5053.20190212>, 2020.
- 6895 Silva, C. V. J., Aragão, L. E. O. C., Young, P. J., Espirito-Santo, F., Berenguer, E., Anderson, L. O., Brasil, I.,  
 6896 Pontes-Lopes, A., Ferreira, J., Withey, K., França, F., Graça, P. M. L. A., Kirsten, L., Xaud, H., Salimon,  
 6897 C., Scaranello, M. A., Castro, B., Seixas, M., Farias, R., and Barlow, J.: Estimating the multi-decadal  
 6898 carbon deficit of burned Amazonian forests, *Environ. Res. Lett.*, 15, 114023,  
 6899 <https://doi.org/10.1088/1748-9326/abb62c>, 2020.
- 6900 Silva Junior, C. H. L., Pessoa, A. C. M., Carvalho, N. S., Reis, J. B. C., Anderson, L. O., and Aragão, L. E. O. C.:  
 6901 The Brazilian Amazon deforestation rate in 2020 is the greatest of the decade, *Nat Ecol Evol*, 5,  
 6902 144–145, <https://doi.org/10.1038/s41559-020-01368-x>, 2021.
- 6903 Silva, P. S., Geirinhas, J. L., Lapere, R., Laura, W., Cassain, D., Alegría, A., and Campbell, J.: Heatwaves and  
 6904 fire in Pantanal: Historical and future perspectives from CORDEX-CORE, *Journal of Environmental*  
 6905 *Management*, 323, 116193, <https://doi.org/10.1016/j.jenvman.2022.116193>, 2022.
- 6906 Silva Trigo, M.: Bolivia alquilará aviones para combatir el fuego y espera la llegada de más brigadistas  
 6907 internacionales, available at:  
 6908 [https://www.infobae.com/america/america-latina/2024/09/10/bolivia-alquilara-aviones-para-combatir-el-f](https://www.infobae.com/america/america-latina/2024/09/10/bolivia-alquilara-aviones-para-combatir-el-fuego-y-espera-la-llegada-de-mas-brigadistas-internacionales/)  
 6909 [uego-y-espera-la-llegada-de-mas-brigadistas-internacionales/](https://www.infobae.com/america/america-latina/2024/09/10/bolivia-alquilara-aviones-para-combatir-el-fuego-y-espera-la-llegada-de-mas-brigadistas-internacionales/) (last access: 6th August 2025), 2024.
- 6910 Silveira, M. V. F., Petri, C. A., Broggio, I. S., Chagas, G. O., Macul, M. S., Leite, C. C. S. S., Ferrari, E. M. M.,  
 6911 Amim, C. G. V., Freitas, A. L. R., Motta, A. Z. V., Carvalho, L. M. E., Silva Junior, C. H. L., Anderson, L.  
 6912 O., and Aragão, L. E. O. C.: Drivers of Fire Anomalies in the Brazilian Amazon: Lessons Learned from  
 6913 the 2019 Fire Crisis, *Land*, 9, 516, <https://doi.org/10.3390/land9120516>, 2020.
- 6914 Silveira, M. V. F., Silva-Junior, C. H. L., Anderson, L. O., and Aragão, L. E. O. C.: Amazon fires in the 21st  
 6915 century: The year of 2020 in evidence, *Global Ecology and Biogeography*, 31, 2026–2040,  
 6916 <https://doi.org/10.1111/geb.13577>, 2022.
- 6917 SitRep: No. 77 – Informe de Situación Nacional. Incendios Forestales, available at:  
 6918 [https://www.gestionderiesgos.gob.ec/wp-content/uploads/2024/11/SitRep-No.-77-Incendios-Forestales-0](https://www.gestionderiesgos.gob.ec/wp-content/uploads/2024/11/SitRep-No.-77-Incendios-Forestales-01012024-al-21112024.pdf)  
 6919 [1012024-al-21112024.pdf](https://www.gestionderiesgos.gob.ec/wp-content/uploads/2024/11/SitRep-No.-77-Incendios-Forestales-01012024-al-21112024.pdf) (last access: 6th August 2025), 2024.
- 6920 Skakun, R., Castilla, G., Metsaranta, J., Whitman, E., Rodrigue, S., Little, J., Groenewegen, K., and Coyle, M.:  
 6921 Extending the National Burned Area Composite Time Series of Wildfires in Canada, *Remote Sensing*,  
 6922 14, 3050, <https://doi.org/10.3390/rs14133050>, 2022.
- 6923 Skakun, R., Castilla, G., and Jain, P.: Mapping wildfires in Canada with Landsat MSS to extend the National  
 6924 Burned Area Composite (NBAC) time series back to 1972, *Int. J. Wildland Fire*, 33,  
 6925 <https://doi.org/10.1071/WF24138>, 2024.
- 6926 Sloan, S., Locatelli, B., Andela, N., Cattau, M. E., Gaveau, D., and Tacconi, L.: Declining severe fire activity on  
 6927 managed lands in Equatorial Asia, *Commun Earth Environ*, 3, 1–12,  
 6928 <https://doi.org/10.1038/s43247-022-00522-6>, 2022.
- 6929 Smith, A. B.: U.S. Billion-dollar Weather and Climate Disasters, 1980 - present (NCEI Accession 0209268),  
 6930 <https://doi.org/10.25921/STKW-7W73>, 2020.



- 6931 Smith, H. G., Sheridan, G. J., Lane, P. N. J., Nyman, P., and Haydon, S.: Wildfire effects on water quality in forest  
 6932 catchments: A review with implications for water supply, *Journal of Hydrology*, 396, 170–192,  
 6933 <https://doi.org/10.1016/j.jhydrol.2010.10.043>, 2011.
- 6934 Smith, S., Geden, O., Nemet, G., Gidden, M., Lamb, W., Powis, C., Bellamy, R., Callaghan, M., Cowie, A., Cox,  
 6935 E., Fuss, S., Gasser, T., Grassi, G., Greene, J., Lueck, S., Mohan, A., Müller-Hansen, F., Peters, G.,  
 6936 Pratama, Y., Repke, T., Riahi, K., Schenuit, F., Steinhauser, J., Streffer, J., Valenzuela, J., and Minx, J.:  
 6937 State of Carbon Dioxide Removal - 1st Edition, OSF, <https://doi.org/10.17605/OSF.IO/W3B4Z>, 2023.
- 6938 Sofiev, M., Ermakova, T., and Vankevich, R.: Evaluation of the smoke-injection height from wild-land fires using  
 6939 remote-sensing data, *Atmos. Chem. Phys.*, 12, 1995–2006, <https://doi.org/10.5194/acp-12-1995-2012>,  
 6940 2012.
- 6941 Song, Z., Zhang, L., Tian, C., Fu, Q., Shen, Z., Zhang, R., Liu, D., and Cui, S.: Development of a  
 6942 high-spatial-resolution annual emission inventory of greenhouse gases from open straw burning in  
 6943 Northeast China from 2001 to 2020, *Atmos. Chem. Phys.*, 24, 13101–13113,  
 6944 <https://doi.org/10.5194/acp-24-13101-2024>, 2024.
- 6945 Soro, T. D., N'Dri, B., Dembélé, B., Kpre, A. J. N., Kouassi, K., Kpangba, K., Kouamé, Y., and Koné, M.: Périodes  
 6946 des feux de végétation en fonction des secteurs phytogéographiques de Côte d'Ivoire: approche par  
 6947 télédétection et perceptions des populations, *Research Journal of Environmental and Earth Sciences*, 6,  
 6948 8–17, 2020.
- 6949 Soro, T. D., Koné, M., N'Dri, A. B., and N'Datchoh, E. T.: Identified main fire hotspots and seasons in Côte  
 6950 d'Ivoire (West Africa) using MODIS fire data, *South African Journal of Science*, 117,  
 6951 <https://doi.org/10.17159/sajs.2021/7659>, 2021.
- 6952 Spessa, A. C., Field, R. D., Pappenberger, F., Langner, A., Englhart, S., Weber, U., Stockdale, T., Siegert, F.,  
 6953 Kaiser, J. W., and Moore, J.: Seasonal forecasting of fire over Kalimantan, Indonesia, *Natural Hazards*  
 6954 and *Earth System Sciences*, 15, 429–442, <https://doi.org/10.5194/nhess-15-429-2015>, 2015.
- 6955 Spuler, F. and Wessel, J.: ibicus v1.0.1, Zenodo [code], , <https://doi.org/10.5281/ZENODO.8101898>, 2023.
- 6956 Spuler, F. R., Wessel, J. B., Comyn-Platt, E., Varndell, J., and Cagnazzo, C.: ibicus: a new open-source Python  
 6957 package and comprehensive interface for statistical bias adjustment and evaluation in climate modelling  
 6958 (v1.0.1), *Geoscientific Model Development*, 17, 1249–1269, <https://doi.org/10.5194/gmd-17-1249-2024>,  
 6959 2024.
- 6960 Spuler, F. and Wessel, J.: State of Wildfires 2024-25: JULES-ES bias adjustment [Code],  
 6961 <https://doi.org/10.5281/ZENODO.15792440>, 2025.
- 6962 Srock, A. F., Charney, J. J., Potter, B. E., and Goodrick, S. L.: The Hot-Dry-Windy Index: A New Fire Weather  
 6963 Index, *Atmosphere*, 9, 279, <https://doi.org/10.3390/atmos9070279>, 2018.
- 6964 Stalhandske, Z., Steinmann, C. B., Meiler, S., Sauer, I. J., Vogt, T., Bresch, D. N., and Kropf, C. M.: Global  
 6965 multi-hazard risk assessment in a changing climate, *Sci Rep*, 14, 5875,  
 6966 <https://doi.org/10.1038/s41598-024-55775-2>, 2024.
- 6967 Starodubtsev, V. M. and Terentiev, A.: Grand fire in the Danube Delta Biosphere Reserve, in: ResearchGate,  
 6968 2025.



- 6969 Staver, A. C., Archibald, S., and Levin, S. A.: The Global Extent and Determinants of Savanna and Forest as  
 6970 Alternative Biome States, *Science*, 334, 230–232, <https://doi.org/10.1126/science.1210465>, 2011.
- 6971 Steinmann, C. B., Meier, S., Jones, M., Koh, J., Kropf, C., Bresch, D. N., and Hantson, S.: State of Wildfires  
 6972 2024-25: Regional Summaries of Asset Exposure and Population Exposure to Burned Area by  
 6973 Continent, Biome, Country, and Administrative Region [Data set] (2025.0),  
 6974 <https://doi.org/10.5281/ZENODO.15755007>, 2025a.
- 6975 Steinmann, C. B.: carmensteinmann/State-of-Wildfires\_2024-25\_CLIMADA: State-of-Wildfires\_2024-25  
 6976 CLIMADA v0.1.0, <https://doi.org/10.5281/zenodo.15831766>, 2025b.
- 6977 Stephens, S. L., McIver, J. D., Boerner, R. E. J., Fettig, C. J., Fontaine, J. B., Hartsough, B. R., Kennedy, P. L.,  
 6978 and Schwikl, D. W.: The Effects of Forest Fuel-Reduction Treatments in the United States, *BioScience*,  
 6979 62, 549–560, <https://doi.org/10.1525/bio.2012.62.6.6>, 2012.
- 6980 Stephens, S. L., Bernal, A. A., Collins, B. M., Finney, M. A., Lautenberger, C., and Saah, D.: Mass fire behavior  
 6981 created by extensive tree mortality and high tree density not predicted by operational fire behavior  
 6982 models in the southern Sierra Nevada, *Forest Ecology and Management*, 518, 120258,  
 6983 <https://doi.org/10.1016/j.foreco.2022.120258>, 2022.
- 6984 Stocks, B. J., Lawson, B. D., Alexander, M. E., Wagner, C. E. V., McAlpine, R. S., Lynham, T. J., and Dubé, D. E.:  
 6985 The Canadian Forest Fire Danger Rating System: An Overview, *The Forestry Chronicle*, 65, 450–457,  
 6986 <https://doi.org/10.5558/tfc65450-6>, 1989.
- 6987 Stott, P. A., Stone, D. A., and Allen, M. R.: Human contribution to the European heatwave of 2003, *Nature*, 432,  
 6988 610–614, <https://doi.org/10.1038/nature03089>, 2004.
- 6989 Sulla-Menashe, D., Gray, J. M., Abercrombie, S. P., and Friedl, M. A.: Hierarchical mapping of annual global land  
 6990 cover 2001 to present: The MODIS Collection 6 Land Cover product, *Remote Sensing of Environment*,  
 6991 222, 183–194, <https://doi.org/10.1016/j.rse.2018.12.013>, 2019.
- 6992 Swain, D.: As extreme California precipitation dipole persists, a high-end offshore wind/fire weather event may  
 6993 unfold in SoCal this week, available at: <https://weatherwest.com/archives/43171> (last access: 6th August  
 6994 2025), Weather West, 2025.
- 6995 Swain, D. L., Langenbrunner, B., Neelin, J. D., and Hall, A.: Increasing precipitation volatility in  
 6996 twenty-first-century California, *Nature Clim Change*, 8, 427–433,  
 6997 <https://doi.org/10.1038/s41558-018-0140-y>, 2018.
- 6998 Swain, D. L., Prein, A. F., Abatzoglou, J. T., Albano, C. M., Brunner, M., Diffenbaugh, N. S., Singh, D., Skinner, C.  
 6999 B., and Touma, D.: Hydroclimate volatility on a warming Earth, *Nat Rev Earth Environ*, 6, 35–50,  
 7000 <https://doi.org/10.1038/s43017-024-00624-z>, 2025.
- 7001 Swart, N. C., Cole, J. N. S., Kharin, V. V., Lazare, M., Scinocca, J. F., Gillett, N. P., Anstey, J., Arora, V., Christian,  
 7002 J. R., Hanna, S., Jiao, Y., Lee, W. G., Majaess, F., Saenko, O. A., Seiler, C., Seinen, C., Shao, A.,  
 7003 Sigmond, M., Solheim, L., Von Salzen, K., Yang, D., and Winter, B.: The Canadian Earth System Model  
 7004 version 5 (CanESM5.0.3), *Geosci. Model Dev.*, 12, 4823–4873,  
 7005 <https://doi.org/10.5194/gmd-12-4823-2019>, 2019.
- 7006 Synolakis, C. E. and Karagiannis, G. M.: Wildfire risk management in the era of climate change, *PNAS Nexus*, 3,  
 7007 pgae151, <https://doi.org/10.1093/pnasnexus/pgae151>, 2024.



- 7008** Syphard, A. and Keeley, J.: Factors Associated with Structure Loss in the 2013–2018 California Wildfires, *Fire*, 2,  
**7009** 49, <https://doi.org/10.3390/fire2030049>, 2019.
- 7010** Tang, W., Llort, J., Weis, J., Perron, M. M. G., Basart, S., Li, Z., Sathyendranath, S., Jackson, T., Sanz Rodriguez,  
**7011** E., Proemse, B. C., Bowie, A. R., Schallenberg, C., Strutton, P. G., Matear, R., and Cassar, N.:  
**7012** Widespread phytoplankton blooms triggered by 2019–2020 Australian wildfires, *Nature*, 597, 370–375,  
**7013** <https://doi.org/10.1038/s41586-021-03805-8>, 2021.
- 7014** Tang, W., He, C., Emmons, L., and Zhang, J.: Global expansion of wildland-urban interface (WUI) and WUI fires:  
**7015** insights from a multiyear worldwide unified database (WUWUI), *Environ. Res. Lett.*, 19, 044028,  
**7016** <https://doi.org/10.1088/1748-9326/ad31da>, 2024.
- 7017** Tang, Y., Rumbold, S., Ellis, R., Kelley, D., Mulcahy, J., Sellar, A., Walton, J., and Jones, C.: MOHC  
**7018** UKESM1.0-LL model output prepared for CMIP6 CMIP, 2019.
- 7019** Tavakoli Hafshejani, M., Nasrollahzadeh, M., and Mirkhani, V.: Better preparation for Iran's forest fires, *Science*,  
**7020** 377, 379–379, <https://doi.org/10.1126/science.add5194>, 2022.
- 7021** Terrill, M.: Measuring the supply chain impact of the LA fires, available at:  
**7022** <https://news.asu.edu/20250121-business-and-entrepreneurship-measuring-supply-chain-impact-la-fires>  
**7023** (last access: 6th August 2025), ASU, 2025.
- 7024** Texas House of Representatives: Texas House of Representatives Investigative Committee on the Panhandle  
**7025** Wildfires, available at:  
**7026** <https://www.house.texas.gov/pdfs/committees/reports/interim/88interim/House-Interim-Committee-on-Th>  
**7027** e-Panhandle-Wildfires-Report.pdf (last access: 6th August 2025), 2024.
- 7028** The Arab Weekly: After years of wildfires, Algeria tames the flames, available at:  
**7029** <https://thearabweekly.com/after-years-wildfires-algeria-tames-flames> (last access: 6th August 2025),  
**7030** AW, 2024.
- 7031** The Nation: Turkey wildfire toll hits 15 as experts flag faulty wires, available at:  
**7032** <https://www.nation.com.pk/25-Jun-2024/turkey-wildfire-toll-hits-15-as-experts-flag-faulty-wires> (last  
**7033** access: 6th August 2025), The Nation, 2024.
- 7034** Thiem, H.: Unusual fire risk across the Northeast in fall of 2024, available at:  
**7035** <https://www.climate.gov/news-features/event-tracker/unusual-fire-risk-across-northeast-fall-2024> (last  
**7036** access: 6th August 2025), NOAA, 2024.
- 7037** Tian, Y., Ghausi, S. A., Zhang, Y., Zhang, M., Xie, D., Cao, Y., Mei, Y., Wang, G., Zhong, D., and Kleidon, A.:  
**7038** Radiation as the dominant cause of high-temperature extremes on the eastern Tibetan Plateau, *Environ.*  
**7039** *Res. Lett.*, 18, 074007, <https://doi.org/10.1088/1748-9326/acd805>, 2023.
- 7040** Tomshin, O. and Solovyev, V.: Features of the Extreme Fire Season of 2021 in Yakutia (Eastern Siberia) and  
**7041** Heavy Air Pollution Caused by Biomass Burning, *Remote Sensing*, 14, 4980,  
**7042** <https://doi.org/10.3390/rs14194980>, 2022.
- 7043** Toreti, A., Bavera, D., Acosta, N. J., Acquafresca, L., Azas, K., Barbosa, P., De, J. A., Ficchi, A., Fioravanti, G.,  
**7044** Grimaldi, S., Hrast, E. A., Magni, D., Mazzeschi, M., McCormick, N., Salamon, P., Santos, N. S., and  
**7045** Volpi, D.: Global Drought Overview September 2024, <https://doi.org/10.2760/7511271>, 2024.



- 7046** Torres-Vázquez, M. Á., Herrera, S., Gincheva, A., Halifa-Marín, A., Cavicchia, L., Di Giuseppe, F., Montávez, J.  
**7047** P., and Turco, M.: Enhancing seasonal fire predictions with hybrid dynamical and random forest models,  
**7048** npj Nat. Hazards, 2, 1–10, <https://doi.org/10.1038/s44304-025-00069-4>, 2025a.
- 7049** Torres-Vázquez, M. Á., Di Giuseppe, F., Moreno-Torreira, A., Gincheva, A., Jerez, S., and Turco, M.: Large  
**7050** increase in extreme fire weather synchronicity over Europe, Environ. Res. Lett., 20, 024045,  
**7051** <https://doi.org/10.1088/1748-9326/ada8c2>, 2025b.
- 7052** Turco, M., Jerez, S., Doblas-Reyes, F. J., AghaKouchak, A., Llasat, M. C., and Provenzale, A.: Skilful forecasting  
**7053** of global fire activity using seasonal climate predictions, Nat Commun, 9, 2718,  
**7054** <https://doi.org/10.1038/s41467-018-05250-0>, 2018.
- 7055** Turco, M., Jones, M. W., and Di Giuseppe, F.: State of Wildfires 2024-25: Anomalies in Extreme Fire Weather  
**7056** Days by Continent, Biome, Country, and Administrative Region, Zenodo [Data set],  
**7057** <https://doi.org/10.5281/zenodo.15538595>, 2025.
- 7058** UK Environment Agency: Water situation: May 2025 summary, available at:  
**7059** [https://www.gov.uk/government/publications/water-situation-national-monthly-reports-for-england-2025/](https://www.gov.uk/government/publications/water-situation-national-monthly-reports-for-england-2025/water-situation-may-2025-summary)  
**7060** [water-situation-may-2025-summary](https://www.gov.uk/government/publications/water-situation-national-monthly-reports-for-england-2025/water-situation-may-2025-summary) (last access: 6th August 2025), 2025.
- 7061** United Nations Environment Programme, U. N.: Spreading like Wildfire: The Rising Threat of Extraordinary  
**7062** Landscape Fires, 2022.
- 7063** United States Geological Survey (USGS): Debris flow in the 2025 Eaton Fire burn area, California, available at:  
**7064** <https://www.usgs.gov/media/images/debris-flow-2025-eaton-fire-burn-area-california> (last access: 6th  
**7065** August 2025), 2025a.
- 7066** United States Geological Survey (USGS): Greater Los Angeles Wildfires - January 2025, available at:  
**7067** <https://www.usgs.gov/media/before-after/greater-los-angeles-wildfires-january-2025> (last access: 6th  
**7068** August 2025), 2025b.
- 7069** US Environmental Protection Agency (EPA): Air Quality System (AQS), available at: <https://www.epa.gov/aqs>  
**7070** (last access: 6th August 2025), 2025.
- 7071** US Forest Service: 2024 Wildfire Year: Record-breaking Intensity and Resilience. USDA Forest Service Pacific  
**7072** Northwest Region, available at:  
**7073** [https://www.fs.usda.gov/sites/nfs/files/legacy-media/r06/Updated%202024%20Fire%20Summary%2012](https://www.fs.usda.gov/sites/nfs/files/legacy-media/r06/Updated%202024%20Fire%20Summary%2012032024.pdf)  
**7074** [032024.pdf](https://www.fs.usda.gov/sites/nfs/files/legacy-media/r06/Updated%202024%20Fire%20Summary%2012032024.pdf) (last access: 6th August 2025), 2024.
- 7075** Valor Económico: Aumento dos custos operacionais cria barreiras no negócio do carvão vegetal, available at:  
**7076** [https://valoreconomico.co.ao/artigo/aumento-dos-custos-operacionais-cria-barreiras-no-negocio-do-carv](https://valoreconomico.co.ao/artigo/aumento-dos-custos-operacionais-cria-barreiras-no-negocio-do-carvao-vegetal)  
**7077** [ao-vegetal](https://valoreconomico.co.ao/artigo/aumento-dos-custos-operacionais-cria-barreiras-no-negocio-do-carvao-vegetal) (last access: 6th August 2025), Valor Económico, 2024.
- 7078** Van Der Wiel, K., Kapnick, S. B., Van Oldenborgh, G. J., Whan, K., Philip, S., Vecchi, G. A., Singh, R. K., Arrighi,  
**7079** J., and Cullen, H.: Rapid attribution of the August 2016 flood-inducing extreme precipitation in south  
**7080** Louisiana to climate change, Hydrol. Earth Syst. Sci., 21, 897–921,  
**7081** <https://doi.org/10.5194/hess-21-897-2017>, 2017.
- 7082** Van Dijk, A. I. J. M., Beck, H. E., Boergens, E., de Jeu, R. A. M., Dorigo, W. A., Edirisinghe, E., Forootan, E.,  
**7083** Guo, E., Güntner, A., Hou, J., Mehrnegar, N., Mo, S., Preimesberger, W., Rahman, J., and Rozas  
**7084** Larraondo, P.: Global Water Monitor 2024, Summary Report, available at:  
**7085** <https://www.globalwater.online/globalwater/report/index.html> (last access: 6th August 2025), 2025.





- 7086** Van Oldenborgh, G. J., Van Der Wiel, K., Kew, S., Philip, S., Otto, F., Vautard, R., King, A., Lott, F., Arrighi, J.,  
**7087** Singh, R., and Van Aalst, M.: Pathways and pitfalls in extreme event attribution, *Climatic Change*, 166,  
**7088** 13, <https://doi.org/10.1007/s10584-021-03071-7>, 2021.
- 7089** Van Wagner, C. E.: Development and structure of the Canadian Forest Fire Weather Index System, *Forestry*  
**7090** Technical Report 35, Canadian Forestry Service, Ottawa, available at:  
**7091** <https://cfs.nrcan.gc.ca/pubwarehouse/pdfs/19927.pdf> (last access: 6th August 2025), 1987.
- 7092** Van Wagtenonk, J. W.: Fire as a Physical Process, in: *Fire in California's Ecosystems*, edited by: Sugihara, N.,  
**7093** University of California Press, 38–57, <https://doi.org/10.1525/california/9780520246058.003.0003>, 2006.
- 7094** Vautard, R., Yiou, P., Otto, F., Stott, P., Christidis, N., van Oldenborgh, G. J., and Schaller, N.: Attribution of  
**7095** human-induced dynamical and thermodynamical contributions in extreme weather events, *Environ. Res.*  
**7096** Lett., 11, 114009, <https://doi.org/10.1088/1748-9326/11/11/114009>, 2016.
- 7097** Verhoeven, E. M., Murray, B. R., Dickman, C. R., Wardle, G. M., and Greenville, A. C.: Fire and rain are one:  
**7098** extreme rainfall events predict wildfire extent in an arid grassland, *International Journal of Wildland Fire*,  
**7099** 702–711, <https://doi.org/10.1071/WF19087>, 2020.
- 7100** Viana, C. R. S., dos Santos, M. C., Muniz, C. C., Filho, M. d S., Ignácio, A. R. A., Vitorino, B. D., da Frota, A. V.  
**7101** B., Bogoni, J. A., Castrillon, S. K. I., Caldas, K. A. dP, da Silva, S. A. A., Rossete, A. N., da Silva, D. J.,  
**7102** Iocca, F. A. dS, dos Santos, F. L., Lázaro, W. L., and Oliveira Junior, E. S.: Impactos das Queimadas na  
**7103** Saúde da População de Cáceres, Pantanal, em 10 de Setembro de 2024. Nota Técnica Conjunta  
**7104** No04/2024. Universidade do Estado do Mato Grosso (UNEMAT), available at:  
**7105** [https://lipan.com.br/wp-content/uploads/2024/09/NOTA\\_TECNICA\\_CONJUNTA\\_04\\_20242.pdf](https://lipan.com.br/wp-content/uploads/2024/09/NOTA_TECNICA_CONJUNTA_04_20242.pdf) (last  
**7106** access: 6th August 2025), 2024.
- 7107** VisiteHuila: Desflorestação da Região Sul é Alarmante, available at:  
**7108** <https://visitehuila.com/en/noticias-eventos/noticias/desflorestacao-regiao-sul-alarmante.html> (last  
**7109** access: 6th August 2025), 2024.
- 7110** Vitolo, C., Di Giuseppe, F., Barnard, C., Coughlan, R., San-Miguel-Ayanz, J., Libertá, G., and Krzeminski, B.:  
**7111** ERA5-based global meteorological wildfire danger maps, *Sci Data*, 7, 216,  
**7112** <https://doi.org/10.1038/s41597-020-0554-z>, 2020.
- 7113** Wang, D., Guan, D., Zhu, S., Kinnon, M. M., Geng, G., Zhang, Q., Zheng, H., Lei, T., Shao, S., Gong, P., and  
**7114** Davis, S. J.: Economic footprint of California wildfires in 2018, *Nat Sustain*, 4, 252–260,  
**7115** <https://doi.org/10.1038/s41893-020-00646-7>, 2021.
- 7116** Wang, Y., Chen, H.-H., Tang, R., He, D., Lee, Z., Xue, H., Wells, M., Boss, E., and Chai, F.: Australian fire  
**7117** nourishes ocean phytoplankton bloom, *Science of The Total Environment*, 807, 150775,  
**7118** <https://doi.org/10.1016/j.scitotenv.2021.150775>, 2022.
- 7119** Wang, Z., Peñuelas, J., Tagesson, T., Smith, W. K., Wu, M., He, W., Sitch, S., and Wang, S.: Evolution of Global  
**7120** Terrestrial Gross Primary Productivity Trend, *Ecosyst Health Sustain*, 10,  
**7121** <https://doi.org/10.34133/ehs.0278>, 2024.
- 7122** Ward, M., Tulloch, A. I. T., Radford, J. Q., Williams, B. A., Reside, A. E., Macdonald, S. L., Mayfield, H. J., Maron,  
**7123** M., Possingham, H. P., Vine, S. J., O'Connor, J. L., Massingham, E. J., Greenville, A. C., Woinarski, J.  
**7124** C. Z., Garnett, S. T., Lintermans, M., Scheele, B. C., Carwardine, J., Nimmo, D. G., Lindenmayer, D. B.,  
**7125** Kooyman, R. M., Simmonds, J. S., Sonter, L. J., and Watson, J. E. M.: Impact of 2019–2020 mega-fires



- 7126 on Australian fauna habitat, *Nat Ecol Evol*, 4, 1321–1326, <https://doi.org/10.1038/s41559-020-1251-1>,  
 7127 2020.
- 7128 van der Werf, G. R., Randerson, J. T., Giglio, L., Collatz, G. J., Kasibhatla, P. S., and Arellano, A. F.: Interannual  
 7129 variability in global biomass burning emissions from 1997 to 2004, *Atmos. Chem. Phys.*, 6, 3423–3441,  
 7130 <https://doi.org/10.5194/acp-6-3423-2006>, 2006.
- 7131 van der Werf, G. R., Randerson, J. T., Giglio, L., Collatz, G. J., Mu, M., Kasibhatla, P. S., Morton, D. C., DeFries,  
 7132 R. S., Jin, Y., and van Leeuwen, T. T.: Global fire emissions and the contribution of deforestation,  
 7133 savanna, forest, agricultural, and peat fires (1997–2009), *Atmospheric Chemistry and Physics*, 10,  
 7134 11707–11735, <https://doi.org/10.5194/acp-10-11707-2010>, 2010.
- 7135 van der Werf, G. R., Randerson, J. T., Giglio, L., van Leeuwen, T. T., Chen, Y., Rogers, B. M., Mu, M., van Marle,  
 7136 M. J. E., Morton, D. C., Collatz, G. J., Yokelson, R. J., and Kasibhatla, P. S.: Global fire emissions  
 7137 estimates during 1997–2016, *Earth Syst. Sci. Data*, 9, 697–720,  
 7138 <https://doi.org/10.5194/essd-9-697-2017>, 2017.
- 7139 Wetterhall, F. and Di Giuseppe, F.: The benefit of seamless forecasts for hydrological predictions over Europe,  
 7140 *Hydrology and Earth System Sciences*, 22, 3409–3420, <https://doi.org/10.5194/hess-22-3409-2018>,  
 7141 2018.
- 7142 WHO: WHO global air quality guidelines: particulate matter (PM<sub>2.5</sub> and PM<sub>10</sub>), ozone, nitrogen dioxide, sulfur  
 7143 dioxide and carbon monoxide, available at: <https://www.who.int/publications/i/item/9789240034228> (last  
 7144 access: 6th August 2025), 2025.
- 7145 Wiedinmyer, C., Kimura, Y., McDonald-Buller, E. C., Emmons, L. K., Buchholz, R. R., Tang, W., Seto, K., Joseph,  
 7146 M. B., Barsanti, K. C., Carlton, A. G., and Yokelson, R.: The Fire Inventory from NCAR version 2.5: an  
 7147 updated global fire emissions model for climate and chemistry applications, *Geoscientific Model  
 7148 Development*, 16, 3873–3891, <https://doi.org/10.5194/gmd-16-3873-2023>, 2023.
- 7149 Wigneron, J.-P., Li, X., Frappart, F., Fan, L., Al-Yaari, A., De Lannoy, G., Liu, X., Wang, M., Le Masson, E., and  
 7150 Moisy, C.: SMOS-IC data record of soil moisture and L-VOD: Historical development, applications and  
 7151 perspectives, *Remote Sensing of Environment*, 254, 112238, <https://doi.org/10.1016/j.rse.2020.112238>,  
 7152 2021.
- 7153 Wikipedia: List of California wildfires, available at: [https://en.wikipedia.org/wiki/List\\_of\\_California\\_wildfires](https://en.wikipedia.org/wiki/List_of_California_wildfires) (last  
 7154 access: 6th August 2025), 2025.
- 7155 Wilken, E., Nava, F., and Griffith, G.: North American terrestrial ecoregions—Level III, available at:  
 7156 [http://ftp://ftp.epa.gov/wed/ecoregions/pubs/NA\\_TerrestrialEcoregionsLevel3\\_Final-2June11\\_CEC.pdf](http://ftp://ftp.epa.gov/wed/ecoregions/pubs/NA_TerrestrialEcoregionsLevel3_Final-2June11_CEC.pdf)  
 7157 (last access: 6th August 2025), 2011.
- 7158 Williams, A. P., Abatzoglou, J. T., Gershunov, A., Guzman-Morales, J., Bishop, D. A., Balch, J. K., and  
 7159 Lettenmaier, D. P.: Observed Impacts of Anthropogenic Climate Change on Wildfire in California, *Earth's  
 7160 Future*, 7, 892–910, <https://doi.org/10.1029/2019EF001210>, 2019.
- 7161 Wittwer, G. and Waschik, R.: Estimating the economic impacts of the 2017–2019 drought and 2019–2020  
 7162 bushfires on regional NSW and the rest of Australia, *Aus J Agri & Res Econ*, 65, 918–936,  
 7163 <https://doi.org/10.1111/1467-8489.12441>, 2021.
- 7164 Woolcott, O. O.: Los Angeles County in flames: responsibilities on fire, *The Lancet Regional Health – Americas*,  
 7165 42, <https://doi.org/10.1016/j.lana.2025.101005>, 2025.



- 7166 Wooster, M. J., Roberts, G. J., Giglio, L., Roy, D. P., Freeborn, P. H., Boschetti, L., Justice, C., Ichoku, C.,  
 7167 Schroeder, W., Davies, D., Smith, A. M. S., Setzer, A., Csiszar, I., Strydom, T., Frost, P., Zhang, T., Xu,  
 7168 W., de Jong, M. C., Johnston, J. M., Ellison, L., Vadrevu, K., Sparks, A. M., Nguyen, H., McCarty, J.,  
 7169 Tanpipat, V., Schmidt, C., and San-Miguel-Ayanz, J.: Satellite remote sensing of active fires: History and  
 7170 current status, applications and future requirements, *Remote Sensing of Environment*, 267, 112694,  
 7171 <https://doi.org/10.1016/j.rse.2021.112694>, 2021.
- 7172 Working on Fire: 34 lives, 4 million hectares, billions of rands in damage: SA's deadliest wildfire season, available  
 7173 at:  
 7174 [https://workingonfire.org/34-lives-4-million-hectares-billions-of-rands-in-damage-sas-deadliest-wildfire-se-](https://workingonfire.org/34-lives-4-million-hectares-billions-of-rands-in-damage-sas-deadliest-wildfire-season/)  
 7175 [ason/](https://workingonfire.org/34-lives-4-million-hectares-billions-of-rands-in-damage-sas-deadliest-wildfire-season/) (last access: 6th August 2025), Working on Fire, 2024.
- 7176 World Bank: Policy Note: Managing Wildfires in a Changing Climate, Washington DC, available at:  
 7177 [https://www.profor.info/sites/default/files/PROFOR\\_ManagingWildfires\\_2020\\_final.pdf](https://www.profor.info/sites/default/files/PROFOR_ManagingWildfires_2020_final.pdf) (last access: 6  
 7178 August 2025), 2020.
- 7179 World Bank: Financially Prepared: The Case for Pre-positioned Finance in European Union Member States and  
 7180 Countries under EU Civil Protection Mechanism, Washington DC,  
 7181 [https://civil-protection-knowledge-network.europa.eu/system/files/2024-05/Financially\\_Prepared\\_-\\_The](https://civil-protection-knowledge-network.europa.eu/system/files/2024-05/Financially_Prepared_-_The_Case_for_Pre-positioned_Finance.pdf)  
 7182 [Case for Pre-positioned Finance.pdf](https://civil-protection-knowledge-network.europa.eu/system/files/2024-05/Financially_Prepared_-_The_Case_for_Pre-positioned_Finance.pdf) (last access: 6 August 2025), 2024a.
- 7183 World Bank: Priorizar a agricultura angolana para desbloquear a diversificação económica, available at:  
 7184 [https://www.worldbank.org/pt/news/feature/2024/03/28/prioritizing-afe-angolan-agriculture-to-unlock-eco-](https://www.worldbank.org/pt/news/feature/2024/03/28/prioritizing-afe-angolan-agriculture-to-unlock-economic-diversification)  
 7185 [nomic-diversification](https://www.worldbank.org/pt/news/feature/2024/03/28/prioritizing-afe-angolan-agriculture-to-unlock-economic-diversification) (last access: 6th August 2025), World Bank, 2024b.
- 7186 World Bank: Wealth Accounting [data set], <https://datacatalog.worldbank.org/search/dataset/0042066>, 2024c.
- 7187 World Meteorological Organization (WMO): State of the Global Climate 2024, <https://library.wmo.int/idurl/4/69455>,  
 7188 2025.
- 7189 World Resources Institute: After Record-Breaking Fires, Can Indonesia's New Policies Turn Down the Heat?,  
 7190 available at:  
 7191 <https://www.wri.org/insights/after-record-breaking-fires-can-indonesias-new-policies-turn-down-heat> (last  
 7192 access: 6th August 2025), 2016.
- 7193 World Weather Attribution: Climate change increased the likelihood of wildfire disaster in highly exposed Los  
 7194 Angeles area, available at:  
 7195 [https://www.worldweatherattribution.org/climate-change-increased-the-likelihood-of-wildfire-disaster-in-hi-](https://www.worldweatherattribution.org/climate-change-increased-the-likelihood-of-wildfire-disaster-in-highly-exposed-los-angeles-area/)  
 7196 [ghly-exposed-los-angeles-area/](https://www.worldweatherattribution.org/climate-change-increased-the-likelihood-of-wildfire-disaster-in-highly-exposed-los-angeles-area/) (last access: 6th August 2025), 2025.
- 7197 World Wildlife Fund: Technical Note: Early Warning to Mitigate Impacts of Drought in the Pantanal, available at:  
 7198 <https://www.wwf.org.br/?89121/Pantanal-may-face-a-historic-water-crisis-in-2024> (last access: 6th  
 7199 August 2025), 2024.
- 7200 Worldwide Fund for Nature (WWF): Com mais de 4 mil focos de fogo em 2024, Roraima vive emergência  
 7201 humanitária, available at:  
 7202 [https://www.wwf.org.br/?88320/Com-mais-de-4-mil-focos-de-fogo-em-2024-Roraima-vive-emergencia-h](https://www.wwf.org.br/?88320/Com-mais-de-4-mil-focos-de-fogo-em-2024-Roraima-vive-emergencia-humanitaria)  
 7203 [umanitaria](https://www.wwf.org.br/?88320/Com-mais-de-4-mil-focos-de-fogo-em-2024-Roraima-vive-emergencia-humanitaria) (last access: 6th August 2025), 2024.
- 7204 Xu, R., Ye, T., Yue, X., Yang, Z., Yu, W., Zhang, Y., Bell, M. L., Morawska, L., Yu, P., Zhang, Y., Wu, Y., Liu, Y.,  
 7205 Johnston, F., Lei, Y., Abramson, M. J., Guo, Y., and Li, S.: Global population exposure to landscape fire



- 7206 air pollution from 2000 to 2019, *Nature*, 621, 521–529, <https://doi.org/10.1038/s41586-023-06398-6>,  
 7207 2023.
- 7208 Xu, R., Ye, T., Huang, W., Yue, X., Morawska, L., Abramson, M. J., Chen, G., Yu, P., Liu, Y., Yang, Z., Zhang, Y.,  
 7209 Wu, Y., Yu, W., Wen, B., Zhang, Y., Hales, S., Lavigne, E., Saldiva, P. H. N., Coelho, M. S. Z. S., Matus,  
 7210 P., Roye, D., Klompmaker, J., Mistry, M., Breitner, S., Zeka, A., Raz, R., Tong, S., Johnston, F. H.,  
 7211 Schwartz, J., Gasparrini, A., Guo, Y., and Li, S.: Global, regional, and national mortality burden  
 7212 attributable to air pollution from landscape fires: a health impact assessment study, *The Lancet*, 404,  
 7213 2447–2459, [https://doi.org/10.1016/S0140-6736\(24\)02251-7](https://doi.org/10.1016/S0140-6736(24)02251-7), 2024.
- 7214 Yebra, M., Dennison, P. E., Chuvieco, E., Riaño, D., Zylstra, P., Hunt, E. R., Danson, F. M., Qi, Y., and Jurdao, S.:  
 7215 A global review of remote sensing of live fuel moisture content for fire danger assessment: Moving  
 7216 towards operational products, *Remote Sensing of Environment*, 136, 455–468,  
 7217 <https://doi.org/10.1016/j.rse.2013.05.029>, 2013.
- 7218 Yebra, M., Quan, X., Riaño, D., Rozas Larraondo, P., van Dijk, A. I. J. M., and Cary, G. J.: A fuel moisture content  
 7219 and flammability monitoring methodology for continental Australia based on optical remote sensing,  
 7220 *Remote Sensing of Environment*, 212, 260–272, <https://doi.org/10.1016/j.rse.2018.04.053>, 2018.
- 7221 Yonhap News Agency: Death toll from wildfires rises to 31, available at:  
 7222 <https://en.yna.co.kr/view/AEN20250402001400315> (last access: 6th August 2025), 2025.
- 7223 Yukimoto, S., Kawai, H., Koshiro, T., Oshima, N., Yoshida, K., Urakawa, S., Tsujino, H., Deushi, M., Tanaka, T.,  
 7224 Hosaka, M., Yabu, S., Yoshimura, H., Shindo, E., Mizuta, R., Obata, A., Adachi, Y., and Ishii, M.: The  
 7225 Meteorological Research Institute Earth System Model Version 2.0, MRI-ESM2.0: Description and Basic  
 7226 Evaluation of the Physical Component, *Journal of the Meteorological Society of Japan. Ser. II*, 97,  
 7227 931–965, <https://doi.org/10.2151/jmsj.2019-051>, 2019.
- 7228 Zachariah, M., Clarke, B., Vahlberg, M., Pereira Marghidan, C., Singh, R., Sengupta, S., Otto, F., Pinto, I., Mistry,  
 7229 M., Arrighi, J., Gale, S., and Rodriguez, L.: Climate change made the deadly heatwaves that hit millions  
 7230 of highly vulnerable people across large parts of Asia more frequent and extreme, *Imperial College*  
 7231 *London*, <https://doi.org/10.25561/111274>, 2024.
- 7232 Zargar, A. R.: India’s worsening, “severe plus” air pollution forces even more dramatic safety measures, available  
 7233 at:  
 7234 <https://www.cbsnews.com/news/delhi-air-pollution-smog-severe-plus-india-safety-measures-restrictions/>  
 7235 (last access: 6th August 2025), *CBS News*, 2024.
- 7236 Zhang, Y., Xu, R., Huang, W., Ye, T., Yu, P., Yu, W., Wu, Y., Liu, Y., Yang, Z., Wen, B., Ju, K., Song, J., Abramson,  
 7237 M. J., Johnson, A., Capon, A., Jalaludin, B., Green, D., Lavigne, E., Johnston, F. H., Morgan, G. G.,  
 7238 Knibbs, L. D., Zhang, Y., Marks, G., Heyworth, J., Arblaster, J., Guo, Y. L., Morawska, L., Coelho, M. S.  
 7239 Z. S., Saldiva, P. H. N., Matus, P., Bi, P., Hales, S., Hu, W., Phung, D., Guo, Y., and Li, S.: Respiratory  
 7240 risks from wildfire-specific PM<sub>2.5</sub> across multiple countries and territories, *Nat Sustain*, 8, 474–484,  
 7241 <https://doi.org/10.1038/s41893-025-01533-9>, 2025.
- 7242 Zheng, B., Ciais, P., Chevallier, F., Chuvieco, E., Chen, Y., and Yang, H.: Increasing forest fire emissions despite  
 7243 the decline in global burned area, *Science Advances*, 7, eabh2646,  
 7244 <https://doi.org/10.1126/sciadv.abh2646>, 2021.
- 7245 Zheng, B., Ciais, P., Chevallier, F., Yang, H., Canadell, J. G., Chen, Y., Van Der Velde, I. R., Aben, I., Chuvieco,  
 7246 E., Davis, S. J., Deeter, M., Hong, C., Kong, Y., Li, H., Li, H., Lin, X., He, K., and Zhang, Q.: Record-high



- 7247 CO<sub>2</sub> emissions from boreal fires in 2021, *Science*, 379, 912–917,  
7248 <https://doi.org/10.1126/science.ade0805>, 2023.
- 7249 Zubkova, M., Boschetti, L., Abatzoglou, J. T., and Giglio, L.: Changes in Fire Activity in Africa from 2002 to 2016  
7250 and Their Potential Drivers, *Geophysical Research Letters*, 46, 7643–7653,  
7251 <https://doi.org/10.1029/2019GL083469>, 2019.
- 7252 Zubkova, M., Giglio, L., Boschetti, L., Roy, D., Hall, J., and Humber, M. L.: The NASA Visible Infrared Imaging  
7253 Radiometer Suite (VIIRS) burned area product - VNP64A1 [dataset], available at:  
7254 <https://ui.adsabs.harvard.edu/abs/2024AGUFMB13I.1644Z> (last access: 6th August 2025), AGU Fall  
7255 Meeting Abstracts, B13I-1644, 2024.
- 7256